



HAL
open science

Optimal control and applications to the environment : mathematical analysis and numerical approximation

Nacer Sellila

► **To cite this version:**

Nacer Sellila. Optimal control and applications to the environment : mathematical analysis and numerical approximation. Analysis of PDEs [math.AP]. Normandie Université, 2021. English. NNT : 2021NORMC248 . tel-03596445

HAL Id: tel-03596445

<https://theses.hal.science/tel-03596445v1>

Submitted on 3 Mar 2022

HAL is a multi-disciplinary open access archive for the deposit and dissemination of scientific research documents, whether they are published or not. The documents may come from teaching and research institutions in France or abroad, or from public or private research centers.

L'archive ouverte pluridisciplinaire **HAL**, est destinée au dépôt et à la diffusion de documents scientifiques de niveau recherche, publiés ou non, émanant des établissements d'enseignement et de recherche français ou étrangers, des laboratoires publics ou privés.



Normandie Université

THÈSE

Pour obtenir le diplôme de doctorat

Spécialité MATHÉMATIQUES

Préparée au sein de l'Université de Caen Normandie

Optimal Control and Applications to the Environment: Mathematical Analysis and Numerical Approximation

Présentée et soutenue par
NACER SELLILA

Thèse soutenue le 03/12/2021
devant le jury composé de

M. LAURENT DI MENZA	Professeur des universités, Université Reims Champagne Ardenne	Rapporteur du jury
M. VINCENT GIOVANGIGLI	Directeur de recherche au CNRS, École Polytechnique	Rapporteur du jury
MME MURIEL BOULAKIA	Professeur des universités, Université Paris Saclay	Membre du jury
M. ABDERRAHIM EL MOATAZ BILLAH	Professeur des universités, Université Caen Normandie	Membre du jury
M. HOUARI MECHKOUR	Enseignant chercheur, ECE Paris	Membre du jury
M. FRANCOIS JOUVE	Professeur des universités, Université de Paris	Président du jury
M. MOHAMMED LOUAKED	Maître de conférences HDR, Université Caen Normandie	Directeur de thèse

Thèse dirigée par **MOHAMMED LOUAKED**, Laboratoire de Mathématiques 'Nicolas Oresme' (Caen)



UNIVERSITÉ
CAEN
NORMANDIE



Acknowledgements

I would like to thank first and foremost to my thesis supervisor Mr. Mohammed Louaked, who was able to guide me in a wise way during these three years of thesis. His consistently accurate advice and constructive remarks were very helpful to me, and his warm welcome as well as our informative and sympathetic discussions made me feel immediately welcome. I thank him for the trust he has placed in me, and I would like to express through these few words my deep gratitude to him.

I would like to thank Mr. Houari Mechkour for all his help. I am delighted to have worked with him because in addition to his scientific support, he has always been there to support and advise me during the development of my thesis.

I would like to thank Mr. Vincent Giovangigli and Mr. Laurent Di Menza for reviewing my thesis. I am also grateful to Mme Muriel Boulakia, Mr. François Jouve, Mr. Abderrahim Elmoataz for agreeing to be part of my thesis defense committee.

I would like to thank Mr. Christophe Baujault (former ECE director) and Mr. François Stephan (ECE director) as well as the Normandy Region for funding my thesis.

I would like to thank all members of the LMNO laboratory as well as the administrative members for their kindness and support.

Next, I would like thank to my current and former colleagues at ECE: Anis, Amina, Waleed, Yves, Jae Yun, Rafik, Benaoumeur, Manolo, Naila, François, Filippo, Serena, Thomas, Aghiles, Raouf, Quentin, Aakash, Maxime for their kindness and support.

A special thanks goes to my colleagues at the LMMO Lab: Dalal, Coumba, Tiphaine, Stavroula, Angelot, Dorian, Emmanuel, Etienne, Julien, Hung, Mostafa, Mohamed, Njaka, Thomas, Thanh, Thien and Tin. Many thanks to you, guys. It has been a pleasure to spend the last three years with you.

Finally, I would like to thank all the members of my family for their support during the period of my studies: my father and my mother, my sister and my brothers for their constant support and encouragement. I associate these thanks to my cousins. A thought to my nephews and nieces. These thanks cannot come to an end without a thought to my second family here in France, my friends with whom I had a great time and with whom I have fond memories.

Abstract

Cette thèse s’articule autour du contrôle optimal et ses applications à des phénomènes naturels tels que les îlots de chaleurs dans des milieux urbains, la pollution dans un environnement marin afin de préserver l’environnement et l’écosystème. Les points d’intérêts des applications de cette thèse rentrent ainsi dans les initiatives internationales et gouvernementales sur les transitions écologiques, énergétiques et aussi du point de vue économique.

Pour répondre aux problématiques citées auparavant, nous explorons différents types de modèles. Des modèles mathématiques paraboliques et hyperboliques sont introduits tels que le modèle Navier-Stokes Forchheimer instationnaire couplé avec les équations de Fourier pour les îlots de chaleur urbains, le modèle du transport avec second membre de type Dirac couplé avec le modèle des eaux peu profondes pour la pollution marine et le modèle stationnaire de Navier-Stokes Forchheimer dans le cas de la migration des poissons des eaux salées vers les eaux douces à travers une structure hydraulique du type passe à poissons.

Dans un premier temps, nous avons analysé ces modèles de manière théorique liée à l’existence et l’unicité de la solution et les estimations d’erreurs des modèles perturbés par rapport aux modèles originaux.

L’étape suivante consistait à une analyse numérique de certaines méthodes éléments finis pour l’approximation des modèles environnementaux.

Les applications ont pour objectif de minimiser la chaleur dans des villes urbaines, la pollution dans le milieu marin ainsi les effets tourbillonnaires dans les passes à poissons. Nous utilisons des algorithmes du type gradient projeté pour optimiser l’emplacement des espaces vert en milieu urbain comme solution du problème d’îlots de chaleur, et la descente du gradient à pas fixe pour minimiser la pollution marine où le gradient de la fonction coût est lié au système adjoint et dans le cas des passes à poissons, la technique d’optimisation topologique de type Lagrangienne. Nous avons implémentés les méthodes proposées sous Freefem++ et nous avons mis en évidence la précision et la robustesse des méthodes numériques suggérées.

Mots clés: Îlots de chaleur urbaines; Milieux poreux; Compressibilité artificielle; Contrôle optimal; Équations paraboliques; Systèmes hyperboliques; Méthode des caractéristiques; Estimations des erreurs; Algorithme de Gradient Projeté; Algorithme de Descente; Algorithme Lagrangien augmenté.

In this work, we are interested to the optimal control and its applications to some natural phenomena such as heat islands in urban environments, marine pollution in order to preserve the environment and the ecosystem.

The interest points of the applications of this thesis fit into international and governmental initiatives on ecological, energy and also economic transitions. To propose solutions to the problems mentioned above, we explore different types of models. Parabolic and hyperbolic mathematical models are introduced such as the unsteady Navier-Stokes Forchheimer model coupled with the Fourier equations for urban heat islands, pointwise control of parabolic problems governed by the linear convection-diffusion coupled with the shallow water models for the marine pollution and the stationary Navier-Stokes Forchheimer model in the case of the migration of fish from salt water to fresh water through a hydraulic structures of the fishways types.

Firstly, we analyzed these models in a theoretical way by studying the existence and the uniqueness of the model solution and give an error estimates between solutions of the perturbed models compared to the original model.

The second step consisted to the numerical analysis of some finite element methods approximation to these environmental models.

The objective is to minimize the heat in urban cities, pollution in the marine environment and the turbulent effects in the fishways.

We use algorithms of the projected gradient type to optimize the location of the green spaces in urban areas as a solution to the problem of heat islands, the descent of the gradient with fixed step to minimize marine pollution where the gradient of the cost function is related to the adjoint state. In the case of the fishways, we use the Lagrangian type topological optimization technique.

We implemented these methods proposed under Freefem++ software and we bring out the precision and the robustness of these suggested numerical methods.

Keywords: Urbain Heat Island; Porous media; Artificial compressibility; Pointwise control problem; Parabolic equation; Hyperbolic system; Characteristic method; Error estimates; Spectral Project Gradient Algorithm; Algorithm of Descent; Augmented Lagrangian Algorithm.

Contents

1	Optimal control and application to reduction of urban heat island intensity in porous city	29
1.1	Introduction	30
1.2	Governing equations in porous city	31
1.2.1	Navier-Stokes Forchheimer equation	31
1.2.2	Energy equation	32
1.3	Existence of solution for the Forchheimer-Fourier system	34
1.4	Main result	35
1.5	Approximation by the artificial compressibility method	44
1.5.1	Existence of solutions of the perturbed problem	45
1.6	Thermal comfort problem	51
1.6.1	Optimal control procedures	52
1.7	Numerical discretization	53
1.7.1	Variational formulation	53
1.7.2	Time semi-discretization	54
1.7.3	Space discretization	55
1.7.4	Gradient project algorithm	56
1.8	Numerical results	57
1.8.1	Effects of numerical and physical parameters	58
1.8.2	Caen Normandy University Campus	63
1.9	Conclusion	64
2	On error estimates of the artificial compressibility for the unsteady Navier-Stokes Forchheimer Fourier problem	67
2.1	Introduction	67
2.2	Prelimanaries	69
2.3	Analysis of the problem	74
2.4	Error estimates for the linearized problem	83
2.5	Error estimates for the nonlinear problem	87
2.6	Numerical resolution	93
2.6.1	Isolated island	98

2.6.2	Domestic frost-free refrigerator application	100
2.7	Conclusion	102
3	Theoretical and numerical analysis of an optimal problem governed by convection diffusion equations	105
3.1	Introduction	105
3.2	Governing equations	107
3.2.1	The transport pollution model	107
3.2.2	Adjoint state	108
3.2.3	2D shallow water model	109
3.2.4	Weak formulation	109
3.3	Control problem	109
3.4	Preliminaries	110
3.5	Characteristic Finite Element Approximation	112
3.6	Numerical resolution	129
3.6.1	Time and space discretization	130
3.6.2	Numerical results	131
3.7	Conclusion	137
4	Analysis and finite element approximation of optimal control problem based on porous media model	141
4.1	Introduction	142
4.2	Mathematical model	144
4.2.1	Preliminaries	144
4.2.2	Perturbed equation	150
4.2.3	Error estimates	153
4.3	Control problem	158
4.3.1	Adjoint system	158
4.3.2	Shape gradient	161
4.4	Finite element method	164
4.5	Numerical approximation and optimization algorithm	174
4.5.1	Optimization procedure	175
4.5.2	Numerical examples	177
4.6	Conclusion	182
4.7	Annex: Control problem of mixed boundary conditions	182
4.7.1	Adjoint system	183
4.7.2	Shape gradient	185
5	The application of adjoint method for shape optimization in porous media model	191
5.1	Introduction	191

5.2	The Navier-Stokes Forchheimer equations	193
5.3	Main results	194
5.3.1	Existence of the weak solution	195
5.3.2	Uniqueness of weak solutions	198
5.4	A shape optimization problem and adjoint states	199
5.5	Finite Element approximation	203
5.5.1	Space discretization : the Finite Element method	205
5.5.2	Algorithmic description of the implemented method	206
5.5.3	Numerical results : academic case	208
5.5.4	Numerical results : practical case	212
5.6	Conclusions	215
	List of Figures	221
	List of Tables	223

Introduction

Un des défis majeurs de notre siècle est de réduire de manière drastique l'impact du réchauffement climatique dans les écosystèmes présents sur terre. Parmi ces problèmes, on note la pollution de l'air et de l'eau, la croissance de la densité urbaine dans des zones rurales et la déforestation, le rejet des déchets industriels et des substances chimiques et d'autres qui génèrent la dégradation de l'environnement et affectent d'une part la santé humaine et d'autre part les espèces animales.

Dans le premier chapitre, nous nous sommes intéressés au problème des îlots de chaleur urbains (Urban Heat Island). Avec le développement de l'urbanisation, les propriétés urbaines changent remarquablement en fonction des activités humaines dans les villes. La chaleur et les nombreuses formes de pollution modifient les propriétés radiatives de l'atmosphère, ce qui entraîne la formation de ces îlots de chaleur urbains. Ils ont des effets négatifs sur la qualité de l'environnement, sur la santé, sur la consommation d'énergie et sur le développement durable des villes. Ils sont aussi responsables de l'augmentation de la température des villes, ce qui engendre une amplification de la concentration d'ozone dans l'air, participant à l'effet de serre indésirable. Di Menza [1] a répondu à la question, comment modéliser l'impact du changement climatique sur un écosystème.

Comment formuler un tel problème du point de vue optimisation ? C'est vers la notion du confort thermique qu'il faut aller pour bien définir le critère d'optimisation de la température dans des villes à forte densité urbaine pour assurer le confort de ses habitants.

Plus précisément, le problème se formule à l'aide de la mécanique des fluides couplée avec les effets de convection thermique reposant sur les équations de Boussinesq.

Nous nous intéressons à l'extension des équations de Boussinesq en ajoutant le terme linéaire de Darcy et le terme non linéaire Forchheimer. Nous exploitons des techniques de contrôle optimal pour l'emplacement des espaces verts et comment faire face aux problèmes environnementaux liés aux îlots de chaleur urbains apparaissant dans les villes. Un modèle climatique tridimensionnel est établi pour étudier les effets de la chaleur anthropique urbaine et l'écoulement de l'air dans les régions urbaines et rurales. Le mécanisme de transport dans les milieux poreux est régi par le système Navier-Stokes Forchheimer. Nous étudions l'existence des solutions faibles

et des solutions fortes en utilisant des conditions aux limites de type Dirichlet dans deux cas différents :

- La première situation consiste à étudier le problème incompressible Navier-Stokes Forchheimer Fourier non-stationnaire,
- Le deuxième contexte repose sur l'étude des solutions faibles et les solutions fortes dans le cas d'un fluide compressible en introduisant la méthode de compressibilité artificielle avec données initiales dans L^2 dans un domaine $\Omega \subset \mathbb{R}^N$ ($N \leq 3$).

Concernant les équations de Boussinesq (stationnaires et non stationnaires), il existe une abondante littérature dédiée au sujet. Canon et DiBenedetto [25] ont démontré l'existence et l'unicité de la solution forte dans les espaces $L^{p,q}$ dans le cas d'un fluide incompressible soumis à un transfert de chaleur convectif en utilisant les opérateurs intégraux singuliers. Cependant, dans le cas de la théorie L^2 , Santos da Rocha et al [29] ont montré l'existence et l'unicité de la solution du problème de Boussinesq stationnaire avec des données non régulières sur le bord dans L^2 . Morimoto [14], [16] a montré l'existence de la solution faible du problème Navier-Stokes stationnaire avec l'équation de convection naturelle dans un domaine borné Ω dans \mathbb{R}^N , ($N \leq 2$) dans le cas où la température sur le bord est imposée par une condition de type mixte, condition de Dirichlet sur certaines parties et de Neumann sur les autres parties, Foias, Manley et Temam [32] ont étudié les solutions fortes avec des données initiales dans L^2 dans un domaine \mathbb{R}^N , ($N \leq 3$), Ōeda [30], [31] a étudié les solutions faibles et fortes dans un domain non cylindrique en employant la méthode de pénalité et la théorie des opérateurs sous-différentiels.

Le système Navier-Stokes Forchheimer Fourier non-stationnaire est le suivant :

$$\left\{ \begin{array}{l} \partial_t u + (u \cdot \nabla)u + au + b |u|u = -\nabla p + \lambda \Delta u + dg [\beta (\theta - \theta_{in}) - 1] \quad \text{dans } \Omega \times [0, T], \\ \partial_t \theta + (u \cdot \nabla)\theta = \eta \Delta \theta + \mathcal{Q}_B + \sum_{i=1}^N \alpha_i \chi_{G_i} \quad \text{dans } \Omega \times [0, T], \\ \operatorname{div} u = 0 \quad \text{dans } \Omega \times [0, T], \\ u(x, t = 0) = a_0(x), \quad \theta(x, t = 0) = \tau_0(x) \quad \text{dans } \Omega, \\ u(x, t) = 0 \quad x \in \Gamma_1, \\ \theta(x, t) = \xi(x, t) \quad x \in \Gamma_1, \\ u(x, t) = 0 \quad \text{sur } (\Gamma_B \cup \Gamma_s) \times [0, T], \\ \frac{\partial \theta}{\partial n} = 0 \quad \text{sur } (\Gamma_B \cup \Gamma_s) \times [0, T], \end{array} \right. \quad (0.1)$$

Avec u est la vitesse du fluide, θ la température, λ et κ sont des coefficients de diffusion, α_i la température dégagée par les feuilles (espaces verts), a, b et d sont des constantes positives telles que a est le coefficient de Darcy, b est le coefficient de Forchheimer, d est le coefficient pour la force de Boussinesq, a_0, τ_0 et ξ sont les conditions initiales de la vitesse, la pression et la température

respectivement, $g(x, t)$ est la fonction vectorielle gravitationnelle et β est le coefficient de dilatation thermique. Q_B est l'intensité de la source de chaleur du bâtiment par unité de surface du sol.

Du point de vue approximation numérique le champs de vitesse et celui de la pression sont dissociés ce qui engendre des difficultés numériques pour approcher les équations Navier-Stokes Forchheimer Fourier liée à la contrainte d'incompressibilité $\operatorname{div} u = 0$. Pour résoudre ce problème et relaxer cette contrainte, il existe plusieurs types de méthodes de relaxation :

- **La méthode de pénalisation:** cette méthode a été introduite par Courant [4], largement étudié dans le cas des équations de Navier-Stokes. Bercovier et Engelman [5] ont utilisé un élément fini parabolique isoparamétrique de type pénalisation où ils ont montré les propriétés de stabilité et de convergence de la méthode. Thomas [6] a utilisé des éléments finis de type Galerkin pour démontrer l'efficacité de la méthode.

$$\operatorname{div} u_\varepsilon + \varepsilon p^\varepsilon = 0.$$

- **La pression stabilisée:** Cette méthode a été introduite par Brezzy et Pitkäranta [7]. Louaked et al [8], Brezzi, Douglas [9], Hughes, Franca, Balestra [10].

$$\operatorname{div} u_\varepsilon + \varepsilon \Delta p^\varepsilon = 0.$$

- **La méthode de pseudo-compressibilité:** Chorin [12], et celle de E et Liu [13] et de Shen [11] ont montré l'efficacité de cette méthode dans la cas de l'analyse de l'erreur des équations de Navier-Stokes.

$$\operatorname{div} u_\varepsilon + \varepsilon \Delta p_t^\varepsilon = 0.$$

- **Méthode de compressibilité artificielle:** cette méthode est largement utilisée par Chorin [3] et Temam [2]

$$\operatorname{div} u^\varepsilon + p_t^\varepsilon = 0.$$

Cette méthode fait l'objet de la suite du couplage des équations Navier-Stokes Forchheimer Fourier.

Alors le problème non perturbé (0.1) se réécrit sous la forme

$$\left\{ \begin{array}{l} \partial_t u_\varepsilon + (u_\varepsilon \cdot \nabla) u_\varepsilon + a u_\varepsilon + b |u_\varepsilon| u_\varepsilon = -\nabla p_\varepsilon + \lambda \Delta u_\varepsilon + dg [\beta (\theta_\varepsilon - \theta_{in}) - 1] \quad \text{dans } \Omega \times [0, T], \\ \partial_t \theta_\varepsilon + (u_\varepsilon \cdot \nabla) \theta_\varepsilon = \eta \Delta \theta_\varepsilon + f \quad \text{dans } \Omega \times [0, T], \\ \varepsilon \partial_t p_\varepsilon + \nabla \cdot u_\varepsilon = 0 \quad \text{dans } \Omega \times [0, T], \\ u_\varepsilon(x, t = 0) = a_0(x) \quad \text{dans } \Omega, \\ \theta_\varepsilon(x, t = 0) = \tau_0(x) \quad \text{dans } \Omega, \\ p_\varepsilon(x, t = 0) = \pi_0(x) \quad \text{dans } \Omega, \\ u_\varepsilon(x, t) = 0 \quad \text{sur } \Gamma_1, \\ \theta_\varepsilon(x, t) = \xi(x, t) \quad \text{sur } \Gamma_1, \\ p_\varepsilon(x, t) = 0 \quad \text{sur } \Gamma_1, \\ u_\varepsilon(x, t) = 0 \quad \text{sur } (\Gamma_B \cup \Gamma_s) \times [0, T], \\ \frac{\partial \theta_\varepsilon}{\partial n} = 0 \quad \text{sur } (\Gamma_B \cup \Gamma_s) \times [0, T], \end{array} \right. \quad (0.2)$$

En premier lieu, nous avons montré l'existence de la solution faible du système non perturbé (0.1). La démonstration est basée sur la construction d'une solution approchée par la méthode de Faedo-Galerkin et le passage aux limites. Soient les espaces fonctionnels suivants :

$$D_\sigma = \{ \text{fonction vecteur } \varphi \in C^\infty(\Omega) | \text{supp} \varphi \subset \Omega, \text{div} \varphi = 0 \quad \text{dans } \Omega \}$$

$$D_0 = \{ \text{fonction scalaire } \varphi \in C^\infty(\bar{\Omega}) | \varphi \equiv 0 \quad \text{au voisinage de } \Gamma_1 \}$$

$$H = \text{adhérence de } D_\sigma \quad \text{sous la norme } L^2(\Omega)$$

$$V = \text{adhérence de } D_\sigma \quad \text{sous la norme } H^1(\Omega)$$

$$W = \text{adhérence de } D_0 \quad \text{sous la norme } H^1(\Omega)$$

Théorème 0.0.1. *Soit Ω un domaine borné dans $\mathbb{R}^d, (d = 2, 3)$. Si $g \in L^\infty(\Omega \times ([0, T]))$, $\xi \in C^1(\bar{\Gamma}_1) \times [0, T]$, $\tau_0 \in L^2(\Omega)$, $a_0 \in H$, $\theta_{in} \in L^2(\Omega)$, a, b sont des constantes positives $a > 0$, $b > 0$, et si $(d\beta \|g\|_{L^\infty}) < c\sqrt{\lambda}\eta$ où $c > 0$, alors il existe une solution faible (u, θ) de (0.1) satisfaisant les conditions initiales.*

$$u \in L^\infty([0, T], H), \quad \theta \in L^\infty([0, T], L^2(\Omega)).$$

De même, dans le cas du système perturbé (0.2) Navier-Stokes Forchheimer Fourier. On a :

Théorème 0.0.2. *Pour $\varepsilon > 0$ fixe et largement petit et $f \in L^2([0, T]; L^2(\Omega))$. De plus, si $g \in L^\infty(\Omega \times ([0, T]))$, $\xi \in C^1(\bar{\Gamma}_1 \times [0, T])$, $\tau_0 \in L^2(\Omega)$, $a_0 \in H$, $\theta_{in} \in L^2(\Omega)$, a, b sont des constantes positives $a > 0$, $b > 0$, si $(d\beta \|g\|_{L^\infty}) < c\sqrt{\lambda}\eta$ où c est une constante positive,*

alors il existe au moins une solution $(u^\varepsilon, \theta^\varepsilon, p^\varepsilon)$ du système perturbé (0.2). En outre,

$$(u^\varepsilon, \theta^\varepsilon, p^\varepsilon) \in L^\infty([0, T]; H) \times L^\infty([0, T]; L^2(\Omega)) \times L^\infty([0, T]; L^2(\Omega))$$

Ensuite, nous avons introduit une procédure d'optimisation de la température dans des villes urbaines afin d'assurer le confort du trafic des piétons. Un îlot de chaleur urbain par définition est la différence de température entre le secteur urbanisé et le secteur environnant dû au résultat des choix d'aménagement des milieux de vie, notamment la minéralisation des surfaces. Il existe plusieurs facteurs, liés à la localisation des espaces verts.

Nous minimisons la température au sol par l'introduction de la fonction coût suivante

$$J_1(\theta) = \frac{1}{n} \int_0^T \int_{\Gamma_{s_i}} \theta^\varepsilon(x, t) dx dt \quad (0.3)$$

Le processus d'optimisation passe par la résolution des équations du système perturbé Navier-Stokes Forchheimer Fourier. Le problème de contrôle est résolu par une méthode itérative. Nous utilisons un algorithme de type gradient projeté.

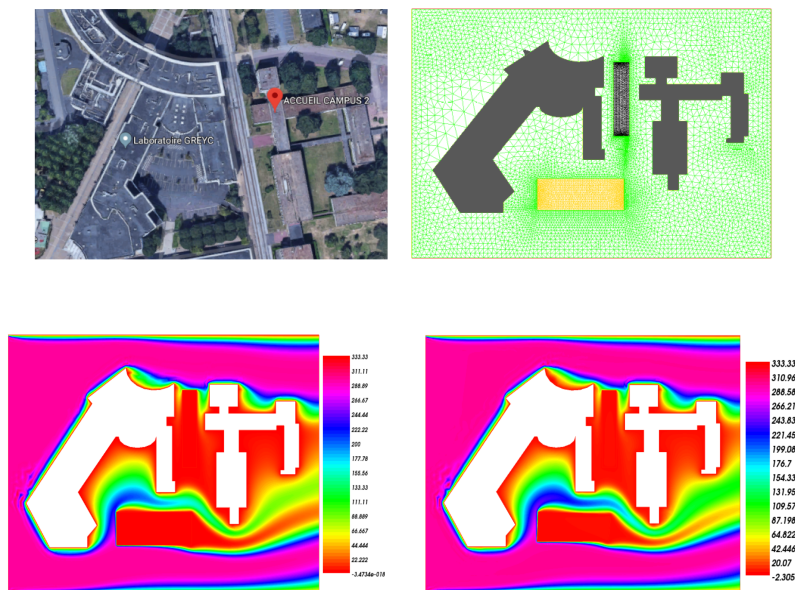


Figure 1: Champs de température de l'air pour les emplacements des espaces verts optimaux et non optimaux (Campus universitaire Caen Normandie).

Dans ce deuxième chapitre, nous nous sommes intéressés aux estimations d'erreurs en introduisant la méthode de compressibilité artificielle pour le système instationnaire de Navier-Stokes Forchheimer Fourier.

Le problème de convection-diffusion couplé avec les équations de Boussinesq incompressibles non-stationnaires sont largement étudiées. Il existe plusieurs méthodes d'approximations numériques pour approcher le problème de convection-diffusion. Shen [42] a analysé l'existence et l'unicité de la solution du problème convection-diffusion stationnaire avec des éléments de Bernard-Raugel. Shi et Ren [43] ont examiné une méthode d'éléments finis mixtes non conforme. Hafien, Fadili et Elmoataz [44] ont étudié l'approximation numérique du problème non local avec des conditions aux limites de types Neumann homogènes sur graphe. Kim et Choi [45] ont considéré la conduction et la convection naturelle entre deux cylindres concentriques sous les effets d'irradiation solaire. Comme on le voit, la vitesse u , la pression p et la température sont couplées par la contrainte d'incompressibilité $\nabla \cdot u = 0$. Pour résoudre ce problème de couplage, nous utilisons les méthodes proposées auparavant (méthode de pénalité, méthode de compressibilité artificielle). Shen [?] a montré l'estimation d'erreur optimal pour les équations de Navier-Stokes instationnaire. He [46] a fait l'extension de l'analyse d'erreur du problème Navier-Stokes stationnaire en utilisant la méthode des éléments finis. Wang et al [47] ont étudié les estimations d'erreurs d'un système pénalisé et une extension à une discrétisation totale du schéma [48]. Giovangigli et Yong [49] ont étudié les estimations à priori des systèmes hyperboliques-paraboliques symétriques linéarisés à faible dissipation. Sun, He et Feng [51] ont proposé la méthode de pénalité pour résoudre le problème couplé Navier-Stokes avec le problème de convection-diffusion non stationnaire dans un domaine Ω de dimension $N = 2$ sous certaines hypothèses sur les données initiales. Ce qui motive notre intérêt pour la résolution de problème couplé plus compliqué réunissant le terme Darcy et le terme de Forchheimer pour les équations de Navier-Stokes est de relaxer la contrainte d'incompressibilité en introduisant la méthode de la compressibilité artificielle.

Nous avons analysé le problème couplé et nous avons établi les estimations d'erreurs entre la solution originale (u, p, θ) et la solution perturbée $(u^\varepsilon, p^\varepsilon, \theta^\varepsilon)$. La preuve des estimations d'erreur se fait en deux étapes : la première consiste à l'analyse de l'erreur dans le cas d'un système linéaire et la deuxième étape concerne l'analyse d'erreur pour le cas d'un système non linéaire. Nous introduisons les espaces fonctionnels suivants :

$$X = H_0^1(\Omega)^2, \quad W = H_0^1(\Omega), \quad V = \{v \in X; \operatorname{div} v = 0\}, \quad H = \{v \in L^2(\Omega)^2; \operatorname{div} v = 0; v \cdot n|_{\partial\Omega} = 0\}$$

Les estimations d'erreurs entre le système perturbé et le non-perturbé sont prouvées sous les conditions suivantes :

- **(H1)** : supposons que la vitesse initiale $u_0 \in V$ et $f \in L^\infty([0, T]; L^2(\Omega))$, la température initiale $\varphi \in W$,

- **(H2)** : supposons que $\varphi \in H^2(\Omega)$ et $tf_t \in L^\infty([0, t]; L^2(\Omega))$ et $t\theta_t \in L^\infty([0, t]; L^2(\Omega))$.

Théorème 0.0.3. *Si $\varphi \in H^2(\Omega)$, le problème perturbé Navier-Stokes Forchheimer Fourier a une solution unique $(u^\varepsilon, p^\varepsilon, \theta^\varepsilon) \in [L^\infty([0, T]; H^2(\Omega)) \cap L^2([0, T]; X)] \times L^2([0, T]; M) \times H^1([0, T]; W)$. La solution $(u^\varepsilon, p^\varepsilon, \theta^\varepsilon)$ converge uniformément vers la solution (u, p, θ) $\varepsilon \rightarrow 0$.*

Le contrôle de l'erreur du problème non-linéaire est illustré par le théorème (0.0.4) suivant :

Théorème 0.0.4. *Supposons **(H1)** et **(H2)** sont validées, ε suffisamment petit, pour tout $t \in [0, T]$, les estimations d'erreurs suivantes sont vérifiées*

$$(at + 1)t\|u - u^\varepsilon\|^2 + t\varepsilon\|p - p^\varepsilon\|^2 + t\|\theta - \theta^\varepsilon\|^2 + \lambda t^2\|\nabla(u - u^\varepsilon)\|^2 + \kappa t^2\|\nabla(\theta - \theta^\varepsilon)\|^2 \leq C\varepsilon^2$$

Concernant l'approximation numérique, nous employons une discrétisation spatio-temporelle reposant sur un schéma d'Euler implicite avec les éléments finis de type Bernadi-Raugel. Nous considérons V_h , Q_h et W_h les espaces éléments finis tels que

$$\begin{aligned} V_h &= \left\{ v_h \in C^0(\bar{\Omega}) \cap H_0^1(\Omega)^d; \forall K \in \mathcal{T}_h, v_h|_K \in \mathbb{P}_K \right\} \\ Q_h &= \left\{ q_h \in L^2(\Omega); \forall K \in \mathcal{T}_h, q_h|_K \in \mathbb{P}_1 \right\} \\ W_h &= \left\{ w_h \in H^1(\Omega); \forall K \in \mathcal{T}_h, w_h|_K \in \mathbb{P}_2 \right\} \end{aligned}$$

La formulation variationnelle du système perturbé (0.2): Trouver $(u_h^{\varepsilon, (k+1)}, p_h^{\varepsilon, (k+1)}, \theta_h^{\varepsilon, (k+1)}) \in (V_h \times Q_h \times W_h)$ pour tout $v_h \in V_h$, $q_h \in Q_h$ et $w_h \in X_h$

$$\begin{aligned} & \frac{\langle u_h^{\varepsilon, (k+1)}, v_h \rangle - \langle u_h^{\varepsilon, (k)}, v_h \rangle}{t_{k+1} - t_k} + \lambda \langle \nabla u_h^{\varepsilon, (k+1)}, \nabla v_h \rangle + a \langle u_h^{\varepsilon, (k+1)}, v_h \rangle + \langle u_h^{\varepsilon, (k)} (\nabla u_h^{\varepsilon, (k+1)}), v_h \rangle \\ & + b \left\langle \left| u_h^{\varepsilon, (k)} \right| u_h^{\varepsilon, (k+1)}, v_h \right\rangle - \langle p_h^{\varepsilon, (k+1)}, \nabla \cdot v_h \rangle = dg\beta \langle \theta_h^{\varepsilon, (k+1)}, v_h \rangle + dg\beta \langle \theta_{in}, v_h \rangle + \langle dg\beta, v_h \rangle \quad \forall v_h \in V_h \end{aligned}$$

$$\varepsilon \frac{\langle p_h^{\varepsilon, (k+1)}, q_h \rangle - \langle p_h^{\varepsilon, (k)}, q_h \rangle}{t_{k+1} - t_k} + \langle \nabla \cdot u_h^{\varepsilon, (k+1)}, q_h \rangle = 0 \quad q_h \in Q_h$$

$$\frac{\langle \theta_h^{\varepsilon, (k+1)}, w_h \rangle - \langle \theta_h^{\varepsilon, (k)}, w_h \rangle}{t_{k+1} - t_k} + \lambda \langle \nabla \theta_h^{\varepsilon, (k+1)}, \nabla w_h \rangle + \langle u_h^{\varepsilon, (k)} (\nabla \theta_h^{\varepsilon, (k+1)}), w_h \rangle = \langle f, w_h \rangle$$

Nous implémentons le schéma ci-dessus dans FreeFem++ [21]. Nous avons effectué plusieurs tests à différent pas de temps pour nous assurer d'atteindre une solution stable. Les résultats obtenus sont illustrés par les figures suivantes :

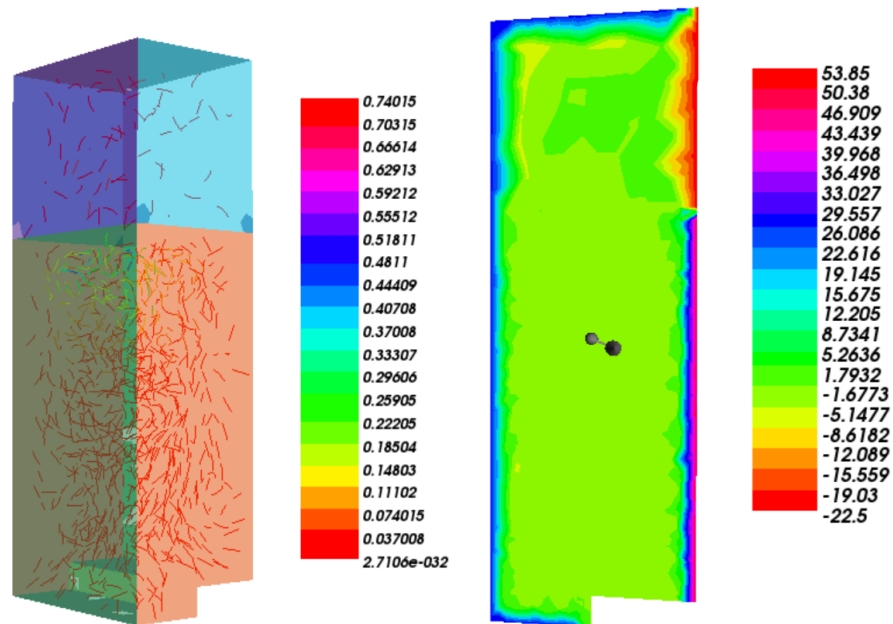


Figure 2: Champs de vitesse et de température dans un réfrigérateur sans étagères.

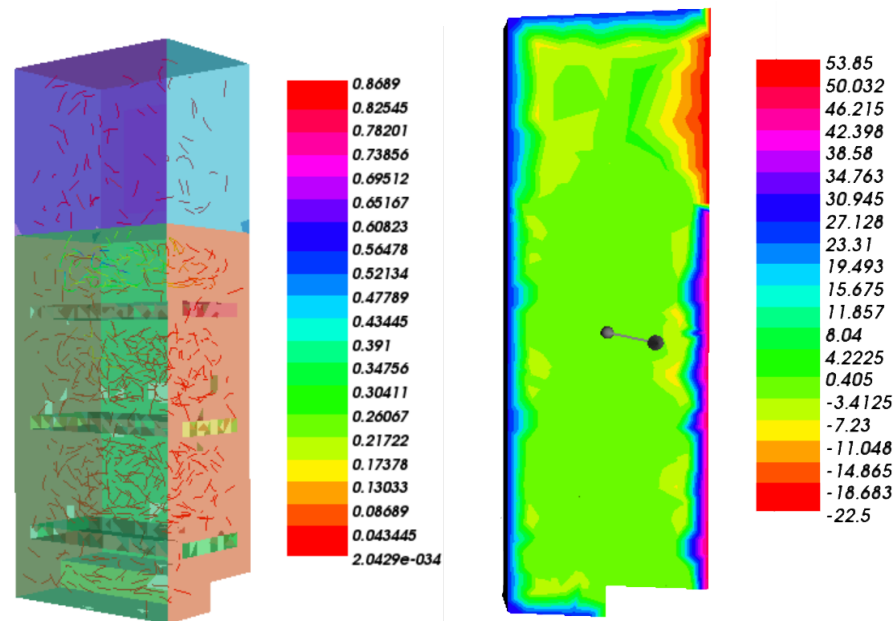


Figure 3: Champs de vitesse et de température dans un réfrigérateur avec étagères.

Dans le troisième chapitre, nous analysons l'approximation par éléments finis des problèmes de contrôle parabolique avec un second membre singulier régi par la convection-diffusion linéaire couplée avec les équations des eaux peu profondes en utilisant la méthode des caractéristiques. Les principales difficultés du problème proviennent de la singularité du second membre dans le système transport-diffusion. Nous développons une analyse théorique du problème. Des estimations d'erreur sont obtenues pour le problème original, adjoint ainsi que le problème de contrôle.

Nous nous intéressons au problème de la pollution marine dont l'activité humaine est directement responsable. Le rejet des eaux usées, les catastrophes industrielles et écologiques se traduisent par la contamination et la diffusion de produits chimiques, des métaux lourds ou d'une importante quantité de produits pétroliers. Ces polluants impactent à la fois les milieux aquatiques et la santé humaine. Ces dernières années, beaucoup de moyens sont donnés pour la préservation et la protection des écosystèmes marins et côtiers. La diminution de la diffusion des polluants provenant des substances chimiques toxiques, ou des rejets d'eaux usées est un vrai défi scientifique et technique. La pollution côtière est généralement contrôlée en traitant les contaminants à la source ou dans les stations d'épuration par des méthodes de traitement des eaux usées afin de réduire leur concentration.

Là encore, le problème de contrôle optimal est régi par des équations de convection-diffusion. Récemment, des recherches approfondies ont été menées sur divers aspects théoriques de ce problème. Boulakia et *al* [33] ont travaillé sur les équations de réaction-diffusion où le terme de réaction est donnée par une fonction cubique dont le but de reconstruire numériquement la partie indépendante du temps de terme source à partir la solution mesurée. Ningning et Zhaojie [34] ont étudié un schéma d'approximation de Galerkin de stabilisation du bord, cette méthode utilise la stabilisation par les moindre carrés des sauts de gradient à travers des bords des éléments. Cette méthode a été proposée par Douglas et Dupont [*"Computing Methods in Applied Sciences, Springer-Verlag, Berlin, 1976"*]. Becker et Vexler [35] ont exploité la discrétisation du problème de contrôle optimal à l'aide de la méthodes des éléments finis stabilisés et montré que ce schéma de stabilisation converge vers des solutions approchées améliorées même sur des maillages grossiers. Luo et Lu [36] ont utilisé la méthode des éléments finis mixtes Petrov/Galerkin avec des moindres carrés. Pour les problèmes de contrôle optimal elliptiques, Casas et Tröltzsch [37] ont adapté, à la discrétisation des fonctions de contrôle, des fonctions constantes par morceaux ou des fonctions linéaires par morceaux. En revanche, pour l'analyse d'erreur à priori, plusieurs chercheurs ont utilisé une discrétisation pure par éléments finis pour des problèmes de contrôle optimal avec des contraintes d'inégalités ponctuelles. Arada, Casas et Tröltzsch [38] ont étudié l'approximation numérique des équations aux dérivées partielles elliptiques semi-linéaire dont le résultat est l'estimation des erreurs en norme infinie pour les contrôles optimaux. Falk [39] a présenté un schéma d'approximation à la fois du problème de contrôle optimal et de la solution de l'équation du contrôle. Fu [40] a analysé le problème de contrôle par une approximation de type éléments finis en utilisant la méthode des caractéristiques où les variables d'états et adjointes sont discrétisées par des fonctions continues linéaires par morceaux, et il a en plus montré l'efficacité de la méthode pour les estimations d'erreurs. Fu et Rui [41] ont appliqué la méthode des caractéristiques aux problèmes de contrôle optimal quadratique. Dans tout ces travaux, les composantes de la vitesse dans le terme de convection apparaissent comme des données constantes.

Le modèle mathématique décrivant les phénomènes physiques dans le cas du transport d'un polluant et de l'évolution de sa concentration, que nous étudions est un modèle de convection-diffusion avec terme source mesure

$$\begin{cases} \partial_t \phi - \mu \Delta \phi + (\mathcal{U} \cdot \nabla) \phi + \sigma \phi = g + \sum_{i=1}^N f_i(t) \delta(r - r_i) & \text{dans } \Omega \times (0, T), \\ \phi(x, t) = 0 & \partial\Omega \times (0, T), \\ \phi(x, 0) = \phi_0(x) & \text{dans } \Omega. \end{cases} \quad (0.4)$$

Et son système rétrograde donné par

$$\begin{cases} -\partial_t \psi - \mu \Delta \psi - (\mathcal{U} \cdot \nabla) \psi + \sigma \psi = \phi - \phi_d & \Omega \times (0, T), \\ \psi(x, T) = 0 & \partial\Omega \times (0, T), \\ \psi(x, t) = 0 & \Omega, \end{cases} \quad (0.5)$$

avec $\mathcal{U} = (u, v)$ est la vitesse du propagation du polluant, ϕ est sa concentration, μ est le coefficient de diffusion, g représente l'accélération de la pesanteur, f le débit de la source et δ est la masse de Dirac. La vitesse du déplacement du contaminant est liée à la vitesse de déplacement des masses d'eau c'est à dire la vitesse de propagation des vagues. Pour calculer cette vitesse, nous utilisons le modèle des équations de Barré de Saint-Venant aussi appelé; "équations en eaux peu profondes" (Shallow Water Model) suivant :

$$\begin{cases} \partial_t u - \mu' \Delta u + (u \cdot \nabla) u & = -g \partial_x H & \text{dans } \Omega \times (0, T), \\ \partial_t v - \mu' \Delta v + (v \cdot \nabla) v & = -g \partial_y H & \text{dans } \Omega \times (0, T), \\ \partial_t H + \partial_x (Hu) + \partial_y (Hv) & = 0 & \text{dans } \Omega \times (0, T), \\ u(x, 0) & = u_0 & \text{dans } \Omega, \\ v(x, 0) & = v_0 & \text{dans } \Omega. \end{cases} \quad (0.6)$$

avec g représente le terme lié aux effets gravitationnels et H la hauteur d'eau par rapport à la surface libre.

Nous nous intéressons à trouver le débit massique optimal à la source $f = (f_1, f_2, \dots, f_n)$. Le problème du contrôle optimal consiste alors à minimiser la concentration du polluant ϕ relative à une concentration cible ϕ_d donnée par la fonction objective suivante :

$$J_2(f) = \int_0^T \left(\frac{1}{2} \|\phi(f) - \phi_d\|^2 + \frac{\alpha}{2} \|f\|^2 \right) dt. \quad (0.7)$$

Les formulations faibles et la condition d'optimalité prennent alors la forme :

$$\begin{cases} (\partial_t \phi, w) + (\mathcal{U} \cdot \nabla \phi, w) + a(\phi, w) + (\sigma \phi, w) = (g + \mathcal{B}u, w), & \forall w \in V = H_0^1(\Omega), \\ \phi(x, 0) = \phi_0(x), \end{cases} \quad (0.8)$$

$$\begin{cases} -(\partial_t \psi, q) - (\mathcal{U} \cdot \nabla \psi, q) + a(q, \psi) + (\sigma \psi, q) = (\phi - \phi_d, w), & \forall q \in V = H_0^1(\Omega), \\ \psi(x, 0) = \psi_0(x), \end{cases} \quad (0.9)$$

avec la condition d'optimalité

$$\int_0^T (\alpha f + \mathcal{B}^* \psi, f - u)_U dt \geq 0 \quad \forall f \in K \subset X = L^2([0, T]; U). \quad (0.10)$$

Les principales difficultés du problème du point de vue théorique sont dues à la singularité du second membre ce qui nous amène à travailler dans des espaces fonctionnels réguliers afin d'obtenir l'expression du système adjoint. L'approximation numérique du problème de transport se fait en utilisant la méthode des caractéristiques [17]. Le but de cette méthode est de transformer l'opérateur de convection en dérivée totale en utilisant une formulation Lagrangienne. Nous considérons l'équation des caractéristiques

$$\begin{cases} \frac{dX}{d\tau}(x, s; \tau) = \phi(X(x, s; \tau), \tau), \\ X(x, s; \tau) = x. \end{cases} \quad (0.11)$$

pour un temps final T , nous introduisons un pas du temps $\Delta t = \frac{T}{N}$. On note $t_n = n\Delta t$, pour $n = 0, \dots, N$ et on pose $\phi^n(x) = \phi(x, t^n)$. En utilisant l'approximation suivante de la dérivée totale le long des courbes caractéristiques, nous approximations $\frac{D\phi}{Dt}$ en temps $t = t_{n+1}$ par

$$\frac{D\phi}{Dt}(x, t) \approx \frac{\phi(x, t^{n+1}) - \phi(X^n(x), t^n)}{\Delta t}. \quad (0.12)$$

Nous construisons ensuite une approximation numérique s'appuyant sur un schéma d'Euler. Considérons (Φ_h^i, F_h^i) comme l'unique solution du problème discret (0.8) et $(\Phi_h^i, F_h^i) \in V^h \times K^h$ est la solution si et seulement s'il y a un état adjoint $\Psi_h^{i-1} \in V^h$, tel que $(\Phi_h^i, \Psi_h^{i-1}, F_h^i) \in V^h \times V^h \times K^h$, $i = \{1, 2, \dots, N^*\}$, satisfaisant la condition d'optimalité suivante :

$$\begin{cases} \left(\frac{\Phi_h^i - \bar{\Phi}_h^{i-1}}{\tau_i}, w_h \right) + a(\Phi_h^i, w_h) + (\sigma \Phi_h^i, w_h) = (g^i + \mathcal{B}F_h^i, w_h), & \forall w_h \in V^h \subset V, \\ \Phi_h^i(x, 0) = \phi_0^h(x), & x \in \Omega, \end{cases} \quad (0.13)$$

$$\begin{cases} \left(\frac{\Psi_h^{i-1} - \bar{\Psi}_h^i \cdot J^i}{\tau_i}, q_h \right) + a(q_h, \Psi_h^{i-1}) + (\sigma \Psi_h^i, q_h) = (\Psi_h^i - \phi_d^i, q_h), & \forall q_h \in V^h \subset V, \\ \Phi_h^{N^*}(x, T) = 0, & x \in \Omega, \end{cases} \quad (0.14)$$

$$(\alpha F_h^i + \mathcal{B}\Psi_h^{i-1}, f_h - F_h^i)_U dt \geq 0 \quad \forall f_h \in K^h \cap U^h, \quad (0.15)$$

avec $\bar{\Psi}_h^i = \Psi_h^i(\bar{x})$

$$x = G(\bar{x}, \tau_i; \tau_{i-1}),$$

avec $J^i = \det DG(\bar{x}, \tau_i; \tau_{i-1})^{-1}$ le déterminant de la matrice transformation Jacobienne à partir de G à x .

L'analyse d'erreur dans le cas des problèmes du contrôle optimal a pris une grande considération dans le cas de la résolution des systèmes paraboliques et elliptiques [18; 17; 19; 20]. Pour obtenir des estimations d'erreurs à priori pour les schémas proposés en (0.13) et (0.15), nous introduisons les problèmes auxiliaires :

Trouver le couple $(\Phi_h^i(f), \Psi_h^i(f)) \in V^h \times V^h$, pour $i = 1, 2, \dots, N^*$ satisfaisant :

$$\begin{cases} \left(\frac{\Phi_h^i(f) - \bar{\Phi}_h^{i-1}(f)}{\tau_i}, w_h \right) + a(\Phi_h^i(f), w_h) + (\sigma \Phi_h^i(f), w_h) = (g^i + \mathcal{B}f_h^i, w_h), & \forall w_h \in V^h \\ \Phi_h^i(u)(x, 0) = \phi_0^h(x), & x \in \Omega. \end{cases} \quad (0.16)$$

$$\begin{cases} \left(\frac{\Psi_h^{i-1}(f) - \bar{\Psi}_h^{i-1}(f) \cdot J^i}{\tau_i}, q_h \right) + a(q_h, \Psi_h^{i-1}(f)) + (\sigma \Psi_h^i(f), q_h) = (\Psi_h^i(u) - \phi_d^i, q_h), & \forall q_h \in V^h \subset V \\ \Phi_h^{N^*}(f)(x, T) = 0, & x \in \Omega. \end{cases} \quad (0.17)$$

Nous avons le résultat de convergence avec estimation d'erreurs suivant :

Théorème 0.0.5. *Considérons (ϕ, ψ, f) et (Φ_h, Ψ_h, F_h) les solutions des équations ((0.8) – (0.10)) et ((0.13) – (0.15)) respectivement. Alors, on a l'estimation d'erreur suivante:*

$$\begin{aligned} & \sqrt{\alpha} \|f - F_h\|_{L^2([0, T]; \mathbb{R}^m)} + \|\phi - \Phi_h\|_{L^\infty([0, T], H_0^1(\Omega))} + \|\psi - \Psi_h\|_{L^\infty([0, T], H_0^1(\Omega))} \\ & \leq Ch_U (\|\psi\|_{L^2([0, T]; H^2(\Omega))} + \|f\|_{L^2([0, T]; L^2(\Omega_{adm}))}) + C_2 h \sum_{v=\phi, \psi} \|v\|_{H^1([0, T]; H^2(\Omega))} \\ & + C_2 \tau \left(\sum_{v=\phi, \psi} \left\| \frac{\partial^2 v}{\partial t^2} \right\|_{L^2([0, T]; L^2(\Omega))} + \sum_{v=\phi, \phi_d} \left\| \frac{\partial^2 v}{\partial t^2} \right\|_{L^2([0, T]; L^2(\Omega))} + \|\psi\|_{L^2([0, T]; L^2(\Omega))} \right). \end{aligned}$$

Nous définissons la fonction coût à minimiser comme suit:

$$J_2(f) = \frac{1}{2} \int_0^t \int_\Omega (\phi(t, x) - \phi_d(t, x))^2 dx dt + \sum_{j=1}^n \int_0^t \frac{\alpha_j}{2} (f_j(t))^2 dt. \quad (0.18)$$

avec $\phi_d \in L^2(\Omega)$. Le vecteur de contrôle $f(t) = (f_j(t))_{j=1, \dots, n}$ appartient à un ensemble de contrôle admissible K . La gestion optimale du système de déuration consiste alors à résoudre

le problème d'optimisation suivant : Trouver $f \in L^2(\Omega)$ tel que

$$\min_{f \in K} J_2(f). \quad (0.19)$$

Le problème de contrôle (0.19) admet une solution unique $f \in K$. Nous donnons l'expression du gradient de la fonction coût (0.18) pour une méthode de descente :

$$\nabla J_2(f)_j = \alpha_j f_j(t) + \psi(t, r_j) \quad \text{avec } j = 1, \dots, n. \quad (0.20)$$

Le processus de contrôle optimal du débit à la source se base sur une méthode itérative en utilisant la méthode du gradient de descente à pas fixe. Les résultats obtenus sont illustrés ci-après

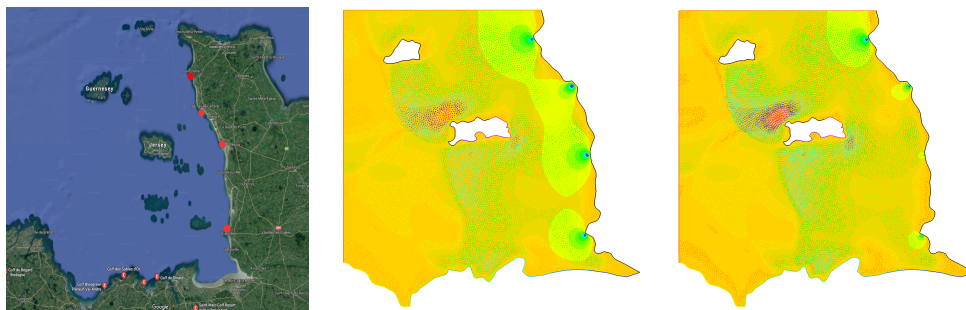


Figure 4: Contrôle optimal de la concentration du polluant dans le golf Normand-Breton.

Afin de valider les estimations d'erreurs développées précédemment, nous évaluons l'erreur pour une séquence de discrétisations avec différents maillages et pas de temps fixes. Nous avons réalisé plusieurs tests numériques reposant sur un algorithme de type gradient. Pour le calcul des erreurs en norme L^2 entre la solution exacte et la solution approchée, on a posé :

$$E(\phi, h_n) = | \phi_h(h_n) - \phi_{ex}(h_n) |_{L^2}$$

$$E(\psi, h_n) = | \psi_h(h_n) - \psi_{ex}(h_n) |_{L^2}$$

$$E(f, h_n) = | f_h(h_n) - f_{ex}(h_n) |_{L^2}$$

et la convergence en espace

$$rate(\phi, h_n) = \frac{\log(E(\phi, h_{n-1})/E(\phi, h_n))}{\log(h_{n-1}/h_n)} \quad (0.21)$$

DDL	$\ \phi - \phi_{ex} \ _{L^2(0,T)}$	Ratio	$\ f - f_{ex} \ _{L^2(0,T)}$	Ratio	$\ \psi - \psi_{ex} \ _{L^2(0,T)}$	Ratio
27	0.0522761	-	0.2429090	-	0.1976700	-
94	0.0350302	0.577554	0.1664970	0.544919	0.1307900	0.595843
332	0.0197525	0.826568	0.0945548	0.816273	0.0733844	0.833702
1280	0.0104595	0.91722	0.0502398	0.912321	0.0386895	0.923532
4963	0.00537356	0.960863	0.0261879	0.939929	0.0198441	0.963229

Table 1: Norme L^2 de l'erreur et le ratio de convergence.

Dans le quatrième chapitre, nous avons exploré l'optimisation des structures hydrauliques de type passes à poissons. Ces structures jouent un rôle important d'un pont de passage entre le milieu marin et les rivières, favorisant et facilitant la migration des espèces aquatiques des eaux salées vers les eaux douces.

La réalisation et l'achèvement de ce chapitre a été le fruit d'un travail collectif avec la collaboration de M. Louaked, M. Kadiri et M. Mechkour où nous avons travaillé sur l'application des équations de Navier-Stokes Forchheimer stationnaire par pénalisation de la contrainte d'incompressibilité dans le but d'optimiser l'effet tourbillonnaire de l'écoulement d'un fluide dans une structure hydraulique de type passe à poissons. Ce travail a été rapporté dans la thèse de M. Kadiri [61].

Dans la littérature, de nombreux types de passes à poissons existent, celle de Denil [60], ou bien à fentes verticales ("*Vertical slot Fishway*"). Dans notre étude nous avons opté pour ce dernier type.

Pour améliorer la fiabilité et l'efficacité de la passe à poissons, le fond des bassins doit toujours avoir une surface rugueuse, et ceci afin de réduire la vitesse d'écoulement à proximité du fond et de faciliter ainsi la remonté des petits poissons. Une surface rugueuse peut être produite en ajoutant des pierres aléatoirement dans le béton avant qu'il ne durcisse. Le comportement de l'écoulement ne peut être représenté avec précision que si la structure des milieux poreux est correctement décrite. Le passage du régime d'écoulement de Darcy au régime de Forchheimer peut se justifier par la nécessité de prendre en compte le comportement du fluide à travers les milieux poreux. Pour clarifier la signification physique de la non-linéarité dans l'équation de Forchheimer, il serait utile de comprendre la dérivation de l'équation de Forchheimer à partir du modèle Navier-Stokes en utilisant les principes de base sous-jacents à la théorie de l'hydrodynamique. Compte tenu des différentes opinions sur l'origine de la non-linéarité, il est maintenant admis que le terme quadratique conduisant à la séparation de la couche limite et à la formation de sillage derrière des obstacles solides. Plusieurs travaux sont disponibles dans le cas des modèles des milieux poreux [57; 58; 59].

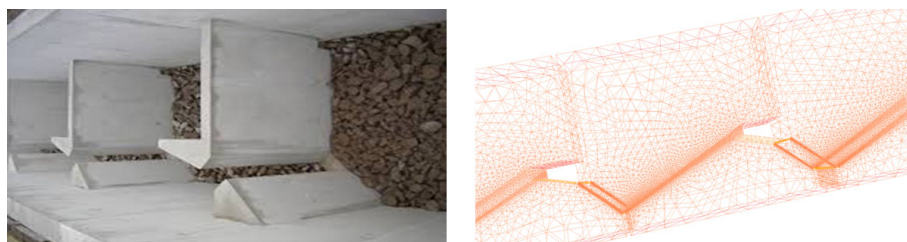


Figure 5: Exemple d'une passe à poissons à fentes obliques et son maillage.

Nous nous intéressons aux équations de Navier-Stokes Forchheimer stationnaire suivantes :

$$\begin{cases} -\nu\Delta u + (u.\nabla)u + a |u|^\alpha u + \nabla p = f & \text{dans } \Omega, \\ \nabla.u = 0 & \text{dans } \Omega, \\ u = 0 & \text{sur } \Gamma_0, \\ u = g & \text{sur } \Gamma_1, \\ \nu \frac{\partial u}{\partial n} - p\mathbf{n} = 0 & \text{sur } \Gamma_2. \end{cases} \quad (0.22)$$

avec u est la vitesse, p est la pression, a est le coefficient de Forchheimer, α est un nombre naturel positif, g est la force de gravité et f est un terme source donné. Le système pénalisé de (0.22) est le suivant :

$$\begin{cases} -\nu\Delta u^\varepsilon + (u^\varepsilon.\nabla)u^\varepsilon + \frac{1}{2}(\nabla.u^\varepsilon)u^\varepsilon + a |u^\varepsilon|^\alpha u^\varepsilon + \nabla p^\varepsilon = f & \text{dans } \Omega, \\ \nabla.u^\varepsilon + \varepsilon p^\varepsilon = 0 & \text{dans } \Omega, \\ u^\varepsilon = 0 & \text{sur } \Gamma_0, \\ u^\varepsilon = g & \text{sur } \Gamma_1, \\ \nu \frac{\partial u^\varepsilon}{\partial n} - p^\varepsilon \mathbf{n} = 0 & \text{sur } \Gamma_2. \end{cases} \quad (0.23)$$

Concernant le modèle non perturbé, nous montrons l'existence et l'unicité d'une solution faible du problème (0.22). L'existence d'une solution faible du problème pénalisé est prouvée en utilisant la méthode de Féado-Galerkin. Nous utilisons les espaces de Sobolev suivants : $X = (H_0^1(\Omega))^d$, $Y = L^2(\Omega)$

Théorème 0.0.6. *Soit Ω un domaine borné dans \mathbb{R}^d ($d = 2, 3$), $f \in X'$ est une fonction donnée. Alors le problème perturbé (0.23) admet une solution qui satisfait*

$$\frac{\nu}{2} \|\nabla u^\varepsilon\|^2 + a \|u^\varepsilon\|_{L^{\alpha+2}}^{\alpha+2} + \varepsilon \|p^\varepsilon\|^2 \leq \frac{1}{2\nu} \|f\|_{X'}^2$$

Nous établissons la convergence de la solution (vitesse en norme H^1 , pression en norme L^2) du système perturbé vers la solution du problème initial.

Théorème 0.0.7. *Soient $(u^\varepsilon, p^\varepsilon)$ la solution du problème perturbé (0.23) et (u, p) la solution dans $X \times Y/\mathbb{R}$ du problème (0.22). Alors, on a*

$$(p^\varepsilon) \in Y \quad \text{est borné uniformément par } \varepsilon,$$

et pour $\varepsilon \rightarrow 0$.

$$u^\varepsilon \rightarrow u \quad \text{dans } X,$$

et

$$p^\varepsilon \rightarrow \tilde{p} \quad \text{dans } Y$$

avec \tilde{p} est la projection orthogonale dans Y de p sur $(\text{Ker} B^*)^\perp$. Nous avons les estimations

suivantes

$$\|u^\varepsilon - u\|_1 + \|p^\varepsilon - \tilde{p}\| \leq C\varepsilon,$$

avec C est une constante positive indépendante de ε , où

$$\text{Ker}B^* = \{q \in Y \mid (q, \nabla \cdot v) = 0 \text{ pour tout } v \in X\} = \{\text{constants}\}.$$

Après l'étude des modèles mathématiques, nous analysons le problème du contrôle optimal. Le problème d'optimisation de forme consiste à minimiser la fonction coût suivante

$$J_3(\Omega) = \frac{1}{2} \int_{\Omega} |u^\varepsilon - u_d|^2 dx + \frac{\sigma}{2} \int_{\Omega} |\text{curl}(u^\varepsilon)|^2 dx. \quad (0.24)$$

avec u^ε est la solution du problème (0.23), u_d est la vitesse cible et σ est le paramètre de vorticit .

Nous donnons l'expression du syst me adjoint associ  au probl me perturb  (0.23)

$$\begin{cases} -\nu \Delta v + (\nabla u^\varepsilon)^T \cdot v - (u^\varepsilon \cdot \nabla) v - \frac{1}{2} \nabla (u^\varepsilon \cdot v) + \frac{1}{2} (\nabla \cdot u^\varepsilon) v + a |u^\varepsilon|^{\alpha-2} (|u^\varepsilon|^2 v \\ + \alpha (u^\varepsilon \cdot v) u^\varepsilon) + \nabla q = (u^\varepsilon - u_d) - \sigma \text{curl}(\text{curl}(u^\varepsilon)) & \text{dans } \Omega, \\ \nabla \cdot v + \varepsilon q = 0 & \text{dans } \Omega, \\ v = 0 & \text{sur } \Gamma_0 \cup \Gamma_1, \\ \nu \frac{\partial v}{\partial n} + 2(u^\varepsilon \cdot n) v - n q = \sigma \text{curl}(u^\varepsilon) \cdot \tau & \text{sur } \Gamma_2. \end{cases} \quad (0.25)$$

Ensuite nous calculons le gradient de forme de la fonction co t en fonction des variables d' tat $(u^\varepsilon, p^\varepsilon)$ et les variables adjointes (v, q)

$$\nabla J_3 = \left[\frac{1}{2} |u^\varepsilon - u_d|^2 + \frac{\sigma}{2} |\text{curl}(u^\varepsilon)|^2 + \frac{\partial u^\varepsilon}{\partial n} \cdot \left(2\nu \frac{\partial v}{\partial n} - \sigma \text{curl}(u^\varepsilon) \wedge n \right) \right] n. \quad (0.26)$$

Nous nous focalisons ensuite sur l'approximation du probl me perturb  par la m thode des  l ments finis. Nous proposons une discr tisation du probl me perturb 

Trouver $u_h^\varepsilon \in X^h$ tel que

$$\begin{aligned} \nu (\nabla u_h^\varepsilon, \nabla v) + ((u_h^\varepsilon \cdot \nabla) u_h^\varepsilon, v_h) &+ \frac{1}{2} (\nabla \cdot u_h^\varepsilon, u_h^\varepsilon \cdot v_h) + a (|u_h^\varepsilon|^\alpha u_h^\varepsilon, v_h) \\ &+ \frac{1}{\varepsilon} I((\nabla \cdot u_h^\varepsilon)(\nabla \cdot v_h)) = (f, v_h) \text{ pour tout } v_h \in X^h. \end{aligned} \quad (0.27)$$

De mani re analogue au probl me continu, nous d montrons l'existence de la solution du probl me discret (0.27). Ensuite, nous  tablissons une estimation d'erreur en terme de la norme H^1 et L^2 pour la vitesse et la pression respectivement.

Th or me 0.0.8. Soient $(u, p) \in X \times Y$ solution du probl me (0.22) et $(u_h^\varepsilon, p_h^\varepsilon)$ d finie par

(0.27). Alors

$$\begin{aligned} \|u - u_h^\varepsilon\|_1 \leq & \left(\frac{3}{r} - 1 + \frac{a}{\nu r} C_1 \right) \left(1 + \frac{C}{\beta_h} \right) \inf_{v_h \in X^h} \|u - v_h\|_1 \\ & + \frac{C_2}{\nu r} \inf_{q_h \in Y^h} \|p - q_h\| + \frac{C_3}{\beta_h} \varepsilon \|p_h\| \end{aligned}$$

et

$$\begin{aligned} \|p - p_h^\varepsilon\|_{Z^h} \leq & \frac{\nu(3-2r) + aC_1}{\beta_h} \left(\frac{3}{r} - 1 + \frac{a}{\nu r} C_2 \right) \left(1 + \frac{C_3}{\beta_h} \right) \inf_{v_h \in X^h} \|u - v_h\|_1 \\ & + \left(1 + \frac{C_4}{\beta_h} \left(\frac{3}{r} - 1 + \frac{a}{\nu r} C_1 \right) \right) \inf_{q_h \in Y^h} \|p - q_h\| + \frac{C''}{\beta_h^2} \varepsilon \|p_h\| \end{aligned}$$

Finalement, pour résoudre le problème d'optimisation et minimiser la fonction objective, nous adoptons une technique de type gradient projeté. Nous appliquons notre algorithme sur des structures hydrauliques de type fentes verticales et obliques. Les résultats obtenus sont présentés par les figures suivantes :

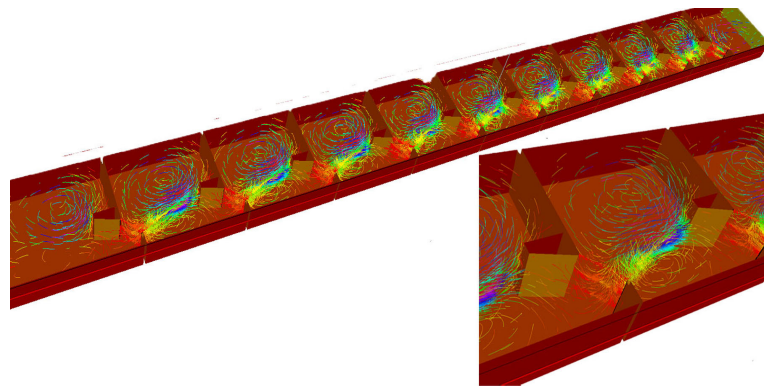


Figure 6: Vitesse non optimale pour dix bassins.

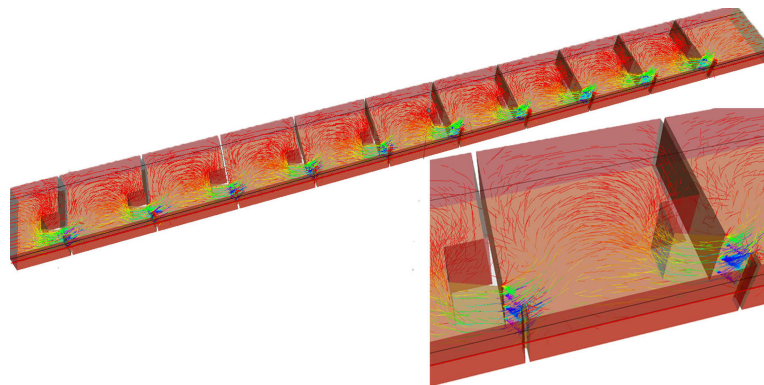


Figure 7: Vitesse optimale pour dix bassins.

Dans le chapitre 5, nous proposons une extension des méthodes d'optimisation de forme proposée récemment par Dapogny et *al* [52] en utilisant le modèle Navier-Stokes Forchheimer à faible nombre de Reynolds. Dans un premier temps, nous donnons les résultats d'existence et d'unicité de la solution de ce système. Ensuite nous construisons le problème d'optimisation de forme en se basant sur un problème adjoint. Nous adoptons une résolution numérique en combinant la méthode des éléments finis et celle d'optimisation de forme.

Il existe une littérature abondante concernant les différentes méthodes d'optimisation de forme adaptées aux problèmes de mécanique des fluides. Parmi elles, on dénombre des méthodes dites paramétriques, géométriques et topologiques. Concernant les méthodes topologiques, Allaire, Dapogny et Frey [52] ont présenté une méthode d'optimisation géométrique et topologique qui s'appuie sur deux façons complémentaires de présenter des formes qui sont maillées exactement afin d'en évaluer les performances par éléments finis et à l'aide d'une fonction de lignes de niveau pour les déformer suivant le gradient de forme. Jouve [50] a travaillé sur l'optimisation topologique des problèmes de conception optimale en élasticité. Osher et Sethian [53] ont prouvé que la méthode de Level Set est un outil très polyvalent dans le cadre de l'optimisation de structures. Choi et Kim [54] ont développé des techniques d'optimisation couplées aux équations de Navier-Stokes tri-dimensionnelles dans l'industrie automobile. Dapogny et *al* [56] ont proposé une méthode d'optimisation de forme, pour les équations de Navier-Stokes stationnaire à faible nombre de Reynolds en utilisant une dérivée de forme de la fonction coût calculée via un Lagrangien augmenté. Nous nous sommes inspirés de ces travaux pour proposer une extension de la méthode aux équations de Navier-Stokes stationnaire couplées au terme linéaire Darcy et au terme non linéaire de Forchheimer. En guise de validation de l'extension proposée, nous avons choisi de reprendre le problème d'ingénierie des structures hydrauliques de type "passe à poisson". Nous nous intéressons à l'optimisation topologique d'une structure hydraulique de type passe à poissons.

Dans la conception d'une passe à poissons, l'objectif principal est de réduire les effets tourbillonnaires dans les bassins. Cette réduction permet aux poissons de minimiser leurs propres efforts pendant la traversée, facilitant ainsi le mouvement d'un bassin à l'autre. Le problème d'optimisation de forme consiste à trouver une forme optimale dans un ensemble admissible en introduisant la fonction objective suivante :

$$J_4(\Omega) = \frac{1}{2} \int_{\Omega} |u - u_{ref}|^2 dx + 2\nu \int_{\Omega} \|\mathbf{e}(u)\|^2 dx. \quad (0.28)$$

avec: u_{ref} la vitesse cible et \mathbf{e} est le tenseur de déformation donné par

$$\mathbf{e}(u) = \frac{1}{2}(\nabla u + {}^T \nabla u)$$

L'écoulement du fluide dans la passe à poissons est décrit par les équations de Navier-Stokes

Forchheimer stationnaire données par le système suivant

$$\begin{cases} -\nu\Delta u + (u.\nabla)u + \nabla p + au + b | u |^\alpha u = f & \text{dans } \Omega, \\ \operatorname{div}(u) = 0 & \text{dans } \Omega, \\ u = u_{in} & \text{sur } \Gamma_{in}, \\ u = 0 & \text{sur } \Gamma, \\ \sigma(u, p)n = 0 & \text{sur } \Gamma_{out}. \end{cases} \quad (0.29)$$

Dans un premier lieu, nous montrons l'existence et l'unicité d'une solution faible du problème (0.29) en utilisant la méthode de Faédo-Galerkin.

Pour cela, nous construisons une solution approchée, nous établissons des estimations a priori et nous vérifions la convergence dans l'espace $(H_0^1(\Omega))^d \cap L^{\alpha+2}$.

Le résultat d'existence de solution faible du système Navier-Stokes Forchheimer est donné par le théorème (0.0.9) suivant :

Théorème 0.0.9. *On considère Ω un domaine borné dans \mathbb{R}^d , ($d = 2, 3$), $f \in H^{-1}(\Omega)$. Si $u = 0$ sur $\partial\Omega$ et $0 \leq \alpha < 10$, il existe au moins une solution faible de (0.29) satisfaisant*

$$\frac{\nu}{2} \|\nabla u_m\|^2 + a \|u_m\|_{L^2}^2 + b \|u_m\|_{L^{\alpha+2}}^{\alpha+2} \leq c \|f\|_{H^{-1}}^2,$$

et

$$\|p\| \leq C \left[(\nu + c_1 + c_2 a) \|u\|_{H^1} + c_3 b \|u\|_{L^{2\alpha+2}}^{\alpha+1} - c_4 \|f\|_{H^{-1}} \right].$$

avec C, c_1, c_2, c_3 et c_4 sont des constantes positives et $\nu > 0$

L'unicité de la solution faible du système Navier-Stokes Forchheimer (0.29) est donnée par le théorème (0.0.10) suivant :

Théorème 0.0.10. *On considère Ω un domaine borné dans \mathbb{R}^d , ($d = 2, 3$) et localement Lipschitzien, $u = 0$ on $\partial\Omega$ et $f \in H^{-1}(\Omega)$. Les solutions de (0.29) existent pour tout nombre de Reynolds; cependant, si ν est assez grand et $\frac{2}{3} \leq \alpha \leq 4$, alors la solution faible du système Navier-Stokes Forchheimer (0.29) est unique.*

Le problème d'optimisation de forme consiste à trouver une forme optimale en minimisant la fonction objective.

$$\min_{\Omega \in Q_{ad}} J_4(\Omega) \quad \text{objet} \quad G(\Omega) = 0. \quad (0.30)$$

avec Q_{ad} est l'ensemble des domaine admissibles.

$$Q_{ad} = \left\{ \Omega \subset \mathbb{R}^d : \sum \Gamma_i \subset \partial\Omega \quad \text{est fixé, } \int_{\Omega} dx = \text{constante} \right\}.$$

Il existe plusieurs méthodes, stratégies ou techniques d'optimisation dans le contexte de la mécanique des fluides [22; 23; 24; 25; 26; 27; 28]. Nous construisons la fonction Lagrangienne par

l'introduction des variables adjointes (v, q) :

$$\mathcal{L}(\Omega, u, p, v, \pi) = J_4(\Omega) - F(\Omega, u, p, v, \pi), \quad (0.31)$$

avec

$$F(\Omega, u, p, v, \pi) = \int_{\Omega} [\nu \nabla u : \nabla v + (u \cdot \nabla)u \cdot v + au \cdot v + b |u|^\alpha u \cdot v - p \operatorname{div} v] dx - \int_{\Omega} \operatorname{div} u \pi dx$$

Alors la solution du problème d'optimisation de forme (0.30) est le minimum du problème suivant

$$\min_{\Omega \in Q_{ad}} \min_{(u,p) \in V_g(\Omega) \times M(\Omega)} \max_{(v,q) \in V_0(\Omega) \times M(\Omega)} \mathcal{L}(\Omega, u, p, v, \pi) \quad (0.32)$$

Le système adjoint établi est de la forme :

$$\begin{cases} -\nu \Delta v + (\nabla u)^T \cdot v - (u \cdot \nabla)v + av + b |u|^\alpha v + \alpha b |u|^{\alpha-2} (u \cdot v)u + \nabla \pi \\ = -(2\nu \Delta u + |u - u_{ref}|) & \text{dans } \Omega, \\ \operatorname{div}(v) = 0 & \text{dans } \Omega, \\ v = 0 & \text{sur } \Gamma_{in}, \\ v = 0 & \text{sur } \Gamma, \\ \sigma(v, \pi)n + (u \cdot n)v = 4\nu(u \cdot n) & \text{sur } \Gamma_{out}. \end{cases} \quad (0.33)$$

Nous adoptons un algorithme basé sur le Lagrangien augmenté pour obtenir la forme optimale de la structure hydraulique.

La résolution numérique par éléments finis repose sur le problème relaxé suivant :

$$\begin{cases} -\nu \Delta u^\varepsilon + (u^\varepsilon \cdot \nabla)u^\varepsilon + \nabla p^\varepsilon + au^\varepsilon + b |u^\varepsilon|^\alpha u^\varepsilon = 0 & \text{dans } \Omega, \\ \operatorname{div}(u^\varepsilon) + \varepsilon p^\varepsilon = 0 & \text{dans } \Omega, \\ u^\varepsilon = u_{in}^\varepsilon & \text{sur } \Gamma_{in}, \\ u^\varepsilon = 0 & \text{sur } \Gamma, \\ \sigma(u^\varepsilon, p^\varepsilon) \cdot n = 0 & \text{sur } \Gamma_{out}. \end{cases} \quad (0.34)$$

avec ε est un paramètre très petit de l'ordre $\varepsilon = 10^{-6}$ dans nos tests numériques.

Les espaces éléments finis utilisés sont :

$$U_h = \{w_1 \in [C(\Omega)]^n : w_1|_T \in [\mathbb{P}_2(T)]^n, \forall T \in \mathcal{T}_h, w_1 \cdot n = 0 \text{ on } \partial\Omega\},$$

$$X_h = \{w_2 \in [C(\Omega)]^n : w_2|_T \in [\mathbb{P}_2(T)]^n, \forall T \in \mathcal{T}_h, w_2 \cdot n = 0 \text{ on } \partial\Omega\},$$

$$M_h = \{q \in C(\Omega) : q|_T \in \mathbb{P}_1(T), \forall T \in \mathcal{T}_h\},$$

$$Q_h = \{\pi \in L^2(\Omega) : \pi|_T \in \mathbb{P}_1(T), \forall T \in \mathcal{T}_h\}.$$

Le problème approché est :

$$\left\{ \begin{array}{l} \text{Trouver } (u_h^\varepsilon, p_h^\varepsilon) \in U_h \times M_h \text{ tel que} \\ \int_{\Omega} \nu \nabla u_h^\varepsilon : \nabla w_1 dx + \int_{\Omega} (u^n \cdot \nabla) u_h^\varepsilon w_1 dx - \int_{\Omega} p_h^\varepsilon \nabla \cdot w_1 dx - \int_{\Omega} q \nabla \cdot u_h^\varepsilon w_1 dx \\ - \int_{\Omega} \varepsilon p_h^\varepsilon q w_1 dx + \int_{\Omega} a u_h^\varepsilon w_1 dx + \int_{\Omega} b |u_h^\varepsilon| u_h^\varepsilon w_1 dx = 0 \quad \forall w_1 \in U_h \quad \text{et} \quad \forall q \in M_h, \end{array} \right. \quad (0.35)$$

les variables adjointes (v_h, π_h) sont solutions de :

$$\left\{ \begin{array}{l} \text{Trouver } (v_h, \pi_h) \in X_h \times M_h \text{ tel que} \\ \int_{\Omega} \nu \nabla v_h : \nabla w_2 dx - \int_{\Omega} (u_h \cdot \nabla) v_h w_2 dx + \int_{\Omega} (\nabla u_h)^T \cdot v_h w_2 dx + \int_{\Omega} v_h w_2 dx \\ + \int_{\Omega} b |u_h|^\alpha v_h w_2 dx + \int_{\Omega} \alpha b |u_h|^{\alpha-2} (u_h \cdot v_h) u_h w_2 dx - \int_{\Omega} \pi_h \nabla \cdot w_2 dx \\ + \int_{\Omega} 2\nu \nabla u_h : \nabla w_2 dx + \int_{\Omega} |u_h - u_{ref}| w_2 dx + \int_{\Gamma_{out}} \sigma(v_h, \pi_h) \cdot n w_2 ds \\ + \int_{\Gamma_{out}} (u_h \cdot n) v_h w_2 ds - 4\nu (u_h) \cdot n w_2 = 0 \quad \forall w_2 \in X_h \quad \text{et} \quad \forall \pi \in Q_h. \end{array} \right. \quad (0.36)$$

L'algorithme de Lagrangien augmenté transforme le problème d'optimisation sous contrainte à une série de problème sans contrainte définie par

$$\inf_{\Omega \in Q_{ad}} \mathcal{L}(\Omega, \lambda^n, b^n),$$

qui prend la forme

$$\mathcal{L}(\Omega, \lambda, b) = J_4(\Omega) - \lambda G(\Omega) + \frac{b}{2} G(\Omega)^2.$$

avec les paramètres λ et b sont le multiplicateur de Lagrange et le coefficient de pénalisation respectivement. $G(\Omega)$ est une contrainte fonctionnelle liée au volume du domaine tel que $G(\Omega) = V(\Omega) - V_d$. La mise à jour des paramètres se fait par

$$\lambda^{n+1} = \lambda^n - b^n G(\Omega^n).$$

avec

$$b^{n+1} = \begin{cases} \delta b^n & \text{si } b < b_d, \\ b & \text{sinon.} \end{cases}$$

La combinaison de la méthode des éléments finis et celle d'optimisation implémentées sous FreeFem++ nous a fournis les résultats numériques suivants :

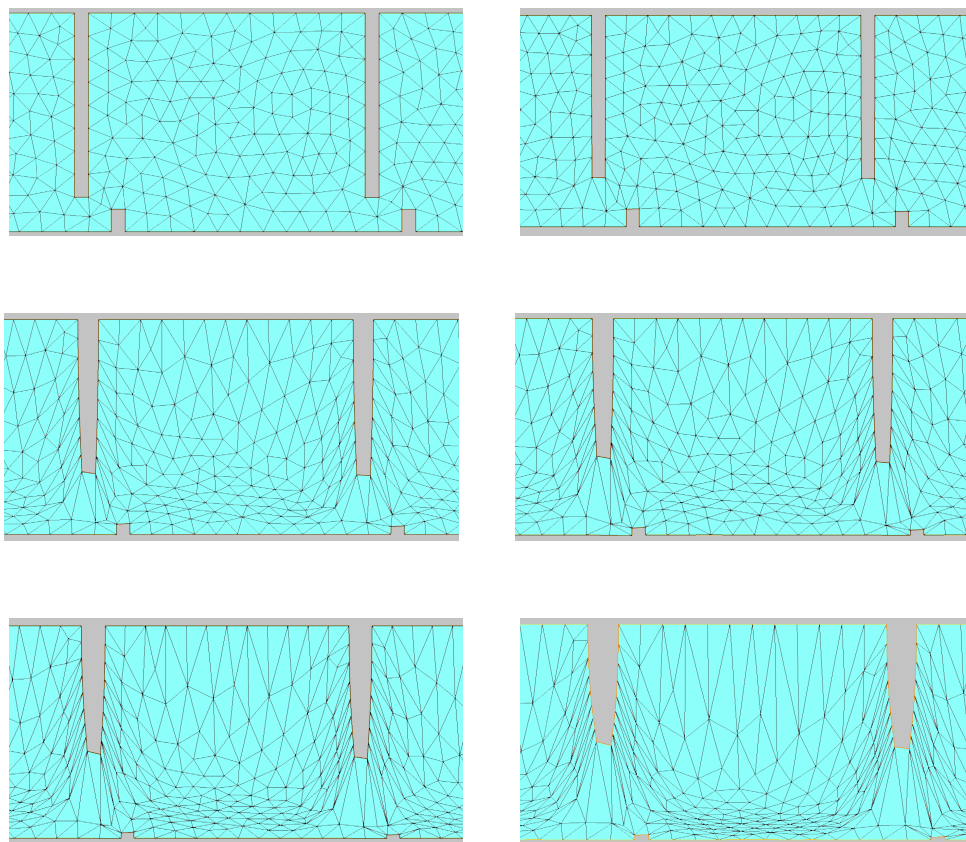


Figure 8: De gauche à droite, de haut en bas de la forme initiale à la forme optimale Ω^n de $n = 0$, à $n = 4000$ iterations.

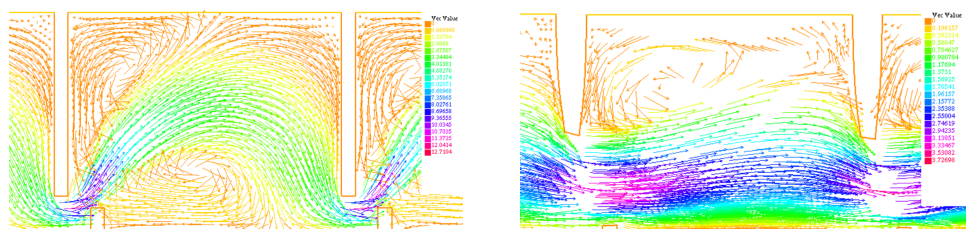


Figure 9: Champs de vitesses non optimal (gauche) et optimal (droite) dans le bassin central d'une passe à poisson.

Bibliography

- [1] L. Di Menza, Comment modéliser l'impact du réchauffement climatique sur un écosystème, Le journal du CNRS, Novembre 2017.
- [2] R. Temam, Sur l'approximation de la solution des équations de Navier-Stokes par la méthode des pas fractionnaires (i). *Archive for Rational Mechanics and Analysis*, 32(2) : 135 – 153, 1969.
- [3] A. J. Chorin, Numerical solution of the Navier-Stokes equations, *Mathematics of computation*, 22(104) : 745 – 762, 1968.
- [4] R. Courant, variational methods for the solution of problems of equilibrium and vibrations, *Bull. Amer. Math. Soc.*, 49(1943), *pp.*1 – 23.
- [5] M. Bercover, M. Engelman, A finite element for the numerical solution of viscous incompressible flows, *J. Comp. Phys.*, 30(1979), *pp.*181 – 201.
- [6] T. J. R. Hughes, W. T. Liu, A. J. Brooks, finite element analysis of incompressible viscous flows by the penalty function formulation, *J. Comp., Phys.*, 30(1979), *pp.* 1-60.
- [7] F. Brezzi AND J. P. Itkaranta, On the stabilization of finite element approximation of the Stokes problem, in *Efficient Solutions of Elliptic Systems, Notes on Numerical Fluid Mechanics*, Vol. 10, W. Hackbusch, ed., Viewig, 1984, *pp.*11 – 19.
- [8] M. Louaked, N. Seloula, and S. Trabelsi. Approximation of the unsteady Brinkman-Forchheimer equations by the pressure stabilization method. *Numerical Methods for Partial Differential Equations*, 33(6) : 1949 – 1965, 2017.
- [9] F. Brezzi and J. Douglas. Stabilized mixed methods for the Stokes problem. *Numerische Mathematik*, 53(1) : 225 – 235, 1988.
- [10] T. JR. Hughes, L. P. Franca and M. Balestra. A new finite element formulation for computational fluid dynamics: V. circumventing the Babuvska-Brezzi condition: a stable Petrov-Galerkin formulation of the Stokes problem accommodating equal-order interpolations. *Computer Methods in Applied Mechanics and Engineering*, 59(1) : 85 – 99, 1986.
- [11] J. Shen. On pressure stabilization method and projection method for unsteady Navier-Stokes equations. In *Advances in Computer Methods for Partial Differential Equations*. Citeseer, 1992.
- [12] A. J. Chorin: On the convergence of discrete approximations to the Navier-Stokes equations. *Mathematics of computation*, 23(106):341–353, 1969.
- [13] W. E and J. G. Liu. Projection method i: convergence and numerical boundary layers. *SIAM journal on numerical analysis*, 2006.

-
- [14] H. Morimoto: On the existence of the weak solutions of equation of natural convection, J. Fac. Sci. Univ. Tokyo Sect. IA Math. 36(1989), 87 – 102.
- [25] J. R. Canon and E. DiBenedetto, The initial value problem for the Boussinesq equations with data in L^p , In: Rautmann R. (eds) Approximation Methods for Navier-Stokes Problems. Lecture Notes in Mathematics, vol 771. Springer, Berlin, Heidelberg.
- [16] H. Morimoto, Non-stationary Boussinesq equations, J. Fac. Sci. Univ. Tokyo Sect. IA Math. 39(1992), 61 – 75.
- [17] O. Pironneau. : On the Transport-Diffusion Algorithm and Its Applications to the Navier-Stokes Equations. Numer. Math. 38, 309 – 332(1982).
- [18] W. Gong, M. Hinze, Z. Zhou, A priori error analysis for finite element approximation for the parabolic optimal control problems with pointwise control, Society for Industrial and applied Mathematics (2014), SIAM J. CONTROL OPTIM. Vol. 52, No. 11, pp. 97-119
- [19] D. Tiba : Lectures on the Optimal Control of Elliptic Equations. University of Jyvaskyla Press, Finland (1995)
- [20] P.G. Ciarlet : The Finite Element Method for Elliptic Problems. SIAM, Philadelphia (2002)
- [21] F. Hecht, New development in FreeFem++. J. Numer. Math. 20(2012), no. 3 – 4, 251 – 265.65Y15.
- [22] M. D. Gunzburger, Perspectives in flow control and optimization, vol. 5, Siam, 2003.
- [23] B. Mohammadi and O. Pironneau, Applied shape optimization for fluids, Oxford University Press, 2010.
- [24] M. P. Bendsoe and O. Sigmund, Topology optimization: theory, methods, and applications, Springer Science & Business Media, 2013.
- [25] N. Aage, T. H. Poulsen, A. Gersborg-Hansen, and O. Sigmund, Topology optimization of large scale stokes flow problems, Struct. Multidisc. Optim., 35 (2008), pp. 175-180.
- [26] T. Borrvall and J. Petersson, Topology optimization of fluids in Stokes flow, Int. J. Numer. Meth. Fluids, 41 (2003), pp. 77-107.
- [27] G. Pingen, A. Evgrafov, and K. Maute, Topology optimization of flow domains using the lattice Boltzmann method, Structural and Multidisciplinary Optimization, 34 (2007), pp. 507-524.
- [28] J. A. Sethian and A. Wiegmann, Structural Boundary Design via Level Set and Immersed Interface Methods, Journal of Computational Physics 163, 489-528 (2000).

- [29] M. Santos da Rocha, Marko A. Rojas-Medar and M. Drina Rojas-Medar, On the Existence and Uniqueness of the Stationary Solution to Equations of Natural Convection with Boundary Data in L^2 , *Mathematical, Physical and Engineering Sciences*, Mar. 8, 2003, Vol. 459, No. 2031(Mar.8, 2003), pp.609 – 621.
- [30] K. Ōeda, On the initial value problem for heat convection equation Boussinesq approximation in time-dependent domain, *Proc. Japan Acad., Ser. A*, 64(1988), 143 – 146.
- [31] K. Ōeda, Weak and strong solutions of the heat convection equations in region with moving boundaries, *J. Fac. Sci. Univ. Tokyo, sect., IA*, 36(1989), 491 – 536.
- [32] C. Foias, O. Manley, R. Temam, Attractors for the Bernard problem: existence and physical bounds on their fractal dimension, *Nonlinear Anal. T. M. A.*, 11(1987), 939 – 967.
- [33] M. Boulakia, M. De Buhan, E. L. SCHWINDT, Numerical reconstruction based on Carleman estimates of source term in reaction-diffusion equation, *ESAIM: COCV* 27(2021) S27.
- [34] Y. Ningning, Z. Zhaojie, A priori and posteriori error analysis of edge stabilization Galerkin method for the optimal control problem governed by convection-dominated diffusion equation, *Journal of Computational and Applied Mathematics* 223(2009)198 – 217.
- [35] R. Becker, B. Vexler, Optimal control of the convection-diffusion equation using stabilized finite element methods, *Numer. Math.* (2007)106 : 349 – 367.
- [36] Z. D. Luo and X. M. Lu, a least squares Galerkin/Petrov mixed finite element method for the stationary conduction-convection problems, *Math. Numer. Sinica*, 25(2)(2003)231 – 244.
- [37] E. Casas, F. Tröltzsch, Error estimates for linear-quadratic elliptic control problems. In: Barbu, V., et al. (ed.) *Analysis and Optimization of Differential Systems*, pp. 89-100. Kluwer, Boston (2003);
- [38] N. Arada, E. Casas, F. Tröltzsch, Error Estimates for the Numerical Approximation of a Semilinear Elliptic Control Problem, *Comput. Optim. Approx.* 23, 201 – 229(2002).
- [39] R. Falk, Approximation of a class of optimal control problems with order of convergence estimates. *J. Math. Anal. Appl.* 44, 28 – 47(1973).
- [40] H. Fu, A characteristic finite element method for optimal control problems governed by convection-diffusion equations, *Journal of Computational and Applied Mathematics* 235(2010)825 – 836.
- [41] H. Fu, H. Rui, A Priori Error Estimates for Optimal Control Problems Governed by Transient Advection-Diffusion Equation, *J Sci Comput* (2009)38 : 290 – 315.
- [42] J. Shen, On error estimates of the penalty method for unsteady Navier-Stokes equations, *SIAM J. Numer. Anal.* 32(2)(1995)386 – 403.

-
- [43] D. Y. Shi and J. C. Ren, Nonconforming mixed finite element method for the stationary conduction-convection problem, *Int. J. Numer. Anal. Mod.* 6(2)(2009) 293-310.
- [44] Y. Hafiene, J. Fadili, A. Elmoataz (2018) The Nonlocal p-Laplacian Evolution Problem on Graphs: The Continuum Limit. In: A. Mansouri, A. El Moataz, F. Nouboud, D. Mammass (eds) *Image and Signal Processing. ICISP 2018. Lecture Notes in Computer Science*, vol 10884. Springer, Cham.
- [45] D. C. Kim and Y. D. Choi, Analysis of conduction – natural convection conjugate heat transfer in the gap between concentric cylinders under solar irradiation, *Int. J. Therm. Sci.* 48(8)(2009)1247 – 1258.
- [46] Y. N. He, Optimal error estimate of the penalty finite element method for time-dependent Navier-Stokes equations, *Math. Comp.* 74(251)1201 – 1216
- [47] K. Wang, Y. N. He, X. L. Feng, On error estimates of the penalty method cor viscoelastic flow problem I: Time discretization, *Appl. Math. Model.* 34(12)(2010)4089 – 4105.
- [48] K. Wang, Y. N. He, X. L. Feng, On error estimates of the fully discrete penalty method cor viscoelastic flow problem, *Int. J. Comput. Math.* 88(10)(2011)2199 – 2220.
- [49] V. Giovandigli, W. A. Yong, Volume viscosity and internal energy relaxation: Error estimates, *Nonlinear Analysis: Real World Applications* 43(2018)213 – 244.
- [50] F. Jouve, Structural shape and topology optimization, *Topology Optimization in Structural and Continuum Mechanics*, G. Rozvany and T. Lewinski eds., CISM International Centre for Mechanical Sciences, 549 (2014), Springer, pp.129-173.
- [51] H. Sun, Y. He, X. Peng, On error estimates of the penalty method for the unsteady conduction-convection problem I: Time discretization, *International Journal of Numerical Analysis and Modeling*, Volume 9, Number 4, 876 – 891.
- [52] G. Allaire, C. Dapogny, P. Frey, Topology and geometry optimization of elastic structures by exact deformation of simplicial mesh, *C. R. Acad. Sci. Paris, Ser. I* 349(2011)999 – 1003.
- [53] S. J. Osher, J. A. Sethian, Fronts propagating with curvature-dependent speed: algorithms based on Hamilton-Jacobi formulations, *J. Comput. Phys.* 79(1988)12 – 49.
- [54] J. H. Choi, K. Y. Kim, and D. S. Chung, Numerical optimization for design of an automotive cooling fan, tech. rep., SAE Technical Paper, 1997.
- [56] C. Dapogny, P. Frey, F. Omnès, Y. Privat, Geometrical shape optimization in fluid mechanics using FreeFem++, *Structural and Multidisciplinary* (2018)50 : 2761 – 2788.
- [57] Z. Chen, S. Lyons, G. Qin, Derivation of the Forchheimer law via homogenization. *Transp. Porous Media.* 44(2001)325 – 335.

- [58] S. Irmay, On the theoretical derivation of Darcy and Forechheimer formulas, *Trans. Amer. Geophys. Union.* 84(1958)702 – 707.
- [59] D. A. Nield, Resolution of a paradox involving viscous dissipation and nonlinear drag in a porous medium, *Transport in Porous Media*, 41, (2000)349 – 357.
- [60] N. Rajaratnam, C. Katopodis, Hydraulics of Denil fishways, *J Hydraulic Eng.* 110 : 1219 – 1233(1984).
- [61] M. Kadiri, Shape optimization and applications to hydraulic structures : mathematical analysis and numerical apprximation, Thèse doctorat, Université De Caen Normandie, 2019.

Chapter 1

Optimal control and application to reduction of urban heat island intensity in porous city

Contents

1.1	Introduction	30
1.2	Governing equations in porous city	31
1.2.1	Navier-Stokes Forchheimer equation	31
1.2.2	Energy equation	32
1.3	Existence of solution for the Forchheimer-Fourier system	34
1.4	Main result	35
1.5	Approximation by the artificial compressibility method	44
1.5.1	Existence of solutions of the perturbed problem	45
1.6	Thermal comfort problem	51
1.6.1	Optimal control procedures	52
1.7	Numerical discretization	53
1.7.1	Variational formulation	53
1.7.2	Time semi-discretization	54
1.7.3	Space discretization	55
1.7.4	Gradient project algorithm	56
1.8	Numerical results	57
1.8.1	Effects of numerical and physical parameters	58
1.8.2	Caen Normandy University Campus	63
1.9	Conclusion	64

1.1 Introduction

The urban territory, dense in infrastructure and limited vegetation cover, subject to solar radiation accumulates heat and creates special thermal conditions called Urban Heat Islands (UHI). UHI is a climatic physical phenomenon, affects human health and its energy consumption. In addition, UHI increases the temperature of cities, which leads to an increase in the concentration of ozone in the air, resulting in an undesirable greenhouse effect. Heat urban islands influence not only the quality of the air but also the property and quantity of the water.

Several factors favor the formation of urban heat islands; the density of the population in cities that leads to the formation of anthropogenic heat and the pollution [1], the rise of humidity in the air, the lack of wind, can develop the sensation of the heat produced by the UHI, the phase change from water to steam allows a transfer of energy [2]. Air conditioning and industries account for 48% of all heat anthropogenic [3]. There are also another factor influencing the UHI such thermal mass of buildings and coatings [4]. The more the urban coatings are dense, the more short waves from solar radiations are absorbed.

To treat the problem of progressive loss of green spaces caused by urbanization, [5] showed the utility of these green spaces to reduce urban heat islands. [6] have also shown the importance of vegetation and water surfaces in the regulation of the urban climate and in the prevention of UHI. Beyond aesthetic value and the landscape function, the use of trees makes it possible to modify the local climate. Individually, trees act as solar masks and windbreaks, altering radiation fields and airflow around buildings.

In recent years, much attention has been paid to study the the phenomenon of the urban heat islands [7], [8] and deal with problems related to the optimal location of green zones in metropolitan areas to mitigate the urban heat island effect.

In the first part of this chapter, we introduce and develop a mathematical model to carry out environmental problems connected to urban heat islands. The set of porous media and heat equations with the artificial compressibility term used in the UHI model is described in Section II. We use also the classical Faedo-Galerkin method and the Fourier transform technique to prove the existence of a weak solution for the incompressible and the compressible Navier-Stokes Forcheimer Fourier system Section IV and Section V respectively. In Section VI, The optimal control formulation is explained. The numerical discretization of the primal equations, the derivation of the optimality system and the numerical implementation of the minimizing process, in particular the Spectral Projected Gradient algorithm is detailed in Section IV. Several numerical results are presented to give an overview of the computational capability of the proposed design approach to control heat processes produced by urban heat islands.

1.2 Governing equations in porous city

The transport phenomena in porous media refers to a solid having space that is filled with fluid is present in several fields. Designated flow regimes can be classified into: Darcy and Forchheimer for unsteady laminar flows, and post-Forchheimer for turbulent flows. To analyze the urban heat islands, cities are considered as porous media. Moreover, the drag force of buildings and ground surface can be represented by the Darcy term, the Forchheimer term and the Brinkman term in the momentum equation. Based on these assumptions, a coupled Navier-Stokes Forchheimer and temperature model is derived.

1.2.1 Navier-Stokes Forchheimer equation

The Navier-Stokes Forchheimer extended Darcy model can be used in various area, such as industries and engineering applications in the nuclear, geological, environment [15]. The turbulent Navier-Stokes Forchheimer with the gravity and the buoyancy terms equation inside the urban canopy is given by

$$\partial_t u + \frac{1}{\Phi \rho} \nabla p - \left[\frac{\mu}{\rho \Phi} + \frac{2\mu_t}{\rho} \right] \Delta u + (u \cdot \nabla) u + \frac{\mu}{K \rho} \Phi u + \frac{C}{\sqrt{K}} \Phi^2 |u| u - \delta \frac{g}{\Phi} [\beta(\theta - \theta_{in}) - 1] = 0 \quad (1.1)$$

where u is the fluid velocity, p is the pressure, θ is the temperature, ρ is the air density, μ is the dynamic viscosity, Φ is the porosity, K is the permeability, C is the Forchheimer inertia coefficient, β is the thermal expansion coefficient, $g(x, t)$ is the gravitational vector function and μ_t is the turbulent viscosity, in which the turbulent viscosity $\mu_t = \frac{c_\mu \rho k^2}{\xi}$ (see [16], [17]) with c_μ value is close to the value for clear flow $c_\mu = 0.09$.

In order to assume an equilibrium turbulent flow, the expressions of the dissipation rate ξ and the turbulent kinetic energy k (see [18]) are given by

$$k = 0.01 u^2 \quad (1.2)$$

$$\xi = \frac{c_\mu^{\frac{3}{4}} k^{\frac{3}{2}}}{V_k z} \quad (1.3)$$

The V_k Von-Karman constant is taken to be 0.4.

The governing equations (1.1) are general and valid for forced convection in variable porosity media. To analyse the convection in packed beds some constitutive equations have to be supplied for the Forchheimer inertia coefficient C and the permeability K . These constitutive equations are obtained from experimental results of *Ergun*(1952). The constitutive equations are related to the porosity Φ and height of roughness element h . The equations may be expressed

in the following form :

$$K = \frac{h^2 \Phi^3}{150(1 - \Phi)^2} \quad (1.4)$$

$$C = \frac{1.75}{\sqrt{150\Phi^3}} \quad (1.5)$$

The urban porosity is assumed to be constant in the horizontal direction and varies in the vertical direction as follows

$$\Phi = \begin{cases} (1 - \Phi_0) \left(\frac{z}{H}\right)^{0.5} + \Phi_0 & \text{if } z \leq H \\ 1 & \text{if } z > H \end{cases} \quad (1.6)$$

in the case of a study in real cities, Φ_0 varies from 0.38 to 0.82 (see [19]).

1.2.2 Energy equation

Urban structures emit anthropogenic heat absorbed by the effect of solar radiation in the ambient air, so the hypothesis of local thermal equilibrium cannot be used in a porous city. In the absence of this effect of thermal equilibrium, the energy equation must be replaced by a model with two non-local thermal equilibrium equations, one for the solid phase and the other for the fluid phase. However, we are interested in the temperature of the fluid outside buildings. The energy equation for the fluid phase can be written as

$$\rho C_p \Phi u \nabla \theta = \nabla (\lambda \Phi \nabla \theta) + (1 - \Phi)q \quad (1.7)$$

After adding the unsteady term and by employing the time averaging method to the energy relationship, the heat transfer equation in a porous city can be obtained as follows:

$$\partial_t \theta + u \nabla \theta = \nabla \left[\left(\frac{\mu}{\rho P r} + \frac{\mu_t}{\rho \sigma_T} \right) \nabla \theta \right] + \frac{(1 - \Phi)}{\rho \Phi C_p} q \quad (1.8)$$

The value of σ_T is close to the value for the clear flow which is equals to 1. Fixing the quantity of heat provided by the vegetation (for more detail of the vegetation model (see [20])) the equation becomes

$$\partial_t \theta + u \nabla \theta - \nabla \left[\left(\frac{\mu}{\rho P r} + \frac{\mu_t}{\rho \sigma_T} \right) \nabla \theta \right] - \frac{(1 - \Phi)}{\rho \Phi C_p} q - \sum_{i=1}^N \alpha_i \chi_{G_i} = 0 \quad (1.9)$$

where G_i represents the green spaces, α_i is the foliage temperature and χ is the characteristic function

$$\chi_{G_i}(x) = \begin{cases} 1 & \text{if } x \in G_i \\ 0 & \text{otherwise} \end{cases} \quad (1.10)$$

The intensity of the heat source in a city is always based on the area of the soil surface. Urban heat sources are mainly composed of the heat released from buildings absorbed by the effect of radiation and the heat released from the ground surface. The two spatial locations of the two heat sources are different and their effects on the urban thermal environment are also different. Some numerical studies of all heat sources have a uniform distribution over the entire urban area [21]. The thermal flux of the heat source is related to the density of buildings and the density of buildings varies in the vertical direction

$$q = \frac{Q_b}{V_b} \quad (1.11)$$

$$V_b = \int_0^H (1 - \Phi) dz \quad (1.12)$$

where Q_b is the intensity of building heat source per unit area of ground surface, V_b is the volume of buildings per unit area of ground surface and H is the height of urban canopy.

Finally, the system for heat transfer in a porous city can be summarized as follows

$$\begin{cases} \partial_t u + \frac{1}{\Phi \rho} \nabla p - \left[\frac{\mu}{\rho \Phi} + \frac{2\mu_t}{\rho} \right] \Delta u + (u \cdot \nabla) u + \frac{\mu}{K \rho} \Phi u + \frac{C}{\sqrt{K}} \Phi^2 |u| u \\ - \delta \frac{g}{\Phi} [\beta(\theta - \theta_{in}) - 1] = 0 \quad \text{in } \Omega \times (0, T) \\ \partial_t \theta + u \nabla \theta - \nabla \cdot \left[\left(\frac{\mu}{\rho Pr} - \frac{\mu_t}{\rho \sigma_T} \right) \nabla \theta \right] - \frac{(1 - \Phi)}{\rho \Phi C_p} q - \sum_{i=1}^N \alpha_i \chi_{G_i} = 0 \quad \text{in } \Omega \times (0, T) \\ \nabla \cdot u = 0 \quad \text{in } \Omega \times (0, T) \\ u(x, 0) = a_0(x), \quad \theta(x, 0) = \tau_0(x) \quad \text{in } \Omega \end{cases} \quad (1.13)$$

here $\Omega \subset \mathbb{R}^n$ ($n = 2$ or 3) is bounded connected domain with Lipschitz continuous boundary $\partial\Omega$. The artificial compressibility approximation was introduced by [11], [12] and [14] in order to deal with the difficulty induced by the incompressibility constraints in the numerical approximations to the Navier Stokes equation.

The unsteady incompressible Navier-Stokes Forchheimer with heat transfer equations may be written in pseudo-compressibility approach as

$$\begin{cases} \partial_t u^\varepsilon + \alpha \nabla p^\varepsilon - \lambda \Delta u^\varepsilon + (u^\varepsilon \cdot \nabla) u^\varepsilon + a u^\varepsilon + b |u^\varepsilon| u^\varepsilon \\ - dg [\beta(\theta^\varepsilon - \theta_{in}^\varepsilon) - 1] = 0 \quad \text{in } \Omega \times (0, T) \\ \partial_t \theta^\varepsilon + u^\varepsilon \nabla \theta^\varepsilon - \nabla \cdot [\eta \nabla \theta^\varepsilon] - Q_B - \sum_{i=1}^N \alpha_i \chi_{G_i} = 0 \quad \text{in } \Omega \times (0, T) \\ \varepsilon \partial_t p^\varepsilon + \text{div} u^\varepsilon = 0 \quad \text{in } \Omega \times (0, T) \end{cases} \quad (1.14)$$

where $\lambda = \left(\frac{\mu}{\rho \Phi} + \frac{2\mu_t}{\rho} \right)$, $\eta = \left(\frac{\mu}{\rho Pr} - \frac{\mu_t}{\rho \sigma_T} \right)$, $Q_B = \frac{(1 - \Phi)}{\rho \Phi C_p} q$, $\alpha = \frac{1}{\Phi \rho}$, $a = \frac{\mu}{K \rho} \Phi$, $b = \frac{C}{\sqrt{K}} \Phi^2$, $d = \frac{\delta}{\Phi}$.

In the rest of the proof of the existence of the solution of this system, by choice we take $\alpha = 1$.

1.3 Existence of solution for the Forchheimer-Fourier system

Let Ω be a bounded domain in \mathbb{R}^n (with $n = 2, 3$) and its boundary satisfies the following

$$\partial\Omega = \Gamma_1 \cup \Gamma_s \cup \Gamma_B \quad (1.15)$$

and

$$\Gamma_1 \cap \Gamma_s \cap \Gamma_B = \emptyset \quad (1.16)$$

The measure of $\Gamma_1 \neq 0$, and the intersection of $\bar{\Gamma}_1 \cap \bar{\Gamma}_2$ (with $\Gamma_2 = \Gamma_B \cup \Gamma_s$) is an $n - 2$ dimensionnal C^1 manifold.

We consider the following problem with initial and boundary conditions

$$\left\{ \begin{array}{l} \partial_t u + (u \cdot \nabla)u + au + b |u| u = -\nabla p + \lambda \Delta u + dg [\beta (\theta - \theta_{in}) - 1] \quad \Omega \times [0, T] \\ \partial_t \theta + (u \cdot \nabla)\theta = \eta \Delta \theta + \mathcal{Q}_B + \sum_{i=1}^N \alpha_i \chi_{G_i} \quad \text{in } \Omega \times [0, T] \\ \operatorname{div} u = 0 \quad \text{in } \Omega \times [0, T] \\ u(x, t = 0) = a_0(x) \quad \text{in } \Omega \\ \theta(x, t = 0) = \tau_0(x) \quad \text{in } \Omega \\ u(x, t) = 0 \quad x \in \Gamma_1 \\ \theta(x, t) = \xi(x, t) \quad x \in \Gamma_1 \\ u(x, t) = 0 \quad \text{on } (\Gamma_B \cup \Gamma_s) \times [0, T] \\ \frac{\partial \theta}{\partial n} = 0 \quad \text{on } (\Gamma_B \cup \Gamma_s) \times [0, T] \end{array} \right. \quad (1.17)$$

where u is the fluid velocity, p is the pressure, θ is the temperature, $\frac{\partial \theta}{\partial n}$ denote the normal derivative of θ at x to $\partial\Omega$, λ is the kinematic viscosity, η is the thermal diffusivity, $a > 0$ is the Darcy coefficient, $b > 0$ is the Forchheimer coefficient, g is gravitational vector function, $\beta > 0$ is the coefficient of volume expansion, and d is a positive constant.

We consier $L^p(\Omega)$ the vector space of functions and $W_p^l(\Omega)$ the Sobolev space. We define the inner product and the norm of $L^2(\Omega)$ as follows : $\|u\| = \sqrt{(u, u)}$, for vector $L^2(\Omega)$ -functions $u = (u_1, \dots, u_n)$, and $\|\theta\| = \sqrt{(\theta, \theta)}$, for $L^2(\Omega)$ -functions θ .

We give the following function spaces

$$D_\sigma = \{\text{vector function } \varphi \in C^\infty(\Omega) | \operatorname{supp} \varphi \subset \Omega, \operatorname{div} \varphi = 0 \quad \text{in } \Omega\}$$

$$D_0 = \{\text{scalar function } \varphi \in C^\infty(\bar{\Omega}) | \varphi \equiv 0 \quad \text{in a neighborhood of } \Gamma_1\}$$

$$H = \text{completion of } D_\sigma \quad \text{under the } L^2(\Omega) \text{ - norm}$$

$V =$ completion of D_σ under the $H^1(\Omega) - norm$

$W =$ completion of D_0 under the $H^1(\Omega) - norm$

where $V = H_0^1(\Omega) \cap H$, and $H_0^1(\Omega)$ is the completion of $C_0^\infty(\Omega)$ under the $H^1(\Omega)$. We also introduce \tilde{V} the completion of D_σ under the norm $\|u\|_{L^n(\Omega)} + \|u\|_V$, and \tilde{W} the completion of D_0 under the norm $\|\theta\|_{L^n(\Omega)} + \|\theta\|_W$. The spaces \tilde{V}' and \tilde{W}' are the dual of \tilde{V} and \tilde{W} respectively. We introduce the following bilinear form

$$B(u, u) = (u \cdot \nabla)u \quad B(u, \theta) = (u \cdot \nabla)\theta$$

Let (u, p, θ) the solution of (1.17). For all $v \in D_\sigma$ and $\tau \in D_0$ we have

$$\frac{d}{dt} \langle u, v \rangle + B \langle u, u, v \rangle + \langle au, v \rangle + \langle b | u | u, v \rangle = \langle p, \nabla \cdot v \rangle - \lambda \langle \nabla u, \nabla v \rangle + \langle dg [\beta (\theta - \theta_{in}) - 1], v \rangle \quad (1.18)$$

$$\frac{d}{dt} \langle \theta, \tau \rangle + B \langle u, \theta, \tau \rangle = -\eta \langle \nabla \theta, \nabla \tau \rangle + \left\langle \mathcal{Q}_B + \sum_{i=1}^N \alpha_i \chi_{G_i}, \tau \right\rangle \quad (1.19)$$

Definition 1.3.1. A pair functions (u, θ) is called a weak solution of (1.17) if $u \in L^2([0, T]; V)$, $(\theta - \theta_0) \in L^2([0, T]; W)$, for some function $\theta_0 \in L^2([0, T]; H^1(\Omega))$ such that $\theta_0(x, t) = \xi(x, t)$, on $\Gamma_1 \times (0, T)$, and (u, θ) satisfy (1.18), (1.19) for any $v \in \tilde{V}$, $\tau \in \tilde{W}$, where the derivative with respect to t is in the distribution sens $\mathcal{D}'(0, T)$.

1.4 Main result

Lemma 1.4.1. *Let*

$$\begin{aligned} u &\in L^2([0, T]; V), & p &\in L^2([0, T]; L^2(\Omega)), & (\theta - \theta_0) &\in L^2([0, T]; W), \\ \theta_0 &\in L^2([0, T]; H^1(\Omega)), & g &\in L^\infty(\Omega \times ([0, T])) \\ v &\in \tilde{V}, & \tau &\in \tilde{W} \end{aligned}$$

where (u, p, θ) satisfy (1.18) and (1.19) for all $v \in \tilde{V}$, $\tau \in \tilde{W}$. So u and θ are a continuous function from $[0, T]$ into \tilde{V}' and \tilde{W}' .

Lemma 1.4.2. *Let Ω be a bounded domain and $\xi(x, t) \in C^1(\bar{\Gamma}_1 \times [0, T])$. Then for each $\varepsilon > 0$ and $1 < p < \infty$ (p is a strictly positive real number), there exists a function $\theta_0(x, t)$ such that*

$$\theta_0 \in C^1(\bar{\Omega} \times [0, T]), \quad \theta_0(x, t) = \xi(x, t) \quad \text{on} \quad \bar{\Gamma}_1 \times [0, T] \quad \sup_{x \leq t \leq T} \|\theta_0\|_{L^p(\Omega)} < \varepsilon$$

For the proof of this Lemma, see [27] (Lemma 6.38) and also [28]

Lemma 1.4.3. *Let $g_\infty = \|g\|_{L^\infty(\Omega \times (0,T))}$, there exists a positive constant c_1 depending on Ω such that*

$$\|u\| \leq c_1 \|\nabla u\| \quad \text{for } \forall u \in V$$

And there is a positive constant c_2 depending on Ω such that

$$\|\theta\| \leq c_2 \|\nabla \theta\| \quad \text{for } \forall \theta \in W$$

where V and W are the functions spaces defined previously.

Lemma 1.4.4. *Let $n \geq 3$, There exist positive constants c_B and $c_{\tilde{B}}$ such that*

$$\begin{aligned} |B(u, v, w)| &\leq c_B \|\nabla u\| \|\nabla v\| \|w\|_n \quad \text{for } \forall u \in V, \quad \forall v \in H^1, \quad w \in L^n \\ |\tilde{B}(u, \theta, \tau)| &\leq c_{\tilde{B}} \|\nabla u\| \|\nabla \theta\| \|\tau\|_n \quad \text{for } \forall u \in V, \quad \forall \theta \in H^1, \quad \tau \in L^n \end{aligned}$$

Using the integration by parts, we obtain:

Lemma 1.4.5.

$$B(u, v, w) = -B(u, w, v) \quad \text{for } \forall u \in V, \text{ and } \forall v, w \in \tilde{V}$$

holds. In particular,

$$B(u, v, v) = 0 \quad \forall u \in V, \quad \forall v \in \tilde{V}$$

and

$$\tilde{B}(u, \theta, \tau) = -\tilde{B}(u, \tau, \theta) \quad \forall u \in V, \quad \forall \theta \in W, \quad \tau \in \tilde{W}$$

holds. In particular

$$\tilde{B}(u, \theta, \theta) = 0, \quad \forall u \in V, \quad \forall \theta \in W$$

Lemma 1.4.6. *Let $2 \leq n \leq 4$, There exist positive constants c_B and $c_{\tilde{B}}$ such that*

$$\begin{aligned} |B(u, v, w)| &\leq c_B \|\nabla u\| \|\nabla v\| \|\nabla w\| \quad \text{for } \forall u, v, w \in V \\ |\tilde{B}(u, \theta, \tau)| &\leq c_{\tilde{B}} \|\nabla u\| \|\nabla \theta\| \|\nabla \tau\| \quad \text{for } \forall u \in V, \quad \forall \theta, \tau \in W \end{aligned}$$

Lemma (1.4.4), (1.4.6) are proved by Hölder and Poincaré's inequalities.

The space \tilde{V} and \tilde{W} are contained and dense in H and $L^2(\Omega)$, respectively, and

$$\tilde{V} \subset H \subset \tilde{V}', \quad \tilde{W} \subset L^2 \subset \tilde{W}',$$

hold where each space is dense in the following one and the injections are continuous. Furthermore the injections $\tilde{V} \hookrightarrow H$, $\tilde{W} \hookrightarrow L^2(\Omega)$ are compact.

Since $(\nabla u, \nabla v)$ ($u \in V$) is continuous linear functional on \tilde{V} , it defines a continuous linear

mapping A from V to \tilde{V} and \tilde{A} from $H^1(\Omega)$ to \tilde{W}' as follows

$$\begin{aligned} \tilde{v}, \langle Au, v \rangle_{\tilde{V}} &= (\nabla u, \nabla v), & u \in V, v \in \tilde{V} \\ \tilde{w}, \langle \tilde{A}\theta, v \rangle_{\tilde{W}} &= (\nabla\theta, \nabla\tau), & \theta \in H^1(\Omega), \tau \in \tilde{W} \end{aligned}$$

and we have the estimate:

$$\begin{aligned} \|Au\|_{\tilde{V}} &\leq \|\nabla u\| \\ \|A\theta\|_{\tilde{V}} &\leq \|\nabla\theta\| \end{aligned} \tag{1.20}$$

According to Lemma (1.4.4), we can define a continuous (nonlinear) mapping B from V to \tilde{V} , and the bilinear bounded operator \tilde{B} from $V \times H^1$ to \tilde{W}' as follows:

$$\begin{aligned} \tilde{v}, \langle B(u, u), v \rangle_{\tilde{V}} &= B(u, u, v), & u \in V, v \in \tilde{V} \\ \tilde{w}, \langle \tilde{B}(u, \theta), \tau \rangle_{\tilde{W}} &= \tilde{B}(u, \theta, \tau) & u \in V, \theta \in H^1(\Omega), \tau \in \tilde{W} \end{aligned} \tag{1.21}$$

Theorem 1.4.7. *Let Ω a bounded domain in \mathbb{R}^n , ($n = 2, 3$) with C^1 boundary satisfying (1.15) and (1.16). if $g \in L^\infty(\Omega \times ([0, T]))$, $\xi \in C^1(\bar{\Gamma}_1 \times [0, T])$, $\tau_0 \in L^2(\Omega)$, $a_0 \in H$, $\theta_{in} \in L^2(\Omega)$ and a, b are a positive constant $a > 0$, $b > 0$ and if $(d\beta\|g\|_{L^\infty}) < c\sqrt{\lambda}\eta$ (with $c > 0$), then there exists a weak solution (u, θ) of (1.17) satisfying the periodic condition in time.*

$$u \in L^\infty([0, T], H), \quad \theta \in L^\infty([0, T], L^2(\Omega)), \tag{1.22}$$

Proof. Assume that (u, p, θ) the solution of (1.17). Let us take the inner product of $v \in D_\sigma$ and $w \in D_0$. Using the integration by parts, we obtain

$$\frac{d}{dt} \langle u, v \rangle + B \langle u, u, v \rangle + \langle au, v \rangle + \langle b |u| u, v \rangle = \langle p, \nabla \cdot v \rangle - \lambda \langle \nabla u, \nabla v \rangle + \langle dg [\beta(\theta - \theta_{in}) - 1], v \rangle \tag{1.23}$$

$$\frac{d}{dt} \langle \theta, w \rangle + \tilde{B} \langle u, \theta, w \rangle = -\eta \langle \nabla\theta, \nabla w \rangle + \left\langle \mathcal{Q}_B + \sum_{i=1}^N \alpha_i \chi_{G_i}, w \right\rangle \tag{1.24}$$

where $f = \mathcal{Q}_B + \sum_{i=1}^N \alpha_i \chi_{G_i}$, and $f \in L^2([0, T]; L^2(\Omega))$.

and

$$B(u, u, v) = ((u \cdot \nabla) u, v) = \int_{\Omega} \sum_{j=1}^n u_j(x) \frac{\partial u_i(x)}{\partial x_j} v_i(x) dx$$

$$\tilde{B}(u, \theta, w) = ((u \cdot \nabla) \theta, w) = \int_{\Omega} \sum_{j=1}^n u_j(x) \frac{\partial \theta_i(x)}{\partial x_j} w(x) dx$$

We construct the weak solution of (1.17) using the Galerkin method for $2 \leq n \leq 4$. Since V is separable and D_σ is dense in V , there exists a sequence $(u)_i$ ($1 \leq i \leq n$) of elements of D_σ , which is a basis of V and orthonormal in H and there exists a sequence $(\theta)_j$ ($1 \leq j \leq n$) of elements of

D_0 , which is a basis of W and orthonormal in $L^2(\Omega)$.

We consider the approximation solutions $(u^{(m)}(t), \theta^{(m)}(t) + \theta_0)$ of (1.23) and (1.24) as follows

$$u^{(m)}(t) = \sum_{i=1}^m f_i^{(m)} u_i \quad (1.25)$$

$$\theta^{(m)}(t) = \sum_{j=1}^m g_j^{(m)} \theta_j \quad (1.26)$$

$$\begin{aligned} & \left\langle \frac{\partial}{\partial t} u^{(m)}, u_k \right\rangle + B \left\langle u^{(m)}, u^{(m)}, u_k \right\rangle + \left\langle a u^{(m)}, u_k \right\rangle + \left\langle b | u^{(m)} | u^{(m)}, u_k \right\rangle \\ & = -\lambda \left\langle \nabla u^{(m)}, \nabla u_k \right\rangle + \left\langle dg \left[\beta \left(\theta^{(m)} - \theta_{in} \right) - 1 \right], u_k \right\rangle, \quad 1 \leq k \leq m \end{aligned} \quad (1.27)$$

$$\begin{aligned} & \left\langle \frac{\partial}{\partial t} \theta^{(m)}, \theta_k \right\rangle + \tilde{B} \left\langle u^{(m)}, \theta^{(m)}, \theta_k \right\rangle \\ & = - \left\langle \frac{\partial}{\partial t} \theta_0, \theta_k \right\rangle - \eta \left\langle \nabla \theta^{(m)}, \nabla \theta_k \right\rangle + \left\langle \mathcal{Q}_B + \sum_{i=1}^N \alpha_i \chi_{G_i}, \theta_k \right\rangle, \quad 1 \leq k \leq m \end{aligned} \quad (1.28)$$

and

$$u^m(x, t = 0) = u_{m0} \quad \theta^m(x, t = 0) = \theta_{m0}$$

Substituting ((1.25), (1.26)) into (1.27), (1.28) we obtain a system of nonlinear differential equations for $f_i^{(m)}(t)$, $g_j^{(m)}(t)$, $1 \leq i \leq m$ and $1 \leq j \leq m$, with the initial conditions

$$f_i^{(m)}(0) = (a_0, u_i), \quad g_j^{(m)}(0) = (\tau_0 - \theta_0(\cdot, 0), \theta_j)$$

This ordinary differential system has a solution $(u^{(m)}, \theta^{(m)})$ defined on $[0, t_m]$. The following a priori estimate shows that $t_m = T$.

Multiplying (1.27) by $f_k^{(m)}$ and (1.28) by $g_k^{(m)}$ respectively, and summing with respect to k , we have

$$\begin{aligned} & \frac{1}{2} \frac{d}{dt} \|u^{(m)}\|_{L^2}^2 + \lambda \|\nabla u^{(m)}\|_{L^2}^2 + B \left\langle u^{(m)}, u^{(m)}, u^{(m)} \right\rangle + \left\langle a u^{(m)}, u^{(m)} \right\rangle \\ & + \left\langle b | u^{(m)} | u^{(m)}, u^{(m)} \right\rangle = \left\langle d\beta g \theta^{(m)}, u^{(m)} \right\rangle - \left\langle d\beta g \theta_{in}, u^{(m)} \right\rangle - \left\langle dg, u^{(m)} \right\rangle \end{aligned} \quad (1.29)$$

and for the Fourier equation we have

$$\frac{1}{2} \frac{d}{dt} \|\theta^{(m)}\|_{L^2}^2 + \eta \|\nabla \theta^{(m)}\|_{L^2}^2 = \tilde{B} \left\langle u^{(m)}, \theta_0, \theta^{(m)} \right\rangle - \left\langle \frac{\partial}{\partial t} \theta_0, \theta^{(m)} \right\rangle + \left\langle f, \theta^{(m)} \right\rangle \quad (1.30)$$

We have $B \left\langle u^{(m)}, u^{(m)}, u^{(m)} \right\rangle = 0$ and $\tilde{B} \left\langle u^{(m)}, \theta^{(m)}, \theta^{(m)} \right\rangle = 0$. Using Schwartz and Poincaré's

inequality for the right hand side of (1.29), we have

$$\begin{aligned}
 & \frac{1}{2} \frac{d}{dt} \|u^{(m)}\|_{L^2}^2 + \lambda \|\nabla u^{(m)}\|_{L^2}^2 + a \|u^{(m)}\|_{L^2}^2 + b \|u^{(m)}\|_{L^3}^3 \\
 & \leq d\beta \|g\|_{L^\infty} \|\theta^{(m)}\|_{L^2} \|u^{(m)}\|_{L^2} + \beta d \|g\|_{L^\infty} \|\theta_{in}\|_{L^2} \|u^{(m)}\|_{L^2} + d \|g\|_{L^\infty} \|u^{(m)}\|_{L^2} \\
 & \frac{1}{2} \frac{d}{dt} \|u^{(m)}\|_{L^2}^2 + \lambda \|\nabla u^{(m)}\|_{L^2}^2 + a \|u^{(m)}\|_{L^2}^2 + b \|u^{(m)}\|_{L^3}^3 \\
 & \leq c_1 d\beta \|g\|_{L^\infty} \|\theta^{(m)}\|_{L^2} \|\nabla u^{(m)}\|_{L^2} + c_1 \beta d \|g\|_{L^\infty} \|\theta_{in}\|_{L^2} \|\nabla u^{(m)}\|_{L^2} \\
 & \quad + c_6 d \|g\|_{L^\infty} \|\nabla u^{(m)}\|_{L^2} \\
 & \frac{1}{2} \frac{d}{dt} \|u^{(m)}\|_{L^2}^2 + \lambda \|\nabla u^{(m)}\|_{L^2}^2 + a \|u^{(m)}\|_{L^2}^2 + b \|u^{(m)}\|_{L^3}^3 \\
 & \leq \frac{3(c_1 d\beta \|g\|_{L^\infty})^2}{2\lambda} \|\theta^{(m)}\|_{L^2}^2 + \frac{\lambda}{6} \|\nabla u^{(m)}\|_{L^2}^2 \\
 & \quad + \frac{3(c_1 d\beta \|g\|_{L^\infty})^2}{2\lambda} \|\theta_{in}\|_{L^2}^2 + \frac{\lambda}{6} \|\nabla u^{(m)}\|_{L^2}^2 + \frac{3(c_6 d \|g\|_{L^\infty})^2}{2\lambda} + \frac{\lambda}{6} \|\nabla u^{(m)}\|_{L^2}^2
 \end{aligned}$$

Thus, we have

$$\begin{aligned}
 & \frac{1}{2} \frac{d}{dt} \|u^{(m)}\|_{L^2}^2 + \frac{\lambda}{2} \|\nabla u^{(m)}\|_{L^2}^2 + a \|u^{(m)}\|_{L^2}^2 + b \|u^{(m)}\|_{L^3}^3 \\
 & \leq \frac{3(c_1 d\beta \|g\|_{L^\infty})^2}{2\lambda} \left(\|\theta^{(m)}\|_{L^2}^2 + \|\theta_{in}\|_{L^2}^2 \right) + \frac{3(c_6 d \|g\|_{L^\infty})^2}{2\lambda}
 \end{aligned} \tag{1.31}$$

Similarly for the Fourier equation

$$\begin{aligned}
 & \frac{1}{2} \frac{d}{dt} \|\theta^{(m)}\|_{L^2}^2 + \eta \|\nabla \theta^{(m)}\|_{L^2}^2 = \tilde{B} \langle u^{(m)}, \theta_0, \theta^{(m)} \rangle - \left\langle \frac{\partial}{\partial t} \theta_0, \theta^{(m)} \right\rangle + \langle f, \theta^{(m)} \rangle \\
 & \frac{1}{2} \frac{d}{dt} \|\theta^{(m)}\|_{L^2}^2 + \eta \|\nabla \theta^{(m)}\|_{L^2}^2 \leq \frac{3c_3}{2\eta} \|\theta_0\|_{L^4} \|\nabla u^{(m)}\|_{L^2} \|\nabla \theta^{(m)}\|_{L^2} + \frac{3c_4}{2\eta} \left\| \frac{\partial}{\partial t} \theta_0 \right\|_{L^2} \|\nabla \theta^{(m)}\|_{L^2} \\
 & \quad + \frac{3c_5}{2\eta} \|f\|_{L^2} \|\nabla \theta^{(m)}\|_{L^2} \\
 & \frac{1}{2} \frac{d}{dt} \|\theta^{(m)}\|_{L^2}^2 + \eta \|\nabla \theta^{(m)}\|_{L^2}^2 \leq \frac{3c_3}{2\eta} \|\theta_0\|_{L^4}^2 \|\nabla u^{(m)}\|_{L^2}^2 + \frac{\eta}{6} \|\nabla \theta^{(m)}\|_{L^2}^2 + \frac{3c_4^2}{2\eta} \left\| \frac{\partial}{\partial t} \theta_0 \right\|_{L^2}^2 \\
 & \quad + \frac{\eta}{6} \|\nabla \theta^{(m)}\|_{L^2}^2 + \frac{3c_5^2}{2\eta} \|f\|_{L^2}^2 + \frac{\eta}{6} \|\nabla \theta^{(m)}\|_{L^2}^2 \\
 & \frac{1}{2} \frac{d}{dt} \|\theta^{(m)}\|_{L^2}^2 + \frac{\eta}{2} \|\nabla \theta^{(m)}\|_{L^2}^2 \leq \frac{3c_3}{2\eta} \|\theta_0\|_{L^4}^2 \|\nabla u^{(m)}\|_{L^2}^2 + \frac{3c_4^2}{2\eta} \left\| \frac{\partial}{\partial t} \theta_0 \right\|_{L^2}^2 + \frac{3c_5^2}{2\eta} \|f\|_{L^2}^2
 \end{aligned} \tag{1.32}$$

where c_3, c_4, c_5 are constants depending only Ω . We integrate (1.31) (1.32) with respect to t , we

obtain

$$\begin{aligned}
& \|u^{(m)}(t)\|_{L^2}^2 + \frac{\lambda}{2} \int_0^t \|\nabla u^{(m)}(s)\|_{L^2}^2 ds + a \int_0^t \|u^{(m)}(s)\|_{L^2}^2 ds + b \int_0^t \|u^{(m)}(s)\|_{L^3}^3 ds \\
& \leq \|u_{m0}\|_{L^2}^2 + \frac{3(c_1 d \beta \|g\|_{L^\infty})^2}{2\lambda} \int_0^t \left(\|\theta^{(m)}(s)\|_{L^2}^2 + \|\theta_{in}(s)\|_{L^2}^2 \right) ds \\
& + \frac{3(c_6 d \|g\|_{L^\infty})^2}{2\lambda} \int_0^t ds, \quad 0 \leq t \leq T
\end{aligned} \tag{1.33}$$

$$\begin{aligned}
& \|\theta^{(m)}(t)\|_{L^2}^2 + \frac{\eta}{2} \int_0^t \|\nabla \theta^{(m)}(s)\|_{L^2}^2 ds \leq \|\theta_{m0}\|_{L^2}^2 \\
& + \frac{3c_3}{\eta} \int_0^t \|\theta_0(s)\|_{L^4}^2 \|\nabla u^{(m)}(s)\|_{L^2}^2 ds + \frac{3c_4^2}{\eta} \int_0^t \left\| \frac{\partial}{\partial t} \theta_0 \right\|_{L^2}^2 ds + \frac{3c_5^2}{\eta} \int_0^t \|f\|_{L^2}^2 ds
\end{aligned} \tag{1.34}$$

From (1.34) we have

$$\begin{aligned}
& \int_0^t \|\nabla \theta^{(m)}(s)\|_{L^2}^2 ds \leq \frac{2}{\eta} \left(\|\theta_{m0}\|_{L^2}^2 - \|\theta^{(m)}(t)\|_{L^2}^2 \right) \\
& + \frac{6c_3}{\eta^2} \int_0^t \|\theta_0(s)\|_{L^4}^2 \|\nabla u^{(m)}(s)\|_{L^2}^2 ds + \frac{6c_4^2}{\eta^2} \int_0^t \left\| \frac{\partial}{\partial t} \theta_0 \right\|_{L^2}^2 ds + \frac{6c_5^2}{\eta^2} \int_0^t \|f\|_{L^2}^2 ds
\end{aligned} \tag{1.35}$$

We replace $\|\theta^{(m)}(s)\|^2$ in (1.33) by $c_2^2 \|\nabla \theta^{(m)}(s)\|^2$. Using (1.35), we transform (1.33) and we obtain

$$\begin{aligned}
& \|u^{(m)}(t)\|_{L^2}^2 + \lambda \int_0^t \|\nabla u^{(m)}(s)\|_{L^2}^2 ds + a \int_0^t \|u^{(m)}(s)\|_{L^2}^2 ds + b \int_0^t \|u^{(m)}(s)\|_{L^3}^3 ds \\
& \leq \|u_{m0}\|_{L^2}^2 + \frac{3(c_1 c_2 d \beta \|g\|_{L^\infty})^2}{\lambda \eta} \left(\|\theta_{m0}\|_{L^2}^2 - \|\theta^{(m)}(t)\|_{L^2}^2 \right) + \frac{3(c_1 d \beta \|g\|_{L^\infty})^2}{2\lambda} \int_0^t \|\theta_{in}(s)\|_{L^2}^2 ds \\
& + \frac{9(c_1 c_2 d \beta \|g\|_{L^\infty})^2}{\lambda \eta^2} \left(c_3 \int_0^t \|\theta_0(s)\|_{L^4}^2 \|\nabla u^{(m)}(s)\|_{L^2}^2 ds + c_4^2 \int_0^t \left\| \frac{\partial}{\partial t} \theta_0 \right\|_{L^2}^2 ds + c_5^2 \int_0^t \|f\|_{L^2}^2 ds \right) \\
& + \frac{3(c_6 d \|g\|_{L^\infty})^2}{2\lambda} \int_0^t ds, \quad 0 \leq t \leq T
\end{aligned} \tag{1.36}$$

$$\begin{aligned}
& \|u^{(m)}(t)\|_{L^2}^2 + \lambda \int_0^t \|\nabla u^{(m)}(s)\|_{L^2}^2 ds + a \int_0^t \|u^{(m)}(s)\|_{L^2}^2 ds + b \int_0^t \|u^{(m)}(s)\|_{L^3}^3 ds \\
& \leq \|u_{m0}\|_{L^2}^2 + \frac{3(c_1 c_2 d \beta \|g\|_{L^\infty})^2}{\lambda \eta} \left(\|\theta_{m0}\|_{L^2}^2 - \|\theta^{(m)}(t)\|_{L^2}^2 \right) + \frac{3(c_1 d \beta \|g\|_{L^\infty})^2}{2\lambda} \int_0^t \|\theta_{in}(s)\|_{L^2}^2 ds \\
& + \frac{9c_3^2 (c_1 c_2 d \beta \|g\|_{L^\infty})^2}{\lambda \eta^2} \int_0^t \|\theta_0(s)\|_{L^4}^2 \|\nabla u^{(m)}(s)\|_{L^2}^2 ds \\
& + \frac{9c_4^2 (c_1 c_2 d \beta \|g\|_{L^\infty})^2}{\lambda \eta^2} \int_0^t \left\| \frac{\partial}{\partial t} \theta_0 \right\|_{L^2}^2 ds + \frac{9c_5^2 (c_1 c_2 d \beta \|g\|_{L^\infty})^2}{\lambda \eta^2} \int_0^t \|f\|_{L^2}^2 ds \\
& + \frac{3(c_6 d \|g\|_{L^\infty})^2}{2\lambda} \int_0^t ds, \quad 0 \leq t \leq T
\end{aligned} \tag{1.37}$$

According to Lemma (1.4.2), we can choose θ_0 satisfying the estimate

$$\frac{9c_3^2 (c_1 c_2 d \beta \|g\|_{L^\infty})^2}{\lambda^2 \eta^2} \|\theta_0\|_p^2 < 1$$

Then, we have θ_0 satisfies the inequality

$$\begin{aligned}
\|\theta_0\|_p^2 & < \frac{\lambda^2 \eta^2}{9c_3^2 (c_1 c_2 d \beta \|g\|_{L^\infty})^2} \\
\|\theta_0\|_p & < \frac{\lambda \eta}{3c_1 c_2 c_3 d \beta \|g\|_{L^\infty}}
\end{aligned} \tag{1.38}$$

For a sufficiently high viscosity and taking $p = 4$, we pose

$$\bar{\lambda} = \lambda - \frac{9c_3^2 (c_1 c_2 d \beta \|g\|_{L^\infty})^2}{\lambda \eta^2} \sup_{0 \leq t \leq T} \|\theta_0\|_4^2$$

Using Lemma (1.4.2) we have

$$\begin{aligned}
& \|u^{(m)}(t)\|_{L^2}^2 + \bar{\lambda} \int_0^t \|\nabla u^{(m)}(s)\|_{L^2}^2 ds + a \int_0^t \|u^{(m)}(s)\|_{L^2}^2 ds + b \int_0^t \|u^{(m)}(s)\|_{L^3}^3 ds \\
& \leq \|u_{m0}\|_{L^2}^2 + \frac{3(c_1 c_2 d \beta \|g\|_{L^\infty})^2}{\lambda \eta} \|\theta_{m0}\|_{L^2}^2 + \frac{3(c_1 d \beta \|g\|_{L^\infty})^2}{2\lambda} \int_0^t \|\theta_{in}(s)\|_{L^2}^2 ds \\
& + \frac{9c_3^2 (c_1 c_2 d \beta \|g\|_{L^\infty})^2}{\lambda \eta^2} \int_0^t \|\theta_0(s)\|_{L^4}^2 ds + \frac{9c_4^2 (c_1 c_2 d \beta \|g\|_{L^\infty})^2}{\lambda \eta^2} \int_0^t \left\| \frac{\partial}{\partial t} \theta_0 \right\|_{L^2}^2 ds \\
& + \frac{9c_5^2 (c_1 c_2 d \beta \|g\|_{L^\infty})^2}{\lambda \eta^2} \int_0^t \|f\|_{L^2}^2 ds + \frac{3(c_6 d \|g\|_{L^\infty})^2}{2\lambda} \int_0^t ds, \quad 0 \leq t \leq T
\end{aligned}$$

$$\begin{aligned}
& \|u^{(m)}(t)\|_{L^2}^2 + \bar{\lambda} \int_0^t \|\nabla u^{(m)}(s)\|_{L^2}^2 ds + a \int_0^t \|u^{(m)}(s)\|_{L^2}^2 ds + b \int_0^t \|u^{(m)}(s)\|_{L^3}^3 ds \\
& \leq \|u_{m0}\|_{L^2}^2 + \frac{3(c_1 c_2 d \beta \|g\|_{L^\infty})^2}{\lambda \eta} \|\theta_{m0}\|_{L^2}^2 + \frac{3(c_1 d \beta \|g\|_{L^\infty})^2}{2\lambda} \int_0^t \|\theta_{in}(s)\|_{L^2}^2 ds \\
& + \frac{9(c_1 c_2 d \beta \|g\|_{L^\infty})^2}{\lambda \eta^2} \left(c_3^2 \int_0^t \|\theta_0(s)\|_{L^4}^2 + c_4^2 \int_0^t \left\| \frac{\partial}{\partial t} \theta_0 \right\|_{L^2}^2 + c_5^2 \int_0^t \|f\|_{L^2}^2 \right) ds \\
& + \frac{3(c_6 d \|g\|_{L^\infty})^2}{2\lambda} \int_0^t ds, \quad 0 \leq t \leq T
\end{aligned} \tag{1.39}$$

The right hand side of (1.39) is bounded by a constant independent of m . The sequence $\{u^{(m)}(t)\}_m$ is a bounded sequence in $L^2([0, T], V)$ and $L^\infty([0, T], H)$. Even, $\{\theta^{(m)}(t)\}_m$ is a bounded sequence in $L^2([0, T], W)$ and in $L^\infty([0, T], L^2(\Omega))$. So we can choose a subsequences of $u^{(m)}$ and $\theta^{(m)}$ such that :

$$\begin{aligned}
u^m & \rightharpoonup u \quad \text{weakly} && \text{in } L^2([0, T], V), \\
u^m & \rightharpoonup u \quad \text{weakly-star} && \text{in } L^\infty([0, T], H), \\
|u^m| & u^m \rightharpoonup v \quad \text{weakly} && \text{in } L^{3/2}([0, T], L^{3/2}(\Omega)), \\
\theta^m & \rightharpoonup \theta \quad \text{weakly} && \text{in } L^2([0, T], W), \\
\theta^m & \rightharpoonup \theta \quad \text{weakly-star} && \text{in } L^\infty([0, T], L^2(\Omega)),
\end{aligned} \tag{1.40}$$

■

We consider γ a real positive constant and want to show that the sequence $\{|\tau|^\gamma \hat{u}^{(m)}(\tau)\}_m$ is bounded in $L^2(\mathbb{R} : H)$ and $\{|\tau|^\gamma \hat{\theta}^{(m)}(\tau)\}_m$ is bounded in $L^2(\mathbb{R} : L^2(\Omega))$, for some $\gamma > 0$, where $\hat{u}^{(m)}$ and $\hat{\theta}^{(m)}$ denotes the Fourier transform of extension $\tilde{u}^{(m)}$, $\tilde{\theta}^{(m)}$ respectively of $u^{(m)}$, $\theta^{(m)}$, that is :

$$\begin{aligned}
\tilde{u}^{(m)}(t) &= \begin{cases} u^{(m)}, & 0 \leq t \leq T \\ 0 & \text{otherwise} \end{cases} \\
\tilde{\theta}^{(m)}(t) &= \begin{cases} \theta^{(m)}, & 0 \leq t \leq T \\ 0 & \text{otherwise} \end{cases}
\end{aligned}$$

where $\hat{u}^{(m)}$, $\hat{\theta}^{(m)}$ given by

$$\begin{aligned}
\hat{u}^{(m)}(\tau) &= \int_{\mathbb{R}} e^{2i\pi t \tau} \tilde{u}^{(m)}(t) dt \\
\hat{\theta}^{(m)}(\tau) &= \int_{\mathbb{R}} e^{2i\pi t \tau} \tilde{\theta}^{(m)}(t) dt
\end{aligned}$$

For this pupose, we observe that

$$\frac{d}{dt} \langle \tilde{u}^{(m)}, u_k \rangle = \langle \tilde{h}_m, u_k \rangle + \langle u_0^{(m)}, u_k \rangle \delta(0) - \langle u^{(m)}(T), u_k \rangle \delta(T) \quad 1 \leq k \leq m \quad (1.41)$$

where $\delta(0)$, $\delta(T)$ are Dirac distributions at 0 and T ,

We pose :

$$h_m = -\lambda A u^{(m)} - B u^{(m)} - a u^{(m)} - b |u^{(m)}| u^{(m)} + dg [\beta (\theta^{(m)} - \theta_{in}) - 1]$$

with

$$\tilde{h}^{(m)}(t) = \begin{cases} h^{(m)}, & 0 \leq t \leq T \\ 0 & \text{outside} \end{cases}$$

Since

$$2i\pi\tau \langle \hat{u}^{(m)}, u_k \rangle = \langle \hat{h}_m, u_k \rangle + \langle u_0^{(m)}, u_k \rangle - \langle u^{(m)}(T), u_k \rangle e^{2i\pi T\tau} \quad 1 \leq k \leq m$$

Let $\hat{f}_i^{(m)}(\tau)$ the Fourier transform of $f_i^{(m)}(\tau)$ for $i = 1, \dots, m$ we get

$$2i\pi\tau \|\hat{u}^{(m)}\|^2 = \langle \hat{h}_m, \hat{u}^{(m)} \rangle + \langle u_0^{(m)}, \hat{u}^{(m)} \rangle - \langle u^{(m)}(T), \hat{u}^{(m)} \rangle e^{2i\pi T\tau} \quad (1.42)$$

Note that

$$\begin{aligned} \int_0^T \|h_m(t)\|_{V'} dt &\leq \int_0^T \left(\lambda \|u^{(m)}(t)\| + C \|u^{(m)}(t)\|^2 + a \|u^{(m)}(t)\| + b \|u^{(m)}(t)\|^2 \right) dt \\ &\quad + \int_0^T (\|dg(\beta\theta_{in} - 1)\| + C \|\theta^m\|) dt \end{aligned}$$

and this remains bounded according to (1.34)-(1.35) and (1.39).

Thus

$$\sup_{\tau \in \mathbb{R}} \|\hat{h}_m(\tau)\|_{V'} \leq Const \quad \forall m \quad (1.43)$$

Combining (1.42) and (1.43), we deduce that

$$|\tau| \|\hat{u}^{(m)}\|^2 \leq C \|\hat{u}_m(\tau)\|$$

For fixed $\gamma \leq \frac{1}{4}$, $|\tau|^{2\gamma} \leq C \frac{1+|\tau|}{1+|\tau|^{1-2\gamma}}, \forall \tau \in \mathbb{R}$

Consequently

$$\begin{aligned} \int_{-\infty}^{+\infty} |\tau|^{2\gamma} \|\hat{u}^{(m)}(\tau)\|^2 d\tau &\leq C \int_{-\infty}^{+\infty} \frac{1+|\tau|}{1+|\tau|^{1-2\gamma}} \|\hat{u}^{(m)}(\tau)\|^2 d\tau \\ &\leq \frac{\|\hat{u}^{(m)}(\tau)\| d\tau}{1+|\tau|^{1-2\gamma}} + C \int_{-\infty}^{+\infty} \|\hat{u}^{(m)}(\tau)\|^2 d\tau \end{aligned}$$

Because of (1.39) and Parseval equality, the last integral remains bounded as $m \rightarrow +\infty$.

The first integral is bounded for $\gamma < \frac{1}{4}$ by combining Schwarz and Parseval inequalities. We conclude that for $0 < \gamma < \frac{1}{4}$

$$\int_{\mathbb{R}} |\tau|^{2\gamma} \|\hat{u}^{(m)}(\tau)\|^2 d\tau < +\infty$$

with a similar approach, we prove that

$$\int_{\mathbb{R}} |\tau|^{2\gamma} \|\hat{\theta}^{(m)}(\tau)\|^2 d\tau < +\infty \quad \text{for some } 0 < \gamma < \frac{1}{4}$$

Therefore, by Theorem 2.2, Chap. 3 [29], we can select subsequences which we denote by the same symbol such that

$$\begin{aligned} u^m &\rightarrow u \quad \text{strongly in } L^2([0, T], H), \\ \theta^m &\rightarrow \tilde{\theta} \quad \text{strongly in } L^2([0, T], L^2(\Omega)), \end{aligned} \tag{1.44}$$

and $u, \theta (= \tilde{a} + \theta_0)$ satisfy (1.23)-(1.24) for any $v = u_i, \tau = \theta_j$.

To conclude, we need to demonstrate that $v = |u|u$. To achieve this, we refer the reader to [30] and apply the same technique to get $|u^{(m)}|u^{(m)} \rightharpoonup |u|u$ weak in $L^{3/2}([0, T], L^{3/2}(\Omega))$ and get $v = |u|u$. Theorem (1.4.7) is proved.

1.5 Approximation by the artificial compressibility method

The artificial compressibility method was introduced in order to manage the difficulty induced by the incompressibility constraints in the numerical approximations of the Navier-Stokes equations. The method proposed by Chorin [11] and investigated later by Temam [12]. In this section we study the coupled system of Navier Stokes Forchheimer equations and the Fourier equation through the method of artificial compressibility. We prove the existence of the weak solution and show how the perturbed problem converge to the solution of the state system Navier-Stokes Forchheimer Fourier system when $\varepsilon \rightarrow 0$ ($\varepsilon > 0$ is arbitrary). The artificial compressibility method that we propose to study is to approximate the solution (u, θ, p) of the incompressible Navier-Stokes Forchheimer Fourier equations $(u_\varepsilon, \theta_\varepsilon, p_\varepsilon)$ satisfying the following perturbed system

$$\left\{ \begin{array}{l}
 \partial_t u_\varepsilon + (u_\varepsilon \cdot \nabla) u_\varepsilon + a u_\varepsilon + b |u_\varepsilon| u_\varepsilon = -\nabla p_\varepsilon + \lambda \Delta u_\varepsilon + dg [\beta (\theta_\varepsilon - \theta_{in}) - 1] \quad \Omega \times [0, T] \\
 \partial_t \theta_\varepsilon + (u_\varepsilon \cdot \nabla) \theta_\varepsilon = \eta \Delta \theta_\varepsilon + f \quad \text{in } \Omega \times [0, T] \\
 \varepsilon \partial_t p_\varepsilon + \nabla \cdot u_\varepsilon = 0 \quad \text{in } \Omega \times [0, T] \\
 u_\varepsilon(x, t = 0) = a_0(x) \quad \text{in } \Omega \\
 \theta_\varepsilon(x, t = 0) = \tau_0(x) \quad \text{in } \Omega \\
 p_\varepsilon(x, t = 0) = \pi_0(x) \quad \text{in } \Omega \\
 u_\varepsilon(x, t) = 0 \quad \text{on } \Gamma_1 \\
 \theta_\varepsilon(x, t) = \xi(x, t) \quad \text{on } \Gamma_1 \\
 p_\varepsilon(x, t) = 0 \quad \text{on } \Gamma_1 \\
 u_\varepsilon(x, t) = 0 \quad \text{on } (\Gamma_B \cup \Gamma_s) \times [0, T] \\
 \frac{\partial \theta_\varepsilon}{\partial n} = 0 \quad \text{on } (\Gamma_B \cup \Gamma_s) \times [0, T]
 \end{array} \right. \tag{1.45}$$

where $\pi_0 \in L^2(\Omega)$ is arbitrary and independent of ε

1.5.1 Existence of solutions of the perturbed problem

Let $f \in L^2([0, T]; L^2(\Omega))$, $a_0 \in L^2(\Omega)$, $\tau_0 \in L^2(\Omega)$ and $\pi_0 \in L^2(\Omega)$ are verified, the problem (1.45) is equivalent to the variational formulation : Find $u_\varepsilon \in L^2([0, T]; V)$, $(\theta_\varepsilon - \theta_0) \in L^2([0, T]; W)$ and $p_\varepsilon \in L^2([0, T]; L^2(\Omega))$ such that

$$\begin{aligned}
 & \frac{d}{dt} \langle u_\varepsilon, v \rangle + B \langle u_\varepsilon, u_\varepsilon, v \rangle + \langle a u_\varepsilon, v \rangle + \langle b |u_\varepsilon| u_\varepsilon, v \rangle - \langle p_\varepsilon, \nabla \cdot v \rangle \\
 & = -\lambda \langle \nabla u_\varepsilon, \nabla v \rangle + \langle d\beta g \theta_\varepsilon, v \rangle - \langle d\beta g \theta_{in}, v \rangle - \langle dg, v \rangle \quad \forall v \in \tilde{V}
 \end{aligned} \tag{1.46}$$

$$\frac{d}{dt} \langle \theta_\varepsilon, \tau \rangle + \tilde{B} \langle u_\varepsilon, \theta_\varepsilon, \tau \rangle = -\eta \langle \nabla \theta_\varepsilon, \nabla \tau \rangle + \langle f, \tau \rangle \quad \forall \tau \in \tilde{W} \tag{1.47}$$

$$\langle \nabla \cdot u_\varepsilon, q \rangle = -\langle \varepsilon \partial_t p_\varepsilon, q \rangle \quad \forall q \in L^2(\Omega) \tag{1.48}$$

Theorem 1.5.1. *For $\varepsilon > 0$ fixed, let $f \in L^2([0, T]; L^2(\Omega))$. if $g \in L^\infty(\Omega \times [0, T])$, $\xi \in C^1(\bar{\Gamma}_1 \times [0, T])$, $\tau_0 \in L^2(\Omega)$, $a_0 \in H$, $\theta_{in} \in L^2(\Omega)$ and a, b are a positive constant $a > 0$, $b > 0$ and suppose that $(d\beta \|g\|_{L^\infty}) < c\sqrt{\lambda}\eta$ (with $c > 0$). Then, there exists at least one solution $(u_\varepsilon, \theta_\varepsilon, p_\varepsilon)$ of perturbed problems (1.45). Moreover,*

$$\begin{aligned}
 u_\varepsilon & \in L^\infty([0, T]; H) \\
 \theta_\varepsilon & \in L^\infty([0, T]; L^2(\Omega)) \\
 p_\varepsilon & \in L^\infty([0, T]; L^2(\Omega))
 \end{aligned}$$

Proof. To prove the well-posedness of the problem (1.46), (1.47) and (1.48), we will use the Faedo-Galerkin method.

$$u_\varepsilon^{(m)}(t) = \sum_{i=1}^m \Psi_i^{(m)} u_i \quad (1.49)$$

$$\theta_\varepsilon^{(m)}(t) = \sum_{j=1}^m \Phi_j^{(m)} \theta_j \quad (1.50)$$

$$p_\varepsilon^{(m)}(t) = \sum_{l=1}^m \xi_l^{(m)} r_l \quad (1.51)$$

Where the coefficients u_i , θ_j and r_l satisfy the system

$$\begin{aligned} \frac{d}{dt} \langle u_\varepsilon^{(m)}, u_k \rangle + B \langle u_\varepsilon^{(m)}, u_\varepsilon^{(m)}, u_k \rangle + \langle a u_\varepsilon^{(m)}, u_k \rangle + \langle b | u_\varepsilon^{(m)} | u_\varepsilon^{(m)}, u_k \rangle - \langle p_\varepsilon^{(m)}, \nabla \cdot u_k \rangle \\ = -\lambda \langle \nabla u_\varepsilon^{(m)}, \nabla u_k \rangle + \langle d\beta g \theta_\varepsilon^{(m)}, u_k \rangle - \langle d\beta g \theta_{in}, u_k \rangle - \langle dg, u_k \rangle \quad k = \{1, \dots, m\} \end{aligned} \quad (1.52)$$

$$\frac{d}{dt} \langle \theta_\varepsilon^{(m)}, \theta_k \rangle + \tilde{B} \langle u_\varepsilon^{(m)}, \theta_\varepsilon^{(m)}, \theta_k \rangle = -\eta \langle \nabla \theta_\varepsilon^{(m)}, \nabla \theta_k \rangle + \langle f, \theta_k \rangle \quad (1.53)$$

$$\langle \nabla \cdot u_\varepsilon^{(m)}, r_k \rangle = -\langle \varepsilon \partial_t p_\varepsilon^{(m)}, r_k \rangle \quad k = \{1, \dots, m\} \quad (1.54)$$

with the following initial boundary conditions

$$u_\varepsilon^{(m)}(0, x) = u_{0m}, \quad \theta_\varepsilon^{(m)}(0, x) = \theta_{0m}, \quad p_\varepsilon^{(m)}(0, x) = p_{0m} \quad (1.55)$$

were u_{0m} , θ_{0m} and p_{0m} are the orthogonal projections of u_0 , θ_0 and p_0 onto the subspaces spanned by $\{u^{(1)}, \dots, u^{(m)}\}$, $\{\theta^{(1)}, \dots, \theta^{(m)}\}$ et $\{r^{(1)}, \dots, r^{(m)}\}$ in $\mathbf{L}^2(\Omega)$ for each component. There exist a solution $u_\varepsilon^{(m)}(t)$, $\theta_\varepsilon^{(m)}(t)$ and $p_\varepsilon^{(m)}(t)$ for any $0 \leq t \leq T_m$. In the first step, we multiply (1.52) (1.53) (1.54) by $\Psi_k^{(m)}$, $\Phi_k^{(m)}$ and $\xi_k^{(m)}$ respectively, and we sum over k , we get

$$\begin{aligned} \left\langle \frac{\partial}{\partial t} u_\varepsilon^{(m)}, u_\varepsilon^{(m)} \right\rangle + B \langle u_\varepsilon^{(m)}, u_\varepsilon^{(m)}, u_\varepsilon^{(m)} \rangle + \langle a u_\varepsilon^{(m)}, u_\varepsilon^{(m)} \rangle + \langle b | u_\varepsilon^{(m)} | u_\varepsilon^{(m)}, u_\varepsilon^{(m)} \rangle - \langle p_\varepsilon^{(m)}, \nabla \cdot u_\varepsilon^{(m)} \rangle \\ = -\lambda \langle \nabla u_\varepsilon^{(m)}, \nabla u_\varepsilon^{(m)} \rangle + \langle d\beta g \theta_\varepsilon^{(m)}, u_\varepsilon^{(m)} \rangle - \langle d\beta g \theta_{in}, u_\varepsilon^{(m)} \rangle - \langle dg, u_\varepsilon^{(m)} \rangle \end{aligned} \quad (1.56)$$

Substituting $\nabla \cdot u_\varepsilon^{(m)} = -\varepsilon \partial_t p_\varepsilon^{(m)}$ in (1.56) we get

$$\begin{aligned} \left\langle \frac{\partial}{\partial t} u_\varepsilon^{(m)}, u_\varepsilon^{(m)} \right\rangle + B \langle u_\varepsilon^{(m)}, u_\varepsilon^{(m)}, u_\varepsilon^{(m)} \rangle + \langle a u_\varepsilon^{(m)}, u_\varepsilon^{(m)} \rangle + \langle b | u_\varepsilon^{(m)} | u_\varepsilon^{(m)}, u_\varepsilon^{(m)} \rangle - \langle p_\varepsilon^{(m)}, -\varepsilon \partial_t p_\varepsilon^{(m)} \rangle \\ = -\lambda \langle \nabla u_\varepsilon^{(m)}, \nabla (u_\varepsilon^{(m)}) \rangle + \langle d\beta g \theta_\varepsilon^{(m)}, u_\varepsilon^{(m)} \rangle - \langle d\beta g \theta_{in}, u_\varepsilon^{(m)} \rangle - \langle dg, u_\varepsilon^{(m)} \rangle \end{aligned} \quad (1.57)$$

$$\begin{aligned} & \frac{1}{2} \frac{d}{dt} \left(\|u_\varepsilon^{(m)}\|_{L^2}^2 + \varepsilon \|p_\varepsilon^{(m)}\|_{L^2}^2 \right) + \lambda \|\nabla u_\varepsilon^{(m)}\|_{L^2}^2 + a \|u_\varepsilon^{(m)}\|_{L^2}^2 + b \|u_\varepsilon^{(m)}\|_{L^3}^3 \\ & = \left\langle d\beta g \theta_\varepsilon^{(m)}, u_\varepsilon^{(m)} \right\rangle - \left\langle d\beta g \theta_{in}, u_\varepsilon^{(m)} \right\rangle - \left\langle dg, u_\varepsilon^{(m)} \right\rangle \end{aligned} \quad (1.58)$$

Using Schwarz and Poincaré's inequality for the right hand side of (1.58), we have

$$\begin{aligned} & \frac{1}{2} \frac{d}{dt} \left(\|u_\varepsilon^{(m)}\|_{L^2}^2 + \varepsilon \|p_\varepsilon^{(m)}\|_{L^2}^2 \right) + \lambda \|\nabla u_\varepsilon^{(m)}\|_{L^2}^2 + a \|u_\varepsilon^{(m)}\|_{L^2}^2 + b \|u_\varepsilon^{(m)}\|_{L^3}^3 \\ & \leq c_7 d\beta \|g\|_{L^\infty} \|\theta_\varepsilon^{(m)}\|_{L^2} \|\nabla u_\varepsilon^{(m)}\|_{L^2} + c_8 d\beta \|g\|_{L^\infty} \|\theta_{in}\|_{L^2} \|\nabla u_\varepsilon^{(m)}\|_{L^2} + c_9 d \|g\|_{L^\infty} \|\nabla u_\varepsilon^{(m)}\|_{L^2} \\ & \frac{1}{2} \frac{d}{dt} \left(\|u_\varepsilon^{(m)}\|_{L^2}^2 + \varepsilon \|p_\varepsilon^{(m)}\|_{L^2}^2 \right) + \lambda \|\nabla u_\varepsilon^{(m)}\|_{L^2}^2 + a \|u_\varepsilon^{(m)}\|_{L^2}^2 + b \|u_\varepsilon^{(m)}\|_{L^3}^3 \\ & \leq \frac{3(c_7 d\beta \|g\|_{L^\infty})^2}{2\lambda} \|\theta_\varepsilon^{(m)}\|_{L^2}^2 + \frac{\lambda}{6} \|\nabla u_\varepsilon^{(m)}\|_{L^2}^2 + \frac{3(c_8 d\beta \|g\|_{L^\infty})^2}{2\lambda} \|\theta_{in}\|_{L^2}^2 + \frac{\lambda}{6} \|\nabla u_\varepsilon^{(m)}\|_{L^2}^2 \\ & + \frac{3(c_9 d \|g\|_{L^\infty})^2}{2\lambda} + \frac{\lambda}{6} \|\nabla u_\varepsilon^{(m)}\|_{L^2}^2 \end{aligned}$$

$$\begin{aligned} & \frac{1}{2} \frac{d}{dt} \left(\|u_\varepsilon^{(m)}\|_{L^2}^2 + \varepsilon \|p_\varepsilon^{(m)}\|_{L^2}^2 \right) + \lambda \|\nabla u_\varepsilon^{(m)}\|_{L^2}^2 + a \|u_\varepsilon^{(m)}\|_{L^2}^2 + b \|u_\varepsilon^{(m)}\|_{L^3}^3 \\ & \leq \frac{3(c_7 d\beta \|g\|_{L^\infty})^2}{2\lambda} \|\theta_\varepsilon^{(m)}\|_{L^2}^2 + \frac{3(c_8 d\beta \|g\|_{L^\infty})^2}{2\lambda} \|\theta_{in}\|_{L^2}^2 + \frac{3(c_9 d \|g\|_{L^\infty})^2}{2\lambda} \end{aligned} \quad (1.59)$$

And for the Fourier system, we have

$$\frac{1}{2} \frac{d}{dt} \|\theta_\varepsilon^{(m)}\|_{L^2}^2 + \frac{\eta}{2} \|\nabla \theta_\varepsilon^{(m)}\|_{L^2}^2 \leq \frac{c_{10}}{\eta} \|\theta_{0m}\|_{L^4}^2 \|\nabla u_\varepsilon^{(m)}\|_{L^2}^2 + \frac{c_{11}^2}{\eta} \left\| \frac{\partial}{\partial t} \theta_{0m} \right\|_{L^2}^2 + \frac{c_{12}^2}{\eta} \|f\|_{L^2}^2 \quad (1.60)$$

Integrating both side of (1.59) and (1.60) over the interval $[0, t]$ we get

$$\begin{aligned} & \|u_\varepsilon^{(m)}\|_{L^2}^2 + \varepsilon \|p_\varepsilon^{(m)}\|_{L^2}^2 + \lambda \int_0^t \|\nabla u_\varepsilon^{(m)}(s)\|_{L^2}^2 ds + a \int_0^t \|u_\varepsilon^{(m)}(s)\|_{L^2}^2 ds + b \int_0^t \|u_\varepsilon^{(m)}(s)\|_{L^3}^3 ds \\ & \leq \|u_{0m}(s)\|_{L^2}^2 + \varepsilon \|p_{0m}\|_{L^2}^2 + \frac{3(c_7 d\beta \|g\|_{L^\infty})^2}{2\lambda} \int_0^t \|\theta_\varepsilon^{(m)}\|_{L^2}^2 ds + \frac{3(c_8 d\beta \|g\|_{L^\infty})^2}{2\lambda} \int_0^t \|\theta_{in}(s)\|_{L^2}^2 ds \\ & + \frac{3(c_9 d \|g\|_{L^\infty})^2}{2\lambda} \int_0^t ds \end{aligned} \quad (1.61)$$

$$\|\theta_\varepsilon^{(m)}\|_{L^2}^2 + \frac{\eta}{2} \int_0^t \|\nabla \theta_\varepsilon^{(m)}(s)\|_{L^2}^2 ds \leq \frac{3c_{10}}{2\eta} \|\theta_{0m}\|_{L^4}^2 \|\nabla u_\varepsilon^{(m)}\|_{L^2}^2 + \frac{3c_{11}^2}{2\eta} \int_0^t \left\| \frac{\partial}{\partial s} \theta_{0m} \right\|_{L^2}^2 ds + \frac{3c_{12}^2}{2\eta} \int_0^t \|f\|_{L^2}^2 ds \quad (1.62)$$

From the equation (1.62)

$$\int_0^t \|\nabla \theta_\varepsilon^{(m)}(s)\|_{L^2}^2 ds \leq \frac{3c_{10}}{\eta^2} \int_0^t \|\theta_{0m}\|_{L^4}^2 \|\nabla u_\varepsilon^{(m)}\|_{L^2}^2 - \|\theta_\varepsilon^{(m)}\|_{L^2}^2 + \frac{3c_{11}^2}{\eta^2} \int_0^t \left\| \frac{\partial}{\partial s} \theta_{0m} \right\|_{L^2}^2 ds + \frac{3c_{12}^2}{\eta^2} \int_0^t \|f\|_{L^2}^2 ds \quad (1.63)$$

Thanks to Poincaré inequality, and using (1.63) in (1.61) we get

$$\begin{aligned} & \|u_\varepsilon^{(m)}\|_{L^2}^2 + \varepsilon \|p_\varepsilon^{(m)}\|_{L^2}^2 + \lambda \int_0^t \|\nabla u_\varepsilon^{(m)}(s)\|_{L^2}^2 ds + a \int_0^t \|u_\varepsilon^{(m)}(s)\|_{L^2}^2 ds + b \int_0^t \|u_\varepsilon^{(m)}(s)\|_{L^3}^3 ds \\ & \leq \|u_{0m}\|_{L^2}^2 + \varepsilon \|p_{0m}\|_{L^2}^2 + \frac{9(c_7 c_{10} c_{13} d \beta \|g\|_{L^\infty})^2}{\lambda \eta^2} \|\theta_{0m}\|_{L^4}^2 \|\nabla u_\varepsilon^{(m)}\|_{L^2}^2 \\ & + \frac{9(c_7 c_{11} c_{13} d \beta \|g\|_{L^\infty})^2}{\lambda \eta^2} \int_0^t \left\| \frac{\partial}{\partial s} \theta_{0m} \right\|_{L^2}^2 ds + \frac{9(c_7 c_{12} c_{13} d \beta \|g\|_{L^\infty})^2}{\lambda \eta^2} \int_0^t \|f\|_{L^2}^2 ds \\ & + \frac{3(c_8 d \beta \|g\|_{L^\infty})^2}{2\lambda} \int_0^t \|\theta_{in}(s)\|_{L^2}^2 ds + \frac{3(c_9 d \|g\|_{L^\infty})^2}{2\lambda} \int_0^t ds \end{aligned}$$

For a sufficiently high viscosity, we pose

$$\bar{\lambda} = \lambda - \frac{9(c_7 c_{10} c_{13} d \beta \|g\|_{L^\infty})^2}{\lambda \eta^2} \sup_{0 \leq t \leq T} \|\theta_{\varepsilon 0}\|_4^2$$

$$\begin{aligned} & \|u_\varepsilon^{(m)}\|_{L^2}^2 + \varepsilon \|p_\varepsilon^{(m)}\|_{L^2}^2 + \bar{\lambda} \int_0^t \|\nabla u_\varepsilon^{(m)}(s)\|_{L^2}^2 ds + a \int_0^t \|u_\varepsilon^{(m)}(s)\|_{L^2}^2 ds + b \int_0^t \|u_\varepsilon^{(m)}(s)\|_{L^3}^3 ds \\ & \leq \|u_{0m}\|_{L^2}^2 + \varepsilon \|p_{0m}\|_{L^2}^2 + \frac{9(c_{13} c_7 d \beta \|g\|_{L^\infty})^2}{\lambda \eta^2} \left(c_{10}^2 \|\theta_{0m}\|_{L^4}^2 + c_{11}^2 \int_0^t \left\| \frac{\partial}{\partial s} \theta_{0m} \right\|_{L^2}^2 ds + c_{12}^2 \int_0^t \|f\|_{L^2}^2 ds \right) \\ & \frac{3(c_8 d \beta \|g\|_{L^\infty})^2}{2\lambda} \int_0^t \|\theta_{in}(s)\|_{L^2}^2 ds + \frac{3(c_9 d \|g\|_{L^\infty})^2}{2\lambda} \int_0^t ds \end{aligned} \quad (1.64)$$

The right hand side of (1.64) is bounded by a constant independant of m . The sequence $\{u_\varepsilon^{(m)}\}_m$ is bounded sequence in $L^2([0, T], V)$ and in $L^\infty([0, T], H)$, $\{\theta_\varepsilon^{(m)}\}_m$ is bounded sequence in $L^2([0, T], W)$ and in $L^\infty([0, T], L^2(\Omega))$. $\{p_\varepsilon^{(m)}\}_m$ is bounded sequence in $L^\infty([0, T], L^2(\Omega))$. So we can choose a subsequences of $u_\varepsilon^{(m)}$, $\theta_\varepsilon^{(m)}$ and $p_\varepsilon^{(m)}$ such that :

$$\begin{aligned} u_\varepsilon^m & \rightharpoonup u_\varepsilon \quad \text{weakly} & \text{in } L^2([0, T], V), \\ u_\varepsilon^m & \rightharpoonup u_\varepsilon \quad \text{weakly-star} & \text{in } L^\infty([0, T], H), \\ |u_\varepsilon^m| & u_\varepsilon^m \rightharpoonup v \quad \text{weakly} & \text{in } L^{\frac{3}{2}}([0, T], L^{\frac{3}{2}}(\Omega)), \\ \theta_\varepsilon^m & \rightharpoonup \theta_\varepsilon \quad \text{weakly} & \text{in } L^2([0, T], W), \\ \theta_\varepsilon^m & \rightharpoonup \theta_\varepsilon \quad \text{weakly-star} & \text{in } L^\infty([0, T], L^2(\Omega)), \\ \sqrt{\varepsilon} p_\varepsilon^m & \rightharpoonup \sqrt{\varepsilon} p_\varepsilon \quad \text{weakly-star} & \text{in } L^\infty([0, T], L^2(\Omega)) \end{aligned} \quad (1.65)$$

■

We have the following inequality from (1.64)

$$\sup_{t \in [0, T]} \left(\|u_\varepsilon^{(m)}\|_{L^2}^2 + \varepsilon \|p_\varepsilon^{(m)}\|_{L^2}^2 \right) \leq C_1 \quad (1.66)$$

$$\int_0^t \|\nabla u_\varepsilon^{(m)}(s)\|_{L^2}^2 ds \leq \frac{C_1}{\lambda} \quad (1.67)$$

$$\int_0^t \|u_\varepsilon^{(m)}(s)\|_{L^2}^2 ds \leq \frac{C_1}{a} \quad (1.68)$$

$$\int_0^t \|u_\varepsilon^{(m)}(s)\|_{L^3}^3 ds \leq \frac{C_1}{b} \quad (1.69)$$

where

$$\begin{aligned} C_1 = & \|u_{0m}\|_{L^2}^2 + \varepsilon \|p_{0m}\|_{L^2}^2 + \frac{9(c_{13}c_7d\beta\|g\|_{L^\infty})^2}{\lambda\eta^2} \left(c_{10}^2 \|\theta_{0m}\|_{L^4}^2 + c_{11}^2 \int_0^t \left\| \frac{\partial}{\partial s} \theta_{0m} \right\|_{L^2}^2 ds + c_{12}^2 \int_0^t \|f\|_{L^2}^2 ds \right) \\ & \frac{3(c_8d\beta\|g\|_{L^\infty})^2}{2\lambda} \int_0^t \|\theta_{in}(s)\|_{L^2}^2 ds + \frac{3(c_9d\|g\|_{L^\infty})^2}{2\lambda} \int_0^t ds \end{aligned} \quad (1.70)$$

We consider $\hat{u}_\varepsilon^{(m)}, \hat{\theta}_\varepsilon^{(m)}, \hat{p}_\varepsilon^{(m)}$ the Fourier transform of extension $\tilde{u}_\varepsilon^{(m)}, \tilde{\theta}_\varepsilon^{(m)}, \tilde{p}_\varepsilon^{(m)}$ respectively of $u_\varepsilon^{(m)}, \theta^{(m)}$ and $p_\varepsilon^{(m)}$, that is :

$$\tilde{u}_\varepsilon^{(m)}(t) = \begin{cases} u_\varepsilon^{(m)}, & 0 \leq t \leq T \\ 0 & \text{otherwise} \end{cases}$$

$$\tilde{\theta}_\varepsilon^{(m)}(t) = \begin{cases} \theta_\varepsilon^{(m)}, & 0 \leq t \leq T \\ 0 & \text{otherwise} \end{cases}$$

$$\tilde{p}_\varepsilon^{(m)}(t) = \begin{cases} p_\varepsilon^{(m)}, & 0 \leq t \leq T \\ 0 & \text{otherwise} \end{cases}$$

where $\hat{u}_\varepsilon^{(m)}, \hat{\theta}_\varepsilon^{(m)}$ and $\hat{p}_\varepsilon^{(m)}$ given by

$$\hat{u}_\varepsilon^{(m)}(\tau) = \int_{\mathbb{R}} e^{2i\pi t\tau} \tilde{u}_\varepsilon^{(m)}(t) dt$$

$$\hat{\theta}_\varepsilon^{(m)}(\tau) = \int_{\mathbb{R}} e^{2i\pi t\tau} \tilde{\theta}_\varepsilon^{(m)}(t) dt$$

$$\hat{p}_\varepsilon^{(m)}(\tau) = \int_{\mathbb{R}} e^{2i\pi t\tau} \tilde{p}_\varepsilon^{(m)}(t) dt$$

Then, we obtain

$$\begin{aligned} \frac{d}{dt} \langle \tilde{u}_\varepsilon^{(m)}, u_k \rangle + \langle \tilde{p}_\varepsilon^{(m)}, \nabla \cdot u_k \rangle &= \langle \varpi_m, u_k \rangle + \langle u_{\varepsilon 0}^{(m)}, u_k \rangle \delta(0) \\ &\quad - \langle u_\varepsilon^{(m)}(T), u_k \rangle \delta(T) \quad k = \{1, \dots, m\} \end{aligned} \quad (1.71)$$

$$\langle \nabla \cdot \tilde{u}_\varepsilon^{(m)}, r_k \rangle + \langle \varepsilon \partial_t \tilde{p}_\varepsilon^{(m)}, r_k \rangle = \langle p_{\varepsilon 0}^{(m)}, r_k \rangle \delta(0) - \langle p_\varepsilon^{(m)}(T), r_k \rangle \delta(T) \quad (1.72)$$

where $\delta(0)$ and $\delta(T)$ are Dirac distributions at $t = 0$ and $t = T$ respectively.

and

$$\varpi_m = -\lambda A u_\varepsilon^{(m)} - B u^{(m)} - a u_\varepsilon^{(m)} - b |u_\varepsilon^{(m)}| u_\varepsilon^{(m)} + dg \left[\beta \left(\theta_\varepsilon^{(m)} - \theta_{in} \right) - 1 \right]$$

Such that

$$\tilde{\varpi}^{(m)}(t) = \begin{cases} \varpi^{(m)}, & 0 \leq t \leq T \\ 0 & \text{outside} \end{cases}$$

Next, by taking the Fourier transforms, and let $\hat{\Psi}_i^{(m)}(\tau)$ and $\hat{\xi}_l^{(m)}(\tau)$ be respectively the Fourier transform of $\Psi_i^{(m)}(t)$ and $\xi_l^{(m)}(t)$ with $1 \leq i \leq m$ and $1 \leq l \leq m$. We multiply (1.71) and (1.72) by $\hat{\Psi}_i^{(m)}(\tau)$ and $\hat{\xi}_l^{(m)}(\tau)$ respectively, and summing respect to k .

$$\begin{aligned} &2i\pi\tau \left(\|\hat{u}_\varepsilon^{(m)}(\tau)\|^2 + \varepsilon \|\hat{p}_\varepsilon^{(m)}(\tau)\|^2 \right) \\ &= \langle \varpi_m, \hat{u}_\varepsilon^{(m)}(\tau) \rangle \\ &+ \langle u_{\varepsilon 0}^{(m)}, \hat{u}_\varepsilon^{(m)}(\tau) \rangle + \varepsilon \langle p_{\varepsilon 0}^{(m)}, \hat{p}_\varepsilon^{(m)}(\tau) \rangle \\ &- \left(\langle u_\varepsilon^{(m)}(T), \hat{u}_\varepsilon^{(m)}(\tau) \rangle + \varepsilon \langle p_\varepsilon^{(m)}(T), \hat{p}_\varepsilon^{(m)}(\tau) \rangle \right) e^{-2i\pi\tau T} \end{aligned} \quad (1.73)$$

Note that

$$\begin{aligned} \int_0^T \|\varpi_m(t)\|_{V'} dt &\leq \int_0^T \left(\lambda \|u_\varepsilon^{(m)}(t)\| + C_1 \|u_\varepsilon^{(m)}(t)\|^2 + a \|u_\varepsilon^{(m)}(t)\| + b \|u_\varepsilon^{(m)}(t)\|^2 \right) dt \\ &\quad + \int_0^T (\|dg(\beta\theta_{in} - 1)\| + C_1 \|\theta_\varepsilon^m\|) dt \end{aligned}$$

Thus

$$\sup_{\tau \in \mathbb{R}} \|\hat{\varpi}_m(\tau)\|_{V'} \leq Const \quad \forall m \quad (1.74)$$

and this remains bounded according to (1.62)-(1.63) and (1.64).

$$2\pi |\tau| \left(\|\hat{u}_\varepsilon^{(m)}(\tau)\|^2 + \varepsilon \|\hat{p}_\varepsilon^{(m)}(\tau)\|^2 \right) \leq \|\varpi_m(t)\|_{V'} \|\hat{u}_\varepsilon^{(m)}(\tau)\| + C_1 \|\hat{u}_\varepsilon^{(m)}(\tau)\| + C_1 \varepsilon \|\hat{p}_\varepsilon^{(m)}(\tau)\|$$

But, we have

$$\|\hat{\varpi}_m(\tau)\|_{V'} \leq \int_0^T \|\varpi_m(\tau)\|_{V'} dt \quad (1.75)$$

$$\int_{-\infty}^{+\infty} |\tau|^{2\gamma} \|\hat{u}_\varepsilon^m\|^2 d\tau \leq \text{const}, \quad \text{for } \tau > 0 \quad (1.76)$$

Then, the convergence of the triplet $(u_\varepsilon^m, \theta_\varepsilon^m, p_\varepsilon^m)$ given by

$$\begin{aligned} u_\varepsilon^m &\rightarrow u_\varepsilon \quad \text{strongly} && \text{in } L^2([0, T], H), \\ \theta_\varepsilon^m &\rightarrow \tilde{\theta} \quad \text{strongly} && \text{in } L^2([0, T], L^2(\Omega)), \\ \sqrt{\varepsilon} p_\varepsilon^m &\rightarrow \sqrt{\varepsilon} p_\varepsilon \quad \text{strongly} && \text{in } L^2([0, T], L^2(\Omega)) \end{aligned} \quad (1.77)$$

In the same way as the incompressible system to conclude this proof, for the convergence of the nonlinear term $|u_\varepsilon^{(m)}| u_\varepsilon^{(m)} \rightharpoonup |u_\varepsilon| u_\varepsilon$ weak in $L^{3/2}([0, T], L^{3/2}(\Omega))$. Theorem (1.5.1) is proved.

1.6 Thermal comfort problem

In this section we apply the model and methodology to solve environmental problems in cities. We consider a domain $\Omega \subset \mathbb{R}^n$ (with $n = 2$ or 3), corresponding to the air layer over a city, with boundary $\partial\Omega = \{\Gamma_1, \Gamma_2, \Gamma_3, \Gamma_B, \Gamma_s\}$

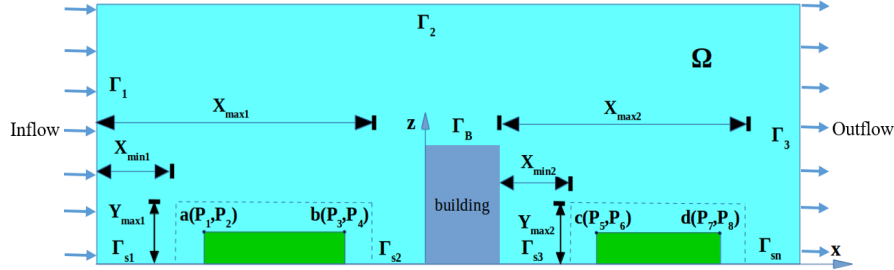


Figure 1.1: 2D Schematic representation.

The approach is based on the development and application of a methodology that employs optimization to seek the locations of the green zones for the purpose of influencing the temperature in the city to ensure the comfort of the pedestrians traffic and to provide planners with a systematic overview of their decision space. For this aim, we introduce the objective function regarding to the environmental implications defined by

$$J = \sum_{i=1}^n \frac{1}{|\Gamma_{s_i}|} \int_0^T \int_{\Gamma_{s_i}} \theta^\varepsilon(x, t) dx dt \quad (1.78)$$

The constraints related to the geometry of the green space are described by the four points (a, b, c, d) which represents the design in term of these variables. We suppose that the four

points are inside the rectangles.

$$\begin{cases} X_{min_1} \leq P_1, & P_2 = Y_{max_1} \\ P_3 \leq X_{max_1}, & P_4 = P_2 \\ X_{min_2} \leq P_5, & P_6 = Y_{max_2} \\ P_7 \leq X_{max_2}, & P_8 = P_6 \end{cases} \quad (1.79)$$

To avoid a zero distance between two ends of the green space, we set

$$\begin{cases} \Delta_1(P_3, P_1) = P_3 - P_1 \geq L_1 \\ \Delta_2(P_5, P_7) = P_5 - P_7 \geq L_2 \end{cases} \quad (1.80)$$

To eliminate complex geometries shape such as the trapezoidal shape, the height variation is fixed

$$\begin{cases} \Delta_3(P_4, P_2) = P_4 - P_2 = h_1 \\ \Delta_4(P_5, P_7) = P_8 - P_6 = h_2 \end{cases} \quad (1.81)$$

1.6.1 Optimal control procedures

We start by providing a general approach to deal with an optimal control problems, then we apply the method to the particular case of the optimal located of the green spaces in the macroscopic climate model.

Abstract formulation for optimal control problem

In order to analyze a shape optimization problem, [26] developed a Lagrangian approach for a general optimal control one. The abstract problem is to minimize a cost function J in the following form

$$\begin{cases} \min J = J(v, \xi) \\ Av = f + B\xi \end{cases} \quad (1.82)$$

where A is a partial differential equation (PDE) operator, v is the state variable, f is a source term, and B is a differential operator acting on the control variable ξ in the state equation. We introduce the Langrangian functional and Lagrange multiplier λ

$$\mathcal{L}(v, \lambda, \xi) = J(v, \xi) - \langle \lambda, f + B\xi - Av \rangle$$

The solution of the problem (1.82) satisfies the PDE system

$$\frac{\partial \mathcal{L}}{\partial \cdot}(v, \lambda, \xi) = 0$$

Considering $v \in L^2([0, T]; V)$, $\xi \in L^2([0, T]; W)$ with V and W being a two Hilbert spaces, we have the following weak form for the state equation (1.82) :

$$a(v, \varphi) = (f, \varphi) + b(\xi, \varphi), \quad \forall \varphi \in V$$

where the (\cdot, \cdot) is the inner product, $a(\cdot, \cdot)$ is a bilinear form of the PDE operator, and $b(v, \varphi) = (B\xi, \varphi)$. Then

$$\mathcal{L}(v, \lambda, \xi) = J(v, \xi) + b(\xi, \lambda) + (f, \lambda) - a(v, \xi)$$

The optimal control consists in solving the following problem

$$\begin{cases} \text{Find } (v, \lambda, \xi) \in V \times V \times Q & \text{such that} \\ \frac{\partial \mathcal{L}}{\partial \cdot}(v, \lambda, \xi) = 0 \end{cases}$$

1.7 Numerical discretization

In this section, we present the numerical resolution of the state system (1.14), which is a previous step in order to find the optimal locations of the green zones by minimizing the objective function.

1.7.1 Variational formulation

For the mathematical setting of conduction-convection problem, we introduce the following Hilbert spaces $X = H_0^1(\Omega)^2$, $W = H_0^1(\Omega)$, $M = \left\{ q \in L^2(\Omega); \int_{\Omega} q dx = 0 \right\}$. The norm corresponding to $H_i(\Omega)^2$ or $H_i(\Omega)$ will be denote $\|\cdot\|_i$ for $i = 1, 2$. In particular, we use (\cdot, \cdot) and $\|\cdot\|_0$ to denote the inner product and norm in $L^2(\Omega)^2$ or $L^2(\Omega)$. The spaces X and W are equipped with their usual scalar product and norm (u, v) , $\|u\| = (u, u)^{1/2}$.

Let $f \in L^2([0, T]; L^2(\Omega))$, $u_0 \in L^2(\Omega)$, $\theta_0 \in L^2(\Omega)$ and $p_0 \in L^2(\Omega)$ are verified, the problem (1.45) is equivalent to the variational formulation : Find $u_\varepsilon \in L^2([0, T]; V)$, $(\theta_\varepsilon - \theta_{in}) \in L^2([0, T]; W)$ et $p_\varepsilon \in L^2([0, T]; L^2(\Omega))$ such that

$$\begin{aligned} & \frac{d}{dt} \langle u_\varepsilon, v \rangle + B \langle u_\varepsilon, u_\varepsilon, v \rangle + \langle a u_\varepsilon, v \rangle + \langle b | u_\varepsilon | u_\varepsilon, v \rangle - \langle p_\varepsilon, \nabla \cdot v \rangle \\ & = -\lambda \langle \nabla u_\varepsilon, \nabla v \rangle + \langle dg \beta \theta_\varepsilon, v \rangle - \langle dg \beta \theta_{in}, v \rangle - \langle dg, v \rangle \quad \forall v \in \tilde{V} \end{aligned} \quad (1.83)$$

$$\frac{d}{dt} \langle \theta_\varepsilon, \tau \rangle + B \langle u_\varepsilon, \theta_\varepsilon, \tau \rangle = -\eta \langle \nabla \theta_\varepsilon, \nabla \tau \rangle + \langle f, \tau \rangle \quad \forall \tau \in \tilde{W} \quad (1.84)$$

$$\langle \nabla \cdot u_\varepsilon, q \rangle = -\langle \varepsilon \partial_t p_\varepsilon, q \rangle \quad \forall q \in L^2(\Omega) \quad (1.85)$$

Let us consider the incompressible Navier-Stokes Forchheimer Fourier system we recall the notion of weak solution that will be used (for more detail see [22]). We say that the triple (u, θ, p) is the weak solution of Navier Stokes Forchheimer system if it satisfies for all $\varphi \in \Omega \times [0, T]$

$$\begin{aligned}
 & \int_0^T \int_{\Omega} \partial_t u \cdot \varphi dx dt + \int_0^T \int_{\Omega} \lambda \nabla u : \nabla \varphi dx dt + \int_0^T \int_{\Omega} (u \cdot \nabla) u \cdot \varphi dx dt \\
 & + \int_0^T \int_{\Omega} \alpha \nabla p \cdot \varphi dx dt + \int_0^T \int_{\Omega} a u \cdot \varphi dx dt + \int_0^T \int_{\Omega} b |u| u \cdot \varphi dx dt \\
 & - \int_0^T \int_{\Omega} dg [\beta(\theta - \theta_{in}) - 1] \varphi dx dt = 0 \\
 & \int_0^T \int_{\Omega} \partial_t \theta \cdot \varphi dx dt + \int_0^T \int_{\Omega} \eta \nabla \theta : \nabla \varphi dx dt + \int_0^T \int_{\Omega} (u \cdot \nabla) \theta \cdot \varphi dx dt \\
 & - \int_0^T \int_{\Omega} Q_B \varphi dx dt - \int_0^T \int_{\Omega} \sum_{i=1}^N \alpha_i \chi_{G_i} \varphi dx dt = 0 \\
 & \int_0^T \int_{\Omega} \varepsilon \partial_t p \cdot \varphi dx dt + \int_0^T \int_{\Omega} \operatorname{div} u \cdot \varphi dx dt = 0
 \end{aligned} \tag{1.86}$$

1.7.2 Time semi-discretization

In order to set the time semi-discretization for the interval $[0, T]$, we chose a number $M \in \mathbb{N}$ and we define the time step $\Delta t = \frac{T}{M}$. Then we consider a set of $M+1$ discrete times $[t_m]_{m=0}^M \subset [0, T]$ given by $t_m = m\Delta t$, for $m = [0, \dots, M]$.

We consider the material derivative of a generic escalar

$$\frac{D\Psi}{Dt}(x, t) = \frac{\partial \Psi}{\partial t}(x, t) + u \cdot \nabla \Psi(x, t) \tag{1.87}$$

Using the characteristic line

$$\frac{dX}{dt} = u(X(t), t) \tag{1.88}$$

we can write

$$\frac{D\Psi}{Dt} = \frac{d}{dt} \Psi(X(t), t) \tag{1.89}$$

So, we can approximate the material derivative in the following way

$$\frac{D\Psi}{Dt}(t^{m+1}) \simeq \frac{\Psi(X(t^{m+1}), t^{m+1}) - \Psi(X(t^m), t^m)}{\Delta t} \tag{1.90}$$

$$\frac{D\Psi}{Dt}(t^{m+1}) = \frac{\Psi^{m+1} - \Psi^m \circ X^m}{\Delta t} \tag{1.91}$$

where $X^m(x) = X(x, (t^{m+1}, t^m))$ represents the position of the particle. Let Δt the time step, the total derivatives for Navier-Stokes Forchheimer energy equation and the artificial compressibility term are discretized according to the method of characteristics. The nonlinear term is approximated using semi-implicit formula while the other linear terms are discretized implicitly.

$$\begin{aligned} & \frac{u_{m+1}^\varepsilon(x) - u_m^\varepsilon \circ X_m(x)}{\Delta t} - \lambda \Delta u_{m+1}^\varepsilon + \alpha \nabla p_{m+1}^\varepsilon + a u_{m+1}^\varepsilon \\ & + b |u_{m+1}^\varepsilon| u_{m+1}^\varepsilon - dg[\beta(\theta_{m+1}^\varepsilon - \theta_{in}) - 1] = 0 \quad \text{in } \Omega \times (0, T) \end{aligned} \quad (1.92)$$

$$\frac{\theta_{m+1}^\varepsilon(x) - \theta_m^\varepsilon \circ X_m(x)}{\Delta t} - \eta \Delta \theta_{m+1}^\varepsilon - Q_B - \sum_{i=1}^N \alpha_i \chi_{G_i} = 0 \quad \text{in } \Omega \times (0, T) \quad (1.93)$$

$$\frac{p_{m+1}^\varepsilon(x) - p_m^\varepsilon(x) \circ X_m(x)}{\Delta t} + \operatorname{div} u_{m+1}^\varepsilon = 0 \quad \text{in } \Omega \times (0, T) \quad (1.94)$$

For $m \in \mathbb{N}$ and

$$u_0^\varepsilon(x) = u_{in}^\varepsilon(x), \quad \theta_0^\varepsilon(x) = \theta_{in}^\varepsilon(x), \quad p_0^\varepsilon(x) = p_{in}^\varepsilon(x) \quad (1.95)$$

A no-slip wall boundary condition was used at the ground surface, and a normal zero-gradient boundary condition was adopted at the domain outlet boundary and the domain top boundary.

1.7.3 Space discretization

To complete the discretization, we use the Finite Element formalism for spatial discretization. We consider \mathcal{T}_h of Ω and, associated to this mesh. Let us denote \hat{u} , $\hat{\theta}$ and \hat{q} the test functions associated to the finite element spaces V_h , X_h and Q_h respectively. We define the following finite spaces

$$\begin{aligned} V_h &= \{ \hat{u} \in [C(\overline{\Omega})]^n : \hat{u}|_T \in [\mathbb{P}_2(T)]^n, \forall T \in \mathcal{T}_h, \hat{u}.n = 0 \} \\ X_h &= \{ \hat{\theta} \in [C(\overline{\Omega})]^n : \hat{\theta}|_T \in [\mathbb{P}_2(T)]^n, \forall T \in \mathcal{T}_h, \hat{\theta}.n = 0 \} \\ Q_h &= \{ \hat{q} \in C(\overline{\Omega}) : \hat{q}|_T \in \mathbb{P}_1(T), \forall T \in \mathcal{T}_h \} \end{aligned}$$

The problem is to find $(u^\varepsilon, \theta^\varepsilon, P^\varepsilon) \in \{V_h, X_h, Q_h\}$ such us

$$\begin{aligned} & \int_{\Omega} \frac{u_{m+1}^\varepsilon(x) - u_m^\varepsilon \circ X_m(x)}{\Delta t} \hat{u} dx + \lambda \int_{\Omega} \nabla u_{m+1}^\varepsilon : \nabla \hat{u} dx - \alpha \int_{\Omega} p_{m+1}^\varepsilon \nabla \hat{u} dx \\ & + a \int_{\Omega} u_{m+1}^\varepsilon \hat{u} dx + b \int_{\Omega} |u_{m+1}^\varepsilon| u_{m+1}^\varepsilon \hat{u} dx \\ & - dg \int_{\Omega} [\beta(\theta_{m+1}^\varepsilon - \theta_{in}) - 1] \hat{u} dx = 0 \quad \forall \hat{u} \in V_h \end{aligned} \quad (1.96)$$

$$\begin{aligned} & \int_{\Omega} \frac{\theta_{m+1}^\varepsilon(x) - \theta_m^\varepsilon \circ X_m(x)}{\Delta t} \hat{\theta} dx + \eta \int_{\Omega} \nabla \theta_{m+1}^\varepsilon : \nabla \hat{\theta} dx \\ & - \int_{\Omega} Q_B \hat{\theta} dx - \sum_{i=1}^N \alpha_i \chi_{G_i} \hat{\theta} dx = 0 \quad \forall \hat{\theta} \in X_h \end{aligned} \quad (1.97)$$

$$\varepsilon \int_{\Omega} \frac{p_{m+1}^{\varepsilon}(x) - p_m^{\varepsilon}(x) \circ X_m(x)}{\Delta t} \hat{q} dx + \int_{\Omega} \operatorname{div} u_{m+1}^{\varepsilon} \hat{q} dx = 0 \quad \forall \hat{q} \in Q_h \quad (1.98)$$

1.7.4 Gradient project algorithm

The control problem is solved by an iterative method with an initial boundary condition for the variable $\xi = \xi^0$. At each step, we solve the state equations, then we compute the value of the cost functional and solve the adjoint equations. Once ξ^i is available, we determine the cost functional derivative ∇J and applying the suitable stopping criteria. If this criteria is not satisfied, we employ an optimization iteration on the control function ξ , for example, we use a steepest-descent method :

$$\xi^{i+1} = \xi^i - \tau^i \nabla J(\xi^i, v^i)$$

where τ^i is a relaxation parameter that can be determined by analyzing the mathematical properties of a control problem.

The optimization problem can be defined as follows :

Problem (\mathbb{P}) : Find the optimal location of the green spaces in the domain Ω , find a vector $P = (a, b, c, d) = (P_1, P_2, P_3, P_4, P_5, P_6, P_7, P_8)^T \in \mathbb{R}^8$ ($P \in \mathbb{R}^{12}$ where $\Omega \subset \mathbb{R}^3$) where the constraints given in (1.79), (1.80), (1.81) are satisfied in such a way θ^{ε} given by the coupled Navier-Stokes Forchheimer with the artificial compressibility and the Fourier equation system (1.83), (1.84), (1.85) respectively, minimize the objective function $J \equiv J(P)$ defined by (1.78).

We denote by Ω the closed and convex subset of \mathbb{R}^8 consisting of all the points $P \in \mathbb{R}^8$ satisfying the constraints (1.79), (1.81), that is defining $l_1 = l_3 = l_5 = l_7 = X_{min}$, $u_1 = u_3 = u_5 = u_7 = Y_{max}$, $l_2 = l_4 = l_6 = l_8 = X_{min}$, $u_2 = u_4 = u_6 = u_8 = Y_{max}$, the admissible Ω given by

$$\Omega = \left\{ P = (P_1, \dots, P_8) \in \mathbb{R}^8 : l_i \leq P_i \leq u_i, i = 1, \dots, 8, \right. \\ \left. P_3 - P_1 \geq L_1, P_5 - P_7 \geq L_2, P_4 - P_2 = h_1, P_8 - P_6 = h_2 \right\} \quad (1.99)$$

So, our problem (\mathbb{P}) can be rewritten in the form :

$$\min_{P \in \Omega} J(P) \quad (1.100)$$

In order to evaluate the objective function J , we first solve the system (37) defined in (3). The numerical approximation of the objective function is given by :

$$J(P) = \sum_{i=1}^n \frac{1}{\Gamma_{s_i}} \sum_{m=1}^M \int_{\tau_h} \int_{\Gamma_{s_i}} \theta_m^{\varepsilon} d\gamma \quad (1.101)$$

To solve this problem, we use the spectral projected gradient algorithm. The projected gradient

method is inspired from the classical gradient methods. Suppose the differentiable function $f : \mathbb{R}^n \rightarrow \mathbb{R}$. Let \mathcal{Q} a closed convex not empty of \mathbb{R}^n . Consider the general following problem

$$\min_{x \in \mathcal{Q}} f(x)$$

it is a way to solve constrained optimization problem. Consider a constraint set \mathcal{Q} , starting from a initial point $x_0 \in \mathcal{Q}$, Project Gradient Descent iterates the following equation until a stopping condition is met :

$$x_{k+1} = P_{\mathcal{Q}}(x_k - t_k \nabla f(x_k))$$

where $P_{\mathcal{Q}}(\cdot)$ is the projection operator. The projection of the point $x \in \mathbb{R}^n$ is obtained as a solution of the following optimization problem

$$P_{\mathcal{Q}}(x_0) = \arg \min_{x \in \mathcal{Q}} \frac{1}{2} \|x - x_0\|_2^2$$

The global convergence is assured under reasonable assumptions [25]. The projected gradient algorithm can be summarized in the following steps :

Algorithm 1 Calculate $\bar{P} = [\bar{P}_1, \bar{P}_2, \bar{P}_3, \bar{P}_4, \bar{P}_5, \bar{P}_6, \bar{P}_7, \bar{P}_8]$

$\bar{P} \in \Omega$
 $\varepsilon > 0$
Ensure: $\bar{P} = [\bar{P}_1, \bar{P}_2, \bar{P}_3, \bar{P}_4, \bar{P}_5, \bar{P}_6, \bar{P}_7, \bar{P}_8]$
 Compute the gradient
 $\rightarrow \frac{\partial J_h^{\Delta t}}{\partial P_i} \approx \frac{J_h^{\Delta t}(P + \zeta e_i) - J_h^{\Delta t}(p)}{\zeta} \quad i = 1, \dots, 8$
 Compute the projection
WHILE $\varsigma > 0$
 Compute
 $\rightarrow d = \Pi_{\Omega}(P - \varsigma \nabla J(P)) - P$
 Compute the new coordinates $\tau > 0$
 $\rightarrow \bar{P} = P + \tau \{\Pi_{\Omega}(P - \varsigma \nabla J(P)) - P\}$
END

1.8 Numerical results

All differential equations are approximated using the finite element method for the space and semi-implicit scheme for the time discretization. In this section, we present the numerical results of the optimal shape of green spaces in high density urban cities that we have obtained by using the approach of the spectral project gradient algorithm in the case of solving a system previously defined with the term of the artificial compressibility for the 2D domain showing in Figure (1.1).

1.8.1 Effects of numerical and physical parameters

Computational domain and grid structure

We consider a rectangular area of $75m$ in length and $25m$ in height. We have a structural model of a city with the random implantation of green spaces. In order to compare and show the temperature distribution in both urban models before and after the optimal shape, we limit our structure to a one built $6m$ in height where the two green spaces to be optimized are located the upstream with $10m$ in length and $2m$ in height, the second downstream of the building with $8m$ in length, $2m$ in height.

For the overall computation time, we have chosen $T = 50s$ for a time step of $0.1s$, for the different space discretization, we tried a several regular triangulations of about 5036 elements. The implementation of our system is realized in FreeFem++ [23].

Boundary conditions

The initial conditions for the velocity, temperature, pressure and simulation parameters are

1. Inlet velocity [18] used a power law as the vertical profile of the wind speed at the domain inlet

$$u_{in}^\varepsilon = u_{ref}^\varepsilon \left(\frac{z}{z_{ref}} \right)^{0.16} \quad (1.102)$$

2. The vertical profiles of the temperature at the domain inlet is given

$$\theta_{in}^\varepsilon = \theta_0^\varepsilon - \gamma z \quad (1.103)$$

where γ is the vertical decrease rate of temperature.

3. The pressure

$$p_{in}^\varepsilon = p_0^\varepsilon - \rho g z \quad (1.104)$$

We ran many numerical simulations,, we present here only an example for this realistic problem. We chose a step size $\zeta = 10^{-3}$, a spectral parameter $\varsigma = 10^{-4}$, and the tolerance $\varepsilon = 10^{-3}$, the value of τ is in an interval $\tau \in [10^{-4}, 10^{-1}]$, in our example we take 10^{-4} . The difference between the temperature in the area of the city and the temperature of the vegetation is 2 degrees. For the all physical parameters used in the simulation, the inlet velocity $u^\varepsilon = 1.43m.s^{-1}$ and the inlet temperature $\theta^\varepsilon = 298.5K$, the density, dynamic viscosity, and kinetic viscosity are respectively $\rho = 1.184Kg.m^{-3}$, $\mu = 1.184 \times 10^{-2}kg.m^{-1}.s^{-1}$ and $\nu = 0.01m^2.s^{-1}$. Account to hold the effects of the turbulence in the city, the turbulence viscosity μ_t depend of the ratio between the density of the fluid multiply with his turbulence kinetic energy k on the dissipation rate of k . The intensity of building heat source $Q_B = 80W.m^{-2}$ with the height of building $z = 6m$ and the reference height $z_{ref} = 8m$. The heat transfer coefficient $h = 5w.m^{-2}.K^{-1}$, the thermal expansion coefficient $\beta = 3.4112 \times 10^{-4}$ and specific heat $C_p = 1006J.Kg^{-1}.K^{-1}$. For the other

parameters, the vertical decrease rate of temperature $\gamma = 0.25$, the Prandtl number $Pr = 0.708$ and the Von-Karman constant $V_k = 0.4$. For the all the test, we take the pseudo-compressibility parameter $\varepsilon = 10^{-5}$. Applying the spectral project gradient algorithm, and after 1000 iterations, from the initial location of the green spaces corresponding to the points $a = (8, 2)$, $b = (18, 2)$, $c = (39, 2)$, $d = (47, 2)$ showed in Figure (1.2), to the best location corresponding to the optimal design variables $a_{SPG} = (6.7370, 2)$, $b_{SPG} = (17.7280, 2)$, $c_{SPG} = (39.8072, 2)$, $d_{SPG} = (45.8966, 2)$ showed in (Figure (1.3)).

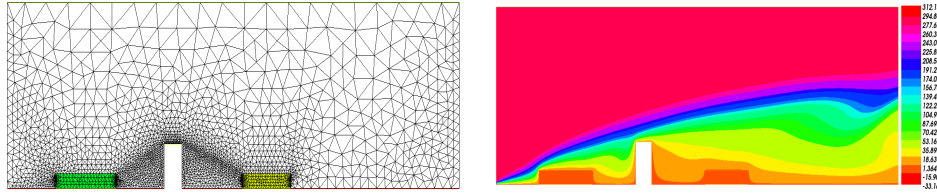


Figure 1.2: Air temperature profile for non optimal green locations.

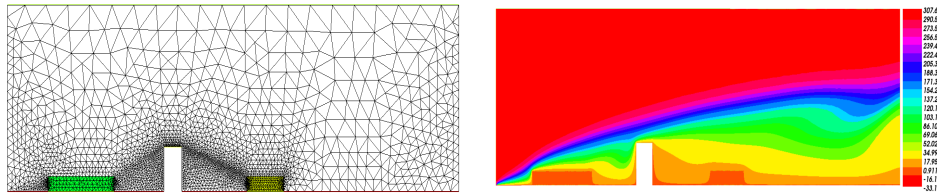


Figure 1.3: Air temperature profile for optimal green locations.

In Figure (1.4), we compare the two scenarios under study, the location of green spaces in the optimal and non-optimal case, we notice the difference of the temperature which is of the order of $0.5^{\circ}C$ before and after the optimization. In our example, to improve the that the location of green spaces, allows us to reduce the temperature in the city. For example, we take a distance of $10m$ from the source of the heat, the temperature drops from $19.85^{\circ}C$ to $19.45^{\circ}C$ showing in Figure (1.4).

We also note that the length of the green space to the left of the building is bigger than the length of the green space at the right as shown in Figure (1.2), (1.3). From this, we can conclude that to have fresh air and lower temperatures, the closer we are to the source, the surface of the green space is larger, and the further away we are from the source, the surface green space decreases.

The convergence history of the cost function is showing in Figure (1.5). From initial cost J of the initial location of the green spaces to the minimum cost J corresponding to the optimal location of the green spaces. To evaluate the sensitivity of the temperature according to the height in the city, to be able to control the evolution of the temperature after the optimal location of the green spaces to ensure the comfort of the pedestrians. The objective of our study is to reduce the temperature, according to the results obtained, we notice that the temperature decreases when approaching the soil as shown in the right of Figure (1.7). And also, we want to show the

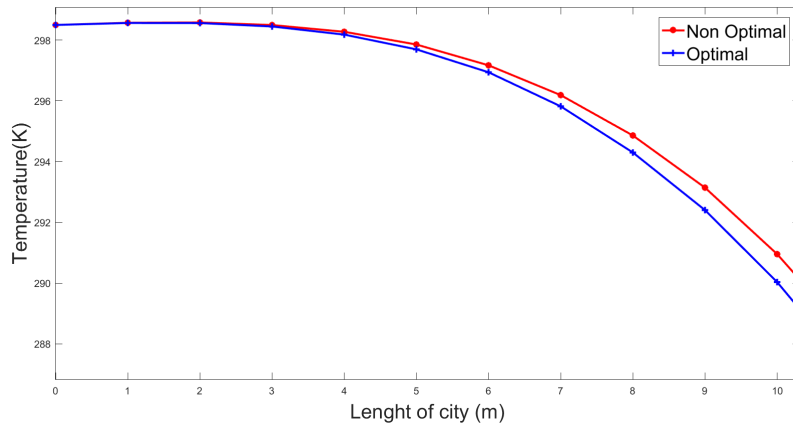


Figure 1.4: Temperature profiles corresponding to the non optimal and optimal and green locations.

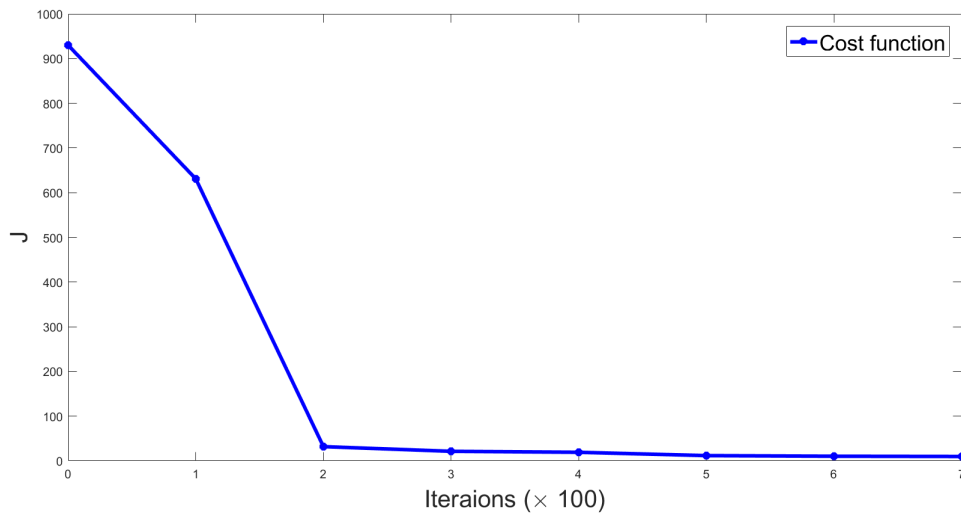


Figure 1.5: Decreasing cost function.

variation of the velocity in the most sensitive area showing in the left of Figure (1.7).

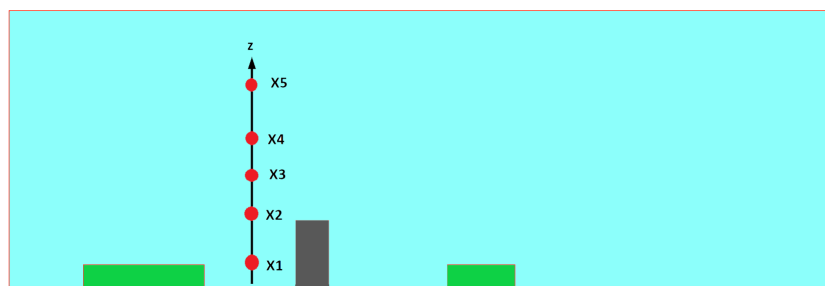


Figure 1.6: Different positions.

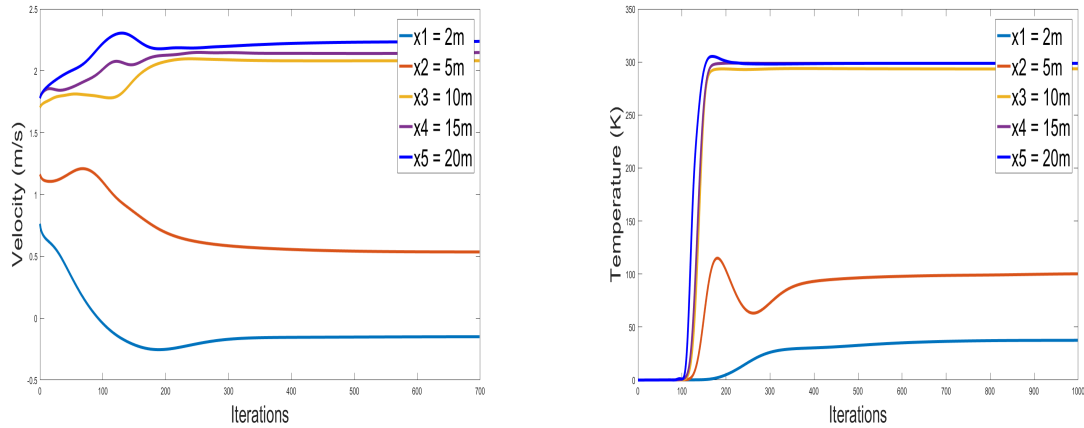


Figure 1.7: Velocity and temperature profiles according to the height in city.

Pseudo-compressibility parameter

The numerical test computed by varying $\varepsilon = [10^{-3}, 10^{-4}, 10^{-5}]$. The numerical results show that the pseudo-compressibility parameter affect a little the computational results. Some results of the fields temperature profiles for different value of ε are showing in Figure (1.8).

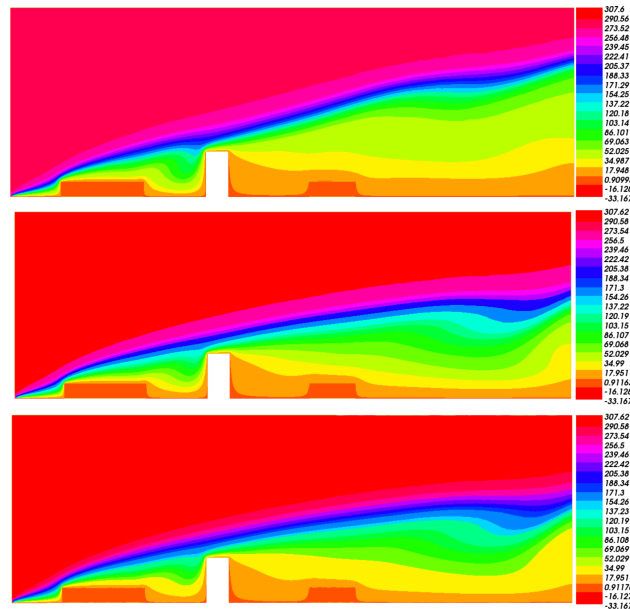


Figure 1.8: Fields Temperature profiles for the difference value of $\varepsilon = 10^{-3}$, $\varepsilon = 10^{-4}$ and $\varepsilon = 10^{-5}$.

Short form of Central Business District

The CBD can be described as follows: we keep the same dimension of the city in length and width, 25m height, and green spaces 10m in length, 16m in width and 2.5m in height for the first space and 2m for the second. For the overall computation time, we have chosen $T = 50s$ for

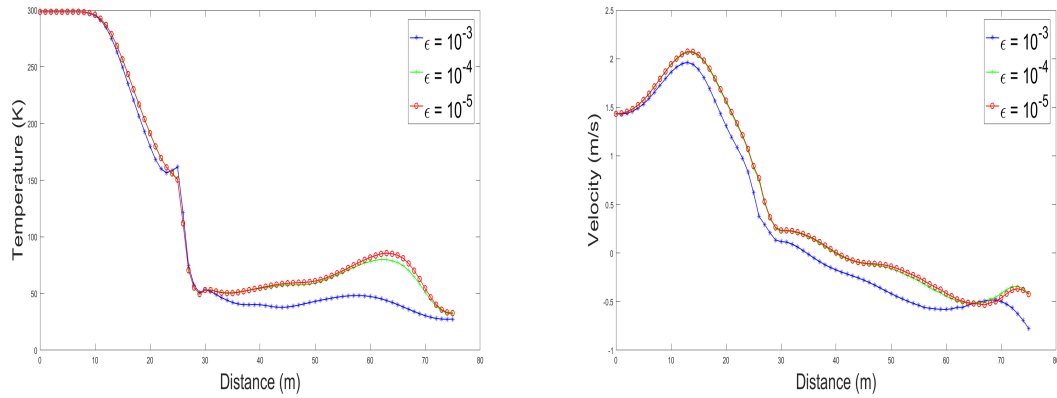


Figure 1.9: Profile temperature and velocity according to the variation of ϵ .

a time step of 0.1s. The numerical results obtained by using the above method of the artificial compressibility for the 3D

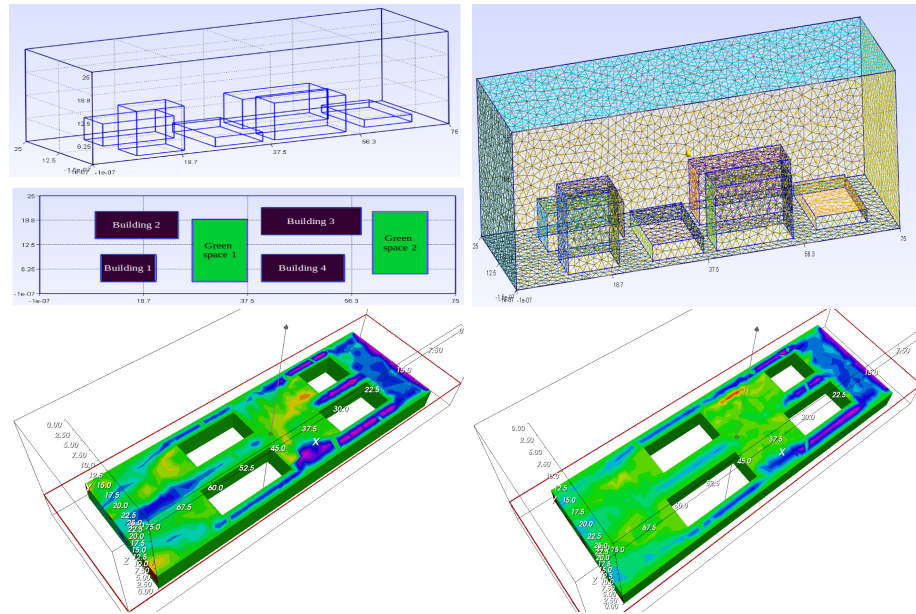


Figure 1.10: Fields Temperature profiles for 3D build: nonoptimal in the left and the optimal in the right .

According to the tests, we have done on the temperature profil before and after the optimal control. Fig. 10 shows the distribution of temperature along the city. From a global point of view, compact cities have a positive impact because they minimize energy consumption, and possibly CO_2 emissions. But from a local point of view, compact cities have a relatively negative impact in creating a dangerous urban climate for human health. Urban morphology and building density can alter the initial flow of the wind. In the addition of green spaces between buildings reduces the formation of vorticity to the ground, which results in the reduction of urban heat islands in the city by the decrease in air speed. The presence of vegetation in the city contributes

to local attenuation of urban heat islands. The cooling effect varies according to the organization of the vegetation, the surface and the type of vegetation. However, the effects of small green spaces is not negligible. In general, the solutions that allow us to reduce urban heat islands is to replace pavement paving materials with green surfaces. The movement of the air at low velocities gives a refreshing, comfortable feeling to people moving in the city. The cooling effect felt can be expressed according to the decrease of the air temperature which would give the same refreshing effect in calm air.

1.8.2 Caen Normandy University Campus

In the second application, we consider a campus area of the university located at ≈ 49.21 latitude and ≈ -0.36 longitude. We consider the domain $\Omega \subset \mathbb{R}^2$ a rectangular shape of $330m \times 235m$. The total duration for this simulation is $T = 10s$ for a time step of $dt = 0.01s$, and 13499 triangles. In the case of this problem for this structure, we consider just one green space because the coordinates in the x and y directions are variable both. From the initial coordinates $p_{1_x} = 100$, $p_{1_y} = 60$, $p_{2_x} = 100$, $p_{2_y} = 30$, $p_{3_x} = 180$, $p_{3_y} = 30$, $p_{4_x} = 180$, $p_{4_y} = 60$, to the new coordinates for the optimal location of the green space $p_{1_{xSPG}} = 103.1644$, $p_{1_{ySPG}} = 59.5934$, $p_{2_{xSPG}} = 101.9247$, $p_{2_{ySPG}} = 32.5414$, $p_{3_{xSPG}} = 177.0478$, $p_{3_{ySPG}} = 32.8829$, $p_{4_{xSPG}} = 179.4662$, $p_{4_{ySPG}} = 57.1102$

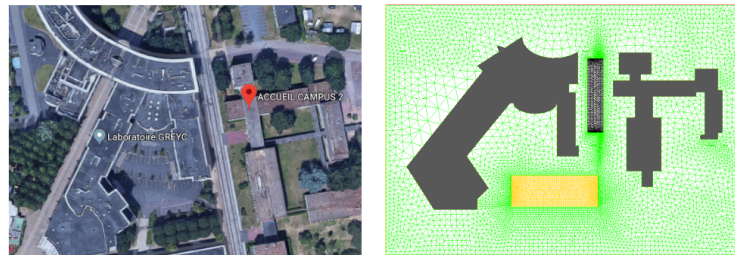


Figure 1.11: Initial mesh of Caen university.

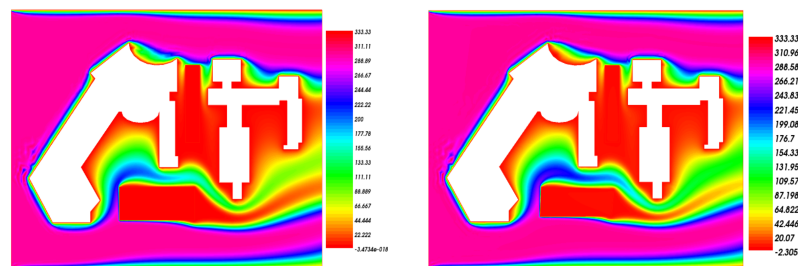


Figure 1.12: Air temperature and velocity profiles for non optimal in the left and optimal green locations in the right.

The results obtained show that the architecture of the green spaces influence the temperature distribution in the urban environment even if we see a small change due to the complexity of the interaction between green spaces and the climate inside the urban environment.

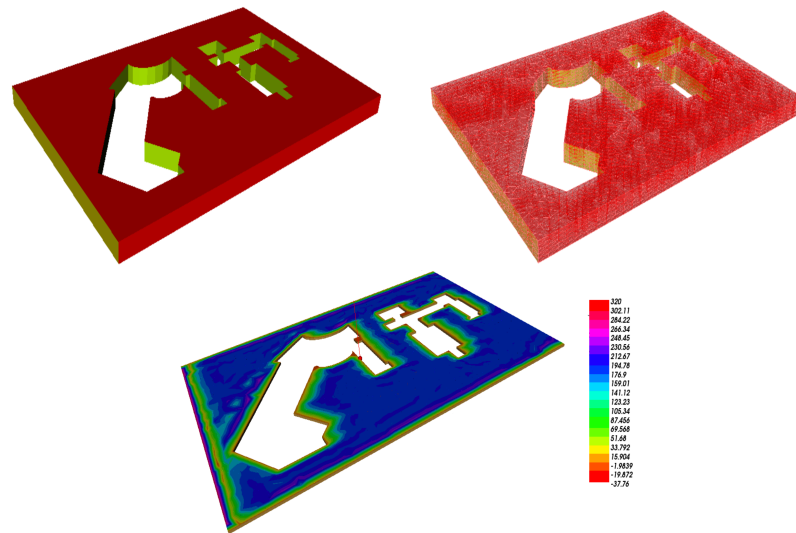


Figure 1.13: 3D air temperature profile for optimal green locations of Caen university.

1.9 Conclusion

The architecture and urbanization of cities have a very important role in preventing overheating, and the generation of urban heat islands.

The contribution of nature in the city is certainly one of the most interesting solutions to reduce the effects of urban heat island, but also for better management of the water cycle, while making the interurban more pleasant.

In this chapter a porous media-based model was developed in order to analyze the mitigation of the urban heat island effect. The focus was placed on presenting the applicability and relevance of a better combination between optimization techniques, and optimal control theory of partial differential equations to ensure the comfort in urban areas. Numerical results illustrate the main features of the developed approach.

Bibliography

- [1] R. Liu, Z. Han, The effects of anthropogenic heat release on urban meteorology and implication for haze pollution in the Beijing-Tianjin-Hebei region, Hindawi Publishing Corporation, Advance in Meteorology, volume 2016, 6178308.
- [2] T. R. Oke, Local climate zones for urban temperature studies, bulletin of the American Meteorological Society (2012).
- [3] D. J. Sailor, L. Lu (2004). A top-down methodology for developing diurnal and seasonal anthropogenic heating profiles for urban areas. Atmospheric Environment, vol. 38, n° 17, $p.27 - 37$.

- [4] W. D. Solecki, C. Rosenzweig, L. Parshall, G. Pope, M. Clark, J. Cox, M. Wiencke, (2005). Mitigation of the heat island effect in urban New Jersey. *Global Environmental Change Part B: Environmental Hazards*, vol. 6, n° 1, $p.39 - 49$.
- [5] D. Aparna, K. M. Buddhiraju, Impact of green roof on micro climate to reduce urban heat island, *remote Sensing Applications: Society and Environment* 10(2018)56 – 69.
- [6] N. E. Theeuwes, G. J. Steeneveld, R. J. Ronda, B. G. Heusinkveld, A. A. M. Holstag, Mitigation of the Urban Heat Island Effect Using Vegetation and Water Bodies, *International Conference of Urban Climates*, 2012.
- [7] F. J. Fernandez, L. J. Alvarez-Vasquez, N. Garcia-Chan, A. Martinez, M. E. Vasquez-Mendez, Optimal location of green zones in metropolitan areas to control the urban heat island, *Journal of Computational and Applied mathematics* 2014.
- [8] A. Mohajerani, J. Bakaric, T. Jeffrey-Bailey, The urban heat island effect, its causes, and mitigation, with reference to the properties as asphalt concrete, *Journal of Environmental Management* 197(2017)522 – 538.
- [9] A. K. Datta, Porous media approaches to studying simultaneous heat and mass transfer in food processes : I: problem formulations, *Journal of Food Engineering* 80(2007)80 – 95.
- [10] Z. Hu, B. Yu, Z. Chen, T. Li, M. Liu, Numerical investigation on the urban heat island in an entire city with an urbanporous media model, *Atmospheric Environment* 47(2012)509 – 518.
- [11] A. J. Chorin, Numerical solution of the Navier-Stokes equations, *Math. Comp.* 22(1968), 745 – 762.
- [12] R. Temam, Sur l’approximation de la solution des equations de Navier-Stokes par la methode des pas fractionnaires. I, *Arch. Rational Mech. Anal.* 32(1969), 135 – 153.
- [13] R. Temam, Sur l’approximation de la solution des equations de Navier-Stokes par la methode des pas fractionnaires. II, *Arch. Rational Mech. Anal.* 33(1969), 377 – 385.
- [14] A. P. Oskolkov, A certain quasilinear parabolic system with small parameter that approximates a system of Navier-Stokes equations, *Zap. Nauch. Sem. Leningrad. Otdel. Mat. Inst. Steklov. (LOMI)* 21(1971), 79 – 103.
- [15] K. Vafai, C. L. Tien (1981). Boundary and inertia effects on flow and heat transfer in porous media. *International Journal of Heat and Mass Transfer*, 24(2), 195 – 203.
- [16] A. V. Rodionov, On the use of Boussinesq approximation in turbulent supersonic jet modeling, *International Journal of Heat and Mass Transfer* 53(2010)889 – 901.

-
- [17] A. Amiri, K. Vafai, Analyse of dispersion effects and non-thermal equilibrium, non Darcian, variable porosity incompressible flow through porous media, *International Journal of Heat and Mass Transfer* 40(1997)3013 – 3024.
- [18] J. Hang, Y. Li, Wind conditions in idealized building clusters: macroscopic simulations using a porous turbulence model. *Boundary-Layer Meteorology* 136(2010)129 – 159.
- [19] C. S. B. Grimmond, T. R. Oke, 1999. Aerodynamic properties of urban areas derived from analysis of surface form. *Journal of Applied Meteorology* 38, 1262 – 1292.
- [20] M. Bruse, H. Fleer, Simulating surface-plant-air interactions inside urban environments with a three dimensional numerical model, *Environmental Modeling & Software* 13(1998)373 – 384.
- [21] H. Fan, J. David Sailor, Modeling the impacts of anthropogenic heating on the urban climate of Philadelphia: a comparison of implementations in two PBL schemes, *Atmospheric Environment* 39(2005)73 – 84.
- [22] P. L. Lions, *Mathematical topics in fluid dynamics, incompressible models*, claredon press, Oxford Science Publications, 1996.
- [23] F. Hecht, O. Pironneau, Antoine Le Hyaric and Kohji Ohtsuka, *Freefem++ Manual*, 2012.
- [24] L. J. Alvarez-vasquez, J. J. Judice, A. martinez, C. Rodriguez, M. E. Vasquez-Mendez, M. A. Vilar, On the optimal design of river fishways, *Optim Eng* (2013)14 : 193 – 211.
- [25] G. Birgin, J. M. Martinez, M. Raydan, Nonmonotone spectral projected gradient methods on convex sets, *SIAM J Optim* 10 : 1196 – 1211(2000).
- [26] J. L. Lions, *Optimal control of system governed by partial differential equations*, Springer-Verlag:New York, 1971.
- [27] D. Gilberg, N. S. Trudinger, *Elliptic partial differential equations of second order*, Springer, 1983.
- [28] H. Morimoto, On the existence of weak solutions of equation of natural convection, *J. Fac. Sci. Univ. Tokyo Sect. IA Math.* 36(1989), 87 – 102.
- [29] R. Temam, *Navier-Stokes Equations*, North-Holland, Amsterdam, 1979.
- [30] J. L. Lions, *Quelques méthodes de résolutions des problèmes aux limites non lineaires*, Etudes mathématiques. Dunod (1969).

Chapter 2

On error estimates of the artificial compressibility for the unsteady Navier-Stokes Forchheimer Fourier problem

Contents

2.1	Introduction	67
2.2	Prelimanaries	69
2.3	Analysis of the problem	74
2.4	Error estimates for the linearized problem	83
2.5	Error estimates for the nonlinear problem	87
2.6	Numerical resolution	93
2.6.1	Isolated island	98
2.6.2	Domestic frost-free refrigerator application	100
2.7	Conclusion	102

2.1 Introduction

Human, industrial activities or natural phenomena significantly influence climate change in cities such as atmospheric pollution by the emission of greenhouse gases and also the formation of heat islands due to solar energy stored by the buildings. Urban Heat Island are a natural phenomenon describing the difference temperature between urban and rural area. Cities are considered porous environments. A porous media refers to a solid full of empty space that is filled with a fluid. The mechanism of transport in the city is governed by the Navier-Stokes Forchheimer equations for air flow and the energy equation for the temperature. When the airflow encounters a city,

it will flow through and over the porous city. The whole domain consists of the porous urban region and a clear fluid region with an interface between them. A lot of theoretical and numerical attention has been paid to Forchheimer models applied to solve some environmental problems in the case of porous media related to urban heat islands, we can cite [16],[17] and [18].

The convection-diffusion problem coupled with the non-stationary incompressible Boussinesq equations are widely studied. There are several methods of numerical approximations have been studied the convection-diffusion problem. Shen [9] analyzed the existence and uniqueness of the solution of the stationary convection-diffusion problem with Bernard-Raugel elements. Shi and Ren [22] proved a nonconforming mixed finite element method. Kim and Choi [23] analyzed conduction and natural convection between two concentric cylinders under the effects of solar irradiation. We know that the velocity u , the pressure p and the temperature θ are coupled by the incompressibility constraint $\nabla \cdot u = 0$. To solve this coupling problem, we use the penalty or artificial compressibility methods. Shen [9] showed the optimal error estimate for the equations of Unsteady Navier-Stokes. He [24] extended the error analysis of the stationary Navier-Stokes problem using the finite element method. Wang and all [25] studied the error estimates of a penalized system and an extension to a total discretization of the scheme [26]. Haiyan, Yinnian and Xinlong [27] proposed the penalty method to solve the Navier-Stokes problem coupled with the nonstationary convection-diffusion problem in a domain of dimension $N = 2$ under assumptions on the initial data.

In this chapter, we propose and analyse the artificial compressibility method for the unsteady incompressible Navier-Stokes Forchheimer Fourier system. We know, in the literature there are several methods to relax the incompressibility constraint to solve the incompressible Navier-Stokes equations [1], [2]. In recent years several authors and works are interested to studying the models of porous media such as the approximation of the unsteady Brinkman-Forchheimer equations by the pressure stabilization method and by the pseudo-compressibility method [3], [4]. In the case of the coupled equations such as the viscous incompressible flow and heat transfer process [5], [6].

Let Ω be a bounded domain in \mathbb{R}^n (with $n = 2, 3$) and its boundary $\partial\Omega$. We consider the

following unsteady Forchheimer Fourier problem :

$$\left\{ \begin{array}{l} u_t - \lambda \Delta u + (u \cdot \nabla)u + au + b |u| u + \nabla p = dg\beta\theta - dg\beta\theta_{in} - dg\beta \quad \Omega \times [0, T] \\ \theta_t - \kappa \Delta \theta + (u \cdot \nabla)\theta = \mathcal{G} \quad \Omega \times [0, T] \\ \operatorname{div} u = 0 \quad \Omega \times [0, T] \\ u(x, t) = 0 \quad \Gamma \times [0, T] \\ \theta(x, t) = 0 \quad \Gamma \times [0, T] \\ p(x, t) = 0 \quad \Gamma \times [0, T] \\ u(x, t = 0) = 0, \quad \theta(x, t = 0) = \varphi(x) \quad x \in \Omega \end{array} \right. \quad (2.1)$$

where $u = (u_1, \dots, u_n)$ is the vector velocity, p the pressure, θ the temperature, $\lambda > 0$ the viscosity, κ the thermal diffusivity, \mathcal{G} , g and $\varphi(x, y)$ are given functions, the constants $a > 0, b > 0$ are the Darcy and Forchheimer coefficients respectively, $\beta > 0$ is the coefficient of volume expansion, and d is a positive constant.

We define also the artificial compressibility system given by

$$\left\{ \begin{array}{l} u_t^\varepsilon - \lambda \Delta u^\varepsilon + (u^\varepsilon \cdot \nabla)u^\varepsilon + au^\varepsilon + b |u^\varepsilon| u^\varepsilon + \nabla p^\varepsilon = dg\beta\theta^\varepsilon - dg\beta\theta_{in} - dg\beta \quad \Omega \times [0, T] \\ \theta_t^\varepsilon - \kappa \Delta \theta^\varepsilon + (u^\varepsilon \cdot \nabla)\theta^\varepsilon = \mathcal{G} \quad \Omega \times [0, T] \\ \varepsilon p_t^\varepsilon + \nabla \cdot u^\varepsilon = 0 \quad \Omega \times [0, T] \\ u^\varepsilon(x, t) = 0 \quad \Gamma \times [0, T] \\ \theta^\varepsilon(x, t) = 0 \quad \Gamma \times [0, T] \\ p^\varepsilon(x, t) = 0 \quad \Gamma \times [0, T] \\ u^\varepsilon(x, t = 0) = 0 \quad \theta^\varepsilon(x, t = 0) = \varphi(x) \quad x \in \Omega \end{array} \right. \quad (2.2)$$

In order to derive the error estimates for the artificial compressibility Navier-Stokes Forchheimer Fourier problem, we organize the chapter as follows. Section 2 is devoted to some notations and preliminaries results related to the problem (2.1). We obtain the regularity of the solution of the system. In the section 3, we provide error estimates for the linearized perturbed system. The nonlinear problem is treated in Section 4. In this part, we obtain an error estimate of order $\mathcal{O}(\varepsilon)$. In section 5, we discretize the problem in space by using finite element method and in time by using the backward Euler explicit scheme. We implement the above scheme in FreeFem++ and we present some numerical results. Finally, we give a conclusion to summarize our contribution.

2.2 Preliminaries

We first introduce some of the notations and results which will be used in the demonstration of this work.

We will use the standard notations $L^2(\Omega)$, $H^k(\Omega)$ and $H_0^k(\Omega)$ to denote the usual Sobelv spaces over Ω . We denote by $\|\cdot\|_k$ and $\|\cdot\|$ respectively the norms in $H^k(\Omega)$ and in $L^2(\Omega)$. We denote

(\cdot, \cdot) the scalar product in $L^2(\Omega)$. We introduce the following Hilbert spaces

$$X = H_0^1(\Omega)^2, \quad W = H_0^1(\Omega), \quad M = \left\{ q \in L^2(\Omega); \int_{\Omega} q dx \right\}$$

We also introduce the Hilbert space H and V defined by

$$\begin{aligned} H &= \{v \in L^2(\Omega)^2; \operatorname{div} v = 0; v.n|_{\partial\Omega}\} \\ V &= \{v \in X; \operatorname{div} v = 0\} \end{aligned}$$

We define $Au = \Delta u$ and $A_{\varepsilon}u = \Delta u - \frac{1}{\varepsilon} \nabla \operatorname{div} u$. They are the positive self-adjoint operators from $D(A) = H^2(\Omega)^2 \cap X$ (or $H^2(\Omega)^2 \cap W$) onto $L^2(\Omega)^2$ (or $L^2(\Omega)$). It is valid that

$$(\tilde{A}u, v) = (\tilde{A}^{1/2}u, \tilde{A}^{1/2}v), \quad \forall u \in D(A), v \in X, (\text{or } W)$$

where $\tilde{A} = A$ or A_{ε} . In paticular

$$(\tilde{A}^{1/2}u, \tilde{A}^{1/2}v) = (\nabla u, \nabla v), \quad \forall u, v \in X (\text{or } W) \quad (2.3)$$

$$(\tilde{A}_{\varepsilon}^{1/2}u, \tilde{A}_{\varepsilon}^{1/2}v) = (A^{1/2}u, A^{1/2}v) + \frac{1}{\varepsilon} (\operatorname{div} u, \operatorname{div} v), \quad \forall u, v \in X \quad (2.4)$$

It is know that (see [7], [8])

$$\|u\|_{L^4} \leq \alpha_0 \|u\|^{1/2} \|A^{1/2}u\|^{1/2}, \quad \|u\| \leq \alpha_0 \|A^{1/2}u\|, \quad \forall u \in X, (\text{or } W) \quad (2.5)$$

$$\|A^{1/2}u\|_{L^4} \leq \alpha_0 \|A^{1/2}u\|^{1/2} \|Au\|^{1/2}, \quad \|A^{1/2}u\| \leq \alpha_0 \|Au\|, \quad \forall u \in D(A) \quad (2.6)$$

where α_0 is a positive constant depending only on Ω . The following Lemma [9] is useful for the remainder of the topic analysis.

Lemma 2.2.1. *There exists a constant $C > 0$, depending only on Ω and such that for ε sufficiently small, we have*

$$\begin{aligned} \|Au\| &\leq C \|A_{\varepsilon}u\| \quad \forall u \in D(A) \\ \|A^{1/2}u\| &\leq C \|A_{\varepsilon}^{1/2}u\| \quad \forall u \in X \\ \|A_{\varepsilon}^{-1}u\| &\leq C \|u\|_{-2} \quad \forall u \in H^{-2}(\Omega)^2 \end{aligned}$$

We define the continuous bilinear forms

$$\begin{aligned} \mathbf{a}(u, v) &= \lambda (\nabla u, \nabla v), \quad \forall u, v \in X \\ \mathbf{a}_{\varepsilon}(u, v) &= \lambda (A_{\varepsilon}^{1/2}u, A_{\varepsilon}^{1/2}v), \quad \forall u, v \in X \\ \bar{\mathbf{a}}(\theta, \varphi) &= \kappa (\nabla \theta, \nabla \varphi), \quad \forall \theta, \varphi \in W \\ \delta(v, q) &= (q, \operatorname{div} v), \quad \forall v \in X, q \in M \end{aligned} \quad (2.7)$$

We now introduce some operators usually associated with Forchheimer-Fourier system and their

approximations.

$$\tilde{B}(u, v, w) = ((u \cdot \nabla) v, w) = \int_{\Omega} \sum_{i,j=1}^n u_j(x) \frac{\partial v_i(x)}{\partial x_j} w_i(x) dx \quad \forall (u, v, w) \in X$$

$$\tilde{\tilde{B}}(u, \theta, \psi) = ((u \cdot \nabla) \theta, \psi) = \int_{\Omega} \sum_{j=1}^n u_j(x) \frac{\partial \theta(x)}{\partial x_j} \psi(x) dx \quad \forall u \in X, \theta \in T, \psi \in W$$

Some estimates of the trilinear $\tilde{B}(\cdot, \cdot, \cdot)$ can be found in [10], [11], [12]

$$\tilde{B}(u, v, w) = -\tilde{B}(u, w, v), \quad \forall u, v, w \in X \quad (2.8)$$

$$|\tilde{B}(u, v, w)| \leq C \|u\|_1 \|v\|_1^{\frac{1}{2}} \|v\|_2^{\frac{1}{2}} \|w\|, \quad \forall u, w \in X, v \in D(A) \quad (2.9)$$

$$\begin{aligned} & |\tilde{B}(u, v, w)| + |\tilde{B}(v, u, w)| + |\tilde{B}(w, v, w)| \\ & \leq C \|u\|_1 \|v\|_2 \|w\|, \quad \forall u \in D(A), v, w \in X \end{aligned} \quad (2.10)$$

Similarly, it is easy to verify that $\tilde{\tilde{B}}(\cdot, \cdot, \cdot)$ the following important property

$$\tilde{\tilde{B}}(u, \theta, \psi) = -\tilde{\tilde{B}}(u, \psi, \theta), \quad \forall u \in X, \theta \in T, \psi \in W \quad (2.11)$$

$$|\tilde{\tilde{B}}(u, \theta, \psi)| \leq C \|u\|_1 \|\theta\|_1^{\frac{1}{2}} \|\theta\|_2^{\frac{1}{2}} \|\psi\|, \quad \forall u \in X, \theta \in D(A), \psi \in W \quad (2.12)$$

$$\begin{aligned} & |\tilde{\tilde{B}}(u, \theta, \psi)| + |\tilde{\tilde{B}}(\theta, u, \psi)| + |\tilde{\tilde{B}}(\psi, \theta, u)| \\ & \leq C \|u\|_1 \|\theta\|_2 \|\psi\|, \quad \forall \theta \in D(A), u \in X, \psi \in W \end{aligned} \quad (2.13)$$

We have also

$$\tilde{B}(u, v, v) = 0 \quad \forall u, v \in X \quad (2.14)$$

The variational formulation of the problem (2.1): Find $(u, p, \theta) \in (X, M, W)$, for all $t \in [0, T]$ and $(\hat{v}, \hat{\phi}, \hat{\psi}) \in (X, M, W)$

$$\begin{cases} (u_t, \hat{v}) + \mathbf{a}(u, \hat{v}) + (au, \hat{v}) + \tilde{B}(u, u, \hat{v}) + (b | u | u, \hat{v}) - \delta(\hat{v}, p) \\ \quad = (dg\beta\theta, \hat{v}) - (dg\beta\theta_{in}, \hat{v}) - (dg\beta, \hat{v}) \\ \delta(u, \hat{\phi}) = 0 \\ (\theta_t, \hat{\psi}) + \bar{\mathbf{a}}(\theta, \hat{\psi}) + \tilde{\tilde{B}}(u, \theta, \hat{\psi}) = (\mathcal{G}, \hat{\psi}) \end{cases} \quad (2.15)$$

The artificial compressibility method applied to (2.15) is that to find:

$(u^\varepsilon, p^\varepsilon, \theta^\varepsilon) \in (X, M, W)$, for all $t \in [0, T]$, such that for all $(\hat{v}, \hat{\phi}, \hat{\psi}) \in (X, M, W)$

$$\begin{cases} (u_t^\varepsilon, \hat{v}) + \mathbf{a}(u^\varepsilon, \hat{v}) + (au^\varepsilon, \hat{v}) + \tilde{B}(u^\varepsilon, u^\varepsilon, \hat{v}) + (b | u | u^\varepsilon, \hat{v}) - \delta(\hat{v}, p^\varepsilon) \\ = (dg\beta\theta^\varepsilon, \hat{v}) - (dg\beta\theta_{in}, \hat{v}) - (dg\beta, \hat{v}) \\ \delta(u^\varepsilon, \hat{\phi}) + \varepsilon(p_t^\varepsilon, \hat{\phi}) = 0 \\ (\theta_t^\varepsilon, \hat{\psi}) + \bar{\mathbf{a}}(\theta^\varepsilon, \hat{\psi}) + \tilde{B}(u^\varepsilon, \theta^\varepsilon, \hat{\psi}) = (\mathcal{G}, \hat{\psi}) \end{cases} \quad (2.16)$$

Theorem 2.2.2. *if $\varphi(x) \in H^2(\Omega)$, problem (2.15) has unique solution $(u, p, \theta) \in [L^2(0, T; X) \cap H^1(0, T; V)] \times L^2(0, T; M) \times H^1(0, T; W)$, satisfies*

$$\|\nabla\theta^{(i)}\| + \|\theta^{(i)}\| + \|\nabla u^{(i)}\| + \|u^{(i)}\| \leq \vartheta(t) \quad 0 \leq i \leq 3$$

where $\vartheta(t)$ is a continuous positive function depends on the data of $\varphi(x)$.

Theorem 2.2.3. *if $\varphi(x) \in H^2(\Omega)$, the artificial compressibility Navier-Stokes Forchheimer Fourier has a unique solution $(u^\varepsilon, p^\varepsilon, \theta^\varepsilon) \in [L^\infty([0, T]; H^2(\Omega)) \cap L^2([0, T]; X)] \times L^2([0, T]; M) \times H^1([0, T]; W)$.*

The solutions $(u^\varepsilon, p^\varepsilon, \theta^\varepsilon)$ converge to the solution (u, p, θ) uniformly as $\varepsilon \rightarrow 0$ has been proved in [20]. We can also refer to the proof of Theorem 3.1 and Theorem 3.2 in [13].

By using a similar argument to [21] we have the following properties

- **(H1).** Assume that the initial velocity $u_0 \in V$ and $f \in L^\infty([0, T]; L^2(\Omega))$, the initial temperature $\varphi \in W$, then $\theta \in L^\infty([0, T]; L^2(\Omega))$, there exists a finite time $t < T$ such that

$$\begin{aligned} u &\in C([0, t]; V) \cap L^2([0, t]; H^2(\Omega)) \\ \theta &\in L^2([0, t]; H^2(\Omega)) \\ p &\in L^2([0, t]; H^1(\Omega)/\mathbb{R}) \end{aligned} \quad (2.17)$$

- **(H2).** Assume that $\varphi \in H^2(\Omega)$ and $tf_t \in L^\infty([0, t]; L^2(\Omega))$, then $t\theta_t \in L^\infty([0, t]; L^2(\Omega))$.

By using the smoothing property of the Navier-Stokes Forchheimer Fourier problem, we has

$$tp_t \in L^2([0, t]; H^1(\Omega)) \quad (2.18)$$

$$t^2 p_{tt} \in L^2([0, t]; H^1(\Omega)) \quad (2.19)$$

$$g \in L^2([0, t]; L^2(\Omega)) \quad (2.20)$$

We recall the property of the monotonicity for any mapping F defined as

$$F : x \mapsto |x| x :$$

$$(|u|u - |v|v, u - v) \geq 0 \quad (2.21)$$

The following Sobolev inequality is useful to deal with the nonlinear form F

$$\|v\|_p \leq \|\nabla v\|, \quad 1 \leq p \leq 6 \quad (2.22)$$

It is known that if $\partial\Omega$ is smooth enough, we have for any $v \in V \cap H^2(\Omega)$

$$\|v\|_2 \leq \|\tilde{\Delta}v\| \quad (2.23)$$

where $\tilde{\Delta}$ is the Stokes operator.

Lemma 2.2.4. *Assume that $u, v \in H_0^1$ satisfy the estimates (2.22). Then*

$$\|F(u) - F(v)\| \leq C\|\nabla(u - v)\| \quad (2.24)$$

For the proof of this Lemma see [14].

For the readers convenience, we recall two lemmas of Gronwall type which which will frequently used.

Lemma 2.2.5. *(Gronwall Lemma). Let $y(t), h(t), g(t), f(t)$ be nonnegative functions satisfying*

$$y(t) + \int_0^t h(s) \leq y(0) + \int_0^t (g(s)y(s) + f(s)) ds \quad \forall 0 \leq t \leq T, \text{ with } \int_0^T g(t)dt \leq M$$

Then

$$y(t) + \int_0^t h(s)ds \leq \exp(M) \left(y(0) + \int_0^t f(s)ds \right), \quad \forall 0 \leq t \leq T$$

Lemma 2.2.6. *(Discrete Gronwall Lemma). Let $y^n(t), h^n(t), g^n(t), f^n(t)$ be nonnegative functions satisfying*

$$y^m + k \sum_{n=1}^m g^n \leq k \sum_{n=1}^m y^n g^n + C, \forall 1 \leq m \leq \frac{T}{k} \quad (2.25)$$

assume $kh^n \leq \frac{1}{2}$ and for all $1 \leq n \leq \frac{T}{k}$ then

$$y^m k \sum_{n=1}^m g^n \leq C \exp \left(2k \sum_{n=1}^{m-1} y^n \right) \quad \forall 1 \leq m \leq \frac{T}{k} \quad (2.26)$$

We recall also the generalization of the Gronwall-Bellman Lemma given by

Lemma 2.2.7. *Let $y(t)$ be a positive differentiable function satisfying the inequality:*

$$y(t) \leq c + \int_a^t (f(s)y(s) + g(s)y^n(s)) ds, \quad t \in I = [a, b] \quad (2.27)$$

where $c \geq 0$; the function $f(t)$ and $g(t)$ are continuous in I and $n > 1$ is a constant. Then:

$$y(t) \leq \frac{c \exp\left(\int_a^t f(s) ds\right)}{\left(1 - (n-1)c^{n-1} \int_a^t g(s) \exp\left((n-1) \int_a^s f(\tau) d\tau\right) ds\right)^{\frac{1}{n-1}}} \quad (2.28)$$

Under assumption, for $t, s \in [a, b]$

$$1 - (n-1)c^{n-1} \int_a^t g(s) \exp\left((n-1) \int_a^s f(\tau) d\tau\right) ds > 0 \quad (2.29)$$

for the proof of this Lemma see [19].

2.3 Analysis of the problem

Let $\Omega \in \mathbb{R}^d$ with ($d=2$ or 3) be an open bounded set with a sufficiently smooth boundary. Before studying the error estimates of the Navier-Stokes Forchheimer Fourier system. In the first step, we demonstrate the regularity of the solution of the system.

The unsteady incompressible Navier-Stokes Forchheimer Fourier equation system is written as

$$u_t - \lambda \Delta u + (u \cdot \nabla) u + au + b |u| u = -\nabla p + dg\beta\theta + f \quad (2.30)$$

$$\theta_t - \lambda \Delta \theta + (u \cdot \nabla) \theta = \mathcal{G} \quad (2.31)$$

$$\nabla \cdot u = 0 \quad (2.32)$$

where $f = -dg(\beta\theta_{in} + 1)$ and $f \in L^2(\Omega)$. The unknowns are the velocity u , the pressure p and the temperature θ . The system (2.30)-(2.31) should be completed with an initial condition

$$u(x, t=0) = u_0 \quad \theta(x, t=0) = \theta_0 \quad x \in \Omega \quad (2.33)$$

and an appropriate boundary condition. For the sake of simplicity, we shall consider only the homogeneous Dirichlet boundary condition for the triplet (u, p, θ) .

Lemma 2.3.1. *We assume that u_0, θ_0 and g satisfy the following regularity*

$$u_0 \in L^2(0, T; X) \cap H^1(0, T; V)$$

$$\theta_0 \in H^1(0, T; W)$$

$$g \in L_\infty, \quad f, f_t \in L^2, \quad \mathcal{G}, \mathcal{G}_t \in L^2$$

and we have the condition

$$\frac{4T}{\lambda} \left[\|\nabla u_0\|^2 + \frac{4T\|\mathcal{G}\|^2 d^2 \beta^2}{\kappa \lambda} \right] < 1$$

Then, there exists $t \leq T$ such the solution of the system (2.30), (2.31) satisfies

$$\|u(t)\|_2 + \|u_t(t)\| + \|p(t)\|_1 \leq C$$

$$\|\theta(t)\|_2 + \|\theta_t(t)\| \leq C$$

Proof. Multiply the equations (2.30) and (2.31) with $\tilde{\Delta}u$ and θ respectively and integrate the resulting equations to obtain

$$\begin{aligned} \frac{1}{2} \frac{d}{dt} \|\nabla u\|^2 + \lambda \|\tilde{\Delta}u\|^2 + a \|\nabla u\|^2 &= (dg\beta\theta, \tilde{\Delta}u) - (b | u | u, \tilde{\Delta}u) \\ &\quad - \tilde{B}(u, u, \tilde{\Delta}u) + (f, \tilde{\Delta}u) \end{aligned} \quad (2.34)$$

and for the Fourier equation, we have

$$\frac{1}{2} \frac{d}{dt} \|\theta\|^2 + \kappa \|\nabla \theta\|^2 = (\mathcal{G}, \theta) - \tilde{B}(u, \theta, \theta) \quad (2.35)$$

Using Cauchy-Schwarz and Young inequalities for the right hand side of (2.34) and (2.35) respectively, we have

$$\begin{aligned} |(dg\beta\theta, \tilde{\Delta}u)| &\leq d\beta \|g\|_{L^\infty} \|\theta\| \|\tilde{\Delta}u\| \\ &\leq \frac{2d^2\beta^2 \|g\|_{L^\infty}^2}{\lambda} \|\theta\|^2 + \frac{\lambda}{8} \|\tilde{\Delta}u\|^2 \\ |(b | u | u, \tilde{\Delta}u)| &\leq \frac{2b^2}{\lambda} \|\nabla u\|_4^4 + \frac{\lambda}{8} \|\tilde{\Delta}u\|^2 \\ |\tilde{B}(u, u, \tilde{\Delta}u)| &\leq \frac{\lambda}{8} \|\tilde{\Delta}u\|^2 + \frac{2}{\lambda} \|\nabla u\|^4 \\ |(f, \tilde{\Delta}u)| &\leq \frac{2}{\lambda} \|f\|^2 + \frac{\lambda}{8} \|\tilde{\Delta}u\|^2 \end{aligned}$$

Substituting all this approximation in (2.34), we get

$$\frac{1}{2} \frac{d}{dt} \|\nabla u\|^2 + \frac{\lambda}{2} \|\tilde{\Delta}u\|^2 + a \|\nabla u\|^2 \leq \frac{2d^2\beta^2 \|g\|_{L^\infty}^2}{\lambda} \|\theta\|^2 + \frac{2}{\lambda} \|\nabla u\|^4 + \frac{2}{\lambda} \|f\|^2 \quad (2.36)$$

Similarly for the Fourier equation (2.35), we have

$$|(\mathcal{G}, \theta)| \leq \|\mathcal{G}\| \|\theta\| \leq \frac{\kappa}{2} \|\nabla \theta\|^2 + \frac{1}{\kappa} \|\mathcal{G}\|^2$$

By replacing these term in (2.35), we get

$$\frac{1}{2} \frac{d}{dt} \|\theta\|^2 + \frac{\kappa}{2} \|\nabla \theta\|^2 \leq \frac{1}{\kappa} \|\mathcal{G}\|^2 \quad (2.37)$$

$$\|\theta\|^2 + \int_0^t \|\nabla\theta(s)\|^2 ds \leq C_1 \quad (2.38)$$

Using (2.38) in (2.36), we have

$$\frac{1}{2} \frac{d}{dt} \|\nabla u\|^2 + \frac{\lambda}{2} \|\tilde{\Delta}u\|^2 \leq C_1 + \frac{2}{\lambda} \|\nabla u\|^4 + \frac{2}{\lambda} \|f\|^2 \quad (2.39)$$

where :

$$C_1 = \frac{T\|\mathcal{G}\|^2}{\kappa} \frac{2d^2\beta^2\|g\|_{L^\infty}^2}{\lambda}$$

In particular, it is equivalent to solve the following equation, and pose $\varepsilon = \frac{2}{\lambda}$

$$\frac{d}{dt}y(t) \leq \varepsilon y(t)^2 \quad \text{with} \quad y(t) = \|\nabla u\|^2 + C_2, \quad y(0) = \|\nabla u(0)\|^2 + C_2$$

Then we have

$$\frac{1}{2} \frac{d}{dt} \|\nabla u\|^2 \leq C_1 + \frac{2}{\lambda} (\|\nabla u\|^2)^2 \quad \text{with} \quad C_1 = \frac{1}{\lambda} \left[\frac{2d^2\beta^2T\|g\|_{L^\infty}^2\|\mathcal{G}\|^2}{\kappa} \right] \quad (2.40)$$

Using Gronwall generalization Lemma (2.2.7), we deduce that

$$\|\nabla u(t)\|^2 \leq C_3 \quad (2.41)$$

Consequently, using (2.39) and (2.41)

$$\sup_{0 \leq t \leq T} \|\nabla u(t)\|^2 + \lambda \int_0^t \|\tilde{\Delta}u(t)\|^2 dt \leq C \quad (2.42)$$

We multiplay the first derivative of (2.30)(2.31) with u_t and θ_t respectively, we integrate the resulting equations, we have

$$\begin{aligned} \frac{1}{2} \frac{d}{dt} \|u_t\|^2 + \frac{\lambda}{2} \|\nabla u_t\|^2 + a \|u_t\|^2 &\leq \frac{4d^2\beta^2\|g\|_{L^\infty}^2}{\lambda} \|\theta\|^2 + \frac{4}{\lambda} (\|u\|_1 \|u\|_2) \|u_t\|^2 \\ &\quad + \frac{4c}{\lambda} \| |u| \|^2 + \frac{4}{\lambda} \|f_t\|^2 \end{aligned} \quad (2.43)$$

$$\frac{1}{2} \frac{d}{dt} \|\theta_t\|^2 + \kappa \|\nabla \theta_t\|^2 \leq \frac{2}{\kappa} (\|\theta\|_1 \|\theta\|_2) \|u_t\|^2 + \frac{2}{\kappa} \|\mathcal{G}_t\|^2 \quad (2.44)$$

We integrate (2.43) and (2.44) with respect to t , we obtain

$$\begin{aligned} \|u_t\|^2 + \lambda \int_0^t \|\nabla u_t(s)\|^2 ds + a \int_0^t \|u_t(s)\|^2 ds &\leq \frac{4d^2\beta^2\|g\|_{L^\infty}^2}{\lambda} \int_0^t \|\theta_t(s)\|^2 ds \\ &+ \frac{4}{\lambda} (\|u\|_1\|u\|_2) \int_0^t \|u_t(s)\|^2 ds \\ &+ \frac{4c}{\lambda} \| |u| \|^2 \int_0^t \|u_t(s)\|^2 ds + \frac{4}{\lambda} \|f_t\|^2 \int_0^t ds \end{aligned} \quad (2.45)$$

$$\|\theta_t\|^2 + \kappa \int_0^t \|\nabla\theta_t(s)\|^2 ds \leq \frac{2}{\kappa} (\|\theta\|_1\|\theta\|_2) \int_0^t \|u_t(s)\|^2 ds + \frac{2}{\kappa} \|\mathcal{G}_t\|^2 \int_0^t ds \quad (2.46)$$

From (2.46), we have

$$\int_0^t \|\nabla\theta_t(s)\|^2 ds \leq \frac{2}{\kappa^2} (\|\theta\|_1\|\theta\|_2) \int_0^t \|u_t(s)\|^2 ds - \frac{2}{\kappa} \|\theta_t\|^2 + \frac{2}{\kappa^2} \|\mathcal{G}_t\|^2 \int_0^t ds \quad (2.47)$$

We replace $\|\theta_t\|^2$ with $c\|\nabla\theta_t\|^2$ in (2.45) and using (2.47), we have

$$\begin{aligned} \|u_t\|^2 + \lambda \int_0^t \|\nabla u_t(s)\|^2 ds + a \int_0^t \|u_t(s)\|^2 ds &\leq \frac{4c^2d^2\beta^2\|g\|_{L^\infty}^2}{\lambda} \int_0^t \|\nabla\theta_t(s)\|^2 ds \\ &+ \frac{4}{\lambda} (\|u\|_1\|u\|_2) \int_0^t \|u_t(s)\|^2 ds \\ &+ \frac{4c}{\lambda} \| |u| \|^2 \int_0^t \|u_t(s)\|^2 ds + \frac{4}{\lambda} \|f_t\|^2 \int_0^t ds \end{aligned} \quad (2.48)$$

$$\begin{aligned} \|u_t\|^2 + \lambda \int_0^t \|\nabla u_t(s)\|^2 ds + a \int_0^t \|u_t(s)\|^2 ds &\leq \frac{8c^2d^2\beta^2\|g\|_{L^\infty}^2}{\kappa^2\lambda} (\|\theta\|_1\|\theta\|_2) \int_0^t \|u_t(s)\|^2 ds \\ &+ \frac{4}{\lambda} (\|u\|_1\|u\|_2) \int_0^t \|u_t(s)\|^2 ds \\ &+ \frac{4c}{\lambda} \| |u| \|^2 \int_0^t \|u_t(s)\|^2 ds \\ &+ \left[\frac{4}{\lambda} \|f_t\|^2 + \frac{8c^2d^2\beta^2\|g\|_{L^\infty}^2}{\kappa^2\lambda} \|\mathcal{G}_t\|^2 \right] \int_0^t ds \end{aligned}$$

So, we have

$$\|u_t\|^2 + \lambda \int_0^t \|\nabla u_t(s)\|^2 ds + a \int_0^t \|u_t(s)\|^2 ds \leq C \quad (2.49)$$

Now, taking the time derivative of (2.30) and (2.31), we obtain

$$u_{tt} - \lambda\Delta u_t + \tilde{B}(u_t, u) + \tilde{B}(u, u_t) + au_t + 2b |u| u_t = -\nabla p_t + dg\beta\theta_t + f_t \quad (2.50)$$

$$\theta_{tt} - \lambda \Delta \theta_t = \mathcal{G}_t - \tilde{B}(u_t, \theta) - \tilde{B}(u, \theta_t) \quad (2.51)$$

Multiplying the relation (2.51) with θ_t , we get

$$\begin{aligned} \frac{1}{2} \frac{d}{dt} \|\theta_t\|^2 + \kappa \|\nabla \theta_t\|^2 &= (\mathcal{G}_t, \theta_t) - \tilde{B}(u_t, \theta, \theta_t) - \tilde{B}(u, \theta_t, \theta_t) \\ &= (\mathcal{G}_t, \theta_t) - \tilde{B}(u_t, \theta, \theta_t) \end{aligned} \quad (2.52)$$

Using Cauchy-Schwarz and Young inequalities for the right hand side of (2.34)

$$\begin{aligned} |(\mathcal{G}_t, \theta_t)| &\leq \|\mathcal{G}\| \|\theta_t\| \leq \frac{\kappa}{4} \|\nabla \theta\|^2 + \frac{2}{\kappa} \|\mathcal{G}\|^2 \\ |\tilde{B}(u_t, \theta, \theta_t)| &\leq \|u_t\| \|\theta\|_1^{1/2} \|\theta\|_2^{1/2} \|\nabla \theta_t\| \\ &\leq \frac{\kappa}{4} \|\nabla \theta_t\|^2 + \frac{2}{\kappa} \|\theta\|_1 \|\theta\|_2 \|u_t\|^2 \\ \frac{1}{2} \frac{d}{dt} \|\theta_t\|^2 + \frac{\kappa}{2} \|\nabla \theta_t\|^2 &\leq \frac{2}{\kappa} (\|\theta\|_1 \|\theta\|_2) \|u_t\|^2 + \frac{2}{\kappa} \|\mathcal{G}_t\|^2 \end{aligned} \quad (2.53)$$

Using Cauchy-Schwarz inequality,

$$\int_0^t \|\theta(s)\|_1 \|\theta(s)\|_2 ds \leq \left(\int_0^t \|\theta(s)\|_1^2 ds \right)^{\frac{1}{2}} \left(\int_0^t \|\theta(s)\|_2^2 ds \right)^{\frac{1}{2}} \leq C \quad (2.54)$$

Applying Gronwall Lemma to (2.53) and (2.49), we obtain

$$\|\theta_t(t)\|_2^2 + \int_0^t \|\nabla \theta_t(s)\|_2^2 ds \leq C \quad (2.55)$$

Now, multiplying the equation (2.50) with u_t , we get

$$\begin{aligned} \frac{1}{2} \frac{d}{dt} \|u_t\|^2 + \lambda \|\nabla u_t\|^2 + a \|u_t\|^2 &= (dg\beta\theta_t, u_t) - (2b | u | u_t, u_t) \\ &\quad - \tilde{B}(u_t, u, u_t) + (f_t, u_t) \end{aligned} \quad (2.56)$$

$$|(dg\beta\theta_t, u_t)| \leq \frac{4d^2\beta^2 \|g\|_{L^\infty}^2}{\lambda} \|\theta_t\|^2 + \frac{\lambda}{8} \|\nabla u_t\|^2$$

$$\begin{aligned} |\tilde{B}(u_t, u, u_t)| &\leq \|u_t\| \|u\|_1^{1/2} \|u\|_2^{1/2} \|\nabla u_t\| \\ &\leq \frac{\lambda}{8} \|\nabla u_t\|^2 + \frac{4}{\lambda} \|u\|_1 \|u\|_2 \|u_t\|^2 \end{aligned}$$

$$|(f_t, u_t)| \leq \frac{4}{\lambda} \|f_t\|^2 + \frac{\lambda}{8} \|\nabla u_t\|^2$$

$$\begin{aligned} |(2b | u | u_t, u_t)| &\leq c \| | u | \| \|u_t\| \|\nabla u_t\| \\ &\leq \frac{4c}{\lambda} \| | u | \|^2 \|u_t\|^2 + \frac{\lambda}{8} \|\nabla u_t\|^2 \end{aligned}$$

By replacing the different terms in the equation (2.56), we get

$$\begin{aligned} \frac{1}{2} \frac{d}{dt} \|u_t\|^2 + \frac{\lambda}{2} \|\nabla u_t\|^2 + a \|u_t\|^2 &\leq \frac{4d^2 \beta^2 \|g\|_{L^\infty}^2}{\lambda} \|\theta_t\|^2 + \frac{4}{\lambda} \|u\|_1 \|u\|_2 \|u_t\|^2 \\ &+ \frac{4c}{\lambda} \| |u| \|^2 \|u_t\|^2 + \frac{4}{\lambda} \|f_t\|^2 \end{aligned} \quad (2.57)$$

Using Cauchy-Schwarz inequality, estimates (2.23) and (2.42), to have

$$\int_0^t \|u(s)\|_1 \|u(s)\|_2 ds \leq \left(\int_0^t \|u(s)\|_1^2 ds \right)^{\frac{1}{2}} \left(\int_0^t \|u(s)\|_2^2 ds \right)^{\frac{1}{2}} \leq C \quad (2.58)$$

Using (2.55) and applying Gronwall Lemma to (2.57), we obtain

$$\|u_t\|^2 + \int_0^t (\lambda \|\nabla u_t(s)\|^2 + a \|u_t(s)\|^2) ds \leq C \quad (2.59)$$

Multiplying the equation (2.30) by $\tilde{\Delta}u$, we get

$$\begin{aligned} \lambda \|\tilde{\Delta}u\| &= - \left(u_t, \tilde{\Delta}u \right) - \left(au_t, \tilde{\Delta}u \right) - \left(b |u| u, \tilde{\Delta}u \right) \\ &\quad - \left(\tilde{B}(u, u, \tilde{\Delta}u) \right) + \left(d\beta g\theta, \tilde{\Delta}u \right) + \left(f, \tilde{\Delta}u \right) \\ &\leq \frac{\lambda}{10} \|\tilde{\Delta}u\|^2 + 2\lambda \|u_t\|^2 + 2a \|\nabla u\|^2 + \frac{\lambda}{10} \|\tilde{\Delta}u\|^2 \\ &\quad + \frac{5b}{\lambda} \|\nabla u\|_4^4 + \frac{\lambda}{10} \|\tilde{\Delta}u\|^2 + \frac{\lambda}{10} \|\tilde{\Delta}u\|^2 + \frac{5}{\lambda} \|\nabla u\|^6 \\ &\quad + \frac{\lambda}{10} \|\tilde{\Delta}u\|^2 + 2d^2 \beta^2 \|g\|_{L^\infty}^2 \|\theta\|^2 + \frac{\lambda}{10} \|\tilde{\Delta}u\|^2 + \frac{10}{\lambda} \|f\|^2 \end{aligned}$$

So, we can deduce

$$\|u\|_2 \leq C \quad \forall t \in [0, T_1] \quad (2.60)$$

$$\|\theta\|_2 \leq C \quad \forall t \in [0, T_1] \quad (2.61)$$

For the pressure estimate, we use the equation (2.30) to have

$$\|\nabla p\| \leq \left(\|u_t\| + \lambda \|\nabla u\| + a \|u\| + b \| |u|^2 \| + \|\tilde{B}(u, u)\| + d\beta \|g\| \|\theta\| + \|f\| \right) \quad (2.62)$$

Using the Hölder's inequality, we have

$$\|\tilde{B}(u, u)\| \leq c \|u\|_4 \|\nabla u\|_4$$

Using Galiardo-Nirenberg's inequalities, we have

$$\|u\|_4 \leq c \|u\|^{1/2} \|Au^{1/2}\|^{1/2}$$

$$\|\nabla u\|_4 \leq c\|\nabla v\|^{3/2}$$

Hence

$$\|\tilde{B}(u, u)\| \leq c\|u\|^{1/2}\|u\|_2^2 \leq C$$

Lemma 2.3.2. *We suppose in addition*

$$f_t, f_{tt} \in C[0, T; L^2(\Omega)]$$

$$\mathcal{G}_t, \mathcal{G}_{tt} \in C[0, T; L^2(\Omega)]$$

The the solution of the system (2.30), (2.31)

$$\|u_t(t)\|_2^2 + \|\nabla p_t\| + \int_0^t (\|u_{tt}(s)\|_2^2 + \|p_{tt}(s)\|_1^2) ds \leq C \quad \forall t \in [0, T_1]$$

$$\|\theta_t(t)\|_2^2 + \int_0^t \|\theta_{tt}(s)\|_2^2 ds \leq C$$

Proof. We have the time derivative of (2.30), (2.31)

$$\begin{aligned} u_{tt} - \lambda\Delta u_t + au_t &= -\nabla p_t + dg\beta\theta_t + f_t \\ &\quad - \tilde{B}(u_t, u) - \tilde{B}(u, u_t) - 2b|u|u_t \end{aligned} \quad (2.63)$$

$$\theta_{tt} - \kappa\Delta\theta_t = \mathcal{G}_t - \tilde{B}(u_t, \theta) - \tilde{B}(u, \theta_t) \quad (2.64)$$

Multiplying the equation (2.63) by $\tilde{\Delta}u_t$ and (2.64) by θ_t , we have

$$\begin{aligned} \frac{1}{2} \frac{d}{dt} \|\nabla u_t\|^2 + \lambda \|\tilde{\Delta}u_t\|^2 + a \|\nabla u_t\|^2 &= (dg\beta\theta_t, \tilde{\Delta}u_t) - (b|u|u_t, \tilde{\Delta}u_t) \\ &\quad - \tilde{B}(u_t, u, \tilde{\Delta}u_t) - \tilde{B}(u, u_t, \tilde{\Delta}u_t) + (f, \tilde{\Delta}u_t) \end{aligned}$$

Using Cauchy-Schwarz and Young inequalities, we have

$$\begin{aligned} |\tilde{B}(u_t, u, \tilde{\Delta}u_t)| &\leq \frac{\lambda}{10} \|\tilde{\Delta}u_t\|^2 + \frac{5}{\lambda} \|u\|_2^2 \|\nabla u_t\|^2 \\ |\tilde{B}(u, u_t, \tilde{\Delta}u_t)| &\leq \frac{\lambda}{10} \|\tilde{\Delta}u_t\|^2 + \frac{5}{\lambda} \|u\|_2^2 \|\nabla u_t\|^2 \\ |(dg\beta\theta_t, \tilde{\Delta}u_t)| &\leq \frac{\lambda}{10} \|\tilde{\Delta}u_t\|^2 + \frac{5d^2\beta^2\|g\|_{L^\infty}^2}{\lambda} \|\theta_t\|^2 \\ |(b|u|u_t, \tilde{\Delta}u_t)| &\leq \frac{\lambda}{10} \|\tilde{\Delta}u_t\|^2 + \frac{5b^2}{\lambda} \|u\|^2 \|u_t\|^2 \\ |(f, \tilde{\Delta}u_t)| &\leq \frac{\lambda}{10} \|\tilde{\Delta}u_t\|^2 + \frac{5}{\lambda} \|f\|^2 \end{aligned}$$

$$\begin{aligned} \frac{1}{2} \frac{d}{dt} \|\nabla u_t\|^2 + \frac{\lambda}{2} \|\tilde{\Delta} u_t\|^2 + a \|\nabla u_t\|^2 &\leq \frac{5d^2 \beta^2 \|g\|_{L^\infty}^2}{\lambda} \|\theta_t\|^2 + \frac{10}{\lambda} \|u\|_2^2 \|\nabla u_t\|^2 \\ &\quad + \frac{5b^2}{\lambda} \|u\|^2 \|u_t\|^2 + \frac{5}{\lambda} \|f\|^2 \end{aligned}$$

Using the previous estimates (2.22), (2.41), (2.60), (2.59) and (2.56), to obtain

$$\frac{1}{2} \frac{d}{dt} \|\nabla u_t\|^2 + \lambda \|\tilde{\Delta} u_t\|^2 \leq C_3 + C \|\nabla u_t\|^2 + \frac{10}{\lambda} \|f\|^2 \quad (2.65)$$

Thanks to Gronwall's inequality, we infer that

$$\sup_{0 \leq t \leq T} \|\nabla u_t(t)\|^2 + \lambda \int_0^t \|\tilde{\Delta} u_t(t)\|^2 dt \leq C \quad (2.66)$$

Subsequently, we take the second time derivative of the system (2.30),(2.31), we have

$$\begin{aligned} u_{ttt} + \lambda \Delta u_{tt} + a u_{tt} &= -\nabla p_{tt} + d\beta g \theta_{tt} - 2b |u_t| u_t - 2b |u| u_{tt} \\ &\quad - \tilde{B}(u_{tt}, u) - \tilde{B}(u, u_{tt}) - 2\tilde{B}(u_t, u_t) + f_{tt} \end{aligned} \quad (2.67)$$

$$\theta_{ttt} + \kappa \Delta \theta_{tt} = \mathcal{G}_{tt} - \tilde{B}(u_{tt}, \theta) - \tilde{B}(u, \theta_{tt}) - 2\tilde{B}(u_t, \theta_t) \quad (2.68)$$

We take the inner product of (2.67), (2.68) with u_{tt} and θ_{tt} respectively, we obtain

$$\begin{aligned} \frac{1}{2} \frac{d}{dt} \|u_{tt}\|^2 + \lambda \|\nabla u_{tt}\|^2 + a \|u_{tt}\|^2 &= (d\beta g \theta_{tt}, u_{tt}) - (f_{tt}, u_{tt}) \\ &\quad - (2b |u_t| u_t, u_{tt}) - (2b |u| u_{tt}, u_{tt}) \\ &\quad - 2\tilde{B}(u_t, u_t, u_{tt}) - \tilde{B}(u_{tt}, u, u_{tt}) \end{aligned} \quad (2.69)$$

$$\frac{1}{2} \frac{d}{dt} \|\theta_{tt}\|^2 + \kappa \|\nabla \theta_{tt}\|^2 = (\mathcal{G}_{tt}, \theta_{tt}) - 2\tilde{B}(u_t, \theta_t, \theta_{tt}) - \tilde{B}(u_{tt}, \theta, \theta_{tt}) \quad (2.70)$$

Using Cauchy-Schwarz and Young inequalities, we have

$$\begin{aligned} |\tilde{B}(u_t, \theta_t, \theta_{tt})| &\leq \frac{\kappa}{6} \|\nabla \theta_{tt}\|^2 + \frac{3}{\kappa} \|u_t\|^2 \|\theta_t\|^2 \\ |\tilde{B}(u_{tt}, \theta, \theta_{tt})| &\leq \frac{\kappa}{6} \|\nabla \theta_{tt}\|^2 + \frac{3}{\kappa} \|u_t\|^2 \|\theta_{tt}\|^2 \\ |(\mathcal{G}_{tt}, \theta_{tt})| &\leq \frac{\kappa}{6} \|\nabla \theta_{tt}\|^2 + \frac{3}{\kappa} \|\mathcal{G}_{tt}\|^2 \end{aligned}$$

Using the estimates (2.66) and applying Gronwall Lemma, we get

$$\|\theta_{tt}\|^2 + \kappa \int_0^t \|\nabla \theta_{tt}(s)\|^2 ds \leq C \quad (2.71)$$

Using Cauchy-Schwarz and Young inequalities for the right hand-side of the equation (2.69), we

have

$$\begin{aligned}
 |(d\beta g\theta_{tt}, u_{tt})| &\leq d\beta\|g\|_\infty\|\theta_{tt}\|\|\nabla u_{tt}\| \\
 &\leq \frac{\lambda}{10}\|\nabla u_{tt}\|^2 + \frac{5d^2\beta^2\|g\|_\infty^2}{\lambda}\|\theta_{tt}\|^2 \\
 |(f_{tt}, u_{tt})| &\leq \frac{\lambda}{10}\|\nabla u_{tt}\|^2 + \frac{5}{\lambda}\|f_{tt}\|^2 \\
 |(b|u_t|u_t, u_{tt})| &\leq \| |u_t| \| \|u_t\| \|\nabla u_{tt}\| \\
 &\leq \frac{\lambda}{10}\|\nabla u_{tt}\|^2 + \frac{5}{\lambda}\| |u_t| \|^2\|u_t\|^2 \\
 |(b|u|u_{tt}, u_{tt})| &\leq \| |u| \| \|u_{tt}\| \|u_{tt}\| \leq \frac{\lambda}{12}\|\nabla u_{tt}\|^2 + \frac{5b^2}{\lambda}\| |u| \|^2\|u_{tt}\|^2 \\
 |\tilde{B}(u_t, u_t, u_{tt})| &\leq \|u_t\|_2\|u_t\|_1\|u_{tt}\| \leq \|\nabla u_t\|^2 + \|u_t\|_2^2\|u_{tt}\|^2 \\
 |\tilde{B}(u_{tt}, u, u_{tt})| &\leq \|u_{tt}\|_1\|u\|_2\|u_{tt}\| \leq \frac{\lambda}{10}\|\nabla u_{tt}\|^2 + \frac{5}{\lambda}\|u_{tt}\|^2 \\
 \frac{1}{2}\frac{d}{dt}\|u_{tt}\|^2 + \lambda\|\nabla u_{tt}\|^2 + a\|u_{tt}\|^2 &\leq \frac{5d^2\beta^2\|g\|_\infty^2}{\lambda}\|\theta_{tt}\|^2 + \frac{5}{\lambda}\| |u_t| \|^2\|u_t\|^2 \\
 &\quad + \frac{5}{\lambda}\| |u| \|^2\|u_{tt}\|^2 + \|\nabla u_t\|^2 \\
 &\quad + \|u_t\|_2^2\|u_{tt}\|^2 + \frac{5}{\lambda}\|u_{tt}\|^2 + \frac{5}{\lambda}\|f_{tt}\|^2
 \end{aligned} \tag{2.72}$$

Using the estimates (2.66) and (2.71) and applying the Gronwall Lemma, we get

$$\|u_{tt}\|^2 + \lambda \int_0^t \|\nabla u_{tt}(s)\|^2 ds \leq C \tag{2.73}$$

Multiplying the equations (2.63) by $\tilde{\Delta}u_t$, we obtain

$$\begin{aligned}
 \lambda\|\tilde{\Delta}u_t\|^2 &= (dg\beta\theta_t, \tilde{\Delta}u_t) + (f_t, \tilde{\Delta}u_t) - (u_{tt}, \tilde{\Delta}u_t) - (\tilde{B}(u_t, u), \tilde{\Delta}u_t) \\
 &\quad - (\tilde{B}(u, u_t), \tilde{\Delta}u_t) - (au_t, \tilde{\Delta}u_t) - (2b|u|u_t, \tilde{\Delta}u_t) \\
 &\leq \frac{10}{\lambda}\|u_{tt}\|^2 + \frac{10d^2\beta^2\|g\|_\infty^2}{\lambda}\|\theta_t\|^2 + \frac{20}{\lambda}\|u\|_2^2\|\nabla u_t\|^2 \\
 &\quad + 2a\|\nabla u_t\|^2 + \frac{10b}{\lambda}\|u\|^2\|u_t\|^2 + \frac{10}{\lambda}\|f\|^2
 \end{aligned}$$

By applying the previous estimates (2.73), (2.66), (2.55), we can deduce

$$\|u_t\|_2 \leq C \quad \forall t \in [0, T] \tag{2.74}$$

$$\|\theta_t\|_2 \leq C \quad \forall t \in [0, T] \tag{2.75}$$

■

2.4 Error estimates for the linearized problem

We consider the following linear problem of the Navier-Stokes Forchheimer Fourier equations. The results in this section will be used in the next section as an intermediate step for analyzing the nonlinear Navier-Stokes Forchheimer Fourier problem.

$$\begin{cases} \partial_t u - \lambda \Delta u + au - \nabla p = dg[\beta(\theta - \theta_{in}) - 1] & \text{in } \Omega \times [0, T] \\ \partial_t \theta - \eta \Delta \theta = \mathcal{G} & \text{in } \Omega \times [0, T] \\ \operatorname{div} u = 0 & \text{in } \Omega \times [0, T] \\ u(x, t = 0) = a_0(x), & \theta(x, t = 0) = \tau_0(x) & \text{in } \Omega \\ u(x, t) = 0, & \theta(x, t) = \xi(x, t) & x \in \Gamma_1 \\ u(x, t) = 0, & \frac{\partial \theta}{\partial n} = 0 & \text{on } (\Gamma_B \cup \Gamma_s) \times [0, T] \end{cases} \quad (2.76)$$

The pseudo-compressibility method applied to (2.76) is

$$\begin{cases} \partial_t u_\varepsilon - \lambda \Delta u_\varepsilon + au_\varepsilon - \nabla p_\varepsilon = dg[\beta(\theta_\varepsilon - \theta_{in}) - 1] & \text{in } \Omega \times [0, T] \\ \partial_t \theta_\varepsilon - \eta \Delta \theta_\varepsilon = \mathcal{G} & \text{in } \Omega \times [0, T] \\ \partial_t p_\varepsilon + \operatorname{div} u_\varepsilon = 0 & \text{in } \Omega \times [0, T] \\ u_\varepsilon(x, t = 0) = a_0(x), & \theta_\varepsilon(x, t = 0) = \tau_0(x) & \text{in } \Omega \\ u_\varepsilon(x, t) = 0, & \theta_\varepsilon(x, t) = \xi(x, t) & x \in \Gamma_1 \\ u_\varepsilon(x, t) = 0, & \frac{\partial \theta_\varepsilon}{\partial n} = 0 & \text{on } (\Gamma_B \cup \Gamma_s) \times [0, T] \end{cases} \quad (2.77)$$

Setting $e = u - u^\varepsilon$, $q = p - p^\varepsilon$ and $\xi = \theta - \theta^\varepsilon$, it follows that $e(0) = q(0) = \xi(0) = 0$. We shall derive a sequence of estimate for the artificial compressibility error e , q and ξ . Subtracting (2.77) from (2.76)

$$\begin{cases} (e_t, \hat{v}) + \mathbf{a}(e, \hat{v}) + (ae, \hat{v}) + \varepsilon(q_t, \hat{\phi}) = \varepsilon(p_t, \hat{\phi}) + (dg\beta\xi, \hat{v}) \\ (\xi, \hat{\psi}) + \bar{\mathbf{a}}(\xi, \hat{\psi}) = 0 \end{cases} \quad (2.78)$$

Lemma 2.4.1. *Suppose (H1) and (H2) are valid, ε sufficiently small, for all $t \in [0, T]$, we have*

$$\int_0^t s^2 \|p_t^\varepsilon(s)\|^2 ds \leq C \quad (2.79)$$

We recall this result from the reference [9]

Lemma 2.4.2. *Suppose (H1) is valid, ε sufficiently small, for all $t \in [0, T]$, we have*

$$\|e\|^2 + \lambda \int_0^t \|\nabla e(s)\|^2 + a \int_0^t \|e(s)\|^2 ds + \varepsilon \int_0^t \|q(s)\|^2 \leq C\varepsilon \quad (2.80)$$

$$\int_0^t \|e(s)\|^2 ds \leq C\varepsilon^2 \quad (2.81)$$

$$\|\xi\|^2 + \kappa \int_0^t \|\nabla \xi(s)\|^2 ds = 0 \quad (2.82)$$

Proof. Taking $(\hat{v}, \hat{\phi}, \hat{\psi}) = (e, q, \xi)$ in (2.78), we obtain

$$\begin{cases} (e_t, e) + \mathbf{a}(e, e) + (ae, e) + \varepsilon(q_t, q) = \varepsilon(p_t, q) + (dg\beta\xi, e) \\ (\xi_t, \xi) - \bar{\mathbf{a}}(\xi, \xi) = 0 \end{cases} \quad (2.83)$$

$$\begin{aligned} & \frac{1}{2} \frac{d}{dt} \|e\|^2 + \lambda \|\nabla e\|^2 + a\|e\|^2 + \frac{\varepsilon}{2} \frac{d}{dt} \|q\|^2 \\ & \leq \frac{\varepsilon}{2} \frac{d}{dt} \|p\|^2 + \frac{\varepsilon}{2} \|q\|^2 + \frac{\lambda}{2} \|\nabla e\|^2 + C\|g\|^2 \|\nabla \xi\|^2 \end{aligned} \quad (2.84)$$

and we have

$$\frac{1}{2} \frac{d}{dt} \|\xi\|^2 + \kappa \|\nabla \xi\|^2 = 0 \quad (2.85)$$

$$\frac{1}{2} \frac{d}{dt} \|e\|^2 + \frac{\lambda}{2} \|\nabla e\|^2 + a\|e\|^2 + \frac{\varepsilon}{2} \frac{d}{dt} \|q\|^2 \leq \frac{\varepsilon}{2} \frac{d}{dt} \|p\|^2 + \frac{\varepsilon}{2} \|q\|^2 \quad (2.86)$$

Intergrating the above two inequalities from $[0, t \leq T]$ thanks to $e(0) = 0$, $q(0) = 0$ and $\xi(0) = 0$, we have

$$\|e\|^2 + \lambda \int_0^t \|\nabla e(s)\|^2 ds + 2a \int_0^t \|e(s)\|^2 ds + \varepsilon \int_0^t \|q(s)\|^2 ds \leq \varepsilon \|p\|^2 + 2 \int_0^t \|q(s)\|^2 ds \quad (2.87)$$

$$\|e\|^2 + \lambda \int_0^t \|\nabla e(s)\|^2 ds + 2a \int_0^t \|e(s)\|^2 ds + \varepsilon \|q\|^2 \leq C\varepsilon \quad (2.88)$$

$$\|\xi\|^2 + \kappa \int_0^t \|\nabla \xi(s)\|^2 ds = 0 \quad (2.89)$$

Now we use the standard parabolic duality argument, for $0 < t \leq T$, we define (w, π) by

$$\begin{cases} w_s + \lambda \Delta w + aw + \nabla \pi = e(s) \\ \nabla \cdot w = 0 \\ w(t) = 0 \end{cases} \quad (2.90)$$

There are the following inequality

$$\lambda \int_0^t \|w(s)\|_2^2 ds + a \int_0^t \|w(s)\|^2 ds + \int_0^t \|\nabla \pi(s)\|^2 ds \leq C \int_0^t \|e(s)\|^2 ds \quad (2.91)$$

We take the inner product of (2.90) with $e(s)$ in right of (2.83) and $\nabla \cdot w = 0$, and we derive

$$\begin{aligned} \|e\|^2 &= (w_s, e) + \lambda(\Delta w, e) + a(w, e) + (\nabla \pi, e) \\ &= \frac{d}{ds}(w, e) - \varepsilon(\pi, p_t^\varepsilon) + (dg\beta\xi, e) \end{aligned} \quad (2.92)$$

Integrating from 0 to t , using Schwarz inequality (2.5), (2.89) and (2.91), since $w(t) = e(0) = 0$, we have

$$\begin{aligned} \int_0^t \|e(s)\|^2 ds &\leq \varepsilon \int_0^t \|\pi(s)\| \|p_t^\varepsilon(s)\| ds + dg\beta \int_0^t \|\xi(s)\| \|e(s)\| ds \\ &\leq C\varepsilon^2 \int_0^t \|\pi(s)\|^2 ds + C\varepsilon^2 \int_0^t \|p_t^\varepsilon(s)\|^2 ds \end{aligned} \quad (2.93)$$

We conclude

$$\int_0^t \|e(s)\|^2 ds \leq C\varepsilon^2 \quad (2.94)$$

■

Theorem 2.4.3. *Suppose (H1) and (H2) are valid, ε sufficiently small, for all $t \in [0, T]$, we have*

$$t\|e\|^2 + \lambda \int_0^t s \|\nabla e(s)\|^2 ds + a \int_0^t s \|e(s)\|^2 ds + t\varepsilon \int_0^t \|q(s)\|^2 ds \leq C\varepsilon^2 \quad (2.95)$$

$$\int_0^t s^2 \|e_t(s)\|^2 ds + \lambda t^2 \|\nabla e\|^2 + at^2 \|e\|^2 + \int_0^t s^2 \varepsilon \|q_{tt}(s)\|^2 ds \leq C\varepsilon^2 \quad (2.96)$$

Proof. We have the following error estimates of the artificial compressibility method

$$e_t - \lambda\Delta e + ae + \nabla q = dg\beta\xi \quad (2.97)$$

$$\nabla \cdot e + \varepsilon q_t = \varepsilon p_t \quad (2.98)$$

$$\xi_t - \kappa\Delta\xi = 0 \quad (2.99)$$

Taking the inner product of (2.97) with te and (2.98) with tq , summing up the two relations and using (2.97), we derive

$$\begin{aligned} &\frac{1}{2} \frac{d}{dt} t \|e\|^2 + \lambda t \|\nabla e\|^2 + at \|e\|^2 + \frac{1}{2} \frac{d}{dt} t \varepsilon \|q\|^2 \\ &= t\varepsilon(p_t, e) + (dg\beta\xi, e) \\ &\frac{1}{2} \frac{d}{dt} t \|e\|^2 + \lambda t \|\nabla e\|^2 + at \|e\|^2 + \frac{1}{2} \frac{d}{dt} t \varepsilon \|q\|^2 \\ &= t\varepsilon(p_t, e) + (dg\beta\xi, e) \\ &\leq \frac{\varepsilon}{2} \frac{d}{dt} t \|p\|^2 + \frac{\varepsilon}{2} t \|q\|^2 + \frac{\lambda}{2} t \|\nabla e\|^2 + Ct \|g\|^2 \|\nabla \xi\|^2 \end{aligned} \quad (2.100)$$

Integrating (2.100) from 0 to t , using the above relation, the Cauchy-Schwarz inequality, Lemma (2.4.2) and **(H2)**, we derive

$$\begin{aligned} & t\|e\|^2 + \frac{\lambda}{2} \int_0^t s \|\nabla e(s)\|^2 ds + a \int_0^t s \|e(s)\|^2 ds + \varepsilon \int_0^t s \|q(s)\|^2 ds \\ & \leq \varepsilon t \|p\|^2 + \frac{\varepsilon}{2} \int_0^t s \|q(s)\|^2 ds + C \int_0^t s \|\nabla \xi(s)\|^2 ds \leq C\varepsilon^2 \end{aligned} \quad (2.101)$$

Next, we take the partial derivative with respect to t of (2.98), we obtain

$$\nabla \cdot e_t + \varepsilon q_{tt} = \varepsilon p_{tt} \quad (2.102)$$

Taking the inner products of (2.97) with $t^2 e_t$ and (2.102) with $t^2 q$, we have

$$t^2(e_t, e_t) - \lambda t^2(\Delta e, e_t) + at^2(e, e_t) + t^2(\nabla q, e_t) = t^2(dg\beta\xi, e_t)$$

$$(\nabla \cdot e_t, e_t) + \varepsilon(q_{tt}, e_t) = \varepsilon(p_{tt}, e_t)$$

summing up the two relations, we obtain

$$\begin{aligned} & t^2(e_t, e_t) - \lambda t^2(\Delta e, e_t) + \frac{a}{2} \frac{d}{dt} t^2(e, e_t) + \varepsilon t^2(q_{tt}, e_t) \\ & = t^2 \frac{\lambda}{2} \|e\|^2 + \varepsilon t^2(p_{tt}, e_t) + t^2(dg\beta\xi, e_t) \\ & t^2\|e_t\|^2 + \frac{\lambda}{2} \frac{d}{dt} t^2 \|\nabla e\|^2 + at^2\|e\|^2 + t^2\varepsilon\|q_{tt}\|^2 \\ & \leq \frac{\lambda}{2} t^2\|e\|^2 + t^2\varepsilon\|p_{tt}\|^2 + t^2\|\nabla e\|^2 + Ct^2\|e\|^2 + \frac{Ct^2}{2} \|g\|^2 \|\xi\|^2 \\ & \int_0^t s^2 \|e_t(s)\|^2 ds + \lambda t^2 \|\nabla e\|^2 + at^2 \|e\|^2 + \int_0^t s^2 \varepsilon \|q_{tt}(s)\|^2 ds \\ & \leq \frac{\lambda}{2} t^2 \|e\|^2 + t^2 \|\nabla e\|^2 + Ct^2 \|e\|^2 + \frac{Ct^2}{2} \|g\|^2 \|\xi\|^2 \leq C\varepsilon^2 \end{aligned} \quad (2.103)$$

■

2.5 Error estimates for the nonlinear problem

We consider the following intermediate unsteady Navier-Stokes Forchheimer Fourier problem : Find u, p and θ such that $T > 0$

$$\left\{ \begin{array}{l} v_t - \lambda \Delta v + av + \nabla \gamma = dg\beta\theta - dg\beta\theta_{in} - dg\beta - \tilde{B}(u, u) - b |u|u \quad \Omega \times [0, T] \\ \theta_t - \kappa \Delta \theta = \mathcal{G} - \tilde{B}(u, \theta) \quad \Omega \times [0, T] \\ \varepsilon \gamma_t + \nabla \cdot v = 0 \quad \Omega \times [0, T] \\ v(x, t) = 0 \quad \Gamma \times [0, T] \\ \theta(x, t) = 0 \quad \Gamma \times [0, T] \\ \gamma(x, t) = 0 \quad \Gamma \times [0, T] \\ \theta(x, t = 0) = \varphi(x) \quad x \in \Omega \end{array} \right. \quad (2.104)$$

and the artificial compressibility unsteady Navier-Stokes Forchheimer Fourier problem : Find $u^\varepsilon, p^\varepsilon$ and θ^ε such that $T > 0$

$$\left\{ \begin{array}{l} u_t^\varepsilon - \lambda \Delta u^\varepsilon + au^\varepsilon + b |u^\varepsilon|u^\varepsilon + \nabla p^\varepsilon = dg\beta\theta^\varepsilon - dg\beta\theta_{in} - dg\beta - \tilde{B}(u^\varepsilon, u^\varepsilon) \quad \Omega \times [0, T] \\ \theta_t^\varepsilon - \kappa \Delta \theta^\varepsilon = \mathcal{G} - \tilde{B}(u^\varepsilon, \theta^\varepsilon) \quad \Omega \times [0, T] \\ \varepsilon p_t^\varepsilon + \nabla \cdot u^\varepsilon = 0 \quad \Omega \times [0, T] \\ u^\varepsilon(x, t) = 0 \quad \Gamma \times [0, T] \\ \theta^\varepsilon(x, t) = 0 \quad \Gamma \times [0, T] \\ p^\varepsilon(x, t) = 0 \quad \Gamma \times [0, T] \\ \theta^\varepsilon(x, t = 0) = \varphi(x) \quad x \in \Omega \end{array} \right. \quad (2.105)$$

where (u, θ) is the solutions of the problem (2.1).

Letting $\rho = v - u$, $\sigma = \gamma - p$ and subtracting (2.1) from (2.104), we obtain

$$\left\{ \begin{array}{l} \rho_t - \lambda \Delta \rho + a\rho + \nabla \sigma = 0 \\ \varepsilon \gamma_t + \nabla \cdot \rho = \varepsilon p_t \\ \rho(x, t) = 0 \\ \sigma(x, t) = 0 \end{array} \right. \quad (2.106)$$

Lemma 2.5.1. *Suppose (H1) and (H2) are valid, ε sufficiently small, for all $t \in [0, T]$, we have*

$$\begin{aligned} & t \|\rho\|^2 + t^2 \|\nabla \rho\|^2 + t\varepsilon \|\sigma\|^2 + at^2 \|\rho\|^2 + a \int_0^t s \|\rho(s)\|^2 ds + \int_0^t s \|\rho(s)\|^2 ds \\ & + \int_0^t s \|\nabla \rho\|^2 ds + \varepsilon \int_0^t s^2 \|\sigma_{tt}(s)\|^2 ds \leq C\varepsilon^2 \end{aligned}$$

Proof. We have $dg\beta\theta - \tilde{B}(u, u) \in L^2([0, T]; L^2(\Omega))$. We note that the assumption **(H1)** for a linear problem can be replaced by the weaker condition $dg\beta\theta \in L^2([0, T]; L^2(\Omega))$. on the other hand, it can be easily shown (see for the instance [8] that $tu_t \in L^2([0, T]; H_0^1(\Omega))$). Hence

$$t \frac{\partial}{\partial t} \left(dg\beta\theta_t - \tilde{B}(u, u) \right) = t \left(dg\beta\theta - \tilde{B}(u_t, u) - \tilde{B}(u, u_t) \in L^2([0, T]; L^2(\Omega)) \right)$$

Lemma (2.5.1) is then a direct consequence of Lemma (2.4.2) and Theorem (2.4.3) applied to (2.106). \blacksquare

Now, letting $\eta = u^\varepsilon - v$, $\zeta = p^\varepsilon - \gamma$ and $\varsigma = \theta^\varepsilon - \theta$ and substracting (2.104) from (2.105)

$$\begin{cases} \eta_t - \lambda\Delta\eta + \tilde{B}(u^\varepsilon, u^\varepsilon) - \tilde{B}(u, u) + a\eta + \nabla\zeta = dg\beta\varsigma - b(|u^\varepsilon| |u^\varepsilon - u| |u|) \\ \varsigma_t - \kappa\Delta\varsigma + \tilde{\tilde{B}}(u^\varepsilon, \theta^\varepsilon) - \tilde{\tilde{B}}(u, \theta) = 0 \\ \varepsilon\zeta_t + \nabla.\eta = 0 \\ \eta(x, t) = 0 \\ \varsigma(x, t) = 0 \\ \zeta(x, t) = 0 \end{cases} \quad (2.107)$$

Since

$$\begin{aligned} \tilde{B}(u^\varepsilon, u^\varepsilon) - \tilde{B}(u, u) &= \tilde{B}(u^\varepsilon, u^\varepsilon - u) + \tilde{B}(u^\varepsilon - u, u) \\ &= \tilde{B}(u^\varepsilon, \eta + \rho) + \tilde{B}(\eta + \rho, u) \end{aligned}$$

and

$$\begin{aligned} \tilde{\tilde{B}}(u^\varepsilon, \theta^\varepsilon) - \tilde{\tilde{B}}(u, \theta) &= \tilde{\tilde{B}}(u^\varepsilon, \theta^\varepsilon - \theta) + \tilde{\tilde{B}}(u^\varepsilon - u, \theta) \\ &= \tilde{\tilde{B}}(u^\varepsilon, \varsigma) + \tilde{\tilde{B}}(\eta + \rho, \theta) \end{aligned}$$

We can rewrite the system (2.107) as

$$\begin{cases} \eta_t - \lambda\Delta\eta + a\eta + \nabla\zeta = dg\beta\varsigma - b(|u^\varepsilon| |u^\varepsilon - u| |u|) - \tilde{B}(u^\varepsilon, \eta + \rho) - \tilde{B}(\eta + \rho, u) \\ \varsigma_t - \kappa\Delta\varsigma = -\tilde{\tilde{B}}(u^\varepsilon, \varsigma) - \tilde{\tilde{B}}(\eta + \rho, \theta) \\ \varepsilon\zeta_t + \nabla.\eta = 0 \\ \eta(x, t) = 0 \\ \varsigma(x, t) = 0 \\ \zeta(x, t) = 0 \end{cases} \quad (2.108)$$

The weak formulation of the problem (2.108) is defined as follows: Find $(\eta, \zeta, \varsigma) \in (X, M, W)$,

for all $t \in [0, T]$, such that for all $(\hat{v}, \hat{\phi}, \hat{\psi}) \in (X, M, W)$

$$\begin{cases} (\eta_t, \hat{v}) + \lambda(\nabla\eta, \nabla\hat{v}) + (a\eta, \hat{v}) - (\zeta, \operatorname{div} \hat{v}) \\ = (dg\beta\varsigma, \hat{v}) - b(|u^\varepsilon| |u^\varepsilon - |u| |u, \hat{v}) - \tilde{B}(u^\varepsilon, \eta + \rho, \hat{v}) - \tilde{B}(\eta + \rho, u, \hat{v}) \\ (\varsigma_t, \hat{\psi}) + \kappa(\nabla\varsigma, \nabla\hat{\psi}) + \tilde{\tilde{B}}(u^\varepsilon, \varsigma, \hat{\psi}) + \tilde{\tilde{B}}(\eta + \rho, \theta, \hat{\psi}) = 0 \\ (\varepsilon\zeta_t, \hat{\phi}) + (\nabla \cdot \eta, \hat{\phi}) = 0 \end{cases} \quad (2.109)$$

$$\begin{cases} (\eta_t, \hat{v}) - \mathbf{a}(\eta, \hat{v}) + (a\eta, \hat{v}) - \delta(\hat{v}, \zeta) \\ = (dg\beta\varsigma, \hat{v}) - b(|u^\varepsilon| |u^\varepsilon - |u| |u, \hat{v}) - \tilde{B}(u^\varepsilon, \eta + \rho, \hat{v}) - \tilde{B}(\eta + \rho, u, \hat{v}) \\ (\varsigma_t, \hat{\psi}) - \bar{\mathbf{a}}(\eta, \hat{\psi}) = -\tilde{\tilde{B}}(u^\varepsilon, \varsigma, \hat{\psi}) - \tilde{\tilde{B}}(\eta + \rho, \theta, \hat{\psi}) \\ (\varepsilon\zeta_t, \hat{\phi}) + (\nabla \cdot \eta, \hat{\phi}) = 0 \end{cases} \quad (2.110)$$

or

$$\begin{cases} (\eta_t, \hat{v}) - \mathbf{a}(\eta, \hat{v}) + (a\eta, \hat{v}) \\ = (dg\beta\varsigma, \hat{v}) - b(|u^\varepsilon| |u^\varepsilon - |u| |u, \hat{v}) - \tilde{B}(u^\varepsilon, \eta + \rho, \hat{v}) - \tilde{B}(\eta + \rho, u, \hat{v}) \\ (\varsigma_t, \hat{\psi}) + \bar{\mathbf{a}}(\eta, \hat{\psi}) = -\tilde{\tilde{B}}(u^\varepsilon, \varsigma, \hat{\psi}) - \tilde{\tilde{B}}(\eta + \rho, \theta, \hat{\psi}) \end{cases} \quad (2.111)$$

Lemma 2.5.2. *Suppose (H1) and (H2) are valid, ε sufficiently small, for all $t \in [0, T]$, the following error estimates holds*

$$t\|\eta\|^2 + t\varepsilon\|\zeta\|^2 + t\|\varsigma\|^2 + t^2\|\nabla\eta\|^2 + t^2\|\nabla\varsigma\|^2 + a \int_0^t s\|\eta(s)\|^2 ds \leq C\varepsilon^2$$

$$\lambda t^2\|\nabla\eta\|^2 + t^2\|\varsigma\|^2 + \varepsilon t^2\|\zeta_{tt}\|^2 + at^2\|\eta\|^2 + \int_0^t s^2\|\eta_t(s)\|^2 ds + \kappa \int_0^t s^2\|\nabla\varsigma(s)\|^2 ds \leq C\varepsilon^2$$

Proof. Taking $\hat{v} = \eta$ in (2.111), we have

$$\begin{aligned} (\eta_t, \eta) + \lambda(\nabla\eta, \nabla\eta) + (a\eta, \eta) &= (dg\beta\varsigma, \eta) - \tilde{B}(u^\varepsilon, \eta + \rho, \eta) - \tilde{B}(\eta + \rho, u, \eta) \\ &\quad - b(|u^\varepsilon| |u^\varepsilon - |u| |u, \eta) \end{aligned} \quad (2.112)$$

Then

$$\begin{aligned} \frac{1}{2} \frac{d}{dt} \|\eta\|^2 + \lambda \|\nabla\eta\|^2 + a \|\eta\|^2 &= (dg\beta\varsigma, \eta) - \tilde{B}(u^\varepsilon, \eta + \rho, \eta) - \tilde{B}(\eta + \rho, u, \eta) \\ &\quad - b(|u^\varepsilon| |u^\varepsilon - |u| |u, \eta) \end{aligned} \quad (2.113)$$

Thanks to Lemma (2.2.1), estimates (2.10) and Schwartz inequality we derive that

$$\begin{aligned} |\tilde{B}(u^\varepsilon, \eta + \rho, \eta)| &\leq C \|u^\varepsilon\| \|\eta + \rho\| \|\nabla\eta\| \\ &\leq C \|u^\varepsilon\|_2 (\|\eta\| + \|\rho\|) \|\nabla\eta\| \\ &\leq \frac{\lambda}{8} \|\eta\|^2 + C \|\rho\|^2 + C \|u^\varepsilon\|_2^2 \|\nabla\eta\|^2 \end{aligned}$$

$$|\tilde{B}(\eta + \rho, u, \eta)| \leq \frac{\lambda}{8} \|\eta\|^2 + C\|\rho\|^2 + C\|u\|_2^2 \|\nabla\eta\|^2$$

We have

$$|(|u^\varepsilon|u^\varepsilon - |u|u, \eta)| = |(|u^\varepsilon|u^\varepsilon - |v|v, \eta)| + |(|v|v - |u|u, \eta)| \quad (2.114)$$

Using (2.21), we have

$$- |(|u^\varepsilon|u^\varepsilon - |v|v, \eta)| \leq 0$$

and

$$|(|v|v - |u|u, \eta)| = |(|v|v - |u^\varepsilon|u^\varepsilon, \eta)| + |(|u^\varepsilon|u^\varepsilon - |u|u, A_\varepsilon^{-1}(-\rho - e))|$$

Same, using (2.21), we have

$$|(|u^\varepsilon|u^\varepsilon - |u|u, -e)| \leq 0$$

The, we return to (2.114), we have

$$|(|u^\varepsilon|u^\varepsilon - |u|u, \eta)| \leq |(|v|v - |u^\varepsilon|u^\varepsilon, \eta)| + |(|u^\varepsilon|u^\varepsilon - |u|u, -\rho)| := T_1 + T_2$$

Based on Lemma (2.2.4) and Young inequality, we get

$$T_1 \leq C\|\nabla\eta\| \|\eta\| \leq \frac{\lambda}{8} \|\nabla\eta\|^2 + C\|\eta\|^2 \quad (2.115)$$

$$\begin{aligned} T_2 &\leq C\|\nabla(\eta + \rho)\| \|\rho\| \leq C(\|\nabla\eta\| + \|\nabla\rho\|) \|\rho\| \\ &\leq \frac{\lambda}{8} \|\nabla\eta\|^2 + C\|\rho\|^2 + C\|\nabla\rho\| \|\rho\| \end{aligned} \quad (2.116)$$

and for the last term

$$\begin{aligned} \|(dg\beta\varsigma, \eta)\| &\leq C\|g\|_\varsigma \|\nabla\eta\| \\ &\leq \frac{\kappa}{4} \|\varsigma\|^2 + C\|g\|_2^2 \|\nabla\eta\|^2 \end{aligned}$$

Similary for the Fourier equation, we take $\hat{\psi} = \varsigma$

$$(\varsigma_t, \varsigma) - \kappa(\nabla\varsigma, \nabla\varsigma) = -\tilde{B}(u^\varepsilon, \varsigma, \varsigma) + \tilde{B}(\eta + \rho, \theta, \varsigma) \quad (2.117)$$

$$\frac{1}{2} \frac{d}{dt} \|\varsigma\|^2 + \kappa \|\nabla\varsigma\|^2 = -\tilde{B}(u^\varepsilon, \varsigma, \varsigma) - \tilde{B}(\eta + \rho, \theta, \varsigma) \quad (2.118)$$

$$\begin{aligned} |\tilde{B}(u^\varepsilon, \varsigma, \varsigma)| &\leq C\|u^\varepsilon\|_2 \|\varsigma\| \|\nabla\varsigma\| \\ &\leq \frac{\kappa}{4} \|\varsigma\|^2 + C\|u^\varepsilon\|_2^2 \|\nabla\varsigma\|^2 \end{aligned}$$

$$|\tilde{B}(\eta + \rho, \theta, \varsigma)| \leq \frac{\lambda}{8} (\|\eta\|^2 + \|\rho\|^2) + C\|\theta\|_2^2 \|\nabla\varsigma\|^2$$

Summerizing the different terms, the Navier-Stokes Forchheimer and Fourier equations (2.113) and (2.118) became for the Navier-Stokes Forchheimer equations

$$\begin{aligned} \frac{d}{dt} \|\eta\|^2 + \lambda \|\nabla \eta\|^2 + a \|\eta\|^2 \leq & C \|\eta\|^2 + C \|\rho\|^2 + C (\|u^\varepsilon\|_2^2 + \|u\|_2^2 + \|g\|_2^2 + 1) \|\nabla \eta\|^2 \\ & + C (\|\rho\| + \|\nabla \rho\|) \|\rho\| + \frac{\kappa}{4} \|\zeta\|^2 \end{aligned} \quad (2.119)$$

and the Fourier equations

$$\frac{1}{2} \frac{d}{dt} \|\zeta\|^2 + \kappa \|\nabla \zeta\|^2 \leq C (\|u^\varepsilon\|_2^2 + \|\theta\|_2^2) \|\nabla \zeta\|^2 + \frac{\lambda}{8} (\|\eta\|^2 + \|\rho\|^2) \quad (2.120)$$

Summing (2.119) and (2.120) we get

$$\begin{aligned} \frac{d}{dt} (\|\eta\|^2 + \|\zeta\|^2) + \lambda \|\nabla \eta\|^2 + \kappa \|\nabla \zeta\|^2 + a \|\eta\|^2 \leq & \frac{\kappa}{2} \|\zeta\|^2 + C (\|u^\varepsilon\|_2^2 + \|u\|_2^2 + \|g\|_2^2 + 1) \|\nabla \eta\|^2 \\ & + C (\|\rho\| + \|\nabla \rho\|) \|\rho\| + C \|\eta\|^2 + C \|\rho\|^2 \\ & + C (\|u^\varepsilon\|_2^2 + \|\theta\|_2^2) \|\nabla \zeta\|^2 + \frac{\lambda}{8} (\|\eta\|^2 + \|\rho\|^2) \end{aligned} \quad (2.121)$$

Since $\int_0^t (\|u^\varepsilon\|_2^2 + \|u\|_2^2 + \|g\|_2^2) ds \leq C$, we can apply Lemma (2.2.5) to above two inequalities, use Lemma (2.5.1) we obtain

$$\|\eta\|^2 + \|\zeta\|^2 + \lambda \int_0^t \|\nabla \eta(s)\|^2 ds + \kappa \int_0^t \|\nabla \zeta(s)\|^2 ds + a \int_0^t \|\eta(s)\|^2 ds \leq C \varepsilon^2 \quad (2.122)$$

We take now $(\hat{v}, \hat{\phi}) = t(\eta, \zeta)$ in (2.109), summing up the two relations, using (2.10) and Schwarz inequality, we derive

$$\begin{aligned} & \frac{1}{2} \frac{d}{dt} t \|\eta\|^2 + t \lambda \|\nabla \eta\|^2 + \frac{1}{2} \frac{d}{dt} t \varepsilon \|\zeta\|^2 + a t \|\eta\|^2 \\ & = \frac{1}{2} \|\eta\|^2 - t \tilde{B}(u^\varepsilon, \eta + \rho, \eta) - t \tilde{B}(\eta + \rho, u, \eta) - b t (|u^\varepsilon| |u^\varepsilon - u|, \eta) + (d g t \beta_\zeta, \eta) \\ & \leq \left(\frac{1}{2} + C t \right) \|\eta\|^2 + C t (\|u^\varepsilon\|_2^2 + \|u\|_2^2 + \|g\|_2^2 + 1) \|\eta\|^2 \\ & \quad + C t \|\rho\|^2 + C t \|\nabla \rho\|^2 \|\rho\| + \frac{\kappa t}{4} \|\nabla \zeta\|^2 \end{aligned} \quad (2.123)$$

Taking $\hat{\psi} = t\zeta$ in (2.109), using (2.8), (2.13) and Schwarz inequality we derive

$$\begin{aligned} \frac{1}{2} \frac{d}{dt} t \|\zeta\|^2 + t \kappa \|\nabla \zeta\|^2 & = \frac{1}{2} \|\zeta\|^2 - \tilde{B}(u^\varepsilon, \zeta, \zeta) - \tilde{B}(\eta + \rho, \theta, \zeta) \\ & \leq \frac{1}{2} \|\zeta\|^2 + C t \|\theta\|^2 \|\zeta\|^2 + t \frac{\lambda}{8} (\|\eta\|^2 + \|\rho\|^2) \end{aligned} \quad (2.124)$$

Integrating over $[0, t]$, we can apply (2.122), Lemma (2.5.1) and Lemma (2.2.1) to above two inequalities, such that

$$t\|\eta\|^2 + t\varepsilon\|\zeta\|^2 + t\|\varsigma\|^2 + \lambda \int_0^t s\|\nabla\eta(s)\|^2 ds + \kappa \int_0^t s\|\nabla\varsigma(s)\|^2 ds + a \int_0^t s\|\eta(s)\|^2 ds \leq C\varepsilon^2 \quad (2.125)$$

Next, we take the partial derivative with respect to t of the second term of (2.109) to obtain

$$(\varepsilon\zeta_{tt}, \hat{\phi}) + (\nabla \cdot \eta_t, \hat{\phi}) = 0 \quad (2.126)$$

Taking $\hat{v} = t^2\eta_t$ in (2.109) and $\hat{\phi} = t^2\zeta$, using (2.8) and Schwarz inequality, we get

$$\begin{aligned} & t^2\|\eta_t\|^2 + \frac{\lambda}{2} \frac{d}{dt} t^2 \|\nabla\eta\|^2 + \frac{\varepsilon}{2} \frac{d}{dt} t^2 \|\zeta_{tt}\|^2 + \frac{a}{2} \frac{d}{dt} t^2 \|\eta\|^2 \\ &= \frac{\lambda t}{2} \|\nabla\eta\|^2 + \varepsilon t \|\zeta\|^2 + \frac{1}{2} t^2 \|\eta\|^2 - t^2 \tilde{B}(u^\varepsilon, \eta + \rho, \eta_t) - t^2 \tilde{B}(\eta + \rho, u, \eta_t) \\ &\quad - bt^2(|u^\varepsilon| |u^\varepsilon - |u||u, \eta_t) + t^2(dg\beta\varsigma, \eta_t) \\ &\leq \frac{\lambda t}{2} \|\nabla\eta\|^2 + \varepsilon t \|\zeta\|^2 + \frac{1}{2} t^2 \|\eta_t\|^2 + C(\|u\|_2^2 + \|u_\varepsilon\|_2^2)(\varepsilon^2 + t^2\|\nabla\eta\|^2) \\ &\quad + \frac{\lambda t}{4} \|\nabla\eta\|^2 + Ct^2\|\eta_t\|^2 + Ct^2\|\rho\|^2 + Ct^2\|\nabla\rho\|^2 + Ct^2\|g\|_2^2\|\nabla\eta\|^2 + \frac{\kappa}{4}\|\varsigma\|^2 \end{aligned}$$

Then

$$\begin{aligned} & t^2\|\eta_t\|^2 + \frac{\lambda}{2} \frac{d}{dt} t^2 \|\nabla\eta\|^2 + \frac{\varepsilon}{2} \frac{d}{dt} t^2 \|\zeta_{tt}\|^2 + \frac{a}{2} \frac{d}{dt} t^2 \|\eta\|^2 \\ &\leq \frac{3\lambda t}{2} \|\nabla\eta\|^2 + \varepsilon t \|\zeta\|^2 + C(\|u\|_2^2 + \|u_\varepsilon\|_2^2)(\varepsilon^2 + t^2\|\nabla\eta\|^2) \\ &\quad + Ct^2\|g\|_2^2\|\nabla\eta\|^2 + \frac{\kappa}{4}\|\varsigma\|^2 + Ct^2\|\eta_t\|^2 + Ct^2\|\rho\|^2 + Ct^2\|\nabla\rho\|^2 \end{aligned} \quad (2.127)$$

We take $\hat{\psi} = t^2\varsigma$ in (2.109), using (2.8), (2.13) and Schwarz inequality, we derive

$$\begin{aligned} \frac{1}{2} \frac{d}{dt} \|\varsigma\|^2 + \kappa t^2 \|\nabla\varsigma\|^2 &= t^2 \|\varsigma\|^2 - t^2 \tilde{B}(u_\varepsilon, \varsigma, \varsigma) - t^2 \tilde{B}(\eta + \rho, \theta, \varsigma) \\ &\leq t \|\varsigma\|^2 + Ct^2 \|\theta\|_2^2 \|\varsigma\|^2 + \mu t^2 (\|\nabla\eta\|^2 + \|\nabla\rho\|^2) \end{aligned} \quad (2.128)$$

Taking the summation of (2.127) and (2.128), integrating over $[0, t]$, using (2.125), Lemma (2.2.5) and Lemma (2.5.1) to above two inequalities and μ sufficiently small, we derive

$$\lambda t^2 \|\nabla\eta\|^2 + t^2 \|\varsigma\|^2 + \varepsilon t^2 \|\zeta_{tt}\|^2 + at^2 \|\eta\|^2 + \int_0^t s^2 \|\eta_t(s)\|^2 ds + \kappa \int_0^t s^2 \|\nabla\varsigma(s)\|^2 ds \leq C\varepsilon^2 \quad (2.129)$$

Taking $\hat{\psi} = t^2\varsigma_t$ in (2.109), using (2.8), (2.13) and Schwarz inequality, we have

$$\begin{aligned} t^2 \|\varsigma\|^2 + \frac{\kappa}{2} \frac{d}{dt} t^2 \|\nabla\varsigma\|^2 &= \kappa t^2 \|\nabla\varsigma\|^2 - t^2 \tilde{b}(u_\varepsilon, \varsigma, \varsigma_t) - t^2 \tilde{b}(\eta + \rho, \theta, \varsigma_t) \\ &\leq \kappa t^2 \|\nabla\varsigma\|^2 + \frac{t^2}{2} \|\varsigma_t\|^2 + Ct^2 \|u_\varepsilon\|^2 \|\nabla\varsigma\|^2 + Ct^2 \|\theta\|_2^2 \|\nabla(\eta + \rho)\|^2 \end{aligned}$$

Integrating over $[0, t]$ using (2.125), (2.129), Lemma (2.2.5) and Lemma (2.5.1), we derive

$$\kappa t^2 \|\nabla \zeta\|^2 + \int_0^t s^2 \|\zeta_t(s)\|^2 ds \leq C\varepsilon^2 \quad (2.130)$$

From (2.108), there holds

$$\nabla \zeta = -\eta_t + \lambda \Delta \eta - \tilde{B}(u^\varepsilon, \eta + \rho) - \tilde{B}(\eta + \rho, u) - a\eta - b(|u^\varepsilon| |u^\varepsilon - |u||u) + dg\beta\zeta$$

Therefore by using previous estimates on the above equation, we derive

$$\int_0^t s^2 \|\zeta\|^2 ds \leq \int_0^t s^2 \|\nabla \zeta\|_1^2 ds \leq C\varepsilon^2 \quad (2.131)$$

■

By combining Lemma (2.5.1) with Lemma (2.5.2), we obtain the following error estimates result.

Theorem 2.5.3. *Suppose (H1) and (H2) are valid, ε sufficiently small, for all $t \in [0, T]$, the following error estimates holds*

$$(at + 1)t\|u - u^\varepsilon\|^2 + t\varepsilon\|p - p^\varepsilon\|^2 + t\|\theta - \theta^\varepsilon\|^2 + \lambda t^2 \|\nabla(u - u^\varepsilon)\|^2 + \kappa t^2 \|\nabla(\theta - \theta^\varepsilon)\|^2 \leq C\varepsilon^2$$

2.6 Numerical resolution

In this section, we present the numerical results of the artificial compressibility Navier-Stokes Forchheimer Fourier system (2.1) with non-homogenous boundary conditions.

$$\left\{ \begin{array}{l} u_t^\varepsilon - \lambda \Delta u^\varepsilon + (u^\varepsilon \cdot \nabla) u^\varepsilon + a u^\varepsilon + b |u^\varepsilon| |u^\varepsilon| + \nabla p^\varepsilon = dg\beta\theta^\varepsilon + \mathcal{F} \quad \Omega \times [0, T] \\ \varepsilon p_t^\varepsilon + \nabla \cdot u^\varepsilon = 0 \quad \Omega \times [0, T] \\ \theta_t^\varepsilon - \kappa \Delta \theta^\varepsilon + (u^\varepsilon \cdot \nabla) \theta^\varepsilon = \mathcal{G} \quad \Omega \times [0, T] \\ u^\varepsilon = \bar{u}_0 \quad \Gamma_1 \\ \theta^\varepsilon = \bar{\theta}_0 \quad \Gamma_1 \\ u^\varepsilon(0) = u_0 \quad \Omega \\ \theta^\varepsilon(0) = \theta_0 \quad \Omega \\ p^\varepsilon(0) = p_0 \quad \Omega \end{array} \right. \quad (2.132)$$

where \bar{u}_0 and $\bar{\theta}_0$ is an imposed velocity and temperature on the boundary and is assumed to be time-independent below for convenience.

We now carry out spatial discretization. We consider a regular triangulation \mathcal{T}_h of the domain Ω , depending on a positive parameter $h > 0$, made up of triangles \mathcal{T}_h and we adopt the

Bernadi Raugel Finite element (for more detail see [14]). It is a 2D coupled finite element, with the Polynomial space is $\mathbb{P}_1^2 + 3$ normals bubbles edges function (\mathbb{P}_2) and the degree of freedom is 6 values at of the 2 components at the 3 vertices and the 3 flux on the 3 edges. So the number degrees of freedom is 9. Let V_h , Q_h and W_h the finite elements spaces such that

$$\begin{aligned} V_h &= \left\{ v_h \in C^0(\bar{\Omega}) \cap H_0^1(\Omega)^d; \forall K \in \mathcal{T}_h, v_h|_K \in \mathbb{P}_K \right\} \\ Q_h &= \left\{ q_h \in L^2(\Omega); \forall K \in \mathcal{T}_h, q_h|_K \in \mathbb{P}_1 \right\} \\ W_h &= \left\{ w_h \in H^1(\Omega); \forall K \in \mathcal{T}_h, w_h|_K \in \mathbb{P}_2 \right\} \end{aligned}$$

Again, we first give the variational formulation for approximated system (2.132):

Find $\left(u_h^{\varepsilon, (k+1)}, p_h^{\varepsilon, (k+1)}, \theta_h^{\varepsilon, (k+1)} \right) \in (V_h \times Q_h \times W_h)$ for all $v_h \in V_h$, $q_h \in Q_h$ and $w_h \in X_h$

$$\begin{aligned} & \frac{\left\langle u_h^{\varepsilon, (k+1)}, v_h \right\rangle - \left\langle u_h^{\varepsilon, (k)}, v_h \right\rangle}{t_{k+1} - t_k} + \lambda \left\langle \nabla u_h^{\varepsilon, (k+1)}, \nabla v_h \right\rangle + a \left\langle u_h^{\varepsilon, (k+1)}, v_h \right\rangle \\ & + \left\langle u_h^{\varepsilon, (k)} \left(\nabla u_h^{\varepsilon, (k+1)} \right), v_h \right\rangle + b \left\langle |u_h^{\varepsilon, (k)}| u_h^{\varepsilon, (k+1)}, v_h \right\rangle - \left\langle p_h^{\varepsilon, (k+1)}, \nabla \cdot v_h \right\rangle \\ & = dg\beta \left\langle \theta_h^{\varepsilon, (k+1)}, v_h \right\rangle + \left\langle \mathcal{F}, v_h \right\rangle \quad \forall v_h \in V_h \end{aligned}$$

$$\varepsilon \frac{\left\langle p_h^{\varepsilon, (k+1)}, q_h \right\rangle - \left\langle p_h^{\varepsilon, (k)}, q_h \right\rangle}{t_{k+1} - t_k} + \left\langle \nabla \cdot u_h^{\varepsilon, (k+1)}, q_h \right\rangle = 0 \quad q_h \in Q_h$$

$$\frac{\left\langle \theta_h^{\varepsilon, (k+1)}, w_h \right\rangle - \left\langle \theta_h^{\varepsilon, (k)}, w_h \right\rangle}{t_{k+1} - t_k} + \lambda \left\langle \nabla \theta_h^{\varepsilon, (k+1)}, \nabla w_h \right\rangle + \left\langle u_h^{\varepsilon, (k)} \left(\nabla \theta_h^{\varepsilon, (k+1)} \right), w_h \right\rangle = \left\langle \mathcal{G}, w_h \right\rangle$$

We implemente the above scheme in FreeFem++ which is used to solve partial differential equations using the finite element method. We run a large number of time steps to ensure that we reach steady state solution. We consider a unit square $\Omega =]0, 1]^2$ and we impose the velocity and the temperature $u = 0, v = 0, \theta = 0$ at all the boundary except at the top $u = 1, v = 0, \theta = 300$ Figure (2.1).

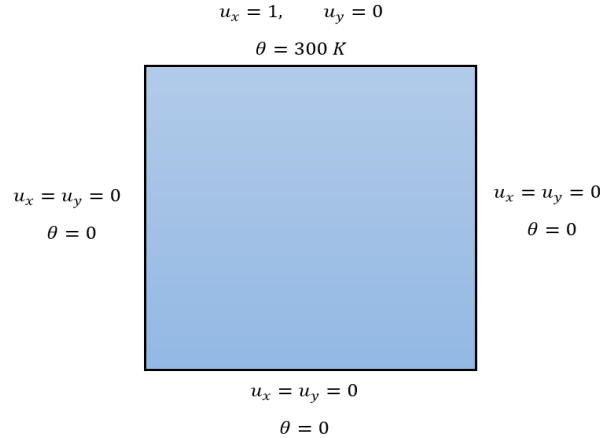


Figure 2.1: Square cavity with free wall.

Figures (2.2) are the numerical results of the lid-driven cavity flow applied to our pseudo-compressibility Navier-Stokes Forchheimer Fourier system. In the first test, we set the time step $dt = 0.1$, $\varepsilon = 0.000001$, $a = 1$, $d = 1$, $Re = 100$, $\kappa = 0.01$, $\beta = 3.38 \times 10^{-4}$, $\theta_{in} = 300K$ and we vary the value of $b = [1, 5, 10]$.

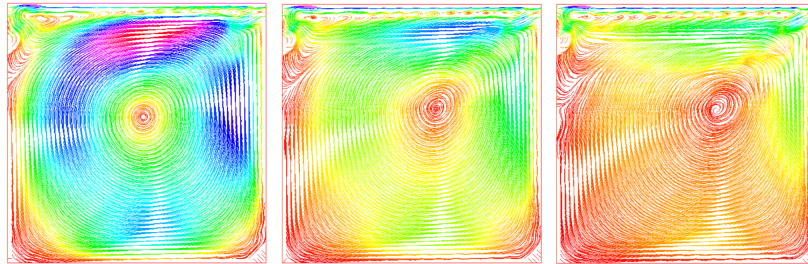


Figure 2.2: Velocity fields in driven cavity $b = 1$, $b = 5$ and $b = 10$.

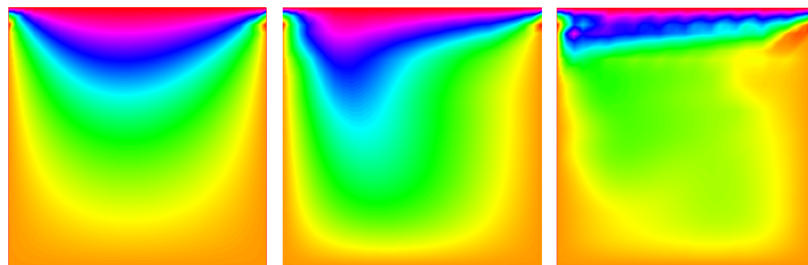


Figure 2.3: Temperature fields in driven cavity $\kappa = 0.01$, $\kappa = 0.001$ and $\kappa = 0.0001$.

Subsequently, we take the same example of the cavity with different initial and boundary conditions of the previous example, as presented in Figure (2.4). In all experiments, the nonlinear systems are solved by the Newton iteration. the physical parameters used for all the tests, $\lambda = 1$, $\kappa = 1$, the time step $dt = 1$, Darcy parameter $a = 1$, Forchheimer parameter $b = 1$ and the total time $T = 50$. For this example, we will investigate the influence of the parameters λ , κ , a , b . As mentioned above, we adopt a finite element spaces of types $(\mathbb{P}_2\mathbb{B}\mathbb{R} - \mathbb{P}_1 - \mathbb{P}_2)$ elements for $(u_h^\varepsilon, p_h^\varepsilon, \theta_h^\varepsilon)$ respectively. The numerical solutions $(u_h^\varepsilon, p_h^\varepsilon, \theta_h^\varepsilon)$ are shown in Figure (2.5).

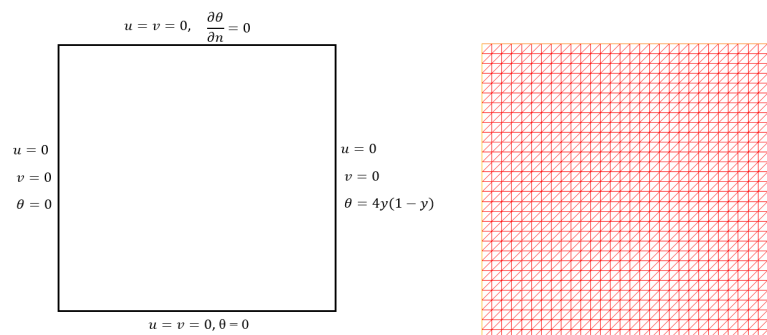
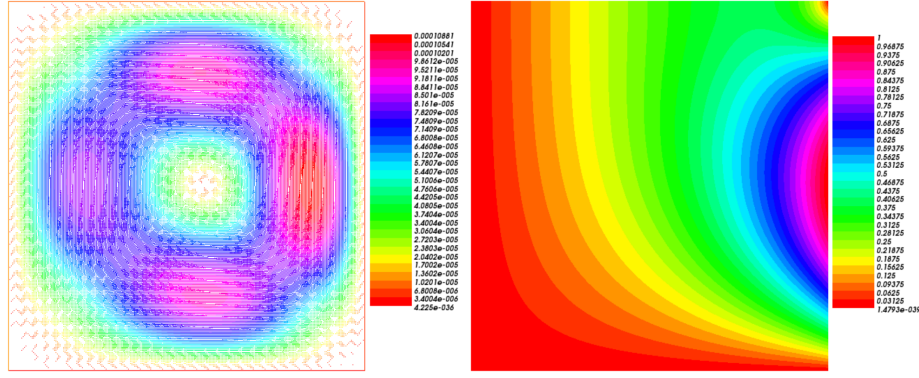


Figure 2.4: Physics model of cavity flows.


 Figure 2.5: Velocity and temperature fields in driven cavity $\lambda = 1$, $\kappa = 1$.

The objective of this part is to test and verify the results of Theorem (2.5.3). We use the L^2 -norm to measure the error of the velocity, pressure and temperature approximations. The error estimates are given by

$$\|u_h^\varepsilon - u_{ex}\|_{L^2(\Omega)} = \left(\int_{\Omega} \sum_{i=1}^2 (u_{i,h}^\varepsilon - u_{i,ex})^2 \right)^{\frac{1}{2}}$$

$$\varepsilon \|p_h^\varepsilon - p_{ex}\|_{L^2(\Omega)} = \left(\varepsilon^2 \int_{\Omega} (p_h^\varepsilon - p_{ex})^2 \right)^{\frac{1}{2}}$$

$$\|\theta_h^\varepsilon - \theta_{ex}\|_{L^2(\Omega)} = \left(\int_{\Omega} (\theta_h^\varepsilon - \theta_{ex})^2 \right)^{\frac{1}{2}}$$

Let $\Omega = [0, 1] \times [0, 1]$ and the exact solution $(u^\varepsilon, p^\varepsilon, \theta^\varepsilon)$ of the artificial compressibility Navier-Stokes Forchheimer Fourier equations to be

$$\begin{cases} u_{ex} = 10x^2(x-1)^2y(y-1)(2y-1) \\ v_{ex} = -10x^2(x-1)(2x-1)y^2(y-1)^2 \\ p_{ex} = 10(2x-1)(2y-1) \\ \theta_{ex} = u_{ex} + v_{ex} \end{cases}$$

The tables (2.1) to (2.6) show the results obtained for the velocity, pressure and temperature approximations according to the different parameters. We see that the numerical results are according with the theoretical results for the artificial compressibility Navier-Stokes Forchheimer Fourier system.

Mesh	N	$\ u_h^\varepsilon - u_{ex}\ _{L^2(\Omega)}$	$\varepsilon \ p_h^\varepsilon - p_{ex}\ _{L^2(\Omega)}$	$\ \theta_h^\varepsilon - \theta_{ex}\ _{L^2(\Omega)}$
5 × 5	50	0.0271462	3.35381e-006	0.382296
20 × 20	800	0.0271162	3.3538e-006	0.382045
35 × 35	2450	0.0271151	3.3538e-006	0.382043
50 × 50	5000	0.0271148	3.3538e-006	0.382043
65 × 65	8450	0.0271147	3.3538e-006	0.382043
80 × 80	12800	0.0271147	3.3538e-006	0.382043
95 × 95	18050	0.0271146	3.3538e-006	0.382043

Table 2.2: Uniform meshes for $\lambda = 0.1$, $\kappa = 1$, $a = 1$, $b = 1$

Mesh	N	$\ u_h^\varepsilon - u_{ex}\ _{L^2(\Omega)}$	$\varepsilon \ p_h^\varepsilon - p_{ex}\ _{L^2(\Omega)}$	$\ \theta_h^\varepsilon - \theta_{ex}\ _{L^2(\Omega)}$
5 × 5	50	0.0252159	3.35378e-006	0.382324
20 × 20	800	0.0251207	3.35376e-006	0.382079
35 × 35	2450	0.0251164	3.35376e-006	0.382078
50 × 50	5000	0.0251154	3.35376e-006	0.382078
65 × 65	8450	0.025115	3.35376e-006	0.382078
80 × 80	12800	0.0251149	3.35376e-006	0.382078
95 × 95	18050	0.0251147	3.35376e-006	0.382078

Table 2.3: Uniform meshes for $\lambda = 0.001$, $\kappa = 1$, $a = 1$, $b = 1$

Mesh	N	$\ u_h^\varepsilon - u_{ex}\ _{L^2(\Omega)}$	$\varepsilon \ p_h^\varepsilon - p_{ex}\ _{L^2(\Omega)}$	$\ \theta_h^\varepsilon - \theta_{ex}\ _{L^2(\Omega)}$
5 × 5	50	0.0274526	3.35381e-006	0.382292
20 × 20	800	0.027449	3.3538e-006	0.38204
35 × 35	2450	0.0274489	3.3538e-006	0.382038
50 × 50	5000	0.0274488	3.3538e-006	0.382038
65 × 65	8450	0.0274488	3.3538e-006	0.382038
80 × 80	12800	0.0274488	3.3538e-006	0.382038
95 × 95	18050	0.0274488	3.3538e-006	0.382038

Table 2.1: Uniform meshes for $\lambda = 1$, $\kappa = 1$, $a = 1$, $b = 1$

Mesh	N	$\ u_h^\varepsilon - u_{ex}\ _{L^2(\Omega)}$	$\varepsilon \ p_h^\varepsilon - p_{ex}\ _{L^2(\Omega)}$	$\ \theta_h^\varepsilon - \theta_{ex}\ _{L^2(\Omega)}$
5 × 5	50	0.027453	3.35426e-006	0.932911
20 × 20	800	0.0274491	3.35425e-006	0.932898
35 × 35	2450	0.0274489	3.35425e-006	0.932897
50 × 50	5000	0.0274489	3.35425e-006	0.932897
65 × 65	8450	0.0274488	3.35425e-006	0.932897
80 × 80	12800	0.0274488	3.35425e-006	0.932897
95 × 95	18050	0.0274488	3.35425e-006	0.932897

Table 2.4: Uniform meshes for $\lambda = 1$, $\kappa = 0.1$, $a = 1$, $b = 1$

Mesh	N	$\ u_h^\varepsilon - u_{ex}\ _{L^2(\Omega)}$	$\varepsilon \ p_h^\varepsilon - p_{ex}\ _{L^2(\Omega)}$	$\ \theta_h^\varepsilon - \theta_{ex}\ _{L^2(\Omega)}$
5 × 5	50	0.0274552	3.35381e-006	0.382292
20 × 20	800	0.027452	3.3538e-006	0.38204
35 × 35	2450	0.0274519	3.3538e-006	0.382038
50 × 50	5000	0.0274518	3.3538e-006	0.382038
65 × 65	8450	0.0274518	3.3538e-006	0.382038
80 × 80	12800	0.0274518	3.3538e-006	0.382038
95 × 95	18050	0.0274518	3.3538e-006	0.382038

Table 2.5: Uniform meshes for $\lambda = 1$, $\kappa = 1$, $a = 5$, $b = 1$

Mesh	N	$\ u_h^\varepsilon - u_{ex}\ _{L^2(\Omega)}$	$\varepsilon \ p_h^\varepsilon - p_{ex}\ _{L^2(\Omega)}$	$\ \theta_h^\varepsilon - \theta_{ex}\ _{L^2(\Omega)}$
5 × 5	50	0.0274526	3.35381e-006	0.382292
20 × 20	800	0.027449	3.3538e-006	0.38204
35 × 35	2450	0.0274489	3.3538e-006	0.382038
50 × 50	5000	0.0274488	3.3538e-006	0.382038
65 × 65	8450	0.0274488	3.3538e-006	0.382038
80 × 80	12800	0.0274488	3.3538e-006	0.382038
95 × 95	18050	0.0274488	3.3538e-006	0.382038

Table 2.6: Uniform meshes for $\lambda = 1$, $\kappa = 1$, $a = 1$, $b = 5$

We can see that after a few iterations the errors tend to the fixed errors which are caused by the finite element approximation of mesh size h . this is consistent with the error of the artificial compressibility method as ε tends to 0.

2.6.1 Isolated island

In this part, we consider a two-dimensional physical model for the numerical studies of the effects of urban anthropogenic heat and wind speed on the UHI of urban region, as shown schematically in Figure (2.6). The numerical results illustrate the performances of the implicit-explicit scheme of the equation (2.132) for the unsteady Navier-Stokes Forchheimer Fourier problem. We use $\mathbb{P}_2\mathbb{B}\mathbb{R}$, \mathbb{P}_1 , \mathbb{P}_2 finite element to approximate the velocity, pressure and the temperature respectively. For overall computation time, we have chosen $T = 10s$ for a time step of 0.1s, for the space discretization, we have a regular triangulations of about 4964 elements. We keep the same parameters as in the cavity, except that for urban heat islands, the boundary and initial conditions are not the same. We did several tests by varying the Forchheimer coefficient to see the evolution of the profile of the velocity and the temperature in the city Figure (2.7) (2.8). We also experimented with the influence of the variation of the compressibility parameter ε showing in Figure (2.9) and Figure (2.10).

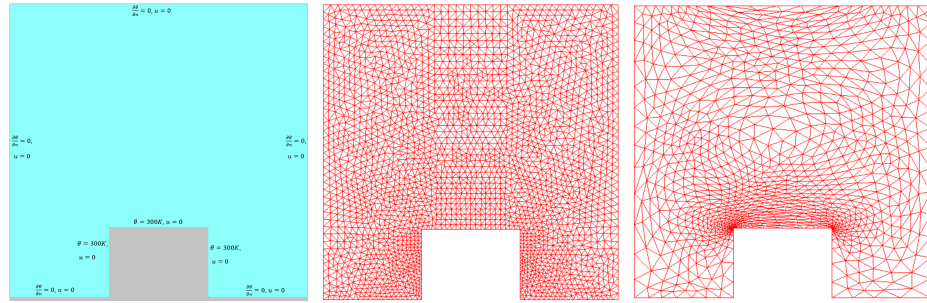


Figure 2.6: The boundary conditions, initial mesh and adaptative mesh.

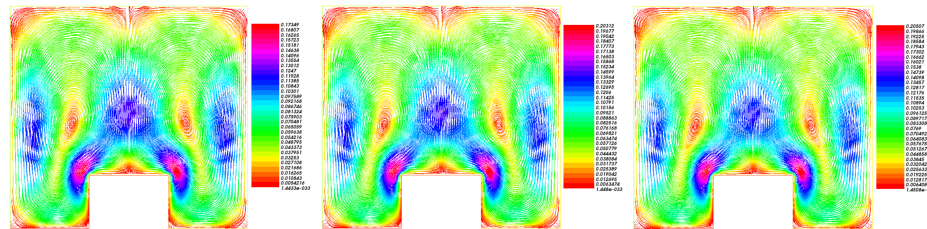


Figure 2.7: Velocity fields in the city $b = 1$, $b = 5$ and $b = 10$ from the left to the right for $\lambda = 0.01$

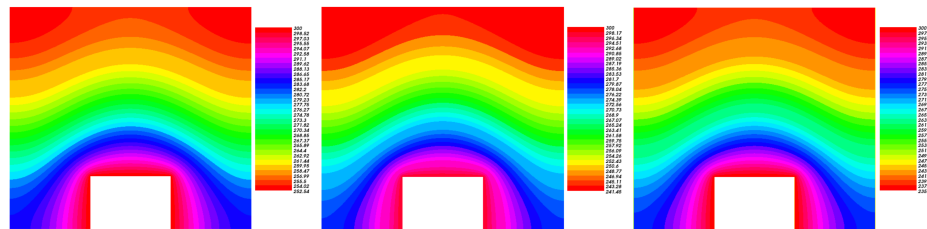


Figure 2.8: Temperature fields in the city $b = 1$, $b = 5$ and $b = 10$ from the left to the right for $\lambda = 0.01$, $\kappa = 0.01$.

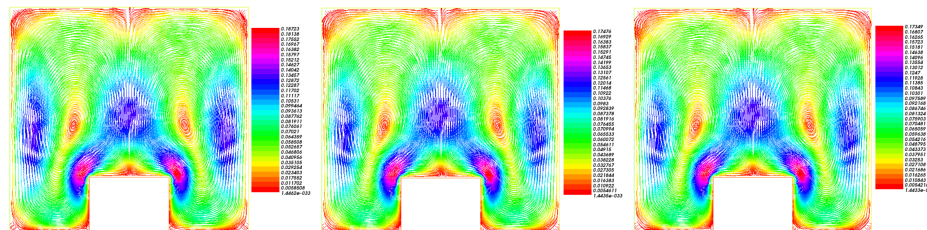


Figure 2.9: Velocity fields in the city $\varepsilon = 10^{-3}$, $\varepsilon = 10^{-4}$ and $\varepsilon = 10^{-6}$ from the left to the right for $\lambda = 1$.

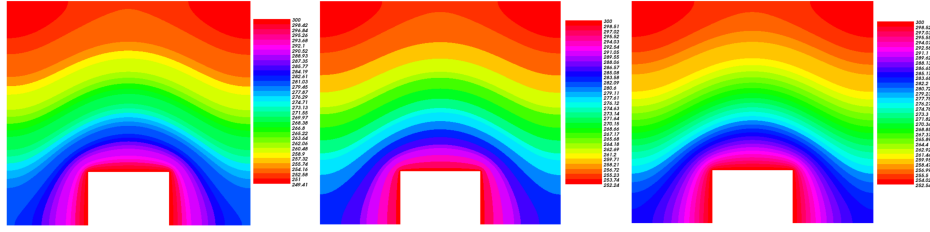


Figure 2.10: Temperature fields in the city $\varepsilon = 10^{-3}$, $\varepsilon = 10^{-4}$ and $\varepsilon = 10^{-6}$ from the left to the right for $\lambda = 0.01$, $\kappa = 0.01$.

2.6.2 Domestic frost-free refrigerator application

In this section we present some numerical results we have obtained for frost-free refrigerator with and without shelves. In the first step we give the result obtained in the case of the frost-free refrigerator without the shelves and in the second case with shelves.

Computational domain and grid structure

We consider a 3D domain with $(1.57, 0.44, 0.44)$ height, length and width respectively. These dimensions represent the interior volume of the refrigerator without taking into consideration the thickness of the different walls. For the overall computation time, we have chosen $T = 40s$ for a time step of $0.1s$, for the different space discretization, we tried a several regular triangulations of about 37839 elements. To simplify the computation, we take the parameters constants $a = b = 1/2$, and $\alpha = 1$, the thermal expansion coefficient $\beta = 3.38 \times 10^{-3}$, the diffusion coefficients $\nu = 1$ and $\kappa = 0.1$ for the fluid flow and heat transfer respectively. All computations are done at a low Reynolds number $Re = 1$.

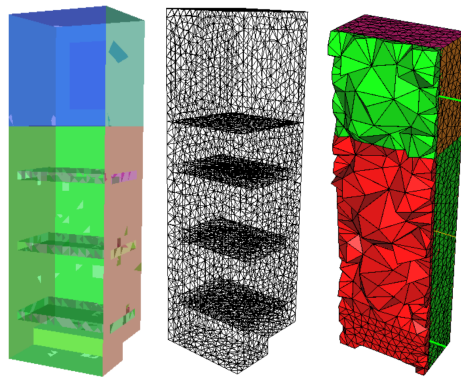


Figure 2.11: Computational domain and 3D mesh of the free-frost refrigerator.

Boundary conditions

For initial conditions for the velocity, temperature, pressure and simulation parameters are

Freeze compartement		
Boundary	Temperature	velocity
Inlet	$T_\infty = 251.7K$	$V_{in} = 0.5(0 \vec{i} + 0 \vec{j} + 1 \vec{k})$
Outlet	Z.N.G	Z.N.G
Top wall	$T_\infty = 302K$	No slip
Bottom	Adiabatic	No slip
Back wall	$T_\infty = 251K$	No slip
Front wall	$T_\infty = 302K$	No slip
Refrigerating compartement		
Inlet	$T_\infty = 253$	$V_{in} = (0.2/\sqrt{2})(0 \vec{i} - 1 \vec{j} + 1 \vec{k})$
Outlet	Z.N.G	Z.N.G
Back wall	$T_\infty = 327K$	No slip
Front wall	$T_\infty = 302K$	No slip
Top wall	Adiabatic	No slip
Bottom	$T_\infty = 302K$	No slip

Table 2.7: Boundary conditions

Figure (2.12) presents the distribution of the temperature in the two compartments of the refrigerator of the two configuration with and without shelves.

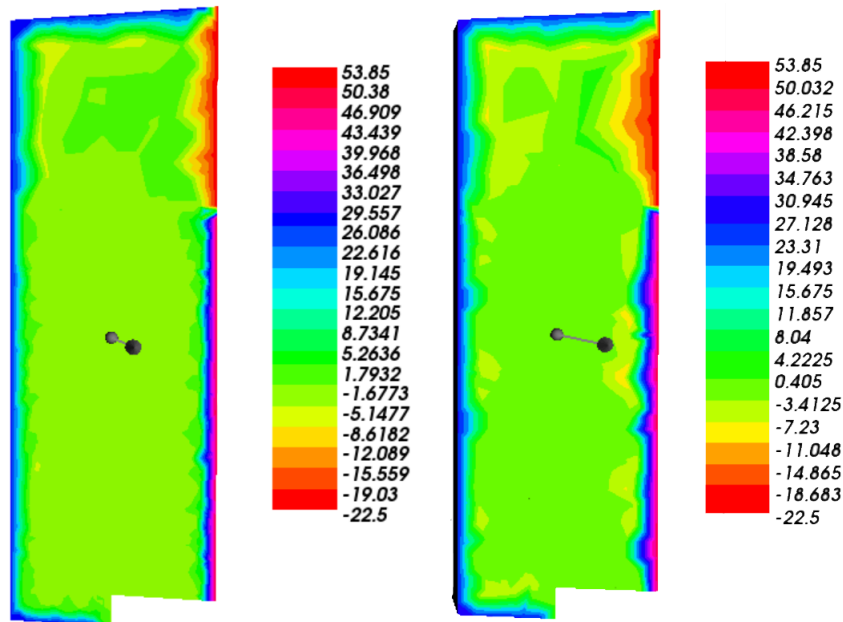


Figure 2.12: Temperature profile in the frost-free refrigerator without shelves in the left and with shelves in the right.

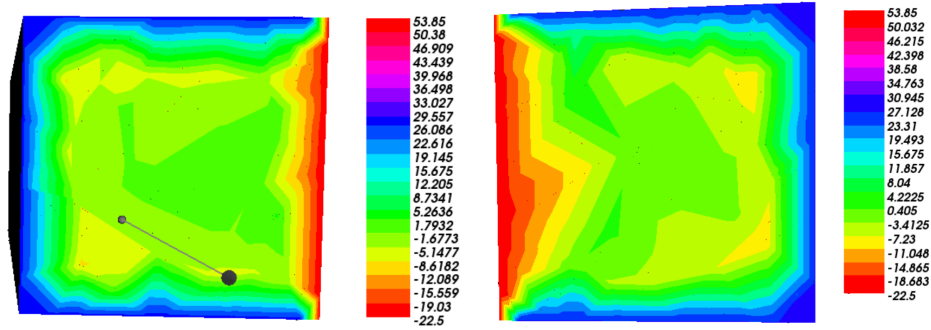


Figure 2.13: Horizontal temperature profile in the freezer compartment without shelves in the left and with shelves in the right.

Figure (2.14) shows the velocity profiles in the two cases of the refrigerator model. The shelves play an important role in the deflection of air in the refrigerator which makes stir on the cold walls and bring fresh air from the top to the bottom.

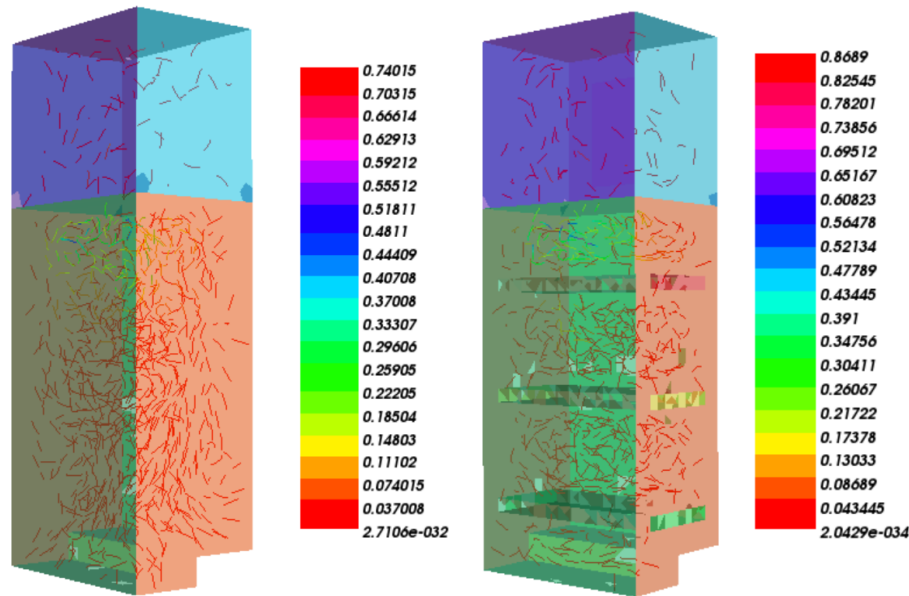


Figure 2.14: Velocity profiles in the refrigerator without shelves in the left and with shelves in the right.

2.7 Conclusion

In this chapter, we studied the artificial compressibility method for the unsteady Navier-Stokes Forchheimer problem coupled with the convection-diffusion equations.

We have shown the relevance of the artificial compressibility method by providing an error estimates for the coupled system.

These optimal error estimates concept the velocity, pressure and temperature in term of L^2 norm. The numerical results are in harmony with the theoretical error estimates. The proposed method

is robust and efficient to deal with practical 3D problems.

Bibliography

- [1] J. Shen, On error estimates of the penalty method for unsteady Navier-Stokes equations. SIAM. J. Numer. Anal. Vol. 32, No. 2, pp 386-403, 1995.
- [2] J. Shen, Pseudo-compressibility methods for the unsteady incompressible Navier-Stokes equations.
- [3] M. Louaked, N. Seloula, S. Trabelsi, Approximation of the unsteady Brinkman-Forchheimer equations by the pressure stabilization method, 2017 Wiley Periodicals, Inc. Numer Methods Partial Differential Eq, 2017.
- [4] M. Louaked, N. Seloula, Pseudocompressibility method for the incompressible Brinkman-Forchheimer equations, Differential and Integral Equations, Volume 28, Numbers 3 – 4(2015), 361 – 382.
- [5] E. Dibenedetto and A. Friedman, Conduction-convection problems with change of phase, J. Differ. Equations, 62(2)(1986)129 – 185.
- [6] R. Temam, Une méthode d’approximation des solution des équations de Navier-Stokes, Bull. Soc. Math. France, 98(1968)115 – 152.
- [7] R.A. Adams, Sobolev Spaces, Academic Press, New York, 1975.
- [8] J.G. Heywood and R. Rannacher, Finite element approximations of the nonstationary Navier-Stokes problem. Part I: Regularity of solutions and second-order spatial discretization, SIAM J. Numer. Anal. 19(2)(1982)275 – 311.
- [9] J. Shen, On error estimates of the penalty method for unsteady Navier-Stokes equations, SIAM J. Numer. Anal. 32(2)(1995)386 – 403.
- [10] Y.N. He and W.W. Sun, Stability and convergence of the Crank-Nicolson/Adams-Bashforth scheme for the time-dependent Navier-Stokes equations, SIAM J. Numer. Anal. 45(2)(2007)837 – 869.
- [11] H.Y. Sun, Y.N. He and X.L. Feng, On error estimates of the pressure-correction projection methods for the time-dependent Navier-Stokes equations, Int. J. Numer. Anal. Mod. 8(1)(2011)70 – 85.
- [12] Y. Zhang, M.F. Feng and Y.N. He, Subgrid model for the stationary incompressible Navier-Stokes equations based on the high order polynomial interpolation, Int. J. Numer. Anal. Mod.7(4)(2010)734 – 748.

-
- [13] T. Zhang, penalty mixed finite element method for non-stationary conduction convection problem.
- [14] C. Bernardi, G. Raugel, Analysis of some finite elements for the Stokes problem. *Math. Comp.* 44, 71 – 79(1985).
- [15] Y.N. He, Optimal error estimate of the penalty finite element method for the time-dependent Navier-Stokes equations, *Math. Comp.* 74(251)(2005)1201 – 1216.
- [16] F.J. Fernández, L.J. Alvarez-Vázquez, N. García-Chan, A. Martínez, M.E. Vázquez-Méndez, Optimal location of green zones in metropolitan areas to control the urban heat island, *Journal of Computational and Applied Mathematics* 289(2015)412 – 425.
- [17] Z. Hu, B. Yu, Z. Chen, T. Lia, M. Liu, Numerical investigation on the urban heat island in an entire city with an urban porous media model, *Atmospheric Environment Volume 47*, February 2012, Pages 509 – 518.
- [18] K. Vafai, C.L. Tien, Boundary and inertia effects on flow and heat transfer in porous media *International Journal of Heat and Mass Transfer*, 24(1981), *pp.*195 – 203.
- [19] Y. Louartassi, E. H. El Mazoudi, N. Elalami, A new Generalization of Lemma Gronwall-Bellman, *Applied Mathematical Sciences*, Vol. 6, 2012, no. 13, 621 - 628.
- [20] N. Sellila, M. Louaked, H. Mechkour, Optimal control and application to reduction of UHI intensity in porous city, (**Submitted**).
- [21] R. Temam, *Navier-Stokes equations: theory and numerical analysis (Third edition)*, North-Holland, Asmterdam, 1984.
- [22] D. Y. Shi and J. C. Ren, Nonconforming mixed finite element method for the stationary conduction-convection problem, *Int. J. Numer. Anal. Mod.* 6(2)(2009) 293-310.
- [23] D. C. Kim and Y. D. Choi, Analysis of conduction – natural convection conjugate heat transfer in the gap between concentric cylinders under solar irradiation, *Int. J. Therm. Sci.* 48(8)(2009)1247 – 1258.
- [24] Y. N. He, Optimal error estimate of the penalty finite element method for time-dependent Navier-Stokes equations, *Math. Comp.* 74(251)1201 – 1216
- [25] K. Wang, Y. N. He, X. L. Feng, On error estimates of the penalty method for viscoelastic flow problem I: Time discretization, *Appl. Math. Model.* 34(12)(2010)4089 – 4105.
- [26] K. Wang, Y. N. He, X. L. Feng, On error estimates of the fully discrete penalty method cor viscoelastic flow problem, *Int. J. Comput. Math.* 88(10)(2011)2199 – 2220.
- [27] H. Sun, Y. He, X. Peng, On error estimates of the penalty method for the unsteady conduction-convection problem I: Time discretization, *International Journal of Numerical Analysis and Modeling*, Volume 9, Number 4, 876 – 891.

Chapter 3

Theoretical and numerical analysis of an optimal problem governed by convection diffusion equations

Contents

3.1	Introduction	105
3.2	Governing equations	107
3.2.1	The transport pollution model	107
3.2.2	Adjoint state	108
3.2.3	2D shallow water model	109
3.2.4	Weak formulation	109
3.3	Control problem	109
3.4	Preliminaries	110
3.5	Characteristic Finite Element Approximation	112
3.6	Numerical resolution	129
3.6.1	Time and space discretization	130
3.6.2	Numerical results	131
3.7	Conclusion	137

3.1 Introduction

Pollution of the aquatic environment is a problem resulting from human activity such as wastewater discharges, or an industrial and ecological disaster that results in the dispersion of a large quantity of crude oil or heavy oil products such as oil spills. Take the example of the sinking of the Torrey Canyon in 1967 transported 120,000 tonnes of unrefined oil Figure (3.1). A large importance of analysis of this problems was approved in recent years [1], [2]. These pollutants

can have consequences for aquatic environments and human health.

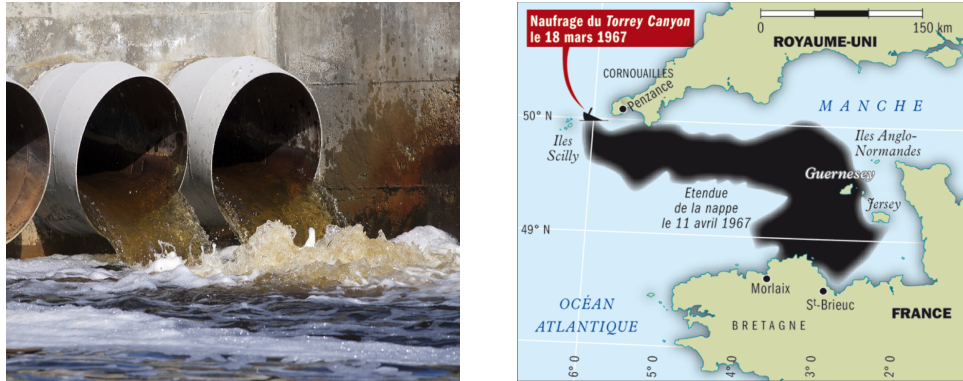


Figure 3.1: Examples of wastewater in the left and a Normand-Breton golf oil spill 1967 in the right.

The preservation of the marine and coastal environment has become a major issue in recent years. Reducing pollutants from toxic chemicals, or wastewater discharges is a challenge. Coastal pollution is generally controlled by treating contaminants at the source or in treatment plants through wastewater treatment methods to reduce their concentration.

The approximation of pollutant transport in the aquatic environment is performed by a numerical procedure using the Galerkin characteristic finite element method [24]. The methods of characteristic combine the convection and capacity terms in governing equations to carry out the temporal discretization in Lagrange coordinates. These methods symmetrize the governing equation and stabilize their numerical approximation [22], that means this approach allows us to avoid theoretically the constraint CFL (Courant-Friedrichs-Levy) on the time step and it has been shown that it has very good stability properties [25], [26]. There are other techniques in the literature for example a hybrid numerical procedure combining a particle method and a finite difference technique [7].

The optimal control problem was introduced by [26] in the case to study the partial differential equations. In recent years, for the optimal control problems, the a priori and posteriori error estimates has taken exponential trend for the parabolic and elliptic equations, for example [15] have studied the numerical solution of state constrained parabolic boundary control problems by finite element approximations, [16] the finite element approximations of parabolic control problems with pointwise control. Other studies of the finite element method for PDEs and control optimal can be found in [17], [18] and [19].

The aim of this studies is to analyse the finite element approximation of parabolic optimal control problem with pointwise control governed by a coupling of the transport pollution model with Shallow Water equations. The main difficulties of the problem from the theoretical point of

view are due to the singularity of the right hand side of the state system includes radon measures and to the presence of pointwise state constraints, which lead us to work in regular functional spaces in order to obtain the adjoint state.

As part of our study, we introduced and developed a mathematical model to solve an environmental problem that consists of studying the marine pollution. In the Sect. 2 we give the model problem and the weak formula and optimality conditions. Then we construct a backward-Euler characteristic finite element approximation, we give an priori error estimates for the control and state approximation. Finally we give the numerical resolution, we propose an algorithm of the minimisation and we show several numerical results and end the chapter with conclusions..

3.2 Governing equations

In this part, we define the governing equations of the studied problem and its mathematical formulation. The equations that governing the phenomenon of pollutant dispersion in the oceans and the transport ensure by the velocity of the fluid or by ocean hydrodynamics. We are interested in the coupling of two systems of equations, advection-diffusion equations and shallow water equations (SWE).

3.2.1 The transport pollution model

The 2D model most used to describe the physical phenomena in the case of the transport of a pollutant by the two processes of diffusion and convection. We are interested in the evolution of oil slick dispersion occurs to the sinking of a ship, and the evolution of the concentration of wastewater discharged into the sea is given by the following model:

$$\partial_t \phi - \mu \Delta \phi + (\mathcal{U} \cdot \nabla) \phi + \sigma \phi = \sum_{i=1}^N F_i(t) \delta(r - r_0) \quad \text{in } \Omega \times (0, T) \quad (3.1)$$

where μ is the diffusion coefficient, and $\delta(r - r_0)$ is the Dirac masse at the accident point r_0 , σ is a positive constant caractérisé the decay of ϕ [11], \mathcal{U} the velocity of the oil or the wastewater propagation is assumed to be known. This velocity can be deduced from the climatic sea surface current and winds [4], or from hydrodynamic Shallow Water model which is the subject of our study.

The initial condition at $t = 0$ is

$$\phi(x, 0) = \phi_0(x) \quad \text{in } \Omega \times (0, T) \quad (3.2)$$

and

$$\phi(x, t) = 0 \quad \text{on } \partial\Omega \times (0, T) \quad (3.3)$$

3.2.2 Adjoint state

The application of the adjoint system is widely used for solving physical problems. For example, [9] to determine the diffusion coefficients and the aerosol transformation coefficients, [[10]] to estimate the concentration of the pollutant in important areas in a region.

Lets the advection-diffusion equations

$$\partial_t \phi - \mu \Delta \phi + (\mathcal{U} \cdot \nabla) \phi + \sigma \phi = \sum_{i=1}^N F_i(t) \delta(r - r_0) \quad \text{in } \Omega \times (0, T) \quad (3.4)$$

Multiply the equation (3.4) by arbitrary, smooth test function ψ and integrate by parts over each element Ω and on an interval $[0, T]$

$$\int_0^T \int_{\Omega} \psi (\partial_t \phi - \mu \Delta \phi + (\mathcal{U} \cdot \nabla) \phi + \sigma \phi) dx dt = \int_0^T \int_{\Omega} \sum_{i=1}^N F_i(t) \delta(r - r_i) \psi dx dt \quad (3.5)$$

Consider the transformation for each terms we get

$$\int_0^T \int_{\Omega} \psi \partial_t \phi dx dt = \int_{\Omega} [\phi \psi]_0^T dx - \int_0^T \int_{\Omega} \phi \partial_t \psi dx dt \quad (3.6)$$

Using Lagrange identity propriety $\langle A\phi, \Psi \rangle = \langle \phi, A^* \Psi \rangle$ to define the adjoint operator such that $A\phi \equiv \mathcal{U} \left(\frac{\partial \Phi}{\partial x} + \frac{\partial \Phi}{\partial y} \right)$ [8]

$$\int_0^T \int_{\Omega} \psi (\mathcal{U} \cdot \nabla) \phi dx dt = - \int_0^T \int_{\Omega} \phi (\mathcal{U} \cdot \nabla) \psi dx dt \quad (3.7)$$

Summarizing

$$\int_0^T \int_{\Omega} \phi (-\partial_t \psi - \mu \Delta \psi - (\mathcal{U} \cdot \nabla) \psi + \sigma \psi) dx dt + \int_{\Omega} [\phi \psi]_0^T dx = p(r, t) \quad (3.8)$$

$$\int_0^T \int_{\Omega} \phi (-\partial_t \psi - \mu \Delta \psi - (\mathcal{U} \cdot \nabla) \psi + \sigma \psi) dx dt + \int_{\Omega} [\Phi_T \psi_T - \phi_0 \psi_0] dx = p(r, t) \quad (3.9)$$

Adding the initial and boundary conditions

$$\psi(x, T) = 0 \quad \text{in } \Omega \times (0, T) \quad (3.10)$$

$$\psi(x, t) = 0 \quad \text{on } \partial\Omega \times (0, T) \quad (3.11)$$

The equation (3.9) became

$$\int_0^T \int_{\Omega} \phi (-\partial_t \psi - \mu \Delta \psi - (\mathcal{U} \cdot \nabla) \psi + \sigma \psi) dx dt = p(r, t) \quad (3.12)$$

with

$$p(r, t) = \phi - \phi_d \quad (3.13)$$

Finally The adjoint system is written in the following form

$$-\partial_t \psi - \mu \Delta \psi - (\mathcal{U} \cdot \nabla) \psi + \sigma \psi = \phi - \phi_d \quad (3.14)$$

3.2.3 2D shallow water model

Generally the unsteady flow of water in two-dimensional space may be described by the shallow water equations. Shallow water Equations (SWE) are commonly used as models of fluid dynamics in the case of the resolution of physical phenomena that are related to the environment [5], [1], [6] and others. The vertical velocity component is negligible compared to the horizontal component. This model is derived from the Navier-Stokes equations. The velocity field (u, v) is related to the elevation of water. We consider the following hyperbolic system

$$\begin{cases} \partial_t u - \mu' \Delta u + (u \cdot \nabla) u & = -g \partial_x H & \Omega \times (0, T) \\ \partial_t v - \mu' \Delta v + (v \cdot \nabla) v & = -g \partial_y H & \text{in in } \Omega \times (0, T) \\ \partial_t H + \partial_x (Hu) + \partial_y (Hv) & = 0 & \text{in } \Omega \times (0, T) \end{cases} \quad (3.15)$$

where (u, v) is the velocity such that $\mathcal{U} = (u, v)$, H water elevation, g is the acceleration due to gravity and μ' is the diffusion coefficient. The system (3.15) can be written in the following form

$$\begin{cases} \partial_t \mathcal{U} - \mu' \Delta \mathcal{U} + (\mathcal{U} \cdot \nabla) \mathcal{U} & = -g \nabla H & \text{in } \Omega \times (0, T) \\ \partial_t H + \nabla \cdot (H\mathcal{U}) & = 0 & \text{in } \Omega \times (0, T) \end{cases} \quad (3.16)$$

3.2.4 Weak formulation

Let \mathcal{U} and H be the solution of the system (3.16), find $(\mathcal{U}, H) \in H_0^1(\Omega) \times H^1(\Omega)$ such that

$$\left(\left(\frac{\mathcal{U}^i - \mathcal{U}^{i-1}}{\tau_i}, w \right) - (gH^i, \nabla \cdot w) + \mu' (\nabla \mathcal{U}^i, \nabla w) \right) = 0 \quad \forall w \in H_0^1(\Omega), \tau \geq 1 \quad (3.17)$$

$$\left(\left(\frac{H^i - H^{i-1}}{\tau_i}, q \right) + (H^i (\nabla \mathcal{U}^i), q) \right) = 0 \quad \forall q \in H^1(\Omega), \tau \geq 1 \quad (3.18)$$

where \mathcal{U}^i and H^i also satisfy the following initial conditions

$$\mathcal{U}(x, 0) = \mathcal{U}_0(x), \quad H_0(x, 0) = H_0(x) \quad (3.19)$$

3.3 Control problem

We are interested in finding the optimal mass flow $f \in \mathcal{M}(\Omega)$ (where $\mathcal{M}(\Omega)$ the space of the real regular Borel measures on Ω) at a discharge points sources. The optimal control problem

consists to minimize the concentration of the pollutant distribution ϕ from a target concentration $\phi_d \in L^2(\Omega)$ using the cost function

$$J(f) = \frac{1}{2} \int \int_{\Omega} (\phi(t, x) - \phi_d(t, x))^2 dx dt + \frac{\alpha_j}{2} \sum_{i=1}^n \int_{\Omega} (f_j(t))^2 dt \quad (3.20)$$

Here $\phi(x, t)$ is the solution of the problem (3.1), (3.2) and (3.3). α_j is a small positive parameter. and the gradient of the cost function is defined

$$\nabla J(f)_j = \alpha_j f_j(t) + \psi(t, r_j) \quad j = 1, \dots, n. \quad (3.21)$$

where ψ is the solution of the adjoint state giving in (3.14), (3.10) and (3.11).

The existence of an optimal control and the expression of the gradient of the cost function are proved in [27] such that

Theorem 3.3.1. *The above control problem (3.1) and (3.20) admits a unique solution $f \in \mathcal{M}(\Omega)$ and the gradient of the cost function is identified as*

$$\nabla J(f)_j = \alpha_j f_j(t) + \psi(t, r_j) \quad j = 1, \dots, n.$$

where the adjoint state function ψ satisfies the following form :

$$\begin{cases} -\partial_t \psi - \mu \Delta \psi - (\mathcal{U} \cdot \nabla) \psi + \sigma \psi = \phi - \phi_d & \text{in } \Omega \times (0, T) \\ \psi(x, T) = 0 & \text{on } \partial\Omega \times (0, T) \\ \psi(x, t) = 0 & \text{in } \Omega \end{cases}$$

3.4 Preliminaries

Let Ω and Ω_{adm} be an open bounded domain in \mathbb{R}^d ($d = 2$ or 3) and are convex polygon with boundary $\partial\Omega$ and $\partial\Omega_{adm}$. We adopt the standard notation Sobolev space $W = L^2([0, T]; V)$ with $V = H_0^1(\Omega)$ and the control space $X = L^2([0, T]; U)$ with $U = L^2(\Omega_{adm})$. Let K be a closed convex set in X and K^h is a closed convex set in U^h where $K^h \subset K \cap U^h$. Let $V^h = \{v_h \in S^h : v_h|_{\partial\Omega}\}$, $W^h = L^2([0, T]; V^h)$ and $V^h \subset V$, $W^h \subset W$. $\mathcal{M}(\Omega)$ the space of the real regular Borel measures on Ω . We define by $C_0^m(\Omega)$, $m \in \mathbb{N}_0$, the linear subspace of continuous functions on Ω . The parameters h and τ denote the spatial and temporal grid size respectively.

$$K = \{v \in X : v \geq 0 \text{ in } \Omega_{adm} \times [0, T]\}$$

Hypothesis 3.4.1. The solution of the shallow water system (3.16) $\mathcal{U} \in H_0^1(\Omega)$ is such that

$$\|\nabla \mathcal{U}\|_{L^\infty} \leq Const$$

We consider the following parabolic problem

$$\begin{cases} \partial_t \phi - \mu \Delta \phi + (\mathcal{U} \cdot \nabla) \phi + \sigma \phi = g + \sum_{i=1}^N f_i(t) \delta(r - r_i) & \text{in } \Omega \times (0, T) \\ \phi(x, t) = 0 & \text{on } \partial\Omega \times (0, T) \\ \phi(x, 0) = \phi_0(x) & \text{in } \Omega \end{cases} \quad (3.22)$$

where $\sigma \geq 0$ for all $(x, t) \in \Omega \times [0, T]$, $\sigma \in L^\infty(\Omega)$, \mathcal{U} fields velocity $\mathcal{U} \in C([0, T], C_0^1(\bar{\Omega})^2)$, $g = g(x, t)$ external sources and sinks, with $g \in L^2(0, T; L^2(\Omega))$. ϕ et f are called state and control variables and ϕ_0 is an initial data where $\phi_0 \in V = H_0^1(\Omega)$.

The adjoint state of the equation (3.22) is define in the following form

$$\begin{cases} -\partial_t \psi - \mu \Delta \psi - (\mathcal{U} \cdot \nabla) \psi + \sigma \psi = \phi - \phi_d & \text{in } \Omega \times (0, T) \\ \psi(x, T) = 0 & \text{on } \partial\Omega \times (0, T) \\ \psi(x, t) = 0 & \text{in } \Omega \end{cases} \quad (3.23)$$

with ϕ_d is a given function, where $\phi_d \in H^1([0, T]; L^2(\Omega))$, and α denotes the regularization parameter $\alpha > 0$.

We consider \mathcal{B} as a linear continuous operator from X to $L^2([0, T]; \mathcal{M}(\Omega))$ such that

$$(\mathcal{B}f)(t) := \sum_{i=1}^N f_i(t) \delta(r - r_i) \quad t \in [0, T], \quad r_i \in \Omega$$

and

$$a(v, w) = \mu \int_{\Omega} \nabla v : \nabla w \quad \forall v, w \in H^1(\Omega)$$

The weak formulation of the problem (3.22) is find : $\phi(f) \in H^1([0, T]; L^2(\Omega)) \cap W$ such that

$$\begin{cases} (\partial_t \phi(f), w) + (\mathcal{U} \cdot \nabla \phi(f), w) + a(\phi(f), w) + (\sigma \phi(f), w) = (g + \mathcal{B}f, w), & \forall w \in V, t \in [0, T] \\ \phi(y)(x, 0) = \phi_0(x), & x \in \Omega \end{cases} \quad (3.24)$$

The problem (3.24) admit a unique solution for all g and f .

Let us suppose that $r_i \in \Omega$ are given locations of point sources. We are interested in estimating the magnitude $f_i(t)$ of the point source from measurements ϕ_d in Ω . The related optimal control problem through an output least square approach and Tikhonov regularization is given by

$$J(v) = \int_0^T \left(\frac{1}{2} \|\phi(v) - \phi_d\|_{L^2(\Omega)}^2 + \frac{\alpha}{2} \|v\|_{L^2([0, T]; \mathbb{R}^m)}^2 \right) dt \quad (3.25)$$

So, the above control problem can be written as follows

$$J(f) = \min_{v \in K} J(v) \quad (3.26)$$

and for all $\phi(v) \in W$, the problem (3.24) can be written

$$\begin{cases} (\partial_t \phi(v), w) + (\mathcal{U} \cdot \nabla \phi(v), w) + a(\phi(v), w) + (\sigma \phi(v), w) = (g + \mathcal{B}v, w), & \forall w \in V, t \in [0, T] \\ \phi(f)(x, 0) = \phi_0(x), & x \in \Omega \end{cases} \quad (3.27)$$

ϕ and f are the unique solution of the control problem (3.27) if and only if the state adjoint $\psi \in W$ such that

$$\begin{cases} (\partial_t \phi, w) + (\mathcal{U} \cdot \nabla \phi, w) + a(\phi, w) + (\sigma \phi, w) = (g + \mathcal{B}u, w), & \forall w \in V = H_0^1(\Omega) \\ \phi(x, 0) = \phi_0(x) \end{cases} \quad (3.28)$$

The adjoint state

$$\begin{cases} -(\partial_t \psi, q) - (\mathcal{U} \cdot \nabla \psi, q) + a(q, \psi) + (\sigma \psi, q) = (\phi - \phi_d, w), & \forall q \in V = H_0^1(\Omega) \\ \psi(x, 0) = \psi_0(x) \end{cases} \quad (3.29)$$

And the optimality condition

$$\int_0^T (\alpha f + \mathcal{B}^* \psi, v - u)_U dt \geq 0 \quad \forall v \in K \subset X = L^2([0, T]; U) \quad (3.30)$$

where \mathcal{B}^* is an adjoint operator of \mathcal{B} , and $(\cdot, \cdot)_U$ is the inner product of U .

3.5 Characteristic Finite Element Approximation

In this section, the characteristics finite element approximation scheme for the control problem is presented. The characteristics method is widely used to solve PDEs, generally adapted to the transport problems. Using the method of characteristic on the hyperbolic part of (3.1) $(\partial_t \phi + (\mathcal{U} \cdot \nabla) \phi)$. The goal of this method is to transform the convection operator into a total derivative by using the Lagrangian formulation. We consider the characteristics equation

$$\begin{cases} \frac{dX}{d\tau}(x, s; \tau) = \phi(X(x, s; \tau), \tau) \\ X(x, s; \tau) = x \end{cases} \quad (3.31)$$

where the characteristics curve $X(x, s; \tau)$ denotes the position at time τ of a fluid particle located at position x at time τ . Let the interval $[0, T]$, we choose $N \in \mathbb{N}$ and define the time step $\Delta t = \frac{T}{N}$. The points $\tau_n = n\Delta t$, for $n = 0, \dots, N$, and we denote $\phi^n(x) = \phi(x, t^n)$. Using the following approximation of the total derivative along the characteristic curves, we approximate $\frac{D\phi}{Dt}$ at the time $\tau = \tau_{n+1}$ by

$$\frac{D\phi}{Dt}(x, t) \approx \frac{\phi(x, t^{n+1}) - \phi(X^n(x), t^n)}{\Delta t} \quad (3.32)$$

where $X^n(x)$ is the approximation of $X(x, t^{n+1}, t^n)$.

Then using the this approximation, the variational formulation with Dirichlet boundary conditions (3.22) becomes

$$\begin{aligned} \frac{1}{\Delta t} (\phi^{n+1} - \phi^n(X^n(x))) - \mu \Delta \phi^{n+1} + \sigma \phi^{n+1} &= g + \sum_{i=1}^N f_i^{n+1}(t) \delta(r - r_i) \quad \text{in } \Omega \times (0, T) \\ \phi(x, t) &= 0 \quad \text{on } \partial\Omega \times (0, T) \end{aligned} \quad (3.33)$$

We consider a quasi-uniform family \mathcal{T}^h of a regular triangulations of $\bar{\Omega}$ such that $\bar{\Omega} = \bigcup_{\beta \in \mathcal{T}^h} \bar{\beta}$, \mathcal{T}^h is a finite dimensional subspace S^h of $C(\bar{\Omega})$ and \mathcal{T}_U^h another finite dimensional subspace U^h of $L^2(\Omega)$. Similary, let \mathcal{T}_U^h of a regular triangulations of $\bar{\Omega}$ such that $\bar{\Omega} = \bigcup_{\beta_U \in \mathcal{T}_U^h} \bar{\beta}_U$, where β and β_U are a diameters bounded by h and h_U . To discretize the optimal control problem some variational discretization approach developed in [12] and [13]. In our case the fully discrete approximation for the optimal control problem we use the characteristic finite element method.

$$J_{h\tau}(v_h^i) = \sum_{i=1}^{N^*} \tau_i \left(\frac{1}{2} \|\phi_h^i - \phi_d\|_{L^2(\Omega)}^2 + \frac{\alpha}{2} \|v_h^i\|_{L^2([0, T]; \mathbb{R}^m)}^2 \right) dt \quad (3.34)$$

where $\tau_i = t_i - t_{i-1}$ and $i = \{1, 2, \dots, N^*\}$ with time interval partition $[0, T] = \{t_0, t_1, \dots, t_{N^*}\}$, $\tau = \max_{1 \leq i \leq N^*} \tau_i$.

So, find $(\phi_h^i, f_h^i) \in V^h \times K^h, i = 1, 2, \dots, N^*$, such that

$$J_{h\tau}(f_h^i) = \min_{v_h^i \in K} J_{h\tau}(v_h^i) \quad (3.35)$$

Subject to

$$\begin{cases} \left(\frac{\phi_h^i - \bar{\phi}_h^{i-1}}{\tau_i}, w_h \right) + a(\phi_h^i, w_h) + (\sigma \phi_h^i, w_h) = (g(x, t_i) + \mathcal{B}v_h^i, w_h), \quad \forall w_h \in V^h \subset V \\ \phi_h^i(x, 0) = \phi_0^h(x), \quad x \in \Omega \end{cases}$$

where $\phi_0^h \in V^h$ is an approxiamtion of ϕ_0 .

Let (Φ_h^i, F_h^i) be the unique solution of the fully discrete problem of (3.28), and $(\Phi_h^i, F_h^i) \in V^h \times K^h$ is the solution if and only if there is a co-state $\Psi_h^{i-1} \in V^h$, such that $(\Phi_h^i, \Psi_h^{i-1}, F_h^i) \in V^h \times V^h \times K^h, i = \{1, 2, \dots, N^*\}$, satisfies the following optimality conditions

$$\begin{cases} \left(\frac{\Phi_h^i - \bar{\Phi}_h^{i-1}}{\tau_i}, w_h \right) + a(\Phi_h^i, w_h) + (\sigma \Phi_h^i, w_h) = (g^i + \mathcal{B}F_h^i, w_h), \quad \forall w_h \in V^h \subset V \\ \Phi_h^i(x, 0) = \phi_0^h(x), \quad x \in \Omega \end{cases} \quad (3.36)$$

$$\begin{cases} \left(\frac{\Psi_h^{i-1} - \bar{\Psi}_h^i \cdot J^i}{\tau_i}, q_h \right) + a(q_h, \Psi_h^{i-1}) + (\sigma \Psi_h^i, q_h) = (\Psi_h^i - \phi_d^i, q_h), & \forall q_h \in V^h \subset V \\ \Psi_h^{N^*}(x, T) = 0, & x \in \Omega \end{cases} \quad (3.37)$$

$$(\alpha F_h^i + \mathcal{B} \Psi_h^{i-1}, v_h - F_h^i)_U \geq 0 \quad \forall v_h \in K^h \cap U^h \quad (3.38)$$

with $\bar{\Psi}_h^i = \Psi_h^i(\bar{x})$. We pose

$$x = G(\bar{x}, \tau_i; \tau_{i-1})$$

where $J^i = \det DG(\bar{x}, \tau_i; \tau_{i-1})^{-1}$ the determinant of the Jacobian transformation from G to x . We know that for each $x \in \Omega$ and $\tau \in [0, T], i \geq 1$, the Jacobian matrix of the transformation x to G is

$$DG(\bar{x}, \tau_i; \tau_{i-1}) = \left[\frac{\partial G(\bar{x}, \tau_i; \tau_{i-1})}{\partial x} \right] = \begin{bmatrix} 1 - \frac{\partial \mathcal{U}_1^i}{\partial x_1} \tau_i & -\frac{\partial \mathcal{U}_1^i}{\partial x_2} \tau_i \\ -\frac{\partial \mathcal{U}_2^i}{\partial x_1} \tau_i & 1 - \frac{\partial \mathcal{U}_2^i}{\partial x_2} \tau_i \end{bmatrix}$$

$$\det DG(\bar{x}, \tau_i; \tau_{i-1}) = 1 - (\nabla \cdot \mathcal{U}^i) \tau_i + \mathcal{O}(\tau_i^2)$$

Using the hypothesis (3.4.1), we have

$$\det DG(\bar{x}, \tau_i; \tau_{i-1}) = 1 + \mathcal{O}(\tau_i^2)$$

For obtaining the error estimates of the proposed scheme in (3.36) and (3.38) using the characteristic finite element approximation of the optimal control problems. For the subsequent analysis it is convenient to introduce the two intermediate variables $(\Phi_h^i(f), \Psi_h^i(f)) \in V^h \times V^h$, for $i = 1, 2, \dots, N^*$ satisfying

$$\begin{cases} \left(\frac{\Phi_h^i(f) - \bar{\Phi}_h^{i-1}(f)}{\tau_i}, w_h \right) + a(\Phi_h^i(f), w_h) + (\sigma \Phi_h^i(f), w_h) = (g^i + \mathcal{B} f_h^i, w_h), & \forall w_h \in V^h \\ \Phi_h^i(u)(x, 0) = \phi_0^h(x), & x \in \Omega \end{cases} \quad (3.39)$$

$$\begin{cases} \left(\frac{\Psi_h^{i-1}(f) - \bar{\Psi}_h^i(f) \cdot J^i}{\tau_i}, q_h \right) + a(q_h, \Psi_h^{i-1}(f)) + (\sigma \Psi_h^i(f), q_h) = (\Psi_h^i(u) - \phi_d^i, q_h), & \forall q_h \in V^h \subset V \\ \Psi_h^{N^*}(f)(x, T) = 0, & x \in \Omega \end{cases} \quad (3.40)$$

We pose

$$\begin{aligned} \theta^i &= \Phi_h^i - \Phi_h^i(u), & \eta^i &= \phi^i - \Phi_h^i(u), & i &= 0, 1, 2, \dots, N^* \\ \zeta^i &= \Psi_h^i - \Psi_h^i(u), & \xi^i &= \psi^i - \Psi_h^i(u), & i &= N^*, \dots, 1, 0 \end{aligned}$$

where $\theta^0 = 0$ et $\zeta^{N^*} = 0$, we suppose that N and M are positive integers which are chosen such

that

$$\begin{aligned}\|v^N\|_V &= \|v\|_{L^\infty([0,T];V)}, & \text{for } v = \theta \text{ and } \eta \\ \|v^M\|_V &= \|v\|_{L^\infty([0,T];V)}, & \text{for } v = \zeta \text{ and } \xi\end{aligned}$$

In the following we will first give the estimates between the approximate solution (Φ_h, Ψ_h) and the intermediate solution $(\Phi_h(f), \Psi_h(f))$

Lemma 3.5.1. *Let (Φ_h, Ψ_h) and $(\Phi_h(f), \Psi_h(f))$ be the solution of (3.36)-(3.37) and (3.39)-(3.40) respectively. Then there are a positive constants C_2 independent of h and τ such that*

$$\|\Phi_h - \Phi_h(f)\|_{L^\infty([0,T];H_0^1(\Omega))} \leq C_2 \|f - F_h\|_{L^2([0,T];L^2(\Omega_{adm}))} \quad (3.41)$$

and

$$\|\Psi_h - \Psi_h(f)\|_{L^\infty([0,T];H_0^1(\Omega))} \leq C_2 \|f - F_h\|_{L^2([0,T];L^2(\Omega_{adm}))} \quad (3.42)$$

Proof. By differentiating between the approximate solution Φ_h and the intermediate solution $\Phi_h(f)$. By subtracting (3.39) from (3.36) we have

$$\left(\frac{\theta^i - \theta^{i-1}}{\tau_i}, w_k \right) + a(\theta^i, w_k) + (\sigma\theta^i, w_k) = (\mathcal{B}(F_h^i - f^i), w_k) - \left(\frac{\theta^i - \bar{\theta}^{i-1}}{\tau_i}, w_k \right) \quad (3.43)$$

■

In order to obtain an error estimates of θ in H^1 , we pose $w_k = d_t\theta^i = \frac{\theta^i - \theta^{i-1}}{\tau_i}$ as a test function.

$$(\partial_t\theta^i, \partial_t\theta^i) + a(\theta^i, \partial_t\theta^i) + (\sigma\theta^i, \partial_t\theta^i) = (\mathcal{B}(F_h^i - f^i), \partial_t\theta^i) - \left(\frac{\theta^i - \bar{\theta}^{i-1}}{\tau_i}, \partial_t\theta^i \right) \quad (3.44)$$

By definition we have the inequality

$$a(a - b) \geq \frac{1}{2}(a^2 - b^2) \quad \forall a, b \in \mathcal{R} \quad (3.45)$$

So,

$$\begin{aligned}a \left(\frac{\theta^i - \theta^{i-1}}{\tau_i}, \theta^i \right) &= \frac{1}{\tau_i} \int_{\Omega} \mu (\nabla(\theta^i - \theta^{i-1}), \nabla\theta^i) \\ &= \frac{1}{2\tau_i} \int_{\Omega} \mu (\nabla\theta^i \cdot \nabla\theta^i) - (\nabla\theta^{i-1} \cdot \nabla\theta^{i-1}) \\ &= \frac{1}{2\tau_i} (a(\theta^i, \theta^i) - a(\theta^{i-1}, \theta^{i-1})) \\ &= \frac{1}{2\tau_i} (\|\theta^i\|_a^2 - \|\theta^{i-1}\|_a^2)\end{aligned} \quad (3.46)$$

The equation (3.44) can be rewritten in the form

$$\|d_t\theta^i\|^2 + \frac{1}{2\tau_i} \left(\|\theta^i\|_a^2 - \|\theta^{i-1}\|_a^2 \right) + (\sigma\theta^i, \partial_t\theta^i) \leq (\mathcal{B}(F_h^i - f^i), \partial_t\theta^i) - \left(\frac{\theta^i - \bar{\theta}^{i-1}}{\tau_i}, \partial_t\theta^i \right) \quad (3.47)$$

We will also make use of Young's inequality: for real numbers a, b and $\varepsilon > 0$

$$|ab| \leq \frac{\varepsilon}{2} a^2 + \frac{1}{2\varepsilon} b^2, \quad \forall a, b, \varepsilon \in \mathcal{R}, \varepsilon > 0 \quad (3.48)$$

for the purpose of the right hand side term, from the continuous property of the \mathcal{B} and the inequality (3.48) with $\varepsilon = \frac{1}{2}$

$$|(\mathcal{B}(F_h^i - f^i), \partial_t\theta^i)| \leq C \|f^i - F_h^i\|_{0,\Omega}^2 + \frac{1}{4} \|d_t\theta^2\|^2 \quad (3.49)$$

Lemma 3.5.2. *Let $f \in V = H_0^1(\Omega)$, and $\bar{f}(x) = f(x - g(x)\tau)$, where g is bounded on $\bar{\Omega}$, then for τ sufficiently small, we have*

$$\|f(x) - \bar{f}(x)\| \leq C_0\tau \|f\|_V \quad (3.50)$$

where the constant $C_0 = C_0(\|g\|_{L^\infty(\Omega)})$ depends proportionably on $\|g\|_{L^\infty(\Omega)}$ and independent on the discrete parameter.

Using the estimate described in Lemma (3.5.2), the Cauchy-Schwarz inequality and the inequality (3.45) with $\varepsilon = \frac{1}{2}$ so

$$\begin{aligned} \left| \left(\frac{\theta^i - \bar{\theta}^{i-1}}{\tau_i}, \partial_t\theta^i \right) \right| &\leq \left\| \frac{\theta^i - \bar{\theta}^{i-1}}{\tau_i} \right\| \|d_t\theta^i\| \\ &\leq C_1 \|\theta^{i-1}\|_V^2 + \frac{1}{4} \|d_t\theta^i\|^2 \end{aligned} \quad (3.51)$$

$$|(\sigma\theta^i, d_t\theta^i)| \leq \|\sigma\theta^i\| \|d_t\theta^i\| \leq C \|\theta^i\|^2 + \frac{1}{2} \|d_t\theta^i\|^2 \quad (3.52)$$

in summary we group together the terms of the equations (3.49),(3.51) and (3.52) in (3.47) we have

$$\begin{aligned} &\|d_t\theta^i\|^2 + \frac{1}{2\tau_i} \left(\|\theta^i\|_a^2 - \|\theta^{i-1}\|_a^2 \right) + C \|\theta^i\|^2 + \frac{1}{2} \|d_t\theta^i\|^2 \\ &\leq C \|f^i - F_h^i\|_{0,\Omega}^2 + \frac{1}{4} \|d_t\theta^2\|^2 + C_1 \|\theta^{i-1}\|_V^2 + \frac{1}{4} \|d_t\theta^i\|^2 \end{aligned} \quad (3.53)$$

$$\|d_t\theta^i\|^2 + \frac{1}{2\tau_i} \left(\|\theta^i\|_a^2 - \|\theta^{i-1}\|_a^2 \right) + C \|\theta^i\|^2 \leq C \|f^i - F_h^i\|_{0,\Omega}^2 + C_1 \|\theta^{i-1}\|_V^2 \quad (3.54)$$

By multiplying the equation (3.54) by $2\tau_i$ and we do the summation on i from 1 to N ,

$$\sum_{i=1}^N \tau_i \|d_t\theta^i\|^2 + a_* \|\theta^N\|_V^2 + C \sum_{i=1}^N \tau_i \|\theta^i\|^2 \leq C_1 \sum_{i=1}^N \tau_i \|\theta^{i-1}\|_V^2 + C \sum_{i=1}^N \tau_i \|f^i - F_h^i\|_{0,\Omega}^2 \quad (3.55)$$

Same for the difference ζ between the approximate solution Ψ_h and the intermediate solution $\Psi_h(f)$ (3.37) - (3.40) we obtain

$$\left(\frac{\zeta^{i-1} - \zeta^i}{\tau_i}, q_h \right) + a(q_h, \zeta^{i-1}) + (\sigma\zeta^{i-1}, q_h) = (\theta^i, q_h) - \left(\frac{\zeta^i - \bar{\zeta}^i}{\tau_i}, q_h \right) - \left(\frac{\bar{\zeta}^i - \bar{\zeta}^i \cdot J}{\tau_i}, q_h \right) \quad (3.56)$$

And we pose $q_h = \bar{d}_t\zeta^{i-1} = \frac{\zeta^{i-1} - \zeta^i}{\tau_i}$ as a test function, the equation (3.56) is of the form

$$\begin{aligned} & (\bar{d}_t\zeta^{i-1}, \bar{d}_t\zeta^{i-1}) + a\left(\frac{\zeta^{i-1} - \zeta^i}{\tau_i}, \zeta^{i-1}\right) + (\sigma\zeta^{i-1}, \bar{d}_t\zeta^{i-1}) \\ &= (\theta^i, \bar{d}_t\zeta^{i-1}) - \left(\frac{\zeta^i - \bar{\zeta}^i}{\tau_i}, \bar{d}_t\zeta^{i-1} \right) - \left(\frac{\bar{\zeta}^i - \bar{\zeta}^i \cdot J}{\tau_i}, \bar{d}_t\zeta^{i-1} \right) \end{aligned} \quad (3.57)$$

Then using the inequality given by (3.45) and Hölder's inequality we get

$$\begin{aligned} & \|\bar{d}_t\zeta^{i-1}\|^2 + \frac{1}{2\tau} \left(\|\zeta^{i-1}\|_a^2 - \|\zeta^i\|_a^2 \right) + C_1 \|\zeta^{i-1}\|^2 + \frac{1}{2} \|\bar{d}_t\zeta^{i-1}\|^2 \\ & \leq (\theta^i, \bar{d}_t\zeta^{i-1}) - \left(\frac{\zeta^i - \bar{\zeta}^i}{\tau_i}, \bar{d}_t\zeta^{i-1} \right) - \left(\frac{\bar{\zeta}^i - \bar{\zeta}^i \cdot J}{\tau_i}, \bar{d}_t\zeta^{i-1} \right) \end{aligned} \quad (3.58)$$

$$\begin{aligned} (\theta^i, \bar{d}_t\zeta^{i-1}) & \leq |(\theta^i, \bar{d}_t\zeta^{i-1})| \\ & \leq C \|\theta^i\|^2 + \frac{1}{6} \|\bar{d}_t\zeta^{i-1}\|^2 \end{aligned} \quad (3.59)$$

$$\begin{aligned}
 \left(\frac{\zeta^i - \bar{\zeta}^i}{\tau_i}, \bar{d}_t \zeta^{i-1} \right) &\leq \left| \left(\frac{\zeta^i - \bar{\zeta}^i}{\tau_i}, \bar{d}_t \zeta^{i-1} \right) \right| \\
 &\leq \left\| \frac{\zeta^i - \bar{\zeta}^i}{\tau_i} \right\| \|\bar{d}_t \zeta^{i-1}\| \\
 &\leq C_1 \|\zeta^i\|_V^2 + \frac{1}{6} \|\bar{d}_t \zeta^{i-1}\|^2
 \end{aligned} \tag{3.60}$$

We have the determinant of the matrix of the Jacobian transformation $J = 1 + \mathcal{O}(\tau_i)$ we have

$$\left(\frac{\bar{\zeta}^i - \bar{\zeta}^i \cdot J}{\tau_i}, \bar{d}_t \zeta^{i-1} \right) \leq \left| \left(\frac{\bar{\zeta}^i - \bar{\zeta}^i \cdot J}{\tau_i}, \bar{d}_t \zeta^{i-1} \right) \right| \leq C \|\zeta^i\|^2 + \frac{1}{6} \|\bar{d}_t \zeta^{i-1}\|^2 \tag{3.61}$$

We replace the terms (3.59),(3.60) and (3.61) in the equation (3.58) we get

$$\begin{aligned}
 &\|\bar{d}_t \zeta^{i-1}\|^2 + \frac{1}{2\tau} \left(\|\zeta^{i-1}\|_a^2 - \|\zeta^{i-1}\|_a^2 \right) + C_1 \|\zeta^{i-1}\|^2 + \frac{1}{2} \|\bar{d}_t \zeta^{i-1}\|^2 \\
 &\leq C \|\theta^i\|^2 + \frac{1}{6} \|\bar{d}_t \zeta^{i-1}\|^2 + C_1 \|\zeta^i\|_V^2 + \frac{1}{6} \|\bar{d}_t \zeta^{i-1}\|^2 + C \|\zeta^i\|^2 + \frac{1}{6} \|\bar{d}_t \zeta^{i-1}\|^2
 \end{aligned} \tag{3.62}$$

By simplification we obtain

$$\begin{aligned}
 &\|\bar{d}_t \zeta^{i-1}\|^2 + \frac{1}{2\tau} \left(\|\zeta^{i-1}\|_a^2 - \|\zeta^{i-1}\|_a^2 \right) + C_1 \|\zeta^{i-1}\|^2 \\
 &\leq C \|\theta^i\|^2 + C_1 \|\bar{d}_t \zeta^i\|_V^2 + C \|\bar{d}_t \zeta^i\|^2
 \end{aligned} \tag{3.63}$$

In the same way by multiplying (3.63) by $2\tau_i$ and we do the summation on i from N^* to $M+1$, the coercivity leads to

$$\begin{aligned}
 &\sum_{i=M+1}^{N^*} \tau_i \|d_t \zeta^{i-1}\|^2 + a_* \|\zeta^M\|_V^2 + C_1 \sum_{i=M+1}^{N^*} \tau_i \|\zeta^{i-1}\|^2 \\
 &\leq C \sum_{i=M+1}^{N^*} \tau_i \|\zeta^i\|_V^2 + C_1 \sum_{i=M+1}^{N^*} \tau_i \|\zeta^i\|^2 + C \sum_{i=M+1}^{N^*} \tau_i \|\theta^i\|^2
 \end{aligned} \tag{3.64}$$

Since $\zeta^{N^*} = 0$, thus it follows from (3.64) and the discrete Gronwall's Lemma for sufficiently small τ_i that

$$\|\zeta\|_{L^\infty([0,T], H_0^1(\Omega))} \leq C_2 \|\Psi_h - \Psi_h(f)\|_{L^2([0,T], L^2(\Omega))} \tag{3.65}$$

Lemma 3.5.3. *Let (ϕ, ψ, f) and (Φ, Ψ, F) be the solutions of ((3.28), (3.29), (3.30)) and ((3.36), (3.37), (3.38)) respectively. Suppose that $f \in L^2([0, T], \mathbb{R}^m)$, $\psi \in L^2([0, T], H_0^1(\Omega_{adm})) \cap L^2([0, T], L^2(\Omega))$,*

$K^h \subset K$. Then there exist a positive constant C independant h_U and τ such that

$$\begin{aligned} \sqrt{\alpha} \|f - F_h\|_{L^2([0,T];\mathbb{R}^m)} &\leq Ch_U (\|\psi\|_{L^2([0,T],H^1(\Omega))} + \|f\|_{L^2([0,T],H^1(\Omega_{adm}))}) \\ &\quad + C\|\psi - \Psi_h(f)\|_{L^2([0,T],H^1(\Omega))} + Ck \left\| \frac{\partial \psi}{\partial t} \right\|_{L^2([0,T],L^2(\Omega))} \end{aligned} \quad (3.66)$$

Proof. We have the variational formulation of the optimality condition (3.30)

$$\begin{aligned} \alpha \|f - F_h\|_{L^2([0,T];\mathbb{R}^m)}^2 &= \sum_{i=1}^{N^*} \tau_i (\alpha f^i, f^i - F_h^i)_U - \sum_{i=1}^{N^*} \tau_i (\alpha F_h^i, f^i - F_h^i)_U \\ &\leq \sum_{i=1}^{N^*} \tau_i (\alpha u^i + \mathcal{B}^* \psi^i, f^i - F_h^i)_U - \sum_{i=1}^{N^*} \tau_i (\alpha U^i + \mathcal{B}^* P_h^{i-1}(f), f^i - F_h^i)_U \\ &\quad + \sum_{i=1}^{N^*} \tau_i (\mathcal{B}^* (\Psi^{i-1}(f) - \psi^i), f^i - F_h^i)_U \\ &\leq \sum_{i=1}^{N^*} \tau_i (\alpha F_h^i + \mathcal{B}^* P_h^{i-1}(f), F_h^i - f^i)_U + \sum_{i=1}^{N^*} \tau_i (\mathcal{B}^* (\Psi^{i-1}(f) - \psi^i), f^i - F_h^i)_U \end{aligned}$$

■

We have $\Pi_h f^i \in K^h$, so from the equation (3.38), where Π_h is an element integral averaging operator from U to U^h such that

$$|\Pi_h v|_{\beta_U} = \frac{1}{|\beta_U|} \int_{\beta_U} v \quad \forall \beta_U \in \mathcal{T}_U^h \quad (3.67)$$

$$\begin{aligned} \alpha \|f - F_h\|_{L^2([0,T];\mathbb{R}^m)}^2 &\leq \sum_{i=1}^{N^*} \tau_i (\alpha U_h^i + \mathcal{B}^* \Psi_h^{i-1}(f), F_h^i - \Pi_h f^i)_U \\ &\quad + \sum_{i=1}^{N^*} \tau_i (\alpha U_h^i + \mathcal{B}^* \Psi_h^{i-1}(f), \Pi_h f^i - f^i)_U \\ &\quad + \sum_{i=1}^{N^*} \tau_i (\mathcal{B}^* (\Psi^{i-1}(f) - \Psi_h^{i-1}(f)), f^i - F_h^i)_U \\ &\quad + \sum_{i=1}^{N^*} \tau_i (\mathcal{B}^* (\Psi^{i-1}(f) - \psi^i), f^i - F_h^i)_U \end{aligned}$$

$$\begin{aligned}
 \alpha \|f - F_h\|_{L^2([0,T];\mathbb{R}^m)}^2 &\leq \sum_{i=1}^{N^*} \tau_i (\alpha F_h^i, \Pi_h f^i - u^i)_U + \sum_{i=1}^{N^*} \tau_i (\mathcal{B}^* \psi^{i-1}, \Pi_h f^i - f^i)_U \\
 &+ \sum_{i=1}^{N^*} \tau_i (\mathcal{B}^* (\psi^{i-1} - \Psi_h^{i-1}(f)), u^i - \Pi_h u^i)_U \\
 &+ \sum_{i=1}^{N^*} \tau_i (\mathcal{B}^* (\Psi_h^{i-1}(f) - \Psi_h^{i-1}), f^i - \Pi_h f^i)_U \\
 &+ \sum_{i=1}^{N^*} \tau_i (\mathcal{B}^* (\Psi_h^{i-1} - \Psi_h^{i-1}(f)), f^i - F_h^i)_U \\
 &+ \sum_{i=1}^{N^*} \tau_i (\mathcal{B}^* (\Psi_h^{i-1}(f) - \psi^i), f^i - F_h^i)_U
 \end{aligned} \tag{3.68}$$

Lemma 3.5.4. *Let integral averaging operator of (3.67) Π_h , then there a positive constante C independent of h_U such that*

$$|v - \Pi_h v|_{0,p,\beta_U} \leq Ch_U |v|_{1,p,\beta_U} \tag{3.69}$$

pour $v \in W^{1,p}(\Omega_{adm})$ et $1 \leq p \leq \infty$

Applying the definition of the integral averaging operator defined in (3.67)

$$\sum_{i=1}^{N^*} \tau_i (\alpha F_h^i, \Pi_h f^i - u^i)_U = 0 \tag{3.70}$$

Then for the second and the third term, by application of Lemme (3.5.4) and the inequality (3.45), we have

$$\begin{aligned}
 \sum_{i=1}^{N^*} \tau_i (\mathcal{B}^* \psi^{i-1}, \Pi_h f^i - f^i)_U &= \sum_{i=1}^{N^*} \tau_i (\mathcal{B}^* \psi^{i-1} - \Pi_h(\mathcal{B}^* \psi^{i-1}), \Pi_h f^i - f^i)_U \\
 &\leq C \sum_{i=1}^{N^*} \tau_i \|\psi^{i-1} - \Pi_h \psi^{i-1}\|_{0,\Omega}^2 + C \sum_{i=1}^{N^*} \tau_i \|f^i - \Pi_h f^i\|_{0,\Omega_{adm}}^2 \\
 &\leq Ch_U^2 \left(\|\psi\|_{L^2([0,T],H^1(\Omega))}^2 + \|f\|_{L^2([0,T],L^2(\Omega))}^2 \right)
 \end{aligned} \tag{3.71}$$

and

$$\begin{aligned}
 \sum_{i=1}^{N^*} \tau_i (\mathcal{B}^* (\psi^{i-1} - \Psi_h^{i-1}(f)), f^i - \Pi_h f^i)_U &\leq C \sum_{i=1}^{N^*} \tau_i \|\psi^{i-1} - \Psi_h^{i-1}(f)\|_{0,\Omega}^2 + C \sum_{i=1}^{N^*} \tau_i \|f^i - \Pi_h f^i\|_{0,\Omega_{adm}}^2 \\
 &\leq C \|\psi - \Psi_h(f)\|_{L^2([0,T],H^1(\Omega))}^2 + Ch_U^2 \|f\|_{L^2([0,T],L^2(\Omega))}^2
 \end{aligned} \tag{3.72}$$

For the fourth terme, from the Lemme(3.5.1), Lemme (3.5.4) and the inequality (3.45), we have

$$\begin{aligned}
\sum_{i=1}^{N^*} \tau_i (\mathcal{B}^* (\Psi_h^{i-1}(f) - \Psi_h^{i-1}), f^i - \Pi_h f^i)_U &\leq C \sum_{i=1}^{N^*} \tau_i \|f - \Pi_h f\|_{0, \Omega_{adm}}^2 + \hat{\varepsilon} \sum_{i=1}^{N^*} \tau_i \|\Psi_h^{i-1}(f) - \Psi_h^{i-1}\|_{0, \Omega_{adm}}^2 \\
&\leq C \|f - \Pi_h f\|_{L^2([0, T], L^2(\Omega_{adm}))}^2 + \hat{\varepsilon} \|\Psi(f) - \Psi\|_{L^2([0, T], L^2(\Omega))}^2 \\
&\leq Ch_U^2 \|f\|_{L^2([0, T], L^2(\Omega))}^2 + \varepsilon \|f - F_h\|_{L^2([0, T], L^2(\Omega_{adm}))}^2
\end{aligned} \tag{3.73}$$

where $\hat{\varepsilon}$ is an arbitrary small number and $\varepsilon = C_2^2 \hat{\varepsilon}$ according to Lemma (3.5.1).

Note that $\theta^0 = \xi^{N^*} = 0$, then it follows from (3.36)-(3.37) and (3.39)-(3.40) that

$$\begin{aligned}
&\sum_{i=1}^{N^*} \tau_i (\mathcal{B}^* (\Psi_h^{i-1} - \Psi_h^{i-1}(f)), f^i - F_h^i)_U = \sum_{i=1}^{N^*} \tau_i (\Psi_h^{i-1} - \Psi_h^{i-1}(f), \mathcal{B}^*(f^i - F_h^i))_U \\
&= \sum_{i=1}^{N^*} \tau_i \left(\Psi_h^{i-1} - \Psi_h^{i-1}(f), \frac{\Psi_h^i(f) - \bar{\Psi}_h^{i-1}(f)}{\tau_i} - \frac{\Psi_h^i - \bar{\Psi}_h^{i-1}}{\tau_i} + a(\Psi_h^i(f), w_\tau) - a(\Psi_h^i, w_\tau) \right) \\
&= \sum_{i=1}^{N^*} \tau_i \left(\xi^{i-1}, -\frac{\Psi_h^i - \Psi_h^i(f)}{\tau_i} - \frac{\bar{\Psi}_h^{i-1} - \bar{\Psi}_h^{i-1}(f)}{\tau_i} \right) - \sum_{i=1}^{N^*} \tau_i a(\theta^i, \xi^{i-1}) \\
&= -\sum_{i=1}^{N^*} \tau_i \left(\frac{\theta^i - \bar{\theta}^{i-1}}{\tau_i}, \xi^{i-1} \right) - \sum_{i=1}^{N^*} \tau_i a(\theta^i, \xi^{i-1}) \\
&= -\sum_{i=1}^{N^*} \tau_i \left(\frac{\xi^{i-1} - \bar{\xi}^i \cdot J^i}{\tau_i}, \theta^i \right) - \sum_{i=1}^{N^*} \tau_i a(\theta^i, \xi^{i-1}) = -\sum_{i=1}^{N^*} \tau_i (\theta^i, \theta^i) = -\|\theta\|_{L^2([0, T], L^2(\Omega))}^2 \leq 0
\end{aligned} \tag{3.74}$$

finally for the last term, for the reason of the continuous proprety of the operator \mathcal{B} and the inequality (3.45) we have

$$\begin{aligned}
\sum_{i=1}^{N^*} \tau_i (\mathcal{B}^* (\Psi_h^{i-1}(f) - \psi^i), f^i - F_h^i)_U &= \sum_{i=1}^{N^*} \tau_i ((\Psi_h^{i-1} - \psi^{i-1}), \mathcal{B}(f^i - F_h^i))_U \\
&\quad + \sum_{i=1}^{N^*} \tau_i ((\psi^{i-1} - \psi^i), \mathcal{B}(f^i - F_h^i))_U
\end{aligned} \tag{3.75}$$

$$\begin{aligned}
 \sum_{i=1}^{N^*} \tau_i (\mathcal{B}^* (\Psi_h^{i-1}(f) - \psi^i), f^i - F_h^i)_U &\leq C \sum_{i=1}^{N^*} \tau_i \|\psi_h^{i-1} - \Psi^{i-1}\|_{0,\Omega}^2 + C \sum_{i=1}^{N^*} \tau_i \|\psi^{i-1} - \psi^i\|_{0,\Omega}^2 \\
 &\quad + \varepsilon \sum_{i=1}^{N^*} \tau_i \|f^i - F_h^i\|_{0,\Omega_{adm}}^2 \\
 &\leq C \|\psi - \Psi(f)\|_{L^2([0,T],L^2(\Omega_{adm}))}^2 + Ck^2 \left\| \frac{\partial \psi}{\partial t} \right\|_{L^2([0,T],L^2(\Omega))}^2 \\
 &\quad + \varepsilon \|f - F_h\|_{L^2([0,T],L^2(\Omega_{adm}))}^2 \tag{3.76}
 \end{aligned}$$

In summary, we replace the different terms previously calculated in (3.68) we obtain

$$\begin{aligned}
 \alpha \|f - F_h\|_{L^2([0,T];\mathbb{R}^m)}^2 &\leq Ch_U^2 \left(\|\psi\|_{L^2([0,T],H^1(\Omega))}^2 + \|f\|_{L^2([0,T],L^2(\Omega_{adm}))}^2 \right) \\
 &\quad + C \|\psi - \Psi_h(f)\|_{L^2([0,T],H^1(\Omega))}^2 + Ch_U^2 \|f\|_{L^2([0,T],L^2(\Omega_{adm}))}^2 \\
 &\quad + Ch_U^2 \|f\|_{L^2([0,T],L^2(\Omega_{adm}))}^2 + \varepsilon \|f - F_h\|_{L^2([0,T],L^2(\Omega_U))}^2 \\
 &\quad + C \|\psi - \Psi_h(f)\|_{L^2([0,T],L^2(\Omega_{adm}))}^2 + Ck^2 \left\| \frac{\partial \psi}{\partial t} \right\|_{L^2([0,T],L^2(\Omega))}^2 \\
 &\quad + \varepsilon \|f - F_h\|_{L^2([0,T],L^2(\Omega_{adm}))}^2 \\
 \alpha \|f - F_h\|_{L^2([0,T];\mathbb{R}^m)}^2 &\leq Ch_U^2 \left(\|p\|_{L^2([0,T],H^1(\Omega))}^2 + \|f\|_{L^2([0,T],L^2(\Omega_{adm}))}^2 \right) \\
 &\quad + C \|\psi - \Psi_h(f)\|_{L^2([0,T],H^1(\Omega))}^2 + Ck^2 \left\| \frac{\partial \psi}{\partial t} \right\|_{L^2([0,T],L^2(\Omega))}^2 \\
 &\quad + \varepsilon \|f - F_h\|_{L^2([0,T],L^2(\Omega))}^2 + C \|\psi - \Psi_h\|_{L^2([0,T],H^1(\Omega))}^2 \tag{3.77}
 \end{aligned}$$

We pose $\varepsilon = \frac{\alpha}{2}$ and the inequality (3.77) writes

$$\begin{aligned}
 \alpha \|f - F_h\|_{L^2([0,T];\mathbb{R}^m)}^2 &\leq Ch_U^2 \left(\|\psi\|_{L^2([0,T],H^1(\Omega))}^2 + \|f\|_{L^2([0,T],L^2(\Omega_{adm}))}^2 \right) \\
 &\quad + C \|\psi - \Psi_h(f)\|_{L^2([0,T],H^1(\Omega))}^2 + Ck^2 \left\| \frac{\partial \psi}{\partial t} \right\|_{L^2([0,T],L^2(\Omega))}^2 \\
 &\quad + \frac{\alpha}{2} \|f - F_h\|_{L^2([0,T],L^2(\Omega))}^2 + C \|\psi - \Psi_h(f)\|_{L^2([0,T],H^1(\Omega))}^2
 \end{aligned}$$

$$\begin{aligned}
 \alpha \|f - F_h\|_{L^2([0,T];\mathbb{R}^m)}^2 &\leq Ch_U^2 \left(\|\psi\|_{L^2([0,T],H^1(\Omega))}^2 + \|f\|_{L^2([0,T],L^2(\Omega_{adm}))}^2 \right) \\
 &\quad + C \|\psi - \Psi_h(f)\|_{L^2([0,T],H^1(\Omega))}^2 + Ck^2 \left\| \frac{\partial \psi}{\partial t} \right\|_{L^2([0,T],L^2(\Omega))}^2 \\
 &\quad + \frac{\alpha}{2} \|f - F_h\|_{L^2([0,T],L^2(\Omega))}^2
 \end{aligned}$$

$$\begin{aligned} \frac{\alpha}{2} \|f - F_h\|_{L^2([0,T];\mathbb{R}^m)}^2 &\leq Ch_U^2 \left(\|\psi\|_{L^2([0,T],H^1(\Omega))}^2 + \|f\|_{L^2([0,T],L^2(\Omega_{adm}))}^2 \right) \\ &\quad + C\|\psi - \Psi_h(f)\|_{L^2([0,T],H^1(\Omega))}^2 + Ck^2 \left\| \frac{\partial\psi}{\partial t} \right\|_{L^2([0,T],L^2(\Omega))}^2 \end{aligned}$$

$$\begin{aligned} \sqrt{\alpha} \|f - F_h\|_{L^2([0,T];\mathbb{R}^m)} &\leq Ch_U \left(\|\psi\|_{L^2([0,T],H^1(\Omega))} + \|f\|_{L^2([0,T],L^2(\Omega_{adm}))} \right) \\ &\quad + C\|\psi - \Psi_h(f)\|_{L^2([0,T],H^1(\Omega))} + Ck \left\| \frac{\partial\psi}{\partial t} \right\|_{L^2([0,T],L^2(\Omega))} \end{aligned} \quad (3.78)$$

Lemma 3.5.5. *Let (ϕ, ψ) et $(\Phi_h(f), \Psi_h(f))$, be the solution of ((3.28) – (3.29)) and ((3.39) – (3.40)) respectively. Suppose that $\phi, \psi \in H^1([0, T], H^2(\Omega)) \cap H^2([0, T], L^2(\Omega))$, $\phi_d \in H^1([0, T], H^1(\Omega))$ and $\|\phi_0 - \phi_0^h\| \leq C\tau$. We have*

$$\|\phi - \Phi_h(f)\|_{L^\infty([0,T],H_0^1(\Omega))} \leq C_2 \left(h \|\phi\|_{H^1([0,T],H^2(\Omega))} + \tau \left\| \frac{\partial^2\phi}{\partial t^2} \right\|_{L^2([0,T],L^2(\Omega))} \right) \quad (3.79)$$

and

$$\begin{aligned} \|\psi - \Psi_h(f)\|_{L^\infty([0,T],H_0^1(\Omega))} &\leq C_2\tau \sum_{v=\phi,\psi} \left\| \frac{\partial^2 v}{\partial t^2} \right\|_{L^2([0,T],L^2(\Omega))} + C_2\tau \sum_{v=\phi,\phi_d} \left\| \frac{\partial^2 v}{\partial t^2} \right\|_{L^2([0,T],L^2(\Omega))} \\ &\quad + C_2\tau \|\psi\|_{L^2([0,T],L^2(\Omega))} + C_2\tau \sum_{v=\phi,\psi} \|\psi\|_{H^1([0,T],H^2(\Omega))} \end{aligned} \quad (3.80)$$

Proof. In the first step, we give an estimate for the difference η between the exact solution and the intermediate solution ψ and $\Psi_h(f)$ respectively. The exact solution ψ satisfies

$$\left(\frac{\phi^i - \bar{\phi}^{i-1}}{\tau_i}, w_h \right) + a(\phi^i, w_h) + (\sigma\phi^i, w_h) = (g^i + \mathcal{B}f^i, w_h) - (\Lambda^i, w_h) \quad \forall w_h \in V^h, i \geq 1 \quad (3.81)$$

where

$$\Lambda^i = \frac{\partial\phi^i}{\partial t} + \mathcal{U} \cdot \nabla\phi^i - \frac{\phi^i - \bar{\phi}^{i-1}}{\tau_i}$$

By differentiating between ((3.39) – (3.81)) we have

$$(\partial_t\eta^i, w_h) + a(\eta^i, w_h) + (\sigma\eta^i, w_h) = -(\Lambda^i, w_h) - \left(\frac{\eta^{i-1} - \bar{\eta}^{i-1}}{\tau_i}, w_h \right) \quad \forall w_h \in V^h, i \geq 1 \quad (3.82)$$

Lemma 3.5.6. *Let \mathcal{Q}_h and \mathcal{R}_h denotes the L^2 -projection operator, $\mathcal{Q}_h\phi \in V^h$, $\mathcal{R}_h\psi \in V^h$ and $\phi \in V$, $\psi \in V$ for each $t \in (0, T]$, there exists a positive constant C independent of h and τ such*

that for $1 \leq s \leq 2$ (for more detail see [20]). Then the following estimates hold

$$\begin{aligned} & \|\phi - \mathcal{Q}_h\phi\|_{L^2([0,T];L^2(\Omega))} + h \|\phi - \mathcal{Q}_h\phi\|_{L^2([0,T];H^1(\Omega))} \leq Ch^s \|\phi\|_{L^2([0,T];H^s(\Omega))}, \\ & \left\| \frac{\partial(\phi - \mathcal{Q}_h\phi)}{\partial t} \right\|_{L^2([0,T];L^2(\Omega))} + h \left\| \frac{\partial(\phi - \mathcal{Q}_h\phi)}{\partial t} \right\|_{L^2([0,T];H^1(\Omega))} \leq Ch^s \|\phi\|_{L^2([0,T];H^s(\Omega))} \end{aligned} \quad (3.83)$$

and

$$\begin{aligned} & \|\psi - \mathcal{R}_h\psi\|_{L^2([0,T];L^2(\Omega))} + h \|\psi - \mathcal{R}_h\psi\|_{L^2([0,T];H^1(\Omega))} \leq Ch^s \|\psi\|_{L^2([0,T];H^s(\Omega))}, \\ & \left\| \frac{\partial(\psi - \mathcal{R}_h\psi)}{\partial t} \right\|_{L^2([0,T];L^2(\Omega))} + h \left\| \frac{\partial(\psi - \mathcal{R}_h\psi)}{\partial t} \right\|_{L^2([0,T];H^1(\Omega))} \leq Ch^s \|\psi\|_{L^2([0,T];H^s(\Omega))} \end{aligned} \quad (3.84)$$

We pose $w_k = d_t\eta^i = \frac{\phi^i - \Phi_h^i(f)}{\tau_i}$ as a test function. Then from the equation (3.81) and the elliptic proction in Lemma (3.5.6)

$$\begin{aligned} \|d_t\eta^i\| + a(\eta^i, d_t\eta^i) + (\sigma\eta^i, d_t\eta^i) &= (d_t\eta^i, d_t(\phi^i - \Phi_h^i(f))) + a(\eta^i, d_t(\phi^i - \Phi_h^i(f))) \\ &= (d_t\eta^i, d_t(\phi^i - \mathcal{Q}_h\phi^i)) + (d_t\eta^i, d_t(\mathcal{Q}_h\phi^i - \Phi_h^i(f))) \\ &\quad + a(\eta^i, d_t(\phi^i - \mathcal{Q}_h\phi^i)) + a(\eta^i, d_t(\mathcal{Q}_h\phi^i - \Phi_h^i(f))) \\ &= (d_t\eta^i, d_t(\phi^i - \mathcal{Q}_h\phi^i)) + a(\eta^i, d_t(\phi^i - \mathcal{Q}_h\phi^i)) \\ &\quad - (\Lambda^i, d_t(\mathcal{Q}_h\phi^i - \Phi_h^i(f))) - \left(\frac{\eta^{i-1} - \bar{\eta}^{i-1}}{\tau_i}, d_t(\mathcal{Q}_h\phi^i - \Phi_h^i(f)) \right) \end{aligned} \quad (3.85)$$

We multiply the equation (3.85) by τ_i and sum it over $1 \leq i \leq N$ and using the inequality defined in (3.48)

$$\begin{aligned} & \sum_{i=1}^{N^*} \tau_i \|d_t\eta^i\|^2 + \frac{1}{2} \|\eta^N\|_a^2 + C \sum_{i=1}^{N^*} \tau_i \|\eta^i\|^2 + \frac{1}{2} \|d_t\eta^i\|^2 \leq \frac{1}{2} \|\eta^0\|_a^2 + \sum_{i=1}^{N^*} \tau_i \|d_t\eta^i\| \|(\phi^i - \mathcal{Q}_h\phi^i)\| \\ & + C \sum_{i=1}^{N^*} \tau_i \|\eta^i\|_V \|d_t(\phi^i - \mathcal{Q}_h\phi^i)\|_V + \sum_{i=1}^{N^*} \tau_i \|\Lambda^i\| (\|d_t(\phi^i - \mathcal{Q}_h\phi^i)\| + \|d_t(\phi^i - \Phi_h(f))\|) \\ & + \sum_{i=1}^{N^*} \tau_i \left\| \frac{\eta^{i-1} - \bar{\eta}^{i-1}}{\tau_i} \right\| (\|d_t(\phi^i - \mathcal{Q}_h\phi^i)\| + \|d_t(\phi^i - \Phi_h(f))\|) \end{aligned}$$

$$\sum_{i=1}^{N^*} \tau_i \|d_t\eta^i\|^2 + \frac{1}{2} \|\eta^N\|_a^2 + C \sum_{i=1}^{N^*} \tau_i \|\eta^i\|^2 + \frac{1}{2} \|d_t\eta^i\|^2 \leq \frac{1}{2} \|\eta^0\|_a^2 + \sum_{i=1}^4 T_i \quad (3.86)$$

We calculate the different terms of the right hand side, then

$$T_1 \leq \frac{1}{6} \sum_{i=1}^{N^*} \tau_i \|d_t \eta^i\|^2 + Ch^4 \|\phi\|_{H^1([0,T];H^2(\Omega))}^2 \quad (3.87)$$

$$T_2 \leq \frac{1}{2} \sum_{i=1}^{N^*} \tau_i \|\eta^i\|_V^2 + Ch^2 \|\phi\|_{H^1([0,T];H^2(\Omega))}^2 \quad (3.88)$$

$$T_3 \leq C\tau^2 \left\| \frac{\partial^2 \phi}{\partial t^2} \right\|_{L^2([0,T];L^2(\Omega))}^2 + Ch^4 \|\phi\|_{H^1([0,T];H^2(\Omega))}^2 + \frac{1}{6} \sum_{i=1}^{N^*} \tau_i \|d_t \eta^i\|^2 \quad (3.89)$$

$$T_4 \leq C_1 \sum_{i=1}^{N^*} \tau_i \|\eta^{i-1}\|_V^2 + Ch^4 \|\phi\|_{H^1([0,T];H^2(\Omega))}^2 + \frac{1}{6} \sum_{i=1}^{N^*} \tau_i \|d_t \eta^i\|^2 \quad (3.90)$$

In summary, we replace the different terms in the equation (3.86) then

$$\begin{aligned} \sum_{i=1}^{N^*} \tau_i \|d_t \eta^i\|^2 + \frac{1}{2} \|\eta^N\|_a^2 + C \sum_{i=1}^{N^*} \tau_i \|\eta^i\|^2 &\leq \frac{1}{2} \|\eta^0\|_a^2 + C\tau^2 \left\| \frac{\partial^2 \phi}{\partial t^2} \right\|_{L^2([0,T];L^2(\Omega))}^2 \\ &+ Ch^2 \|\phi\|_{H^1([0,T];H^2(\Omega))}^2 \\ &+ C_1 \sum_{i=1}^{N^*} \tau_i \left(\|\eta^i\|_V^2 + \|\eta^{i-1}\|_V^2 \right) \end{aligned} \quad (3.91)$$

Next, we give the estimate for the difference θ between the exact solution ψ and the intermediate solution $\Psi_h(f)$. The exact solution ψ satisfies

$$\begin{aligned} &\left(\frac{\psi^i - \bar{\psi}^{i-1} \cdot J^i}{\tau_i}, q_h \right) + a(q_h, \psi^{i-1}) + (\sigma \psi^{i-1}, q_h) \\ &= (\phi^{i-1} - \phi_d^{i-1}, q_h) - (\chi^{i-1}, q_h) + \left(\frac{\bar{\psi}^i - \bar{\psi}^i \cdot J^i}{\tau_i}, q_h \right) \quad \forall q_h \in V^h, i \leq N^* \end{aligned} \quad (3.92)$$

where

$$\chi^{i-1} = \frac{\partial \psi^{i-1}}{\partial t} + \mathcal{U} \cdot \nabla \psi^{i-1} - \frac{\bar{\psi}^i - \psi^{i-1}}{\tau_i}$$

By differentiating between ((3.40) – (3.92)) we have

$$\begin{aligned}
 (\bar{d}_t \xi^{i-1}, q_h) + a(q_h, \xi^{i-1}) + (\sigma \xi^{i-1}, q_h) &= -(\chi^{i-1}, q_h) - \left(\frac{\xi^i - \bar{\xi}^{i-1}}{\tau_i}, q_h \right) - \left(\frac{\bar{\xi}^i - \bar{\xi}^i \cdot J^i}{\tau_i}, q_h \right) \\
 &+ \left(\frac{\bar{\psi}^i - \bar{\psi}^i \cdot J^i}{\tau_i}, q_h \right) + (\phi^i - \Phi_h^i(f), q_h) + (\phi^{i-1} - \Phi^i, q_h) \\
 &+ (\phi_d^i - \phi_d^{i-1}, q_h), \quad \forall q_h \in V^h, i \leq N^* \tag{3.93}
 \end{aligned}$$

Similarly, $t \in (0, T]$, let $\mathcal{R}_h \psi \in V^h$ the elliptic projection of $\psi \in V$. We pose $q_h = \frac{\bar{d}_t \eta^i = \bar{d}_t (\mathcal{R}_h \psi^{i-1} - \Psi_h^{i-1}(f))}{\tau_i}$ as a test function.

$$\begin{aligned}
 \|\bar{d}_t \xi^{i-1}\|^2 + a(\bar{d}_t \xi^{i-1}, \xi^{i-1}) + (\sigma \xi^{i-1}, \bar{d}_t \xi^{i-1}) &= (\bar{d}_t \xi^{i-1}, \bar{d}_t (\mathcal{R}_h \psi^{i-1} - \Psi_h^{i-1})) \\
 &+ a(\bar{d}_t (\psi^{i-1} - \mathcal{R}_h \psi^{i-1}), \xi^{i-1}) \\
 &- (\chi^{i-1}, \bar{d}_t (\mathcal{R}_h \psi^{i-1} - \Psi_h^{i-1}(f))) \\
 &- (\chi^{i-1}, \bar{d}_t (\mathcal{R}_h \psi^{i-1} - \Psi_h^{i-1}(f))) \\
 &- \left(\frac{\xi^i - \bar{\xi}^{i-1}}{\tau_i}, \bar{d}_t (\mathcal{R}_h \psi^{i-1} - \Psi_h^{i-1}(f)) \right) \\
 &+ \left(\frac{\bar{\xi}^i - \bar{\xi}^i \cdot J^i}{\tau_i}, \bar{d}_t (\mathcal{R}_h \psi^{i-1} - \Psi_h^{i-1}(f)) \right) \\
 &+ (\phi^i - \Phi_h^i(f), \bar{d}_t (\mathcal{R}_h \psi^{i-1} - \Psi_h^{i-1}(f))) \\
 &+ (\phi^{i-1} - \Phi^i, \bar{d}_t (\mathcal{R}_h \psi^{i-1} - \Psi_h^{i-1}(f))) \\
 &+ (\phi_d^i - \phi_d^{i-1}, \bar{d}_t (\mathcal{R}_h \psi^{i-1} - \Psi_h^{i-1}(f))) \tag{3.94}
 \end{aligned}$$

Similarly, we multiply both sides of (3.94) by τ_i and sum over i from N^* to $M+1$ and using the inequality defined in (3.48) then

$$\sum_{i=M+1}^{N^*} \tau_i \|\bar{d}_t \xi^{i-1}\|^2 + \frac{1}{2} \|\xi^M\|_a^2 + C \sum_{i=M+1}^{N^*} \tau_i \|\xi^{i-1}\|^2 + \frac{1}{2} \|\bar{d}_t \xi^{i-1}\|^2 \leq \sum_{i=5}^{13} T_i \tag{3.95}$$

$$\begin{aligned}
 T_5 &\leq \sum_{i=M+1}^{N^*} \tau_i \|\bar{d}_t \xi^{i-1}\| \|\bar{d}_t (\psi^{i-1} - \mathcal{R}_h \psi^{i-1})\| \\
 &\leq \frac{1}{16} \sum_{i=M+1}^{N^*} \tau_i \|\bar{d}_t \xi^{i-1}\|^2 + Ch^4 \|\psi\|_{H^1([0, T]; H^2(\Omega))}^2 \tag{3.96}
 \end{aligned}$$

$$\begin{aligned}
T_6 &\leq \sum_{i=M+1}^{N^*} \tau_i \|\xi^{i-1}\|_V^2 + \left\| \frac{\partial(\psi - \mathcal{R}_h\psi)}{\partial t} \right\| \\
&\leq C \sum_{i=M+1}^{N^*} \tau_i \|\xi^{i-1}\|_V^2 + Ch^2 \|\psi\|_{H^1([0,T];H^2(\Omega))}^2
\end{aligned} \tag{3.97}$$

$$\begin{aligned}
T_7 &\leq \sum_{i=M+1}^{N^*} \tau_i \|\chi^{i-1}\| \left(\|\bar{d}_t(\psi^{i-1} - \mathcal{R}_h\psi^{i-1})\| + \|\bar{d}_t(\psi^{i-1} - \mathcal{R}_h\Psi_h^{i-1}(f))\| \right) \\
&\leq C\tau^2 \left\| \frac{\partial^2\psi}{\partial t^2} \right\|_{L^2([0,T];L^2(\Omega))}^2 + Ch^4 \|\psi\|_{H^1([0,T];H^2(\Omega))}^2 + \frac{1}{16} \sum_{i=M+1}^{N^*} \tau_i \|\bar{d}_t\xi^{i-1}\|^2
\end{aligned} \tag{3.98}$$

$$\begin{aligned}
T_8 &\leq \sum_{i=M+1}^{N^*} \tau_i \left\| \frac{\xi^i - \bar{\xi}^i}{\tau} \right\| \left(\|\bar{d}_t(\psi^{i-1} - \mathcal{R}_h\psi^{i-1})\| + \|\bar{d}_t(\psi^{i-1} - \mathcal{R}_h\Psi_h^{i-1}(f))\| \right) \\
&\leq C_1 \sum_{i=M+1}^{N^*} \tau_i \|\xi^{i-1}\|_V^2 + Ch^4 \|\psi\|_{H^1([0,T];H^2(\Omega))}^2 + \frac{1}{16} \sum_{i=M+1}^{N^*} \tau_i \|\bar{d}_t\xi^{i-1}\|^2
\end{aligned} \tag{3.99}$$

$$\begin{aligned}
T_9 &\leq \sum_{i=M+1}^{N^*} \tau_i \left\| \frac{\bar{\xi}^i - \bar{\xi}^i \cdot J}{\tau} \right\| \left(\|\bar{d}_t(\psi^{i-1} - \mathcal{R}_h\psi^{i-1})\| + \|\bar{d}_t(\psi^{i-1} - \mathcal{R}_h\Psi_h^{i-1}(f))\| \right) \\
&\leq C \sum_{i=M+1}^{N^*} \tau_i \|\xi^{i-1}\|^2 + Ch^4 \|\psi\|_{H^1([0,T];H^2(\Omega))}^2 + \frac{1}{16} \sum_{i=M+1}^{N^*} \tau_i \|\bar{d}_t\xi^{i-1}\|^2
\end{aligned} \tag{3.100}$$

$$\begin{aligned}
T_{10} &\leq \sum_{i=M+1}^{N^*} \tau_i \left\| \frac{\bar{\psi}^i - \bar{\psi}^i \cdot J}{\tau} \right\| \left(\|\bar{d}_t(\psi^{i-1} - \mathcal{R}_h\psi^{i-1})\| + \|\bar{d}_t(\psi^{i-1} - \mathcal{R}_h\Psi_h^{i-1}(f))\| \right) \\
&\leq C \sum_{i=M+1}^{N^*} \tau_i^2 \|\psi\|_{L^2([0,T];L^2(\Omega))}^2 + Ch^4 \|\psi\|_{H^1([0,T];H^2(\Omega))}^2 + \frac{1}{16} \sum_{i=M+1}^{N^*} \tau_i \|\bar{d}_t\xi^{i-1}\|^2
\end{aligned} \tag{3.101}$$

$$\begin{aligned}
T_{11} &\leq C \sum_{i=M+1}^{N^*} \tau_i \|\phi^i - \Phi_h^i(f)\| \left(\|\bar{d}_t(\psi^{i-1} - \mathcal{R}_h\psi^{i-1})\| + \|\bar{d}_t(\psi^{i-1} - \mathcal{R}_h\Psi_h^{i-1}(f))\| \right) \\
&\leq C\tau^2 \left\| \frac{\partial^2\phi}{\partial t^2} \right\|_{L^2([0,T];L^2(\Omega))}^2 + Ch^2 \|\phi\|_{H^1([0,T];H^2(\Omega))}^2 + Ch^4 \|\psi\|_{H^1([0,T];H^2(\Omega))}^2 \\
&\quad + \frac{1}{16} \sum_{i=M+1}^{N^*} \tau_i \|\bar{d}_t\xi^{i-1}\|^2
\end{aligned} \tag{3.102}$$

$$\begin{aligned}
 T_{12} &\leq \sum_{i=M+1}^{N^*} \tau_i \|\phi^i - \phi^{i-1}\| \left(\|\bar{d}_t(\psi^{i-1} - \mathcal{R}_h \psi^{i-1})\| + \|\bar{d}_t(\psi^{i-1} - \mathcal{R}_h \Psi_h^{i-1}(f))\| \right) \\
 &\leq C\tau^2 \left\| \frac{\partial \phi}{\partial t} \right\|_{L^2([0,T];L^2(\Omega))}^2 + Ch^4 \|\psi\|_{H^1([0,T];H^2(\Omega))}^2 + \frac{1}{16} \sum_{i=M+1}^{N^*} \tau_i \|\bar{d}_t \xi^{i-1}\|^2 \quad (3.103)
 \end{aligned}$$

$$\begin{aligned}
 T_{13} &\leq \sum_{i=M+1}^{N^*} \tau_i \|\phi_d^{i-1} - \phi_d^i\| \left(\|\bar{d}_t(\psi^{i-1} - \mathcal{R}_h \psi^{i-1})\| + \|\bar{d}_t(\psi^{i-1} - \mathcal{R}_h \Psi_h^{i-1}(f))\| \right) \\
 &\leq C\tau^2 \left\| \frac{\partial \phi_d}{\partial t} \right\|_{L^2([0,T];L^2(\Omega))}^2 + Ch^4 \|\psi\|_{H^1([0,T];H^2(\Omega))}^2 + \frac{1}{16} \sum_{i=M+1}^{N^*} \tau_i \|\bar{d}_t \xi^{i-1}\|^2
 \end{aligned}$$

Summarizing and replaced the different terms in equation (3.95) then

$$\begin{aligned}
 &\sum_{i=M+1}^{N^*} \tau_i \|\bar{d}_t \xi^{i-1}\|^2 + \frac{1}{2} \|\xi^M\|_a^2 + C \sum_{i=M+1}^{N^*} \tau_i \|\xi^{i-1}\|^2 \\
 &\leq C_2 \tau_i^2 \left(\sum_{v=\phi,\psi} \left\| \frac{\partial^2 v}{\partial t^2} \right\|_{L^2([0,T];L^2(\Omega))}^2 + \sum_{v=\phi,\phi_d} \left\| \frac{\partial v}{\partial t} \right\|_{L^2([0,T];L^2(\Omega))}^2 + \|\psi\|_{H^1([0,T];H^2(\Omega))}^2 \right) \\
 &\quad + C_2 h^2 \sum_{i=\psi,\phi} \|v\|_{H^1([0,T];H^2(\Omega))}^2 + C_1 \sum_{i=M+1}^{N^*} \tau_i \left(\|\xi^{i-1}\|_V^2 + \|\xi^i\|_V^2 \right) \quad (3.104)
 \end{aligned}$$

■

Theorem 3.5.7. *Let that (ϕ, ψ, f) and (Φ_h, Ψ_h, F_h) are the solutions of the equations ((3.28) – (3.30)) and ((3.36) – (3.38)) respectively. Moreover, we assume that all conditions in Lemma (3.5.1), (3.5.3) and (3.5.5) are valid. Then the following estimates hold*

$$\begin{aligned}
 &\sqrt{\alpha} \|f - F_h\|_{L^2([0,T];\mathbb{R}^m)} + \|\phi - \Phi_h\|_{L^\infty([0,T],H_0^1(\Omega))} + \|\psi - \Psi_h\|_{L^\infty([0,T],H_0^1(\Omega))} \\
 &\leq Ch_U \left(\|\psi\|_{L^2([0,T];H^2(\Omega))} + \|f\|_{L^2([0,T];L^2(\Omega_{adm}))} \right) + C_2 h \sum_{v=\phi,\psi} \|v\|_{H^1([0,T];H^2(\Omega))} \\
 &\quad + C_2 \tau \left(\sum_{v=\phi,\psi} \left\| \frac{\partial^2 v}{\partial t^2} \right\|_{L^2([0,T];L^2(\Omega))}^2 + \sum_{v=\phi,\phi_d} \left\| \frac{\partial^2 v}{\partial t^2} \right\|_{L^2([0,T];L^2(\Omega))}^2 + \|\psi\|_{L^2([0,T];L^2(\Omega))} \right) \quad (3.105)
 \end{aligned}$$

Proof. From the Lemme (3.5.3) and Lemme (3.5.5) we have

$$\begin{aligned}
\sqrt{\alpha}\|f - F_h\|_{L^2([0,T];\mathbb{R}^m)} &\leq Ch_U (\|\psi\|_{L^2([0,T],H^1(\Omega))} + \|f\|_{L^2([0,T],L^2(\Omega_{adm}))}) \\
&\quad + C\|\psi - \Psi_h(f)\|_{L^2([0,T],H^1(\Omega))} + Ck \left\| \frac{\partial\psi}{\partial t} \right\|_{L^2([0,T],L^2(\Omega))} \\
&\leq Ch_U (\|\psi\|_{L^2([0,T],H^1(\Omega))} + \|f\|_{L^2([0,T],L^2(\Omega_{adm}))}) \\
&\quad + C_2h \sum_{v=\phi,\psi} \|v\|_{H^1([0,T],H^2(\Omega))} + C_2\tau \|\psi\|_{L^2([0,T],L^2(\Omega))} \\
&\quad + C_2\tau \left(\sum_{v=\phi,\psi} \left\| \frac{\partial^2 v}{\partial t^2} \right\|_{L^2([0,T],L^2(\Omega))} + \sum_{v=\phi,\phi_d} \left\| \frac{\partial^2 v}{\partial t^2} \right\|_{L^2([0,T],L^2(\Omega))} \right)
\end{aligned} \tag{3.106}$$

And from the Lemma (3.5.1), (3.5.5) and (3.106) we have

$$\begin{aligned}
&\|\phi - \Phi_h\|_{L^2([0,T],H_0^1(\Omega))} + \|\psi - \Psi_h\|_{L^2([0,T],H_0^1(\Omega))} \leq \|\Phi_h - \Phi_h(f)\|_{L^2([0,T],H_0^1(\Omega))} \\
&+ \|\phi - \Phi_h(f)\|_{L^2([0,T],H_0^1(\Omega))} + \|\Psi - \Psi_h(f)\|_{L^2([0,T],H_0^1(\Omega))} + \|\Psi - \Psi_h(f)\|_{L^2([0,T],H_0^1(\Omega))} \\
&\leq C_2\|f - F_h\|_{L^2([0,T],L^2(\Omega_{adm}))} + C_2h \sum_{v=\phi,\psi} \|v\|_{H^1([0,T],H^2(\Omega))} + C_2\tau \|\psi\|_{L^2([0,T],L^2(\Omega))} \\
&\quad + C_2\tau \left(\sum_{v=\phi,\psi} \left\| \frac{\partial^2 v}{\partial t^2} \right\|_{L^2([0,T],L^2(\Omega))} + \sum_{v=\phi,\psi,\phi_d} \left\| \frac{\partial v}{\partial t} \right\|_{L^2([0,T],L^2(\Omega))} \right)
\end{aligned} \tag{3.107}$$

■

3.6 Numerical resolution

In this part, we present the 2D model that we use to solve the pollutant dispersion problem from four towns on the Normandy coast discharging wastewater into aquatic environments as shown in figure on the right. We consider the domaine $\Omega \in \mathbb{R}^2$ corresponding to the water surface of Normand-Breton gulf delimited by the borders $\partial\Omega = \{\Gamma_1, \Gamma_2, \Gamma_3, \Gamma_4\}$ as shown in the following left Figure (3.2)

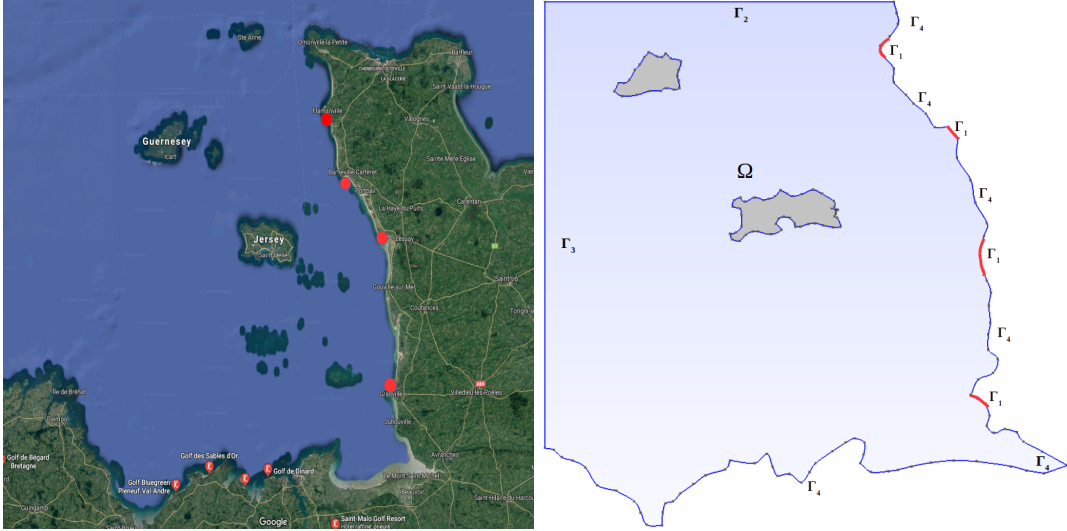


Figure 3.2: 2D geometric model of Normand-Breton gulf.

- Γ_1 corresponding to the boundary of the wastewater discharge.
- Γ_2 and Γ_3 corresponding to the free border of entry and exit of the fluid.
- Γ_4 corresponds to the border of the boundary conditions on the coast of Bretagne and the Normandy coast.

3.6.1 Time and space discretization

In order to set the time semi-discretization for the interval $[0, T]$, we chose a number $M \in \mathbb{N}$ and we define the time step $\Delta t = \frac{T}{M}$. Then we consider a set of $M + 1$ discrete times $[t_m]_{m=0}^M \subset [0, T]$ given by $t_m = m\Delta t$, for $m = [0, \dots, M]$. To complete the discretization, we use the finite element formalism for spatial discretization. We consider \mathcal{T}_h of Ω and, associated to this mesh. Let us denote (\hat{u}, \hat{v}) , \hat{q} and $\hat{\phi}$ the function test associated for the space finite element V_h , Q_h for the shallow water, M_h , \bar{M}_h for the transport equation and the adjoint state respectively. We define the following finite spaces for the shallow water equation such that

$$\begin{aligned} V_h &= \{ \hat{u} \in [C(\bar{\Omega})]^n, \hat{v} \in [C(\bar{\Omega})]^n : \hat{u}|_T \in [\mathbb{P}_1(T)]^n, \forall T \in \mathcal{T}_h, \hat{u} \cdot n = 0, \hat{v} \cdot n = 0 \text{ on } \partial\Omega \} \\ Q_h &= \{ \hat{H} \in C(\bar{\Omega}) : \hat{H}|_T \in \mathbb{P}_1(T), \forall T \in \mathcal{T}_h \} \end{aligned}$$

And the finite element spaces for the pollution model and the adjoint state we give

$$\begin{aligned} M_h &= \{ \hat{\Phi} \in [C(\bar{\Omega})]^n : \hat{\Phi}|_T \in [\mathbb{P}_1(T)]^n, \forall T \in \mathcal{T}_h \} \\ \bar{M}_h &= \{ \hat{\psi} \in [C(\bar{\Omega})]^n : \hat{\psi}|_T \in [\mathbb{P}_1(T)]^n, \forall T \in \mathcal{T}_h \} \end{aligned}$$

Find $(u, v) \in V_h, H \in Q_h$ such that

$$\int_{\Omega} \frac{u_{m+1}(x) - u_m \circ X_m(x)}{\Delta t} \hat{u} dx + \mu \int_{\Omega} \nabla u_{m+1} : \nabla \hat{u} dx + \int_{\Omega} g \nabla \cdot H_{m+1} \hat{u} dx = 0 \quad (3.108)$$

$$\int_{\Omega} \frac{v_{m+1}(x) - v_m \circ X_m(x)}{\Delta t} \hat{v} dx + \mu \int_{\Omega} \nabla v_{m+1} : \nabla \hat{v} dx + \int_{\Omega} g \nabla \cdot H_{m+1} \hat{v} dx = 0 \quad (3.109)$$

$$\int_{\Omega} \frac{H_{m+1}(x) - H_m \circ X_m(x)}{\Delta t} \hat{H} dx + \int_{\Omega} u_{m+1} \nabla \cdot H_{m+1} \hat{H} dx = 0 \quad (3.110)$$

For all $\hat{\Phi} \in M_h$, the weak formulation, find $\Phi_{m+1} \in M_h$ such that

$$\begin{aligned} & \int_{\Omega} \frac{\Phi_{m+1}(x) - \Phi_m \circ X_m(x)}{\Delta t} \hat{\Phi} dx + \mu \int_{\Omega} \nabla \Phi_{m+1} : \nabla \hat{\Phi} dx \\ & + \int_{\Omega} \sigma \Phi_{m+1} \hat{\Phi} dx = \int_{\Omega} \Phi_0 \hat{\Phi} dx + \int_{\Omega} \sum_{i=1}^4 F_i(t) \delta(r - r_i) \hat{\Phi} dx \quad \forall \hat{\Phi} \in M_h \end{aligned} \quad (3.111)$$

For all $m = [M - 1, \dots, 0]$, find $\psi \in \bar{M}_h$ is the solution of the adjoint state equation ($\psi^M = 0$)

$$\begin{aligned} & - \int_{\Omega} \frac{\psi_{m+1}(x) - \psi_m \circ X_m(x)}{\Delta t} \hat{\psi} dx + \mu \int_{\Omega} \nabla \psi_{m+1} : \nabla \hat{\psi} dx \\ & + \int_{\Omega} \sigma \psi_{m+1} \hat{\psi} dx = \int_{\Omega} (\phi_{m+1} - \phi_d) \hat{\psi} dx \quad \forall \hat{\psi} \in \bar{M}_h \end{aligned} \quad (3.112)$$

3.6.2 Numerical results

In this part, we present some 2D numerical results for the schemes discussed before. we consider two test, where the configuration geometric is defined in Figure (3.2) and Figure (3.3). Our scheme, which consists of piecewise linear finite elements in space and the and implicit backward Euler method in time. We use the descent of gradient to solve the linear system that arise on each time step.

To solve the optimal control problem, we use an algorithm of decsent. The methode of gradient is computed from the adjoint state given by (3.14). The algorithm of the decsent of gradient can be summarized in the following steps

Algorithm 2 Find $f(t)$, $\nabla J(f, \psi)$

$(u^{(0)}(x, t), v^{(0)}(x, t), H^{(0)}(x, t)) \leftarrow \text{comp. an approx. sol. by solving(3.15)}$
 Choose : $\phi^{(0)}(x, t), f(t) = f^{(0)}(t) \leftarrow \text{comp. an approx. sol. by solving(3.1)}$
 $\psi^{(0)}(x, t) \leftarrow \text{comp. an approx. sol. by solving(3.14)}$
 $\nabla J_j^{(0)} = \mu_j f^{(0)}(t) + \psi^{(0)}(t, r_j) \leftarrow \text{comp. the gradient of descent}$
 $j = \{1, \dots, N\}$
for $\{i = 0, \dots, n - \text{iteration}\}$ **do**
 1. Update the control $\leftarrow f^{(i+1)}(t) = f^{(i)}(t) + \rho \nabla J^{(i)}(t)$
 $(u^{(i+1)}(x, t), v^{(i+1)}(x, t), H^{(i+1)}(x, t)) \leftarrow \text{comp. an approx. sol. by solving(3.15)}$
 $\phi^{(i+1)}(x, t), f(t) = f^{(i+1)}(t) \leftarrow \text{comp. an approx. sol. by solving(3.1)}$
 $\psi^{(i+1)}(x, t) \leftarrow \text{comp. an approx. sol. by solving(3.14)}$
 $\nabla J_j^{(i+1)} = \alpha_j f^{(i)}(t) + \psi^{(i)}(t, r_j) \leftarrow \text{comp. the gradient of descent}$
 $j = \{1, \dots, N\}$
 2. $\left| \frac{\nabla J^{(i+1)}}{\nabla J^{(i)}} \right| < \text{tol}$ then put
 $f^{(i)}(t) = f^{(i+1)}(t)$,
 $\nabla J^{(i)} = \nabla J^{(i+1)}$ and go to $\Rightarrow 1$
end for

Test 1

The first test, we consider a rectangular structure of $10m \times 10m$. For the overall computation time, we have chosen $T = 20$ for a time step of 0.01s, for the different space discretization, we tried a several regular triangulations of about 9392 elements. The implementation of our system is realized in FreeFem++ [21]. We have developed many test, the results obtained are presented below. Figure (3.3) shows the nonoptimal solution of the advection-diffusion problem of the pollutant.

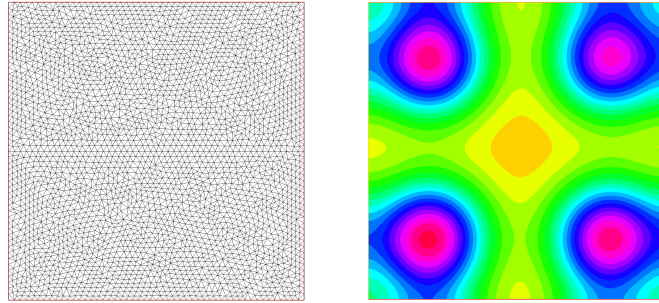


Figure 3.3: The nonoptimal solution of the pollutant.

To reduce the pollutant in the aquatic environment, we control the sources of the pollutant using the descent of the gradient algorithm. We have realised several tests by varying the diffusion parameter μ and the regulation parameter α . The initial value for the concentration of the pollutant $\phi(0, x) = 1$, the initial velocity $u(0, x) = 1, v(0, x) = 1$ and the initial elevation $H(0, x) = 0.5$. The step of the descent of the gradient $\rho = 0.01$. The different results we obtained are presented in the following Figure (3.4).

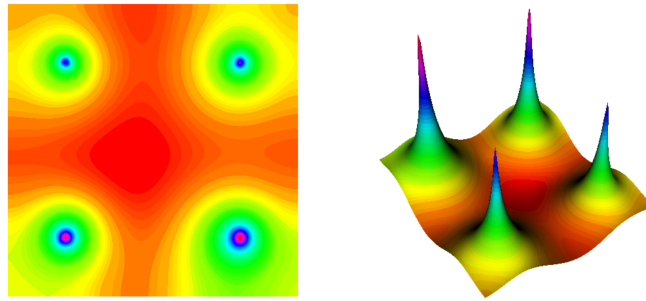


Figure 3.4: Optimal control of the pollutant with $\alpha = 1$ and $\mu = 1m^2.s^{-1}$.

In the first case, we vary the diffusion coefficient and we fix the regulation parameter. The different results obtained are showing in Figure (3.5), Figure (3.6) and Figure (3.7)

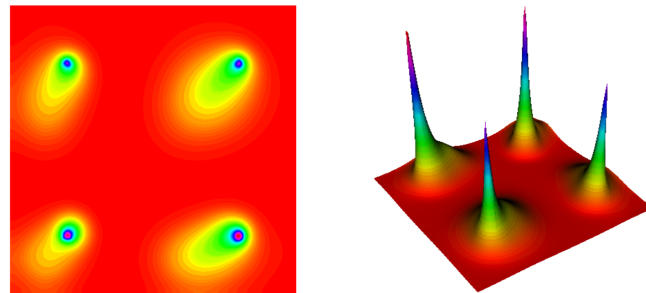


Figure 3.5: Optimal control of the pollutant with $\alpha = 1$ and $\mu = 0.1m^2.s^{-1}$

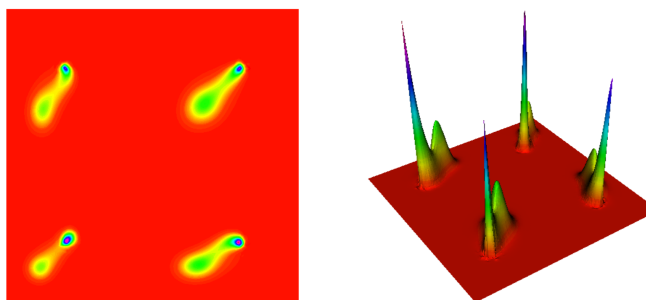


Figure 3.6: Optimal control of the pollutant with $\alpha = 1$ and $\mu = 0.01m^2.s^{-1}$.

In the second case, when the ragulation parameter $\alpha = 0$,

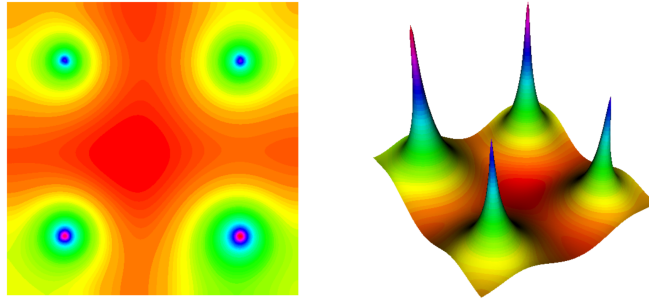


Figure 3.7: Optimal control of the pollutant with $\alpha = 0$ and $\mu = 1m^2.s^{-1}$.

Finally, we fix the diffusion parameter and we vary the regulation parameter. The obtained results are showing in Figure (3.8)

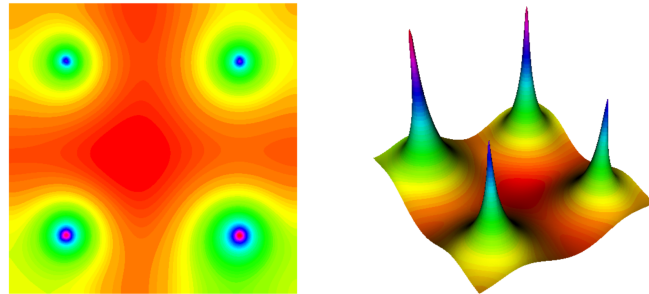


Figure 3.8: Optimal control of the pollutant with $\alpha = 0.1$ and $\mu = 1m^2.s^{-1}$.

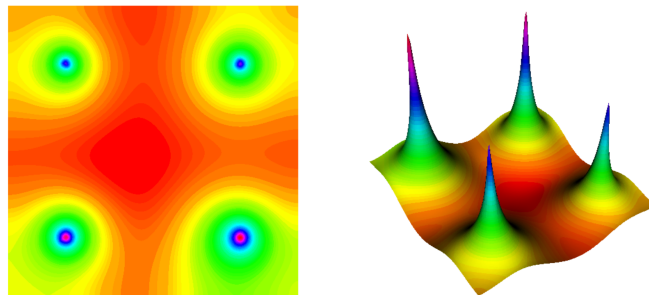


Figure 3.9: Optimal control of the pollutant with $\alpha = 0.01$ and $\mu = 1m^2.s^{-1}$.

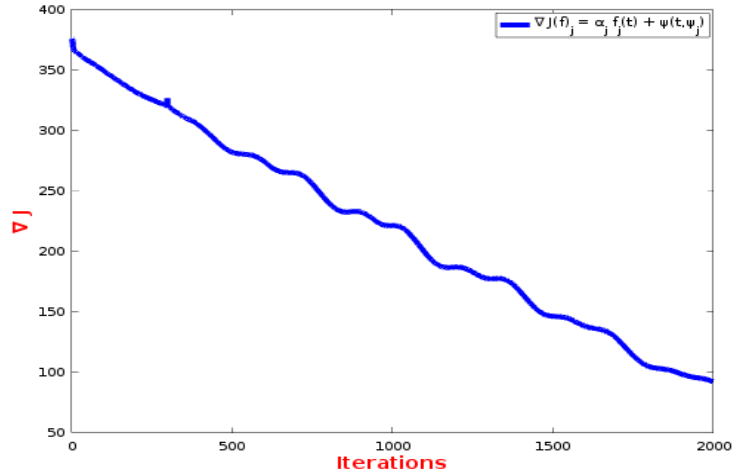


Figure 3.10: Gradient of the cost function evolution depending iteration number.

In order to validate the estimates developed in the previously. We consider the behavior of the error for a sequence of discretizations with different mesh size and fixed time steps. we set Ω to be unit square $[0, 1] \times [0, 1]$ and we take the exact solution as

$$\begin{aligned}\phi_{ex}(x, t) &= -\frac{1}{2\pi} \log |x| \cdot t(1-t) \\ f(t) &= t(1-t)\end{aligned}$$

and the exact solution for the adjoint state

$$\psi(x, t) = -\cos\left(\frac{\pi}{2} |x|^2\right) \cdot t(1-t)$$

and also we take the exact solution of the desired concentration value ϕ_d

$$\begin{aligned}\phi_d &= -\frac{1}{2\pi} \log |x| \cdot t(1-t) - \cos\left(\frac{\pi}{2} |x|^2\right) \cdot t(1-t) \\ &\quad + \left(2\pi \sin\left(\frac{\pi}{2} |x|^2\right) + \pi^2 |x|^2 \cos\left(\frac{\pi}{2} |x|^2\right)\right) \cdot t(1-t)\end{aligned}$$

The concentration of the Dirac mass is concentrated at $[x, y] = [0.5, 0.5]$. numerically, the implementation of mass dirac is done by the construction of the interpolation matrix at a array of points x, y from a finite element space.

In order to obtain the L^2 norm of the error between the exact solution and the numerical one

$$E(\phi, h_n) = \|\phi_h(h_n) - \phi_{ex}(h_n)\|_{L^2}$$

and the rate of convergence in space

$$rate(\phi, h_n) = \frac{\log(E(\phi, h_{n-1})/E(\phi, h_n))}{\log(h_{n-1}/h_n)} \quad (3.113)$$

where h denotes the mesh size of the triangulation or the step τ .

In order to investigate the convergence order with respect to space discretization we fix the time discretization $N = 100$ and we vary the mesh size of the triangulation from 27 until 4963 Degrees of freedom. The results are listed in Table 1, and Figure (3.11) presents the numerical result at time $t = 0.1$ for grid with 4963 Dofs. We can see from Table 1 that the convergence order for the control f , the state ϕ and the adjoint state ψ is only 1.

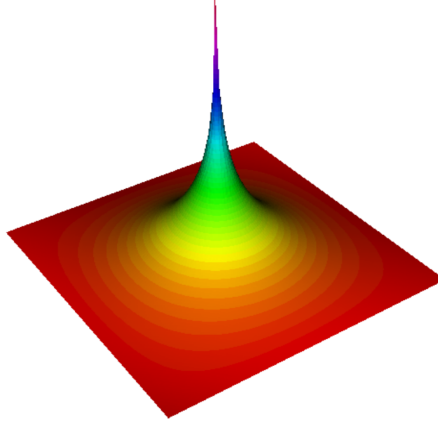


Figure 3.11: The discrete state $\Phi_{h\tau}$ at time $t = 0.1$ with 12106

Dof	$\ \phi - \phi_{ex}\ _{L^2(0,T)}$	Rate	$\ f - f_{ex}\ _{L^2(0,T)}$	Rate	$\ \psi - \psi_{ex}\ _{L^2(0,T)}$	Rate
27	0.0522761	-	0.2429090	-	0.1976700	-
94	0.0350302	0.577554	0.1664970	0.544919	0.1307900	0.595843
332	0.0197525	0.826568	0.0945548	0.816273	0.0733844	0.833702
1280	0.0104595	0.91722	0.0502398	0.912321	0.0386895	0.923532
4963	0.00537356	0.960863	0.0261879	0.939929	0.0198441	0.963229

Table 1: L^2 norm of the error and the rate convergence.

Test 2

in the second test, we consider the domain $\Omega \subset \mathbb{R}^2$. The domain Ω is occupied by shallow waters. The problem area is the Normand-Breton Gulf is located in northwestern of France between $\approx 50^\circ$ to 48° altitude and between $\approx -1.4^\circ$ to -2.28° longitude. The four sources are located at $\approx (49.51^\circ, -1.88^\circ)$, $\approx (49.37^\circ, -1.79^\circ)$, $\approx (49^\circ, -1.58^\circ)$ and $\approx (48.71^\circ, -1.52^\circ)$ in altitude and longitude respectively, with a source of energy $f = 10000kg$. To solve the coupled system shallow water and transport equations we took a diffusion coefficient $\mu' = 1m^2/s$ and $\mu = 0.1m^2/s$, the height of the initial elevation $H = 1m$, the initial velocity $u = v = 1m/s$ and the step time $\Delta t = 0.01s$, the decay of the concentration of the pollutant is taken $\sigma = 0.02$, the regulation parameter $\alpha = 0.2$ and the step of descent $\rho = 0.01$. For the discretization of the computing space, we have a regular triangulation of about 28763 triangles. The mesh is generated under GMSH then imported to Freefem++. The overall computation time we have $M = \frac{T}{\Delta t}$ with $T = 20$. Figure (3.12) show the nonoptimal solution in the left and the optimal solution in the right.

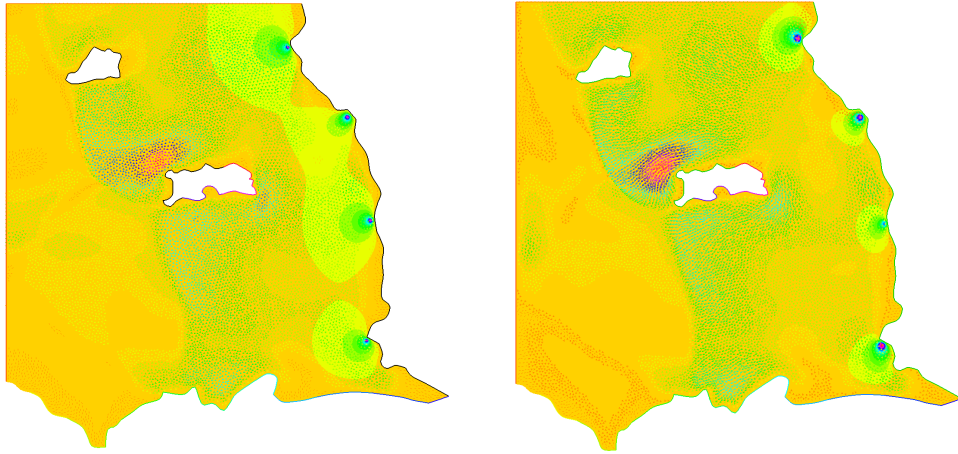


Figure 3.12: Nonoptimal (left) and optimal control (right) of the pollutant in the Normand-Breton Gulf.

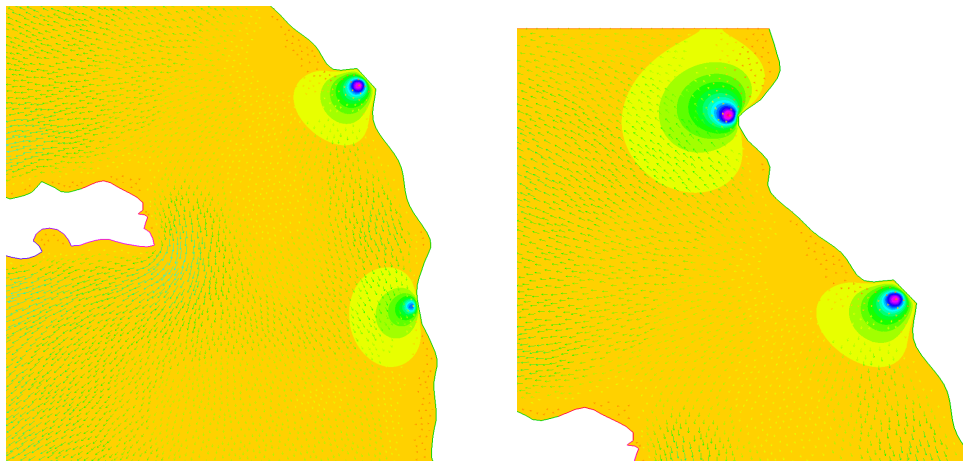


Figure 3.13: Zoom for the differents sources of the pollutant.

3.7 Conclusion

Nowadays, environmental pollution is a major factor that can cause degradation of the natural aquatic environment, and also on human health. To reduce the risk of this pollution effect is to minimize the rejection of the amount of wastewater in the sea.

In the first part of the work, the mathematically well-posed formulation of the different environmental problems related the transport pollution model and the shallow water equations. We study a finite element approximation of quadratic optimal control problems governed by the coupled system advection-diffusion equations and the shallow water, where the state and the adjoint state are discretized using the characteristic finite element method.

After, we treat the numerical part in which we give the implementation of a complete numerical

algorithm, and the optimization process by solving the fully discretized problem, which includes the resolution of coupled model and the adjoint state variables.

finally, the efficient procedure for the direct control concentration pollutant problem of the method presented here is evaluated by an academic and with a realistic test developed in FreeFem++. The numerical results obtained proved the robustness of the technique for studying the control of the pollution.

Bibliography

- [1] M. Louaked, A. Saïdi, Pointwise control and hybrid scheme for water quality equation, *Nonlinear Analysis* 71(2009)e2337-e2349.
- [2] Q. A. Dang, M. Ehrhardt, G. L. Tran, D. Le, Mathematical modeling and numerical algorithms for simulation of oil spill, *Environ Model Assess* (2012) 17:275-288.
- [3] R. M., Johansen, P. J. Brandvik, P. Daling, A. Lewis, R. Fiocco and all. (1999). Oil spill modeling towards the close of 20th century: overview of the state of the art. *Spill Science & Technology Bulletin*, 5, 3-16.
- [4] J. W. Doerffer, *Oil spill response in the marine environment*. Oxford: Pergamon, 1992.
- [5] I. Fent, M. Putti, C. Gregoretti, S. Lanzoni, Modeling shallow water flows on general terrains, *Advanced in water Resources* 121 (2018) 316-332.
- [6] M. M. Mousa, Efficient numerical scheme based on the method of lines for the shallow water equations, *Journal of Ocean Engineering and Science* 3 (2018) 303–309.
- [7] M. Louaked, A. Saïdi, 2D Control Problem and TVD-Particle Method for Water Treatment System, *Application of Mathematics in Technical and Natural Sciences*, AIP Conf. Proc. 1404, 405-413 (2011); doi: 10.1063/1.3664788
- [8] Y. N. Skiba, Direct and Adjoint Oil Spill Estimates, *Environmental Monitoring and Assessment* · October 1999.
- [9] Q. A. Dang, M. Ehrhardt, G. L. Tran, D. Le, On the numerical solution of some problems of environmental pollution, *Air Pollution Research Advances*, Corin G. Bodine, pp. 171-200 (2014).
- [10] Y. N. Skiba, D. Parra-Guevara, Application of Adjoint Approach to Oil Spill Problems, *Environ Model Assess* (2017) 22:379–395.
- [11] M. Reed, Ø. Johansen, P. J. Brandvik, P. Daling, A. Lewis, R. Fiocco and al (1999). oil spill modeling towards the close of the 20th century: Overview of the state of the art. *Spill Science & Technology Bulletin*, 5, 3-16.

- [12] M. Hinze, A variational discretization concept in control constrained optimization: The linear quadratic case, *Comput. Optim. Appl.*, 30 (2005), pp. 45–63.
- [13] M. Hinze, R. Pinnau, M. Ulbrich, and S. Ulbrich, *Optimization with PDE Constraints*, *Math. Model. Theory Appl.* 23, Springer, New York, 2009.
- [14] J.L. Lions, *Optimal control of systems governed by partial differential equations*. Springer, Berlin (1971).
- [15] W. Alt and U. Mackenroth, Convergence of finite element approximations to state constrained convex parabolic boundary control problems, *SIAM J. Control Optim.*, 27 (1989), pp. 718-736.
- [16] W. Gong, M. Hinze, Z. Zhou, A priori error analysis for finite element approximation for the parabolic optimal control problems with pointwise control, *Society for Industrial and applied Mathematics* (2014), *SIAM J. CONTROL OPTIM.* Vol. 52, No. 1 1, pp. 97-119
- [17] O. Pironneau, *Optimal Shape Design for Elliptic Systems*. Springer, Berlin (1984).
- [18] D. Tiba, *Lectures on the Optimal Control of Elliptic Equations*. University of Jyväskylä Press, Finland (1995)
- [19] P. G. Ciarlet, *The Finite Element Method for Elliptic Problems*. SIAM, Philadelphia (2002)
- [20] V. Thomée, *Galerkin Finite Element Methods for Parabolic Problems*. Springer Series in Computational Mathematics. Springer, Berlin (1997)
- [21] F. Hecht, New development in FreeFem++. *J. Numer. Math.* 20 (2012), no. 3-4, 251–265. 65Y15.
- [22] H. Fu. A Characteristic finite element method for optimal control problems governed by convection-diffusion equations. *Journal of Computational and Applied Mathematics.* 235(2010) 825-836.
- [23] O. Pironneau. : On the Transport-Diffusion Algorithm and Its Applications to the Navier-Stokes Equations. *Numer. Math.* 38, 309-332 (1982).
- [24] O. Pironneau. and M. Tabata : stability and convergence of a Galerkin-characteristics finite element scheme of lumped mass type. *Int. J. Numer. Meth. Fluids* 2000; 00:1-6.
- [25] G. Fournestey, Stabilité des méthodes de Lagrange-Galerkin du premier et du second ordre , *Technical Report 4505*, INRIA Rocquencourt, (2002).
- [26] K.W. Morton , A. Priestley, and E. Suli, Stability of the Lagrange-Galerkin method with non-exact integration, *RAIRO-Modélisation mathématique et analyse numérique*, 22(4) : 625 – 653(1988).

- [27] M. Louaked , A. Saïdi, 2D control problem and TVD-particle method for water treatment system, 2011, hal-00579797.

Chapter 4

Analysis and finite element approximation of optimal control problem based on porous media model

The realization and the completion of this chapter was the collective work with the collaboration of M. Louaked, M. Kadiri and M. Mechkour where we worked on the application of the stationary Navier-Stokes Forchheimer equations by penalization of the incompressibility constraint in order to optimize the vortex effect of the flow of a fluid in a hydraulic structure of the fishway. This work was reported in M. Kadiri's thesis [22]. My contribution in this work consists first of all in the analysis of the existence and uniqueness of the solution of the problem. In the second part, the implementation of the optimization procedure in terms of numerical resolution of the design of 2D and 3D fishway, implementation of the mathematical model, the choice of physical parameters, optimization algorithm, obtaining and processing of the numerical results.

Contents

4.1	Introduction	142
4.2	Mathematical model	144
4.2.1	Preliminaries	144
4.2.2	Perturbed equation	150
4.2.3	Error estimates	153
4.3	Control problem	158
4.3.1	Adjoint system	158
4.3.2	Shape gradient	161
4.4	Finite element method	164
4.5	Numerical approximation and optimization algorithm	174
4.5.1	Optimization procedure	175
4.5.2	Numerical examples	177
4.6	Conclusion	182

4.7 Annex: Control problem of mixed boundary conditions	182
4.7.1 Adjoint system	183
4.7.2 Shape gradient	185

4.1 Introduction

The purpose of this chapter is the study of different proprieties for the porous media equations based on the Navier Stokes equations with damping. We begin by showing the existence and uniqueness of the solution for the following boundary problem

$$\left\{ \begin{array}{ll} -\nu\Delta u + (u.\nabla)u + a |u|^\alpha u + \nabla p = f & \text{in } \Omega \\ \nabla.u = 0 & \text{in } \Omega \\ u = 0 & \text{on } \partial\Omega \end{array} \right. \quad (4.1)$$

where $\Omega \in \mathbb{R}^d$ ($d=2, 3$) is the fluid domain with a sufficiently smooth boundary $\partial\Omega$; u is the velocity; p is the pressure; ν is the viscosity. The damping term $\alpha \in [0, 2]$ and the Forchheimer coefficient $a > 0$ are real numbers.

Applications of these water flow models include problems related to the optimization of fish passage structures. We look for finding an optimal shape of fishways by minimizing a cost function. Such optimal structure allow to a maximum number of fishes to cross to the river upstream.

The construction of dams is a very old activity; the first known works date back to 5,000 years and are located in the Middle East. It has continued to grow ever since. These structure are used usually for agriculture, electricity, or for navigation, But they constitute impassable obstacles to the free movement of fish and may contribute to the extinction of fish populations as Salomon, Trout, and Eels. To overcome these barriers, men think to built hydraulic structures which permit to migratory species to cross to the river upstream. Fishways represent a comfortable way for migratory species to across through dams. Our objective in this chapter is to simply the fishes passage to their production or feeding areas and assure to provide a rest area between pools. In our study we are interested by the vertical slots fishways (see [3]).

Vertical slots fishways are used frequently in the world. The vertical slots provide a good energy dissipation and create a quiet areas between pool which allows to fishes to have some rest before crossing one pool to another. Such structure is designed with a slope to the ground. It permits to small species to pass the circulation zones in the pool with less efforts which is not the case for other types of fishways; as the pool and weir type (Clay [1]) and the Denil type (Katopodis et al. [2]).

In real world engineering applications, in order to improve the reliability of fishway attraction

and passage efficiency, the bottom of the pools must always have a rough surface in order to reduce the flow velocity in the vicinity of the bottom and make it easier for the benthic fauna and small fish to ascend. A rough surface can be produced by embedding stones closely together into the concrete before it sets. The flow behavior can only be represented accurately if the structure of porous media is properly described. Transition from the Darcy flow regime to the Forchheimer regime can be justified by the need to take into account the behavior of the fluid through the pore space. To clarify the physical meaning of the non-linearity in the Forchheimer equation, it would be wise to understand the derivation of the Forchheimer equation from the Navier-Stokes model using the basic principles underlying the theory of hydrodynamics. Considering the different opinions on the origin of the non-linearity, it is now admitted that the quadratic term leads to boundary layer separation and wake formation behind solid obstacles. Several discussions are available in [5; 9; 11].

We aim to study these structures through the use of the steady-state model of porous media and evaluating the feasibility of computing the flow pattern in vertical slot fish ladder and derive an optimal structure that enables fish to overcome the obstacle under appropriate conditions.

Solving the problem (4.1) may be numerically difficult, due to the incompressibility constraint $\nabla \cdot u = 0$. A common approach to deal with this issue is to relax the incompressibility condition through the penalty type procedure. We intend to use a penalty method, first introduced by Courant and exploited by Temam [15] for the approximation of the Navier Stokes equations, to handle the Navier Stokes Forchheimer system.

The penalization technique consists in establishing an approximation of the pairing (\mathbf{u}, p) solution of (4.1) by $(\mathbf{u}^\varepsilon, p^\varepsilon)$ solution of the given penalized problem

$$\left\{ \begin{array}{ll} -\nu \Delta u^\varepsilon + (u^\varepsilon \cdot \nabla) u^\varepsilon + \frac{1}{2} (\nabla \cdot u^\varepsilon) u^\varepsilon + a |u^\varepsilon|^\alpha u^\varepsilon + \nabla p^\varepsilon = f & \text{in } \Omega \\ \nabla \cdot u^\varepsilon + \varepsilon p^\varepsilon = 0 & \text{in } \Omega \\ u^\varepsilon = 0 & \text{on } \partial\Omega \end{array} \right. \quad (4.2)$$

We investigate the existence and uniqueness of a weak solution by means of a Faedo-Galerkin method. Next, we analyze the penalized problem by deriving a priori error estimates and show that the perturbed problem has a convergent solution in $O(\varepsilon)$ where ε is the penalty parameter. Finally, we establish that the finite element approximation of the penalized solution converges to the solution of the porous medium model.

The perturbed model is used to address an optimization problem involving the structure of the fish ladder, consisting in finding an optimal shape of the fishway by minimizing a cost function linked to the fish passage comfort. We proceed to derive an adjoint equations and compute

the shape gradient of the objective function. The numerical solution combines a finite element method and a gradient type algorithm named projected spectral gradient to deal with the optimization problem.

The rest of the chapter is arranged as described in the following. The next section deals with notations, some preliminary results, the existence of a weak solution based on the use of the standard Faedo-Galerkin method and the derivation of an error estimate to prove the convergence of the penalized solution to the solution of the original porous media model. Section 3 is devoted to the optimal control by which we will minimize a cost function to obtain an optimal design of the fish passage structures. In Section 4 we treat the numerical analysis of the penalty finite element scheme. Numerical simulation for 2D and 3D cases with structures already used for fishway modeling [4], [6] are carried to illustrate that the proposed method is robust and efficient.

4.2 Mathematical model

4.2.1 Preliminaries

We are interesting in the study of the system (4.1). Let denote by (\cdot, \cdot) , $\|\cdot\|$ and $\|\cdot\|_k$ the scalar product in L^2 , the L^2 -norm and the norm of $H^k(\Omega)$ respectively. We therefore introduce the following Sobolev spaces

$$\begin{aligned} X &= (H_0^1(\Omega))^d, \quad Y = L^2(\Omega), \quad M = \left\{ q \in L^2(\Omega); \int_{\Omega} q dx = 0 \right\} \\ \hat{V}_0(\Omega) &= \{u \in (H^1(\Omega))^d \mid u = 0 \text{ on } \Omega\} \\ V_0(\Omega) &= \{u \in (H^2(\Omega))^d \mid u = 0 \text{ on } \Omega\} \end{aligned}$$

We define X' as the dual of the space X .

To ease later analysis, we recall the monotonicity property of any mapping F given by $F : \mathbf{x} \mapsto |\mathbf{x}|^\alpha \mathbf{x}$

$$(|\mathbf{u}|^\alpha \mathbf{u} - |\mathbf{v}|^\alpha \mathbf{v}, \mathbf{u} - \mathbf{v}) \geq 0 \quad (4.3)$$

In addition, we need $C_{0,div}^\infty$ the set of all C^∞ real vector functions $u = (u_1, \dots, u_d)$ ($d=2, 3$) with compact support in Ω such that $\nabla \cdot u = 0$.

We present well-posedness, error analysis and give some features of the weak solution.

Existence of weak solution

The model of fluid motion in porous media reads as

$$\begin{cases} -\nu\Delta u + (u.\nabla)u + a|u|^\alpha u + \nabla p = f & \text{in } \Omega \\ \nabla.u = 0 & \text{in } \Omega \\ u = 0 & \text{on } \partial\Omega \end{cases} \quad (4.4)$$

Integration by parts yields the following weak formulation:

Find $(u, p) \in C_{0,div}^\infty(\Omega) \times Y$ such that

$$\begin{cases} \nu(\nabla u, \nabla v) + ((u.\nabla)u, v) + a(|u|^\alpha u, v) - (p, \nabla.v) = (f, v) \quad \forall v \in C_{0,div}^\infty(\Omega) \\ (\nabla.u, q) = 0 \quad \forall q \in M \end{cases} \quad (4.5)$$

Now let us state the theorem that ensures the existence of a weak solution.

Theorem 4.2.1. *Let Ω be a bounded domain in \mathbb{R}^d ($d = 2, 3$), $f \in X'$ is a given exterior function. There exist at least a weak solution of (4.4) satisfying*

$$\frac{\nu}{2} \|\nabla u\|^2 + a \|u\|_{L^{\alpha+2}}^{\alpha+2} \leq \frac{1}{2\nu} \|f\|_{X'}^2, \quad \text{for } 0 \leq \alpha \leq 10 \quad (4.6)$$

and

$$\|p\| \leq C(\|f\|_{X'} + \|\nabla u\| + \|\nabla u\|^2 + \|u\|_{L^{\alpha+2}}) \quad (4.7)$$

for some positive constant C .

The proof relies mainly on the following lemmas.

Lemma 4.2.2. *Suppose that Ω is a bounded locally Lipschitzian domain of \mathbb{R}^d ($d=2, 3$). Let $F \in X'$ and $u \in X$ such that*

$$(F, u) = 0$$

then there exists a unique $P \in L^2(\Omega)$ satisfying

$$(F, u) = \int_{\Omega} P \nabla.u dx \quad \text{and} \quad \int_{\Omega} P dx = 0$$

For the proof of this Lemma see [21].

Lemma 4.2.3. *Assume that Ω is an arbitrary domain in \mathbb{R}^d ($d=2, 3$), and let $f \in X'$. Then*

1. *The vector $V \in H_{loc}^1(\Omega)$ satisfies (4.5) for all $v \in C_{0,div}^\infty(\Omega)$ if and only if there exists $P \in L_{loc}^2(\Omega)$ satisfying the identity*

$$\nu(\nabla V, \nabla w) + ((V.\nabla)V, w) + (a|V|^\alpha V, w) = (P, \nabla.w) + (f, w) \quad (4.8)$$

for all $w \in C_{0,div}^\infty(\Omega)$.

2. If, Moreover, Ω is bounded and Lipschitzian and $f \in X'$, $V \in (H^1(\Omega))^d$ ($d=2, 3$), then

$$P \in Y, \text{ with } \int_{\Omega} P dx = 0$$

and (4.8) holds for all $w \in X$.

Proof. It is clear that (4.8) implies (4.5). If Ω is locally Lipschitzian, the functional

$$F(w) := \nu(\nabla V, \nabla w) + ((V \cdot \nabla)V, w) + (a|V|^\alpha V, w) - (f, w) \quad (4.9)$$

is linear and bounded in $w \in X$ and it becomes zero when $w \in X$ and $\nabla \cdot w = 0$. Using the Corollary 3.5.1 in [20] and lemma 4.2.2, there exists $P \in Y$ such that

$$F(w) = (P, \nabla \cdot w) \quad (4.10)$$

for all $w \in X$, thus satisfying (4.8). If Ω is an arbitrary domain, we use Corollary 3.5.2 in [20] to deduce the existence of $P \in L^2_{loc}(\Omega)$ satisfying (4.10) $\forall w \in C^\infty_{0,div}(\Omega)$. ■

Lemma 4.2.4. Consider $F: \mathbb{R}^m \rightarrow \mathbb{R}^m$ be a continuous function such that for some $K > 0$

$$F(\xi) \cdot \xi > 0$$

for all $\xi \in \mathbb{R}^m$ with $|\xi| = K$. Then there exists $\xi_0 \in \mathbb{R}^m$ with $|\xi_0| \leq K$ such that $F(\xi_0) = 0$.

The proof of this Lemma is referred to [20].

Proof. (of theorem (4.2.1)) Existence of the velocity field: We consider an orthonormal basis (w_k) in X and define the sequence $(u_m) \in X$ satisfying

$$\nu(\nabla u_m, \nabla w_k) + ((u_m \cdot \nabla)u_m, w_k) + (a|u_m|^\alpha u_m, w_k) = (f, w_k) \quad (4.11)$$

where for each $m \in \mathbb{N}$

$$u_m = \sum_{k=1}^m \xi_{km} w_k \quad (4.12)$$

We multiply (4.11) by ξ_{km} and sum with respect to k to obtain

$$\nu \|\nabla u_m\|^2 + a \|u_m\|_{L^{\alpha+2}}^{\alpha+2} = (f, u_m) \leq \|f\|_{X'} \|\nabla u_m\| \quad (4.13)$$

By Young's inequality we get

$$\frac{\nu}{2} \|\nabla u_m\|^2 + a \|u_m\|_{L^{\alpha+2}}^{\alpha+2} \leq \frac{1}{2\nu} \|f\|_{X'}^2 \quad (4.14)$$

Next, we introduce the following function

$$(F(\xi); \xi) := \nu(\nabla \xi, \nabla \xi) + a(|\xi|^\alpha \xi, \xi) - (f, \xi)$$

We have

$$\begin{aligned} (F(\xi); \xi) &\geq \nu \|\xi\|^2 + a \|\xi\|_{L^{\alpha+2}}^{\alpha+2} - \|f\|_{X'} \|\xi\| \\ &= (\nu \|\xi\| - \|f\|_{X'}) \|\xi\| + a \|\xi\|_{L^{\alpha+2}}^{\alpha+2} \end{aligned}$$

when $\|\xi\| = K$, $K > \frac{1}{\nu} \|f\|_{X'}$. The lemma 4.2.4 gives the existence of u_m solution of (4.11) for each m . Moreover, the sequence (u_m) is bounded by (4.14), then there exists a subsequence denoted (u_m) which

$$u_m \rightharpoonup u \text{ in } X \quad (4.15)$$

From the Sobolev embedding theorem we get

$$u_m \longrightarrow u \text{ in } L^{6-\varepsilon} \quad (4.16)$$

with ε is some positive constant. For the convergence of three quantities in (4.11), we proceed as follow; as $m \rightarrow \infty$ we have

$$(\nabla u_m, \nabla w_k) \longrightarrow (\nabla u, \nabla w_k) \quad (4.17)$$

For the two remaining terms, we develop

$$\begin{aligned} &| ((u_m \cdot \nabla) u_m, w_k) - ((u \cdot \nabla) u, w_k) | \\ &\leq | ((u_m - u) \cdot \nabla) u_m, w_k) | + | ((u \cdot \nabla)(u_m - u), w_k) | \\ &= T^{(1)} + T^{(2)} \end{aligned}$$

The first quantity can be raised by

$$\begin{aligned} T^{(1)} &\leq \|w_k\|_{L^6} \|\nabla u_m\| \|u_m - u\|_{L^3} \\ &\leq c \|w_k\|_1 \|\nabla u_m\| \|u_m - u\|_{L^3} \end{aligned}$$

By (4.16) we obtain

$$\lim_{m \rightarrow \infty} T^{(1)} = 0$$

It remains to raise the term $T^{(2)}$

$$\begin{aligned} T^{(2)} &\leq | ((u \cdot \nabla) w_k, (u_m - u)) | \\ &\leq \|u\|_{L^6} \|\nabla w_k\| \|u_m - u\|_{L^3} \\ &\leq C \|w_k\| \|u_m - u\|_{L^3} \end{aligned}$$

Therefore,

$$\lim_{m \rightarrow \infty} T^{(2)} = 0$$

Finally, we obtain the ensuing convergence result

$$|((u_m \cdot \nabla)u_m, w_k) - ((u \cdot \nabla)u, w_k)| \rightarrow 0, \quad m \rightarrow \infty \quad (4.18)$$

For the last term, we use

$$\begin{aligned} |(|u_m|^\alpha u_m, w_k) - (|u|^\alpha u, w_k)| &\leq |(|u_m|^\alpha(u_m - u), w_k)| + |((|u_m|^\alpha - |u|^\alpha)u, w_k) \\ &= T^{(3)} + T^{(4)} \end{aligned}$$

Regarding the first term $T^{(3)}$, thank to the embedding theorem

$$T^{(3)} \leq C \sup |w_k| \cdot \|u_m\|_{L^{\alpha+2}}^\alpha \|u_m - u\|_{L^{6-\varepsilon}}$$

thus we obtain

$$\lim_{m \rightarrow \infty} T^{(3)} = 0$$

The last term $T^{(4)}$ can be raised with the same approach

$$T^{(4)} \leq C \|u_m - u\|_{L^{6-\varepsilon}} \cdot \|u_m\|_{L^{\alpha+2}}^\alpha \|w_k\|_{L^p}$$

with $p = \infty$. So we have

$$\lim_{m \rightarrow \infty} T^{(4)} = 0$$

Therefore

$$\lim_{m \rightarrow \infty} (|u_m|^\alpha u_m, w_k) = (|u|^\alpha u, w_k) \quad (4.19)$$

From (4.18)-(4.19), the velocity $u \in X$ satisfies the equation

$$\nu(\nabla u, \nabla w_k) + ((u \cdot \nabla)u, w_k) + (a |u|^\alpha u, w_k) = (f, w_k) \quad (4.20)$$

Finally, we write any $\varphi \in X$ as a limit of a linear combination of w_k . Then the velocity $u \in X$ satisfies

$$\nu(\nabla u, \nabla \varphi) + ((u \cdot \nabla)u, \varphi) + (a |u|^\alpha u, \varphi) = (f, \varphi) \quad \text{for all } \varphi \in X \quad (4.21)$$

Using (4.14) one gets

$$\frac{\nu}{2} \|\nabla u\| + a \|u\|_{L^{\alpha+2}}^{\alpha+2} \leq \frac{1}{2\nu} \|f\|_{X'}^2 \quad (4.22)$$

Existence of the pressure field: Supposing that Ω is locally Lipschitzian, thanks to lemma (4.2.3): there exists $p \in Y$ satisfying (4.5) and

$$\int_{\Omega} p dx = 0 \quad (4.23)$$

Consider the problem

$$\begin{aligned}\nabla \cdot W &= p \\ W &\in X\end{aligned}\tag{4.24}$$

$$\|W\|_1 \leq \|p\|$$

As $p \in Y$ and satisfies (4.23), the problem (4.24) has a solution thanks to the theorem 3.3.1 in [20]. Setting $w = W$ in (4.8) to obtain

$$\|p\|^2 \leq C (\|f\|_{X'} + \|u\|_1 + \|u\|_{L^{\alpha+2}} + \|u\|_1^2) \|p\|\tag{4.25}$$

■

Lemma 4.2.5. *Consider $u, v \in X$ such that (4.22) holds for u and v , then*

$$\||u|^\alpha u - |v|^\alpha v\| \leq C \|\nabla(u - v)\|\tag{4.26}$$

For the proof of this Lemma see [14]-[13].

In what follows, we address the question of the uniqueness of the solution.

Uniqueness of weak solution

We shall prove the following theorem for the boundary value problem (4.4).

Theorem 4.2.6. *Let Ω be a bounded domain in \mathbb{R}^d ($d=2, 3$), locally Lipschitz, and $f \in X'$. If ν is "big enough" and $\frac{2}{3} \leq \alpha \leq 2$, then the weak solution of (4.4) is unique.*

Proof. Let us suppose that the problem (4.4) has two weak solutions u_1 and u_2 .

Define $\varphi = u_1 - u_2$ and write

$$\nu \|\nabla(u_1 - u_2)\|^2 + ((u_1 - u_2) \cdot \nabla)u_1, u_1 - u_2 + (a|u_1|^\alpha u_1 - a|u_2|^\alpha u_2, u_1 - u_2) = 0$$

which leads to

$$\begin{aligned}\nu \|\nabla(u_1 - u_2)\|^2 &+ ((u_1 - u_2) \cdot \nabla)u_1, u_1 - u_2 \\ &+ (a|u_1|^\alpha (u_1 - u_2), (u_1 - u_2)) + a(|u_1|^\alpha - |u_2|^\alpha)u_2, u_1 - u_2 = 0\end{aligned}$$

This gives

$$\begin{aligned}
 \nu \|\nabla(u_1 - u_2)\|^2 &= -(((u_1 - u_2) \cdot \nabla)u_1, u_1 - u_2) \\
 &\quad - (a|u_1|^\alpha(u_1 - u_2), (u_1 - u_2)) \\
 &\quad - a((|u_1|^\alpha - |u_2|^\alpha)u_2, u_1 - u_2)
 \end{aligned} \tag{4.27}$$

The first term on the right hand side in (4.27) implies

$$\begin{aligned}
 | -(((u_1 - u_2) \cdot \nabla)u_1, u_1 - u_2) | &\leq \|\nabla u_1\| \cdot \|u_1 - u_2\|_{L^4}^2 \\
 &\leq \frac{c_1}{\nu} \|f\|_{X'} \|u_1 - u_2\|_{L^6}^2
 \end{aligned} \tag{4.28}$$

Using the embedding of $L^6 \hookrightarrow H^1$

$$| -(((u_1 - u_2) \cdot \nabla)u_1, u_1 - u_2) | \leq \frac{c_1}{\nu} \|f\|_{X'} \|u_1 - u_2\|_1^2 \tag{4.29}$$

We now turn to the other terms using $1 \leq \frac{3\alpha}{2} \leq \alpha + 2$, i.e., $\frac{2}{3} \leq \alpha \leq 4$, we obtain

$$\begin{aligned}
 | - (a|u_1|^\alpha(u_1 - u_2), (u_1 - u_2)) | &= |a|u_1|^\alpha|u_1 - u_2|^2| \\
 &\leq a \| |u_1|^\alpha \|_{\frac{3}{2}} \| |u_1 - u_2|^2 \|_{L^3} \\
 &\leq a \| |u_1|^\alpha \|_{\frac{3\alpha}{2}} \| |u_1 - u_2|^2 \|_{L^6}^2 \\
 &\leq ca \| |u_1|^\alpha \|_{L^{\alpha+2}} \|\nabla(u_1 - u_2)\|^2 \\
 &\leq c_2 a \|f\|_{X'} \|\nabla(u_1 - u_2)\|^2
 \end{aligned} \tag{4.30}$$

The last term on the right of (4.27), and according to $1 \leq \frac{3\alpha}{2} \leq \alpha + 2$, i.e., $\frac{2}{3} \leq \alpha \leq 4$ we obtain

$$| - a((|u_1|^\alpha - |u_2|^\alpha)u_2, (u_1 - u_2)) | \leq c_3 a \alpha \|f\|_{X'} \|\nabla(u_1 - u_2)\|^2 \tag{4.31}$$

Replacing (4.28), (4.30) and (4.31) in (4.27) yields

$$\nu \|\nabla(u_1 - u_2)\|^2 - \left(\frac{c_1}{\nu} \|f\|_{X'} + c_2 a \|f\|_{X'} + c_3 a \alpha \|f\|_{X'} \right) \|\nabla(u_1 - u_2)\|^2 \leq 0$$

We conclude, for ν big enough, that $u_1 = u_2$. ■

The incompressibility constraint makes the Navier Stokes equations with damping (4.4) difficult. A penalty reformulation is therefore introduced to obtain a better behaving problem, where a direct discretization can then be performed.

4.2.2 Perturbed equation

We give the penalty problem.

$$\begin{cases} \nu \Delta u^\varepsilon + (u^\varepsilon \cdot \nabla) u^\varepsilon + \frac{1}{2} (\nabla \cdot u^\varepsilon) u^\varepsilon + a |u^\varepsilon|^\alpha u^\varepsilon + \nabla p^\varepsilon = f & \text{in } \Omega \\ \varepsilon p^\varepsilon + \nabla \cdot u^\varepsilon = 0 & \text{in } \Omega \\ u^\varepsilon = 0 & \text{on } \partial\Omega \end{cases} \quad (4.32)$$

The penalized weak formulation of the equation (4.32) writes for $\varepsilon > 0$

Find $(u^\varepsilon, p^\varepsilon) \in X \times Y$ such that

$$\begin{cases} \nu (\nabla u^\varepsilon, \nabla v) + ((u^\varepsilon \cdot \nabla) u^\varepsilon, v) + \frac{1}{2} ((\nabla \cdot u^\varepsilon), u^\varepsilon \cdot v) + a (|u^\varepsilon|^\alpha u^\varepsilon, v) + \frac{1}{\varepsilon} (\nabla \cdot u^\varepsilon, \nabla \cdot v) = (f, v) \\ \varepsilon (p^\varepsilon, q) + (\nabla \cdot u^\varepsilon, q) = 0 \end{cases} \quad (4.33)$$

for all $v \in X$ and $q \in Y$.

We recall some elementary properties of the functional defined by $T(w, u, v) = ((w \cdot \nabla) u, v) + \frac{1}{2} ((\nabla \cdot w), u \cdot v)$ for $(w, u, v) \in X^3$. T is trilinear and there exists a positive constant $C > 0$ such that

$$T(w, u, v) \leq C \|w\|_1 \|u\|_1 \|v\|_1 \quad \forall (w, u, v) \in X^3 \quad (4.34)$$

Moreover, T satisfies

$$((w \cdot \nabla) v, v) + \frac{1}{2} ((\nabla \cdot w), v \cdot v) = 0 \quad \text{for all } w, v \in X \quad (4.35)$$

and

$$((w \cdot \nabla) u, v) + \frac{1}{2} ((\nabla \cdot w), u \cdot v) = -((w \cdot \nabla) v, u) - \frac{1}{2} ((\nabla \cdot w), v \cdot u) \quad \text{for all } (w, u, v) \in X^3 \quad (4.36)$$

We begin with an existence result.

Existence of weak solution of the perturbed problem

The following theorem asserts that the solution for the perturbed problem (4.32) exists and it is bounded.

Theorem 4.2.7. *Let Ω a bounded domain in \mathbb{R}^d ($d = 2, 3$), $f \in X'$ is a given exterior function.*

Then the perturbed problem (4.32) has a weak solution satisfying

$$\frac{\nu}{2} \|\nabla u^\varepsilon\|^2 + a \|u^\varepsilon\|_{L^{\alpha+2}}^{\alpha+2} + \varepsilon \|p^\varepsilon\|^2 \leq \frac{1}{2\nu} \|f\|_{X'}^2 \quad (4.37)$$

Proof. We consider (w_k) an orthonormal basis of X and (r_j) an orthonormal basis of Y . Let $X_m = \langle w_1, \dots, w_m \rangle$ and $Y_m = \langle r_1, \dots, r_m \rangle$ for some positive integer m . We define the sequence (u_m^ε) and (p_m^ε)

$$u_m^\varepsilon = \sum_{k=1}^m \xi_{km} w_k, \quad p_m^\varepsilon = \sum_{k=1}^m \psi_{km} r_k \quad (4.38)$$

the approximate solution of u^ε and p^ε such that

$$\begin{aligned} \nu(\nabla u_m^\varepsilon, \nabla w_k) + (u_m^\varepsilon \cdot \nabla) u_m^\varepsilon, w_k &+ \frac{1}{2}(\nabla \cdot u_m^\varepsilon, u_m^\varepsilon \cdot w_k) + a(|u_m^\varepsilon|^\alpha u_m^\varepsilon, w_k) \\ &- (p_m^\varepsilon, \nabla \cdot w_k) = (f, w_k) \quad \text{for } k = 1, \dots, m \end{aligned} \quad (4.39)$$

$$\varepsilon(p_m^\varepsilon, r_j) + (\nabla \cdot u_m^\varepsilon, r_j) = 0, \quad \text{for } j = 1, \dots, m \quad (4.40)$$

We multiply by ξ_{km} the equation (4.39) and by ψ_{jm} the equation (4.39) and sum with respect to k and j to get

$$\nu \|\nabla u_m^\varepsilon\|^2 + a \|u_m^\varepsilon\|_{L^{\alpha+2}}^{\alpha+2} + \varepsilon \|p_m^\varepsilon\|^2 = (f, u_m^\varepsilon) \leq \|f\|_{X'} \|\nabla u_m^\varepsilon\| \quad (4.41)$$

Using the Young's inequality to have

$$\frac{\nu}{2} \|\nabla u_m^\varepsilon\|^2 + a \|u_m^\varepsilon\|_{L^{\alpha+2}}^{\alpha+2} + \varepsilon \|p_m^\varepsilon\|^2 \leq \frac{1}{2\nu} \|f\|_{X'}^2 \quad (4.42)$$

For the convergence of the all terms on the left hand side in (4.39), we follow a similar process as in the previous section. the function u^ε satisfies

$$\begin{aligned} \nu(\nabla u^\varepsilon, \nabla w_k) + (u^\varepsilon \cdot \nabla) u^\varepsilon, w_k &+ \frac{1}{2}(\nabla \cdot u^\varepsilon, u^\varepsilon \cdot w_k) + a(|u^\varepsilon|^\alpha u^\varepsilon, w_k) \\ &- (p^\varepsilon, \nabla \cdot w_k) = (f, w_k) \quad \text{for } k = 1, \dots, m \end{aligned} \quad (4.43)$$

For all $\varphi \in H^1(\Omega)$ written as a linear combination of w_k , u^ε and p^ε satisfy

$$\begin{aligned} \nu(\nabla u^\varepsilon, \nabla \varphi) + (u^\varepsilon \cdot \nabla) u^\varepsilon, \varphi &+ \frac{1}{2}(\nabla \cdot u^\varepsilon, u^\varepsilon \cdot \varphi) + a(|u^\varepsilon|^\alpha u^\varepsilon, \varphi) \\ &- (p^\varepsilon, \nabla \cdot \varphi) = (f, \varphi) \quad \forall \varphi \in H^1(\Omega) \end{aligned} \quad (4.44)$$

Using (4.42) to infer that

$$\frac{\nu}{2} \|\nabla u^\varepsilon\|^2 + a \|u^\varepsilon\|_{L^{\alpha+2}}^{\alpha+2} + \varepsilon \|p^\varepsilon\|^2 \leq \frac{1}{2\nu} \|f\|_{X'}^2 \quad (4.45)$$

■

Now let us state the boundness of the quantities u^ε and p^ε and obtain the error estimates between the exact solution and the different iterations.

4.2.3 Error estimates

We consider that $(u^\varepsilon, p^\varepsilon)$ are solutions of the problem (4.32) and let s be the norm

$$s = \sup_{u,v,w \in X} \frac{|((w \cdot \nabla)u \cdot v) + \frac{1}{2}(\nabla \cdot w, u \cdot v)|}{\|w\|_1 \|u\|_1 \|v\|_1} \quad (4.46)$$

Then, the data ν and f are assumed to satisfy

$$\frac{s}{\nu^2} \|f\|_{X'} < 1 \quad (4.47)$$

The equation (4.47) can be written differently; there is a fixed r with $0 < r < 1$ such that

$$\frac{s}{\nu^2} \|f\|_{X'} \leq 1 - r \quad (4.48)$$

The above easy lemma gives the convergence of the different nonlinear terms. We give an indication of the proof of the assertions.

Lemma 4.2.8. *If $u_k \rightarrow u \in X$. Then for all $v \in X$*

$$\begin{aligned} \lim_{k \rightarrow \infty} ((u_k \cdot \nabla)u_k, v) &= ((u \cdot \nabla)u, v) \\ \lim_{k \rightarrow \infty} (\nabla \cdot u_k, u_k \cdot v) &= (\nabla \cdot u, u \cdot v) \\ \lim_{k \rightarrow \infty} (\nabla \cdot u_k, \nabla \cdot v) &= (\nabla \cdot u, \nabla \cdot v) \\ \lim_{k \rightarrow \infty} (|u_k|^\alpha |u_k, v) &= (|u|^\alpha |u, v) \end{aligned} \quad (4.49)$$

Proof. The term $((u_k \cdot \nabla)u_k, v) - ((u \cdot \nabla)u, v)$ can be bounded as

$$\begin{aligned}
 |((u_k \cdot \nabla)u_k, v) - ((u \cdot \nabla)u, v)| &\leq |((u_k - u) \cdot \nabla)u_k, v| + |(u \cdot \nabla)(u_k - u), v| \\
 &\leq \|v\|_{L^6(\Omega)} \|\nabla u_k\| \|u_k - u\|_{L^3(\Omega)} \\
 &\quad + \|u\|_{L^6(\Omega)} \|\nabla u_k\| \|u_k - u\|_{L^3(\Omega)} \\
 &\leq c \|v\|_{H^1(\Omega)} \|\nabla u_k\| \|u_k - u\|_{L^3(\Omega)} \\
 &\quad + C \|\nabla u_k\| \|u_k - u\|_{L^3(\Omega)}
 \end{aligned} \tag{4.50}$$

The second term $(\nabla \cdot u_k, u_k \cdot v) - (\nabla \cdot u, u \cdot v)$ can be cast into

$$\begin{aligned}
 (\nabla \cdot u_k, u_k \cdot v) - (\nabla \cdot u, u \cdot v) &= (\nabla(u_k - u), u_k \cdot v) + (\nabla u, (u_k - u) \cdot v) \\
 &\leq \|\nabla u_k - u\| \|u_k\|_{L^3(\Omega)} \|v\|_{L^6(\Omega)} \\
 &\quad + \|\nabla u\| \|u_k - u\|_{L^3(\Omega)} \|v\|_{L^6(\Omega)} \\
 &\leq c \|\nabla u_k - u\| \|u_k\|_{L^3(\Omega)} \|v\|_{H^1(\Omega)} \\
 &\quad + C \|\nabla u\| \|u_k - u\|_{L^3(\Omega)} \|v\|_{H^1(\Omega)}
 \end{aligned} \tag{4.51}$$

The latest convergence is a straightforward consequence of the Lemma 4.2.5

$$\|(|u_k|^\alpha u_k - |u|^\alpha u)\| \leq C \|\nabla(u_k - u)\|.$$

■

In order to study the convergence, we recall the Inf-sup condition: there exists a constant $\beta > 0$ such that

$$\sup_{v \in X(v \neq 0)} \frac{(q, \nabla \cdot v)}{\|v\|_1} \geq \beta \|\hat{q}\|_Z \quad \text{for all } q \in Y \tag{4.52}$$

where

$$\hat{q} = \{\bar{q} \in Y | \bar{q} - q = \text{constant}\}, \quad Z = \{\hat{q} | q \in Y\} \quad \text{and} \quad \|\hat{q}\|_Z = \inf_{x \in \mathbb{R}} \|q + x\| \tag{4.53}$$

We also define the operators $B \in \mathcal{L}(X, Y')$ and $B^* \in \mathcal{L}(Y, X')$ by

$$(q, \nabla \cdot v) = (q, Bv)_{Y \times Y'} = (B^*q, v)_{X' \times X} \tag{4.54}$$

In such a way that

$$Bv = \nabla \cdot v \quad \text{and} \quad B^*q = \nabla q \tag{4.55}$$

and

$$\text{Ker } B^* = \{q \in Y | (q, \nabla \cdot v) = 0 \text{ for all } v \in X\} = \{\text{constants}\}$$

We show the convergence of the solution sequence of the perturbed problem and we give an error estimate corresponding to the order $O(\varepsilon)$.

Theorem 4.2.9. *Let $(u^\varepsilon, p^\varepsilon)$ be solution of the problem (4.32) and (u, p) the solution in $X \times Y/\mathbb{R}$ of the problem (4.4). Then we have*

$$(p^\varepsilon) \in Y \quad \text{is uniformly bounded in } \varepsilon \quad (4.56)$$

and as $\varepsilon \rightarrow 0$.

$$u^\varepsilon \rightarrow u \quad \text{in } X \quad (4.57)$$

and

$$p^\varepsilon \rightarrow \tilde{p} \quad \text{in } Y \quad (4.58)$$

where \tilde{p} is the orthogonal projection in Y of p onto $(\text{Ker}B^*)^\perp$. And we have the following estimates

$$\|u^\varepsilon - u\|_1 + \|p^\varepsilon - \tilde{p}\| \leq C\varepsilon \quad (4.59)$$

with C is a positive constant non depending of ε .

Proof. We use the second equation in (4.32) into the first equation in (4.33) we obtain

$$-(p^\varepsilon, \nabla \cdot v) = (f, v) - \nu(\nabla u^\varepsilon, \nabla v) - ((u^\varepsilon \cdot \nabla)u^\varepsilon, v) - \frac{1}{2}(\nabla u^\varepsilon, u^\varepsilon \cdot v) - (a|u^\varepsilon|^\alpha u^\varepsilon, v) \quad \text{for all } v \in X$$

Thanks to (4.34) and Lemma 4.2.5

$$|(p^\varepsilon, \nabla \cdot v)| \leq (\|f\|_{X'} + \nu \|u^\varepsilon\|_1 + C_1 \|u^\varepsilon\|_1^2 + C_2 a \|u^\varepsilon\|_1) \|v\|_1 \quad \text{for all } v \in X$$

Applying this in the inf-sup condition with $q = p^\varepsilon \in Y$, and using the fact that ∇u^ε is uniformly bounded, we get

$$\|p^\varepsilon\|_Z \leq \frac{C}{\beta} \quad (4.60)$$

with C is a constant no depending of ε . Using the second equation of (4.32) and the definition of $\text{ker}B^*$

$$(p^\varepsilon, q) = 0 \quad \text{for all } q \in \text{Ker}B^*$$

Then

$$p^\varepsilon \in (\text{Ker}B^*)^\perp \quad \text{in } Y$$

Since

$$\|p^\varepsilon\|_Z = \|p^\varepsilon\|$$

Therefore

$$\|p^\varepsilon\| \leq \frac{C}{\beta} \quad (4.61)$$

(p^ε) is uniformly bounded in ε .

The couple $(u^\varepsilon, p^\varepsilon)$ is uniformly bounded in $X \times Y$. Then there exists a subsequence without lose of generality denoted $(u^\varepsilon, p^\varepsilon)$ convergent to $(u, \tilde{p}) \in X \times Y$. We know already that $(\ker B^*)^\perp$ is closed and convex that is gives $(\ker B^*)^\perp$ is weakly closed and $p^\varepsilon \in (\ker B^*)^\perp \rightarrow \tilde{p} \in (\ker B^*)^\perp$. Let us now show that (u, \tilde{p}) is solution of the problem (4.4). We use the second equation of (4.32), we have

$$(q, \nabla \cdot u^\varepsilon) = -\varepsilon \left(q, -\frac{1}{\varepsilon} \nabla \cdot u^\varepsilon \right) = -\varepsilon (q, p^\varepsilon)$$

Therefore

$$|(q, \nabla \cdot u^\varepsilon)| \leq \varepsilon \|q\| \|p^\varepsilon\| \quad (4.62)$$

And by lemma (4.2.8), $\nabla \cdot u^\varepsilon \rightarrow \nabla \cdot u$ in $L^2(\Omega)$. we get

$$(q, \nabla \cdot u^\varepsilon) \rightarrow (q, \nabla \cdot u) \text{ as } \varepsilon \rightarrow 0$$

Passing to limits in (4.62) and using (4.61) yields

$$(q, \nabla \cdot u) = 0 \text{ for all } q \in Y$$

Therefore the second equation of (4.4) is verified.

Using lemma 4.2.8 and the previous result gives

$$\begin{aligned} \lim_{\varepsilon \rightarrow 0} (\nabla u^\varepsilon, \nabla v) &= (\nabla u, \nabla v) && \text{for all } v \in X \\ \lim_{\varepsilon \rightarrow 0} ((u^\varepsilon \cdot \nabla) u^\varepsilon, \nabla v) &= ((u \cdot \nabla) u, \nabla v) && \text{for all } v \in X \\ \lim_{\varepsilon \rightarrow 0} (\nabla \cdot u^\varepsilon, u^\varepsilon \cdot v) &= 0 && \text{for all } v \in X \\ \lim_{\varepsilon \rightarrow 0} (|u^\varepsilon|^\alpha u^\varepsilon, \nabla v) &= (|u|^\alpha u, \nabla v) && \text{for all } v \in X \\ \lim_{\varepsilon \rightarrow 0} (p^\varepsilon, \nabla \cdot v) &= (p, \nabla \cdot v) && \text{for all } v \in X \end{aligned} \quad (4.63)$$

We replace these limits in the first equation (4.32) implies that the limit of $(u^\varepsilon, p^\varepsilon)$ is solution of the problem (4.4).

Finally, it remains to establish the estimate (4.59). Subtracting the first equation (4.4) from the first equation of (4.32) and using the second equation of (4.32) gives

$$\begin{aligned} (p^\varepsilon - \tilde{p}, \nabla \cdot v) &= \nu (\nabla (u^\varepsilon - u), \nabla v) + ((u^\varepsilon \cdot \nabla) u^\varepsilon, v) - ((u \cdot \nabla) u, v) + \frac{1}{2} (\nabla \cdot u^\varepsilon, u^\varepsilon \cdot v) \\ &\quad + (a |u^\varepsilon|^\alpha u^\varepsilon, v) - (a |u|^\alpha u, v) \quad \forall v \in X \end{aligned} \quad (4.64)$$

Taking $v = u^\varepsilon - u$ yields

$$\begin{aligned} (p^\varepsilon - p, \nabla \cdot (u^\varepsilon - u)) &= \nu \|u^\varepsilon - u\|_1^2 + ((u^\varepsilon \cdot \nabla) u^\varepsilon, u^\varepsilon - u) + \frac{1}{2} (\nabla \cdot u^\varepsilon, u^\varepsilon \cdot (u^\varepsilon - u)) \\ &\quad - ((u \cdot \nabla) u, (u^\varepsilon - u)) + a(|u^\varepsilon|^\alpha u^\varepsilon, (u^\varepsilon - u)) - a(|u|^\alpha u, (u^\varepsilon - u)) \end{aligned} \quad (4.65)$$

Rewriting the fourth term on the right hand side in (4.65),

$$\begin{aligned}
 -((u.\nabla)u, u^\varepsilon - u) &= (((u^\varepsilon - u - u^\varepsilon).\nabla)(u^\varepsilon + u - u^\varepsilon), (u^\varepsilon - u)) \\
 &= (((u^\varepsilon - u).\nabla)u^\varepsilon, (u^\varepsilon - u)) + (((u^\varepsilon - u).\nabla)(u - u^\varepsilon), (u^\varepsilon - u)) \\
 &\quad - ((u^\varepsilon.\nabla)u^\varepsilon, (u^\varepsilon - u)) - ((u^\varepsilon.\nabla)(u - u^\varepsilon), (u^\varepsilon - u))
 \end{aligned}$$

We note that

$$\begin{aligned}
 -((u.\nabla)u, u^\varepsilon - u) &= (((u^\varepsilon - u).\nabla)u, (u^\varepsilon - u)) - ((u^\varepsilon.\nabla)u, (u^\varepsilon - u)) \\
 &\quad \frac{1}{2}(\nabla.(u^\varepsilon - u), u^\varepsilon.(u^\varepsilon - u)) - \frac{1}{2}(\nabla.u^\varepsilon, u^\varepsilon.(u^\varepsilon - u))
 \end{aligned} \tag{4.66}$$

Replacing the previous result in (4.65) yields to

$$\begin{aligned}
 (p^\varepsilon - \tilde{p}, \nabla.(u^\varepsilon - u)) &= \nu \| u^\varepsilon - u \|_1^2 + (((u^\varepsilon - u).\nabla)u^\varepsilon, (u^\varepsilon - u)) \\
 &\quad + \frac{1}{2}(\nabla.(u^\varepsilon - u), u^\varepsilon.(u^\varepsilon - u)) + a(|u^\varepsilon|^\alpha u^\varepsilon - |u|^\alpha u, (u^\varepsilon - u)) \\
 &\geq \nu \| u^\varepsilon - u \|_1^2 - s \| u^\varepsilon - u \|_1^2 \| u^\varepsilon \|_1
 \end{aligned} \tag{4.67}$$

We use the fact that (u^ε) is bounded and by the inequality (4.48) we obtain

$$\| u^\varepsilon \|_1 \leq \frac{\nu}{s}(1 - r)$$

Consequently

$$((p^\varepsilon - \tilde{p}), \nabla.(u^\varepsilon - u)) \geq \nu r \| u^\varepsilon - u \|_1^2$$

By the second equation in (4.32) we have

$$\| u^\varepsilon - u \|_1^2 \leq \frac{\varepsilon}{\nu r} (\tilde{p} - p^\varepsilon, p^\varepsilon) = \frac{\varepsilon}{\nu r} (\tilde{p} - p^\varepsilon, \tilde{p}) - \frac{\varepsilon}{\nu r} \| \tilde{p} - p^\varepsilon \|^2 \tag{4.68}$$

Therefore

$$\| u^\varepsilon - u \|_1^2 \leq \frac{\varepsilon}{\nu r} \| \tilde{p} - p^\varepsilon \| \| \tilde{p} \|. \tag{4.69}$$

We now observe that

$$((u^\varepsilon.\nabla)u^\varepsilon, v) = (((u^\varepsilon.\nabla)u^\varepsilon, v)) + ((u.\nabla)u^\varepsilon, v) \tag{4.70}$$

$$-((u.\nabla)u, v) = ((u.\nabla)(u^\varepsilon - u), v) - ((u.\nabla)u^\varepsilon, v) \tag{4.71}$$

$$\frac{1}{2}(\nabla.u^\varepsilon, u^\varepsilon.v) = \frac{1}{2}(\nabla.(u^\varepsilon - u), u^\varepsilon.v) \tag{4.72}$$

Injecting (4.70)-(4.72) in (4.64) to get

$$\begin{aligned} (p^\varepsilon - \tilde{p}, \nabla \cdot v) &= \nu(\nabla(u^\varepsilon - u), \nabla v) + (((u^\varepsilon - u) \cdot \nabla)u^\varepsilon, v) + ((u \cdot \nabla)(u^\varepsilon - u), v) \\ &\quad + \frac{1}{2}(\nabla \cdot (u^\varepsilon - u), u^\varepsilon \cdot v) + a(|u^\varepsilon|^\alpha u^\varepsilon - |u|^\alpha u, v) \end{aligned} \quad (4.73)$$

Using (4.73) in the condition inf-sup (4.52) gives with $q = p - \tilde{p}$

$$\|p^\varepsilon - \tilde{p}\|_Z \leq \frac{1}{\beta} (\nu \|u^\varepsilon - u\|_1 + s(\|u^\varepsilon\|_1 + \|u\|_1) \|u^\varepsilon - u\|_1 + C_1 a \|u^\varepsilon - u\|_1)$$

Note that $p^\varepsilon, \tilde{p} \in (\ker B^*)^\perp$, and from (4.48) we obtain

$$\|p^\varepsilon - \tilde{p}\| \leq \frac{1}{\beta} (\nu + 2(1-r)\nu + C_1 a) \|u^\varepsilon - u\|_1$$

Therefore

$$\|p^\varepsilon - \tilde{p}\| \leq \frac{A}{\beta} \|u^\varepsilon - u\|_1 \quad (4.74)$$

where $A = (3 - 2r)\nu + C_1 a$.

Putting (4.74) in (4.69) to have

$$\|u^\varepsilon - u\|_1 \leq \frac{A}{\nu r \beta} \|\tilde{p}\| \varepsilon. \quad (4.75)$$

Finally, we substitute (4.75) in (4.74) to infer that

$$\|p^\varepsilon - \tilde{p}\| \leq \frac{A^2}{\nu r \beta^2} \|\tilde{p}\| \varepsilon. \quad (4.76)$$

■

Remark 4.2.1. *The inequality (4.61) shows that the perturbed pressure (p^ε) is uniformly bounded in ε .*

4.3 Control problem

Shape optimization is the process of finding the optimal shape of a domain that minimizes a given criterion called objective function with respect to a set of design variables. To make the calculation of the gradients easier we use the based adjoint system techniques.

4.3.1 Adjoint system

We begin by deriving the adjoint system associated with the penalized model (4.77).

$$\begin{cases} -\nu\Delta u^\varepsilon + (u^\varepsilon \cdot \nabla)u^\varepsilon + \frac{1}{2}(\nabla \cdot u^\varepsilon)u^\varepsilon + a|u^\varepsilon|^\alpha u^\varepsilon + \nabla p^\varepsilon = f & \text{in } \Omega \\ \nabla \cdot u^\varepsilon + \varepsilon p^\varepsilon = 0 & \text{in } \Omega \\ u^\varepsilon = 0 & \text{on } \partial\Omega \end{cases} \quad (4.77)$$

and compute the shape gradient of the cost function in terms of state and adjoint variables.

We define the objective function that combines two constraints: A comfort constraint and a turbulence reduction constraint.

$$J(\Omega) = J_1(\Omega) + J_2(\Omega) \quad (4.78)$$

where

$$J_1(\Omega) = \frac{1}{2} \int_{\Omega} |u^\varepsilon - u_d|^2 dx, \text{ and } J_2(\Omega) = \frac{\sigma}{2} \int_{\Omega} |\text{curl}(u^\varepsilon)|^2 dx$$

and u_d is a target velocity.

We introduce also the following function

$$\begin{aligned} F(\Omega, u, p, v, q) = & \int_{\Omega} \left(\nu \nabla u^\varepsilon : \nabla v + (u^\varepsilon \cdot \nabla)u^\varepsilon \cdot v + \frac{1}{2}(\nabla \cdot u^\varepsilon)u^\varepsilon \cdot v + a|u^\varepsilon|^\alpha u^\varepsilon \cdot v - p^\varepsilon \nabla \cdot v \right) dx \\ & - \int_{\Omega} q \nabla \cdot u^\varepsilon dx - \varepsilon \int_{\Omega} q p^\varepsilon dx - \int_{\Omega} f \cdot v dx \end{aligned} \quad (4.79)$$

We define the set of admissible domains

$$\Omega_{ad} = \{ \Omega \subset \mathbb{R}^2 | \Omega \text{ with piecewise } C^{1,1} \text{ boundary and } \partial\Omega \text{ is fixed} \}$$

Then the optimization problem can be expressed as

$$\begin{aligned} \min_{\Omega \in \Omega_{ad}} J(\Omega) = & \frac{1}{2} \int_{\Omega} |u^\varepsilon - u_d|^2 dx + \frac{\sigma}{2} \int_{\Omega} |\text{curl}(u^\varepsilon)|^2 dx \\ & \text{such that } (u^\varepsilon, p^\varepsilon) \text{ satisfies the equation (4.77)} \end{aligned} \quad (4.80)$$

Without loss of generality, we assume that the function f is zero.

Let state the result which describes the adjoint system related to the general penalized problem (4.77).

Theorem 4.3.1. *Let $(u^\varepsilon, p^\varepsilon) \in \hat{V}_0(\Omega) \times Y$. The adjoint system associated to the equation (4.77)*

$$\begin{aligned}
 & -\nu\Delta v + (\nabla u^\varepsilon)^T \cdot v - (u^\varepsilon \cdot \nabla)v - \frac{1}{2}\nabla(u^\varepsilon \cdot v) + \frac{1}{2}(\nabla \cdot u^\varepsilon)v + a|u^\varepsilon|^{\alpha-2}(|u^\varepsilon|^2v + \alpha(u^\varepsilon \cdot v)u^\varepsilon) \\
 & + \nabla q = (u^\varepsilon - u_d) - \sigma \underline{\text{curl}}(\text{curl}(u^\varepsilon))
 \end{aligned}$$

An arbitrary \tilde{u} in $\partial\Omega$ gives

$$\nu \frac{\partial v}{\partial n} - nq = \sigma \text{curl}(u^\varepsilon) \cdot \tau \quad \text{on } \partial\Omega$$

Finally we obtain the adjoint system

$$\left\{ \begin{array}{ll}
 -\nu\Delta v + (\nabla u^\varepsilon)^T \cdot v - (u^\varepsilon \cdot \nabla)v - \frac{1}{2}\nabla(u^\varepsilon \cdot v) + \frac{1}{2}(\nabla \cdot u^\varepsilon)v + a|u^\varepsilon|^{\alpha-2}(|u^\varepsilon|^2v + \alpha(u^\varepsilon \cdot v)u^\varepsilon) \\
 + \nabla q = (u^\varepsilon - u_d) - \sigma \underline{\text{curl}}(\text{curl}(u^\varepsilon)) & \text{in } \Omega \\
 \nabla \cdot v + \varepsilon q = 0 & \text{in } \Omega \\
 \nu \frac{\partial v}{\partial n} - nq = \sigma \text{curl}(u^\varepsilon) \cdot \tau & \text{on } \partial\Omega
 \end{array} \right. \quad (4.84)$$

■

4.3.2 Shape gradient

In this subsection, we express the shape gradient using the state and adjoint systems.

Consider Ω be a reference domain in \mathbb{R}^d , the perturbation of Ω by the velocity method is described as the flow defined by the initial value problem

$$\left\{ \begin{array}{l}
 \frac{d\chi}{dt}(t, \mathbf{X}) = \mathbf{V}(t, \chi(t)) \\
 \chi(0, \mathbf{X}) = \mathbf{X}
 \end{array} \right. \quad (4.85)$$

We consider the mapping T_t such that $T_t(\mathbf{X}) = \chi(t, \mathbf{X})$, $\forall \mathbf{X} \in \Omega$.

Let Ω_t be a perturbation domain of Ω and $J(\Omega)$ be a functional associated to Ω_t . The shape derivative of the functional $J(\Omega_t)$ at Ω in the direction of the deformation field \mathbf{V} is written as

$$dJ(\Omega; \mathbf{V}) = \lim_{t \rightarrow 0} \frac{1}{t} (J(\Omega_t) - J(\Omega)).$$

If $dJ(\Omega; \mathbf{V})$ exists for all $\mathbf{V} \in \mathcal{C}([0, T]; (\mathcal{D}^k(\mathbb{R}^d))^2)$, for small positive constant T , the functional J is called shape differentiable at Ω and its shape gradient satisfies

$$dJ(\Omega, \mathbf{V}) = (\nabla J, \mathbf{V})_{((\mathcal{D}^k(\mathbb{R}^d))^2)' \times (\mathcal{D}^k(\mathbb{R}^d))^2}$$

We define the velocity field admissible domain as follow

$$V_{ad} = \{ \mathbf{V} \in \mathcal{C}^0(0, \tau; (\mathcal{C}^2(\mathbb{R}^d))^2) \mid \mathbf{V} = 0 \quad \text{on } \partial\Omega \}$$

The use of the velocity \mathbf{V} for $t \geq 0$, implies the transformation of the domain Ω into $\Omega_t = T_t(\Omega)$ by the velocity method with formulation (4.85).

Let us find an expression of the derivative of the saddle point problem $j(t)$ with respect to t , where

$$j(t) = \min_{(u_t^\varepsilon, p_t^\varepsilon) \in V_0(\Omega_t) \times Y(\Omega_t)} \max_{(v_t, q_t) \in V_0(\Omega_t) \times Y(\Omega_t)} L(\Omega_t, u_t^\varepsilon, p_t^\varepsilon, v_t, q_t)$$

where (u_t, p_t) and (v_t, q_t) are solutions of (4.77) and (4.81) in the perturbed domain Ω_t , respectively.

We consider the Hilbert spaces which depend on the parameter t defined by

$$V_0(\Omega_t) = \{u^\varepsilon \circ T_t^{-1} : u^\varepsilon \in V_0(\Omega)\}$$

$$Y(\Omega_t) = \{p^\varepsilon \circ T_t^{-1} : p^\varepsilon \in Y(\Omega)\}$$

Since T_t and T_t^{-1} are diffeomorphisms, the parametrisation do not influence $j(t)$, and we have

$$j(t) = \min_{(u^\varepsilon, p^\varepsilon) \in V_0(\Omega) \times Y(\Omega)} \max_{(v, q) \in V_0(\Omega) \times Y(\Omega)} L(\Omega_t, u^\varepsilon \circ T_t^{-1}, p^\varepsilon \circ T_t^{-1}, v \circ T_t^{-1}, q \circ T_t^{-1})$$

We introduce the following functions which depend on the parameter t

$$l_1(t) = \frac{1}{2} \int_{\Omega_t} |u^\varepsilon \circ T_t^{-1} - u_d|^2 dx + \frac{\sigma}{2} \int_{\Omega_t} |\text{curl}(u^\varepsilon \circ T_t^{-1})|^2 dx,$$

$$\begin{aligned} l_2(t) &= \int_{\Omega_t} [\nu \nabla(u^\varepsilon \circ T_t^{-1}) : \nabla(v \circ T_t^{-1}) + ((u^\varepsilon \circ T_t^{-1}) \cdot \nabla)(u^\varepsilon \circ T_t^{-1}) \cdot (v \circ T_t^{-1}) \\ &\quad + a |u^\varepsilon \circ T_t^{-1}|^\alpha (u^\varepsilon \circ T_t^{-1}) \cdot (v \circ T_t^{-1}) - (p^\varepsilon \circ T_t^{-1}) \nabla \cdot (v \circ T_t^{-1}) - (f \circ T_t^{-1}) \cdot (v \circ T_t^{-1})] dx \\ &\quad - \int_{\Omega_t} (q \circ T_t^{-1}) \nabla \cdot (u^\varepsilon \circ T_t^{-1}) dx - \varepsilon \int_{\Omega_t} (q \circ T_t^{-1}) (p^\varepsilon \circ T_t^{-1}) dx \end{aligned}$$

The Lagrangian functional writes

$$L(\Omega_t, u^\varepsilon \circ T_t^{-1}, p^\varepsilon \circ T_t^{-1}, v \circ T_t^{-1}, q \circ T_t^{-1}) = l_1(t) - l_2(t)$$

If $\Phi : [0, \tau] \times \mathbb{R}^d \rightarrow \mathbb{R}$ is sufficiently smooth, we have the following Hadamard's formula

$$\frac{d}{dt} \int_{\Omega_t} \Phi(t, x) dx|_{t=0} = \int_{\Omega} \frac{\partial \Phi}{\partial t}(0, x) dx + \int_{\partial \Omega} \Phi(0, x) \mathbf{V}(0, X) \cdot \mathbf{n} ds \quad (4.86)$$

Let $\mathbf{V}(0, X) \in V_{ad}$, and observe that $\mathbf{V}(0, X) = \mathbf{V}$. Therefore we can derive the shape gradient using the formula (4.86):

$$\frac{d}{dt} L(\Omega_t, u^\varepsilon \circ T_t^{-1}, p^\varepsilon \circ T_t^{-1}, v \circ T_t^{-1}, q \circ T_t^{-1})|_{t=0} = l'_1(0) - l'_2(0) \quad (4.87)$$

where

$$\begin{aligned} l'_1(0) &= \int_{\Omega} (u^\varepsilon - u_d) \cdot (-\nabla u^\varepsilon \cdot \mathbf{V}) dx + \sigma \int_{\Omega} \text{curl}(u^\varepsilon) \text{curl}(-\nabla u^\varepsilon \cdot \mathbf{V}) dx \\ &\quad + \frac{1}{2} \int_{\partial \Omega} (|u^\varepsilon - u_d|^2 \mathbf{V} \cdot \mathbf{n}) ds + \frac{\sigma}{2} \int_{\partial \Omega} (|\text{curl}(u^\varepsilon)|^2 \mathbf{V} \cdot \mathbf{n}) ds \end{aligned} \quad (4.88)$$

$$\begin{aligned}
l'_2(0) &= \int_{\Omega} [\nu \nabla(-\nabla u^\varepsilon \cdot \mathbf{V}) : \nabla v + \nu \nabla u^\varepsilon : \nabla(-\nabla v \cdot \mathbf{V}) \\
&\quad + ((-\nabla u^\varepsilon \cdot \mathbf{V}) \cdot \nabla u^\varepsilon) \cdot v + (u^\varepsilon \cdot \nabla(-\nabla u^\varepsilon \cdot \mathbf{V})) \cdot v + (u^\varepsilon \cdot \nabla u^\varepsilon) \cdot (-\nabla v \cdot \mathbf{V}) \\
&\quad + \frac{1}{2} \nabla \cdot (-\nabla u^\varepsilon \cdot \mathbf{V}) u^\varepsilon \cdot v + \frac{1}{2} \nabla \cdot u^\varepsilon (-\nabla u^\varepsilon \cdot \mathbf{V}) \cdot v + \frac{1}{2} \nabla \cdot u^\varepsilon u^\varepsilon \cdot (-\nabla v \cdot \mathbf{V}) \\
&\quad + a\alpha |u^\varepsilon|^{\alpha-2} (-\nabla u^\varepsilon \cdot \mathbf{V} \cdot u^\varepsilon) (u^\varepsilon \cdot v) + a |u^\varepsilon|^\alpha (-\nabla u^\varepsilon \cdot \mathbf{V}) \cdot v \\
&\quad + a |u^\varepsilon|^\alpha u^\varepsilon \cdot (-\nabla v \cdot \mathbf{V}) - (f \cdot \mathbf{V}) \cdot v - f \cdot ((-\nabla v) \cdot \mathbf{V}) - (\nabla p^\varepsilon \cdot \mathbf{V}) \nabla \cdot v \\
&\quad - p^\varepsilon \nabla \cdot (-\nabla v \cdot \mathbf{V}) - q \nabla \cdot (-\nabla u^\varepsilon \cdot \mathbf{V}) - (\nabla \cdot u^\varepsilon) (-\nabla q \cdot \mathbf{V})] dx
\end{aligned}$$

Using Green's formula and the condition $u^\varepsilon = 0$ on $\partial\Omega$, we obtain

$$\begin{aligned}
l'_2(0) &= - \int_{\Omega} [(-\nu \Delta u^\varepsilon + (u^\varepsilon \cdot \nabla) u^\varepsilon + \frac{1}{2} \nabla \cdot u^\varepsilon u^\varepsilon + a |u^\varepsilon|^\alpha u^\varepsilon + \nabla p^\varepsilon - f) \cdot (\nabla v \cdot \mathbf{V})] dx \\
&\quad + \int_{\Omega} (\nabla \cdot u^\varepsilon) (\nabla q \cdot \mathbf{V}) dx + \int_{\Omega} (\nabla \cdot v) (\nabla p \cdot \mathbf{V}) dx + \int_{\Omega} [-\nu \Delta v + (\nabla u^\varepsilon)^T \cdot v - (u^\varepsilon \cdot \nabla) v \\
&\quad - \frac{1}{2} \nabla \cdot (u^\varepsilon \cdot v) + \frac{1}{2} (\nabla \cdot u^\varepsilon) v + a |u^\varepsilon|^{\alpha-2} (|u^\varepsilon|^2 v + \alpha (u^\varepsilon \cdot v) u^\varepsilon) - \nabla q] \cdot (\nabla u^\varepsilon \cdot \mathbf{V}) dx \\
&\quad - \int_{\partial\Omega} [\nu \frac{\partial v}{\partial \mathbf{n}} - nq] \cdot (\nabla u^\varepsilon \cdot \mathbf{V}) ds - \int_{\partial\Omega} [\frac{\partial u^\varepsilon}{\partial \mathbf{n}} - np^\varepsilon] \cdot (\nabla v \cdot \mathbf{V}) ds \\
&\quad + \int_{\partial\Omega} [\nu \nabla u^\varepsilon : \nabla v + (u^\varepsilon \cdot \nabla u^\varepsilon) \cdot v + a |u^\varepsilon|^\alpha u^\varepsilon \cdot v - p^\varepsilon \nabla \cdot v - q \nabla \cdot u^\varepsilon] \mathbf{V} \cdot \mathbf{n} ds
\end{aligned} \tag{4.89}$$

Replacing (4.161) and (4.89) in (4.87) and using the fact that $(u^\varepsilon, p^\varepsilon)$ is solution of (4.77) and (v, q) is solution of (4.81) respectively yields to

$$\begin{aligned}
dJ(\Omega; \mathbf{V}) &= \frac{d}{dt} L|_{t=0} \\
&= \frac{1}{2} \int_{\partial\Omega} ((|u^\varepsilon - u_d|^2 + \sigma |\operatorname{curl}(u^\varepsilon)|^2) \mathbf{V} \cdot \mathbf{n}) ds + \int_{\partial\Omega} [\nu \frac{\partial v}{\partial \mathbf{n}} - nq] \cdot (\nabla u^\varepsilon \cdot \mathbf{V}) ds \\
&\quad + \int_{\partial\Omega} [\nu \frac{\partial u^\varepsilon}{\partial \mathbf{n}} - np] \cdot (\nabla v \cdot \mathbf{V}) ds - \int_{\partial\Omega} [(\nu \nabla u^\varepsilon : \nabla v) \mathbf{V} \cdot \mathbf{n} ds \\
&\quad - \sigma \int_{\partial\Omega} (\frac{\partial u^\varepsilon}{\partial \mathbf{n}} \cdot (\operatorname{curl}(u^\varepsilon) \wedge \mathbf{n})) \mathbf{V} \cdot \mathbf{n} ds
\end{aligned} \tag{4.90}$$

Note that $u^\varepsilon = 0, v = 0$ in $\partial\Omega$ we have

$$\mathbf{n} \cdot (\nabla u^\varepsilon \cdot \mathbf{V}) = \nabla u^\varepsilon \cdot (\mathbf{n} \otimes \mathbf{n}) \cdot \mathbf{V} \cdot \mathbf{n} = \nabla u^\varepsilon \cdot \mathbf{n} \cdot \mathbf{n} (\mathbf{V} \cdot \mathbf{n}) = (\nabla \cdot u^\varepsilon) (\mathbf{V} \cdot \mathbf{n}) = 0, \quad \forall x \in \partial\Omega \tag{4.91}$$

$$\frac{\partial v}{\partial \mathbf{n}} \cdot (\nabla u^\varepsilon \cdot \mathbf{V}) = \nabla u^\varepsilon \cdot (\mathbf{n} \otimes \mathbf{n}) \cdot \mathbf{V} \cdot \frac{\partial v}{\partial \mathbf{n}} = \frac{\partial u^\varepsilon}{\partial \mathbf{n}} \cdot \frac{\partial v}{\partial \mathbf{n}} (\mathbf{V} \cdot \mathbf{n}) = (\nabla u^\varepsilon : \nabla v) \mathbf{V} \cdot \mathbf{n} \tag{4.92}$$

With a similar manner we obtain

$$\mathbf{n} \cdot (\nabla v \cdot \mathbf{V}) = 0, \quad \frac{\partial u^\varepsilon}{\partial \mathbf{n}} \cdot (\nabla v \cdot \mathbf{V}) = \frac{\partial u^\varepsilon}{\partial \mathbf{n}} \cdot \frac{\partial v}{\partial \mathbf{n}} (\mathbf{V} \cdot \mathbf{n}) = (\nabla u^\varepsilon : \nabla v) \mathbf{V} \cdot \mathbf{n} \quad (4.93)$$

Substituting (4.91)-(4.93) in (4.90) the shape derivative takes the form

$$dJ(\Omega; \mathbf{V}) = \int_{\partial\Omega} \left[\frac{1}{2} |u^\varepsilon - u_d|^2 + \frac{\sigma}{2} |\operatorname{curl}(u^\varepsilon)|^2 + \frac{\partial u^\varepsilon}{\partial \mathbf{n}} \cdot \left(\nu \frac{\partial v}{\partial \mathbf{n}} + \sigma \operatorname{curl}(u^\varepsilon) \wedge \mathbf{n} \right) \right] \mathbf{V} \cdot \mathbf{n} \, ds \quad (4.94)$$

Consequently, the shape gradient writes

$$\nabla J = \left[\frac{1}{2} |u^\varepsilon - u_d|^2 + \frac{\sigma}{2} |\operatorname{curl}(u^\varepsilon)|^2 + \frac{\partial u^\varepsilon}{\partial \mathbf{n}} \cdot \left(\nu \frac{\partial v}{\partial \mathbf{n}} + \sigma \operatorname{curl}(u^\varepsilon) \wedge \mathbf{n} \right) \right] \mathbf{n} \quad (4.95)$$

4.4 Finite element method

In this section, we give the discrete formulation for the penalized problem. To this end, we first introduce the finite element space Ω_h of Ω . Let $\bar{\Omega}_h = \cup_k \bar{T}_k$, with $\{T_k\}$ is a partition of Ω into non overlapping elements. Let us introduce the finite element dimensional space X^h of $X = (H_0^1(\Omega))^d$, $d=2$ or 3 as follow

$$X^h = \left\{ v \in (C(\bar{\Omega}))^d \mid v|_{T_k} \in Q^k \text{ for all } T_k \subset \Omega_h \right\} \quad (4.96)$$

where Q^k is the space of polynomials functions of degree d^*k given by

$$Q^k = \operatorname{span} \left\{ \prod_{i=1}^d x_i^{b_i} \mid 0 \leq b_i \leq k \right\} \quad (4.97)$$

We define the integration rule $I(\cdot)$ by

$$\int_{\Omega} g \, dx \simeq I(g) = \sum_{k=1}^E \sum_{i=1}^{G_k} g(x_i^k) w_i^k \quad (4.98)$$

where $x_i^k \in \bar{\Omega}_k$, are the integration point coordinates, w_i^k , $1 \leq i \leq G_k$, $1 \leq k \leq E$, are the integration weights of the Gauss rule $I(\cdot)$ on any element Ω_k . E is the number of elements in the mesh and G_k is the number of points integration in one element Ω_k .

The pressure space Y^h is piecewise discontinuous defined with the points in the integration above. We have for any $q_h \in Y^h$

$$I(q_h \nabla \cdot v_h) = (q_h, \nabla \cdot v_h) \quad \text{for all } v_h \in X^h \quad (4.99)$$

For $f \in (X^h)'$, and for $\varepsilon > 0$ fixed we introduce the approximate perturbed problem reads as

Find $u_h^\varepsilon \in X^h$ such that

$$\begin{aligned} \nu(\nabla u_h^\varepsilon, \nabla v) + ((u_h^\varepsilon \cdot \nabla) u_h^\varepsilon, v_h) + \frac{1}{2}(\nabla \cdot u_h^\varepsilon, u_h^\varepsilon \cdot v_h) + a(|u_h^\varepsilon|^\alpha u_h^\varepsilon, v_h) \\ + \frac{1}{\varepsilon} I((\nabla \cdot u_h^\varepsilon)(\nabla \cdot v_h)) = (f, v_h) \quad \text{for all } v_h \in X^h \end{aligned} \quad (4.100)$$

Moreover, the approximate pressure verifies

$$p_h^\varepsilon(x_i^e) = -\frac{1}{\varepsilon} \nabla \cdot u_h^\varepsilon(x_i^e), \quad 1 \leq i \leq G, \quad 1 \leq e \leq E \quad (4.101)$$

We assume again that the condition (4.48) is satisfied by f

$$\frac{sh}{\nu} \|f\|_{(X^h)'} \leq \frac{s}{\nu^2} \|f\|_{X'} \leq 1 - r \quad (4.102)$$

The next result focuses on the existence of a weak solution for the approximate perturbed problem (4.100).

Theorem 4.4.1. *Assume that the regularity of the data (4.102) holds for $h, \varepsilon > 0$. We have the following proprieties*

1. *There exists a solution to the approximate perturbed problem (4.100).*
2. *The sequence $(u_h^\varepsilon) \in X^h$ is uniformly bounded in ε .*
3. *The following estimates*

$$\frac{\nu}{2} \|\nabla u_h^\varepsilon\|^2 + a \|u_h^\varepsilon\|_{L^{\alpha+2}}^{\alpha+2} + \varepsilon \|p_h^\varepsilon\|^2 \leq \frac{1}{2\nu} \|f\|_{X'}^2 \quad (4.103)$$

hold.

Proof. We follow similar steps as for the continuous problem in theorem 4.2.1 to obtain

$$\|u_h^\varepsilon\|_{X^h} \leq \frac{1}{\nu} \|f\|_{(X^h)'} \quad (4.104)$$

■

We set the Inf-sup stability condition for the approximate problem. We suppose, there exists a constant $\beta_h > 0$, such that

$$\sup_{v_h \in X^h} \frac{I(q_h \nabla \cdot v_h)}{\|v_h\|_V} \geq \beta_h \|\hat{q}_h\|_{Z^h} \quad \text{for all } q_h \in Y^h \quad (4.105)$$

We introduce the finite element space Z^h with

$$\hat{q}_h = \left\{ \bar{q}_h \in Y^h \mid \bar{q}_h - q_h \in \text{Ker } B_h^* \right\} \quad (4.106)$$

We also define the operators $B_h \in \mathcal{L}(X^h, (Y^h)'), B_h^* \in \mathcal{L}(Y^h, (X^h)'),$ by

$$I(q_h \nabla \cdot v_h) = (q_h, B_h v_h)_{(Y^h)' \times Y^h} = (B_h^* q_h, v_h)_{(X^h)' \times X^h}, \quad \text{for all } (v_h, q_h) \in X^h \times Y^h \quad (4.107)$$

The kernel of the operator B_h^* is defined by

$$\text{Ker } B_h^* = \left\{ q_h \in Y^h \mid I(q_h \nabla \cdot v_h) = 0 \quad \forall v_h \in X^h \right\} \quad (4.108)$$

The norm on Z^h in (4.105) writes

$$\| \hat{q}_h \|_{Z^h} = \inf_{q_h^0 \in \text{Ker } B_h^*} \| q_h^0 + q_h \| \quad (4.109)$$

The main idea of these results is that the pressure is bounded in ε and that the solution for the approximate penalized problem (4.100) converges to the solution of a boundary approximate problem.

Theorem 4.4.2. *Consider that u_h^ε is solution of the problem (4.100) in X^h and the pressure p_h^ε defined by (4.101) in Y^h . Then*

- (i) *The approximate discrete pressure p_h^ε is uniformly bounded in ε .*
- (ii) *The couple $(u_h^\varepsilon, p_h^\varepsilon)$ converges to the solution (u_h, p_h) of the problem*

Find $(u_h, p_h) \in X^h \times Y^h$ such that

$$\begin{cases} \nu(\nabla u_h, \nabla v_h) + ((u_h \cdot \nabla) u_h, v_h) + \frac{1}{2}((\nabla \cdot u_h), u_h \cdot v_h) + a(|u_h|^\alpha u_h, v_h) \\ - (p_h, \nabla \cdot v_h) = (f, v_h) \quad \text{for all } v_h \in X^h \\ (q_h, \nabla \cdot u_h) = 0 \quad \text{for all } q_h \in Y^h \end{cases} \quad (4.110)$$

Proof. The theorem 4.4.1 ensures that $(u_h^\varepsilon) \in X^h$ is uniformly bounded in ε .

Replacing (4.101) in (4.100)

$$\begin{aligned} I(p_h^\varepsilon \nabla \cdot v_h) = & - (f, v_h) + \nu(\nabla u_h^\varepsilon, \nabla v) + ((u_h^\varepsilon \cdot \nabla) u_h^\varepsilon, v_h) \\ & + \frac{1}{2}(\nabla \cdot u_h^\varepsilon, u_h^\varepsilon \cdot v_h) + a(|u_h^\varepsilon|^\alpha u_h^\varepsilon, v_h) \end{aligned}$$

Substituting this results in the discrete inf-sup condition (4.105),

$$\| \hat{p}_h^\varepsilon \|_{Z^h} \leq \frac{1}{\beta_h} \left\{ \| f \|_{(X^h)'} + \nu \| u_h^\varepsilon \|_1 + c_1 \| u_h^\varepsilon \|_1^2 + c_2 \| u_h^\varepsilon \|_1 \right\} \leq \frac{C}{\beta_h}. \quad (4.111)$$

Or $p_h^\varepsilon \in (\text{Ker } B_h^*)^\perp$, we infer that

$$\| p_h^\varepsilon \|_{Z^h} = \| p_h^\varepsilon \|$$

Therefore, (4.111) gives

$$\| p_h^\varepsilon \| \leq \frac{C}{\beta_h} \quad (4.112)$$

Since C is independent of ε .

The sequence $(u_h^\varepsilon, p_h^\varepsilon)$ is bounded, then there exists a subsequence denoted $(u_h^\varepsilon, p_h^\varepsilon)$ without lose of generality which converge to $(u_h, p_h) \in X^h \times Y^h$. And we have

$$\lim_{\varepsilon \rightarrow 0} I(q_h \nabla \cdot u_h^\varepsilon) = I(q_h \nabla u_h), \quad \text{for all } q_h \in Y^h \quad (4.113)$$

Using (4.101),

$$I(q_h \nabla \cdot u_h^\varepsilon) = -\varepsilon I(q_h p_h^\varepsilon) \leq \varepsilon \| q_h \| \| p_h^\varepsilon \|$$

We use the fact that (p_h^ε) is bounded, and we pass to limits as $\varepsilon \rightarrow 0$ to obtain

$$I(q_h \nabla \cdot v_h) = 0$$

Therefore the second equation of (4.110) is established. For the first equation of (4.110) we use

$$\begin{aligned} \lim_{\varepsilon \rightarrow 0} \nu(\nabla u_h^\varepsilon, \nabla v_h) &= \nu(\nabla u_h, \nabla v_h) && \text{for all } v_h \in X^h \\ \lim_{\varepsilon \rightarrow 0} ((u_h^\varepsilon \cdot \nabla) u_h^\varepsilon, v_h) &= ((u_h \cdot \nabla) u_h, v_h) && \text{for all } v_h \in X^h \\ \lim_{\varepsilon \rightarrow 0} \frac{1}{2}(\nabla \cdot u_h^\varepsilon, u_h^\varepsilon \cdot v_h) &= \frac{1}{2}(\nabla \cdot u_h, u_h \cdot v_h) && \text{for all } v_h \in X^h \\ \lim_{\varepsilon \rightarrow 0} (|u_h^\varepsilon|^\alpha u_h^\varepsilon, v_h) &= (|u_h|^\alpha u_h, v_h) && \text{for all } v_h \in X^h \\ \lim_{\varepsilon \rightarrow 0} (p_h^\varepsilon, \nabla \cdot v_h) &= (p_h, \nabla \cdot v_h) && \text{for all } v_h \in X^h \end{aligned}$$

■

We are now in a position to give an priori estimates of the error for the solution of the discrete penalized problem (4.100) and the solution of the approximate state problem (4.110).

Lemma 4.4.3. *Consider $(u_h^\varepsilon, p_h^\varepsilon) \in X^h \times Y^h$ defined by (4.100) and $(u_h, p_h) \in X^h \times Y^h$ solution of the problem (4.110). Then*

$$\| u_h^\varepsilon - u_h \|_1 \leq \varepsilon \frac{C_1}{\beta_h} \| p_h \| \quad (4.114)$$

and

$$\| p_h^\varepsilon - p_h \| \leq \varepsilon \frac{C_2}{\beta_h^2} \| p_h \| \quad (4.115)$$

where C_1 and C_2 are two positive constant non depending in ε .

Proof. We use the definition of the discrete pressure in (4.101) in the equation (4.100) and we

subtract (4.110) to have

$$\begin{aligned} & \nu(\nabla(u_h^\varepsilon - u_h), \nabla v_h) + ((u_h^\varepsilon \cdot \nabla)u_h^\varepsilon, v_h) + \frac{1}{2}(\nabla \cdot u_h^\varepsilon, u_h^\varepsilon \cdot v_h) + a(|u_h^\varepsilon|^\alpha u_h^\varepsilon - |u_h|^\alpha u_h, v_h) \\ & - ((u_h \cdot \nabla)u_h, v_h) - \frac{1}{2}(\nabla \cdot u_h, u_h \cdot v_h) + (p_h - p_h^\varepsilon, \nabla \cdot v_h) = 0 \text{ for all } v_h \in X^h \end{aligned} \quad (4.116)$$

With some calculus, for $v_h \in X^h$ we obtain

$$((u_h^\varepsilon \cdot \nabla)u_h^\varepsilon, v_h) = (((u_h^\varepsilon - u_h) \cdot \nabla)u_h^\varepsilon, v_h) + ((u_h \cdot \nabla)u_h^\varepsilon, v_h), \quad (4.117)$$

$$-((u_h \cdot \nabla)u_h, v_h) = -((u_h \cdot \nabla)(u_h - u_h^\varepsilon), v_h) - ((u_h \cdot \nabla)u_h^\varepsilon, v_h) \quad (4.118)$$

$$\frac{1}{2}((\nabla \cdot u_h^\varepsilon), u_h^\varepsilon \cdot v_h) = \frac{1}{2}(\nabla \cdot (u_h^\varepsilon - u_h), u_h^\varepsilon \cdot v_h) + \frac{1}{2}(\nabla \cdot u_h^\varepsilon, u_h^\varepsilon \cdot v_h), \quad (4.119)$$

$$-\frac{1}{2}((\nabla \cdot u_h), u_h \cdot v_h) = \frac{1}{2}((\nabla \cdot u_h), (u_h^\varepsilon - u_h) \cdot v_h) - \frac{1}{2}(\nabla \cdot u_h, u_h^\varepsilon \cdot v_h) \quad (4.120)$$

Replacing (4.117)-(4.120) in (4.116), yields to

$$\begin{aligned} (p_h^\varepsilon - p_h, \nabla \cdot v_h) &= \nu(\nabla(u_h^\varepsilon - u_h), \nabla v_h) + (((u_h^\varepsilon - u_h) \cdot \nabla)u_h^\varepsilon, v_h) + ((u_h \cdot \nabla)(u_h^\varepsilon - u_h), v_h) \\ & \quad + \frac{1}{2}(\nabla \cdot (u_h^\varepsilon - u_h), u_h^\varepsilon \cdot v_h) + \frac{1}{2}(\nabla \cdot u_h, (u_h^\varepsilon - u_h) \cdot v_h) + a(|u_h^\varepsilon|^\alpha u_h^\varepsilon - |u_h|^\alpha u_h, v_h) \end{aligned} \quad (4.121)$$

Substituting in (4.105) and using (4.102) and (4.104)

$$\| \hat{p}_h^\varepsilon - \hat{p}_h \|_{Z^h} \leq \frac{\nu + 2\nu(1-r) + aC_3}{\beta_h} \| u_h^\varepsilon - u_h \|_1 \quad (4.122)$$

Or, p_h^ε and p_h are in $(\text{Ker} B_h^*)^\perp$, then

$$\| \hat{p}_h^\varepsilon - \hat{p}_h \|_{Z^h} = \| \hat{p}_h^\varepsilon - \hat{p}_h \|$$

Consequently, (4.122) gives

$$\| p_h^\varepsilon - p_h \| \leq \frac{\nu(3-2r) + aC_3}{\beta_h} \| u_h^\varepsilon - u_h \|_1 \quad (4.123)$$

Consider $v_h = u_h^\varepsilon - u_h$ in the equation (4.116) to write

$$\begin{aligned} (p_h^\varepsilon - p_h, \nabla \cdot (u_h^\varepsilon - u_h)) &= \nu \| u_h^\varepsilon - u_h \|_1^2 + ((u_h^\varepsilon \cdot \nabla)u_h^\varepsilon, u_h^\varepsilon - u_h) + \frac{1}{2}(\nabla \cdot u_h^\varepsilon, u_h^\varepsilon \cdot (u_h^\varepsilon - u_h)) \\ & \quad - ((u_h \cdot \nabla)u_h, u_h^\varepsilon - u_h) - \frac{1}{2}((\nabla \cdot u_h, u_h \cdot (u_h^\varepsilon - u_h)) \\ & \quad + a(|u_h^\varepsilon|^\alpha u_h^\varepsilon, u_h^\varepsilon - u_h) - a(|u_h|^\alpha u_h, u_h^\varepsilon - u_h) \end{aligned} \quad (4.124)$$

Using $u_h = -(u_h^\varepsilon - u_h - u_h^\varepsilon)$ and thanks to (4.3), and the inequality (4.122), (4.124) takes the form

$$\begin{aligned} (p_h^\varepsilon - p_h, \nabla \cdot (u_h^\varepsilon - u_h)) &= \nu \|u_h^\varepsilon - u_h\|_1^2 + ((u_h^\varepsilon - u_h) \cdot \nabla) u_h^\varepsilon, (u_h^\varepsilon - u_h) \\ &\quad + \frac{1}{2} ((\nabla \cdot (u_h^\varepsilon - u_h), u_h^\varepsilon \cdot (u_h^\varepsilon - u_h)) \\ &\quad + a(|u_h^\varepsilon|^\alpha u_h^\varepsilon, u_h^\varepsilon - u_h) - a(|u_h|^\alpha u_h, u_h^\varepsilon - u_h)) \\ &\geq \nu \|u_h^\varepsilon - u_h\|_1^2 - s \|u_h^\varepsilon - u_h\|_1 \|u_h^\varepsilon\|_1. \end{aligned}$$

By (4.102) and (4.104), we infer

$$(p_h^\varepsilon - p_h, \nabla \cdot (u_h^\varepsilon - u_h)) \geq \nu r \|u_h^\varepsilon - u_h\|_1^2$$

Using (4.110)

$$\|u_h^\varepsilon - u_h\|_1^2 \leq \frac{1}{\nu r} (p_h^\varepsilon - p_h, \nabla \cdot u_h^\varepsilon)$$

The use of the property (4.101) gives

$$\begin{aligned} \|u_h^\varepsilon - u_h\|_1^2 &\leq \frac{\varepsilon}{\nu r} (p_h^\varepsilon - p_h, p_h^\varepsilon) \\ &= \frac{\varepsilon}{\nu r} (p_h^\varepsilon - p_h, p_h) - \frac{\varepsilon}{\nu r} \|p_h^\varepsilon - p_h\|^2 \end{aligned}$$

Therefore

$$\|u_h^\varepsilon - u_h\|_1^2 \leq \frac{\varepsilon}{\nu r} \|p_h^\varepsilon - p_h\| \|p_h\| \quad (4.125)$$

Substituting (4.125) in (4.123) gives

$$\|u_h^\varepsilon - u_h\|_1^2 \leq \frac{(3-2r)\nu + aK_1}{\nu r \beta_h} \varepsilon \|p_h\| \quad (4.126)$$

Replacing this results in (4.123) to get

$$\|p_h^\varepsilon - p_h\|_1^2 \leq \frac{(\nu(3-2r) + aK_1)^2}{\nu r \beta_h^2} \varepsilon \|p_h\| \quad (4.127)$$

Finally the desired estimates (4.114) and (4.115) are obtained with $C_1 = \frac{(3-2r)\nu + aK_1}{\nu r}$ and $C_2 = \frac{(\nu(3-2r) + aK_1)^2}{\nu r}$. ■

Theorem 4.4.4. *Assume that (u, p) and (u_h, p_h) are solutions of the problem (4.4) and (4.110) respectively. Then*

$$\|u_h - u\|_1 \leq \left(\frac{3}{r} - 1 + \frac{a}{\nu r} C_1 \right) \left(1 + \frac{C}{\beta_h} \right) \|u - v_h\|_1 + \frac{C_2}{\nu r} \|p - q_h\| \quad (4.128)$$

for all $v_h \in X^h$ and all $q_h \in Y^h$, and

$$\|p - p_h\|_{Z^h} \leq \frac{\nu(3-2r) + aC}{\beta_h} \|u - u_h\|_1 + \left(1 + \frac{C'}{\beta_h}\right) \|p - q_h\| \quad \text{for all } q_h \in Y^h \quad (4.129)$$

Proof. We introduce the finite space $\mathbb{X}^h = \{v_h \in X^h \mid (q_h, \nabla \cdot v_h) = 0 \text{ for all } q_h \in Y^h\}$. Since $u_h \in \mathbb{X}^h$ and $v_h \in \mathbb{X}^h$, substituting $u_h - v_h$ to v_h in (4.110) to get

$$\begin{aligned} \nu(\nabla u_h, \nabla(u_h - v_h)) + ((u_h \cdot \nabla)u_h, u_h - v_h) + \frac{1}{2}(\nabla \cdot u_h, u_h \cdot (u_h - v_h)) \\ + a(|u_h|^\alpha u_h, u_h - v_h) = (f, u_h - v_h) \quad \text{for all } v_h \in \mathbb{X}^h \end{aligned} \quad (4.130)$$

Subtracting the quantity

$$\nu(\nabla v_h, \nabla(u_h - v_h)) + ((v_h \cdot \nabla)v_h, u_h - v_h) + \frac{1}{2}(\nabla \cdot v_h, v_h \cdot (u_h - v_h)) + a(|v_h|^\alpha v_h, u_h - v_h)$$

from the both sides of (4.130), multiplying (4.4) by $v = u_h - v_h$ and substituting here in the right hand side

$$\begin{aligned} \nu(\nabla(u_h - v_h), \nabla(u_h - v_h)) + ((u_h \cdot \nabla)u_h, u_h - v_h) + \frac{1}{2}(\nabla \cdot u_h, u_h \cdot (u_h - v_h)) \\ + a(|u_h|^\alpha u_h, u_h - v_h) - ((v_h \cdot \nabla)v_h, u_h - v_h) - \frac{1}{2}(\nabla \cdot v_h, v_h \cdot (u_h - v_h)) \\ - a(|v_h|^\alpha v_h, u_h - v_h) \\ = \nu(\nabla u, \nabla(u_h - v_h)) + ((u \cdot \nabla)u, u_h - v_h) + a(|u|^\alpha u, u_h - v_h) \\ - (p, \nabla \cdot (u_h - v_h)) - \nu(\nabla v_h, \nabla(u_h - v_h)) - ((v_h \cdot \nabla)v_h, u_h - v_h) \\ - \frac{1}{2}(\nabla \cdot v_h, v_h \cdot (u_h - v_h)) - a(|v_h|^\alpha v_h, u_h - v_h) \quad \text{for all } v_h \in \mathbb{X}^h \end{aligned} \quad (4.131)$$

Or, $v_h \in \mathbb{X}^h$, $(p, \nabla \cdot (u_h - v_h)) = (p - q_h, \nabla \cdot (u_h - v_h))$. Adding and subtracting $((u \cdot \nabla)v_h, u_h - v_h)$ on the right hand side in the previous result

$$\begin{aligned} \nu(\nabla(u_h - v_h), \nabla(u_h - v_h)) + ((u_h \cdot \nabla)u_h, u_h - v_h) + \frac{1}{2}(\nabla \cdot u_h, u_h \cdot (u_h - v_h)) \\ + a(|u_h|^\alpha u_h - |v_h|^\alpha v_h, u_h - v_h) - ((v_h \cdot \nabla)v_h, u_h - v_h) - \frac{1}{2}(\nabla \cdot v_h, v_h \cdot (u_h - v_h)) \\ = \nu(\nabla(u - v_h), \nabla(u_h - v_h)) + ((u \cdot \nabla)(u - v_h), u_h - v_h) + a(|u|^\alpha u - |v_h|^\alpha v_h, u_h - v_h) \\ - (p - q_h, \nabla \cdot (u_h - v_h)) + ((u - v_h \cdot \nabla)v_h, u_h - v_h) - \frac{1}{2}(\nabla \cdot (u - v_h), v_h \cdot (u_h - v_h)) \end{aligned} \quad (4.132)$$

for all $v_h \in \mathbb{X}^h$.

The first part of the equality above can be simplified as

$$\begin{aligned}
& \nu(\nabla(u_h - v_h), \nabla(u_h - v_h)) + ((u_h \cdot \nabla)u_h, u_h - v_h) + \frac{1}{2}(\nabla \cdot u_h, u_h \cdot (u_h - v_h)) \\
& \quad + a(|u_h|^\alpha u_h - |v_h|^\alpha v_h, u_h - v_h) - ((v_h \cdot \nabla)v_h, u_h - v_h) - \frac{1}{2}(\nabla \cdot v_h, v_h \cdot (u_h - v_h)) \\
= & \nu(\nabla(u_h - v_h), \nabla(u_h - v_h)) + ((u_h \cdot \nabla)u_h, u_h - v_h) + \frac{1}{2}(\nabla \cdot u_h, u_h \cdot (u_h - v_h)) \\
& \quad - (((v_h - u_h) \cdot \nabla)(v_h - u_h), u_h - v_h) - ((u_h \cdot \nabla)(v_h - u_h), u_h - v_h) \\
& \quad - (((v_h - u_h) \cdot \nabla)u_h, u_h - v_h) - ((u_h \cdot \nabla)u_h, u_h - v_h) \\
& \quad - \frac{1}{2}(\nabla \cdot (v_h - u_h), (v_h - u_h) \cdot (u_h - v_h)) - \frac{1}{2}((\nabla \cdot u_h), (v_h - u_h) \cdot (u_h - v_h)) \\
& \quad - \frac{1}{2}(\nabla \cdot (v_h - u_h), u_h \cdot (u_h - v_h)) - \frac{1}{2}(\nabla \cdot u_h, u_h \cdot (u_h - v_h)) \\
& \quad + a(|u_h|^\alpha u_h - |v_h|^\alpha v_h, u_h - v_h) \\
= & \nu(\nabla(u_h - v_h), \nabla(u_h - v_h)) + (((u_h - v_h) \cdot \nabla)u_h, u_h - v_h) + \frac{1}{2}(\nabla \cdot (u_h - v_h), u_h \cdot (u_h - v_h)) \\
& \quad + a(|u_h|^\alpha u_h - |v_h|^\alpha v_h, u_h - v_h)
\end{aligned} \tag{4.133}$$

$$\geq \nu \|u_h - v_h\|_1^2 - s \|u_h - v_h\|_1^2 \|u_h\|_1 \geq \nu r \|u_h - v_h\|_1^2 \tag{4.134}$$

Substituting (4.134) in (4.132) and thanks to (4.102), the fact that (u_h) is bounded and the Cauchy Schwartz inequality, we have

$$\begin{aligned}
\|u_h - v_h\|_1 \leq & \frac{1}{r} \left(1 + \frac{s}{\nu} (\|u\|_1 + \|v_h\|_1) + \frac{a}{\nu} C_1 \right) \|u - v_h\|_1 \\
& + \frac{C_2}{\nu r} \|p - q_h\|
\end{aligned} \tag{4.135}$$

for all $v_h \in \mathbb{X}^h$ and $q_h \in Y^h$.

Simplifying (4.135) gives

$$\begin{aligned}
\|u - u_h\|_1 \leq & \left[1 + \frac{1}{r} \left(1 + \frac{s}{\nu} (\|u\|_1 + \|v_h\|_1) + \frac{a}{\nu} C_1 \right) \right] \|u - v_h\|_1 \\
& + \frac{C_2}{\nu r} \|p - q_h\|
\end{aligned} \tag{4.136}$$

We define $v_h = \prod_h u$ as the orthogonal projection of u on \mathbb{X}^h . We have

$$\|u - \prod_h u\|_1 = \inf_{v_h \in \mathbb{X}^h} \|u - v_h\|_1$$

and

$$\| \prod_h u \|_1 \leq \| u \|_1$$

Using these properties in (4.136) and the fact that (u) is bounded yields

$$\| u - u_h \|_1 \leq \left[\frac{3}{r} - 1 + \frac{a}{\nu r} C_1 \right] \inf_{v_h \in \mathbb{X}^h} \| u - v_h \|_1 + \frac{C_2}{\nu r} \| p - q_h \| \quad (4.137)$$

It remains to estimate the term $\inf_{v_h \in \mathbb{X}^h} \| u - v_h \|_1$. For this end, we solve an auxiliary approximate penalized variational Stokes problem:

let $v_h \in X^h$, for all $\varepsilon > 0$, Find $z_h^\varepsilon \in X^h$ such that

$$(\nabla z_h^\varepsilon, \nabla w_h) - \frac{1}{\varepsilon} I((\nabla \cdot z_h^\varepsilon)(\nabla \cdot w_h)) = (\nabla v_h, \nabla w_h) \quad \text{for all } w_h \in X^h \quad (4.138)$$

There exists a unique solution $z_h^\varepsilon \in X^h$ of the problem (4.138). We define the associated pressure $\pi_h^\varepsilon \in Y^h$ as

$$\pi_h^\varepsilon(x_i^e) = -\frac{1}{\varepsilon} \nabla \cdot z_h^\varepsilon(x_i^e), \quad 1 \leq i \leq G, \quad 1 \leq e \leq E \quad (4.139)$$

The sequence $(z_h^\varepsilon, \pi_h^\varepsilon)$ converges in $\mathbb{X}^h \times Y^h$ to the solution $(z_h, \pi_h) \in X^h \times Y^h$ of the problem

Find $(z_h, \pi_h) \in X^h \times Y^h$ such that

$$\begin{aligned} (\nabla z_h, \nabla w_h) - (\pi_h, \nabla w_h) &= (\nabla v_h, \nabla w_h) & \text{for all } w_h \in X^h \\ (q_h, \nabla \cdot z_h) &= 0 & \text{for all } q_h \in Y^h \end{aligned} \quad (4.140)$$

So,

$$\| v_h - z_h \|_1 = \sup_{w_h \in X^h} \frac{(\nabla(v_h - z_h), \nabla w_h)}{\| w_h \|_1}$$

Using (4.140) to infer that

$$\| v_h - z_h \|_1 = \sup_{w_h \in X^h} \frac{(\pi_h, \nabla \cdot w_h)}{\| w_h \|_1}$$

The discrete inf-sup condition gives

$$\| v_h - z_h \|_1 \geq \beta_h \| \hat{z}_h \|_{Z^h} \quad (4.141)$$

Consider $w_h = u_h - z_h$ in (4.140). Since $(\pi_h, \nabla \cdot z_h) = 0$ and combine (4.140) and (4.4) to have $(\pi_h, \nabla \cdot u) = 0$ and since $(q_h, \nabla \cdot (u - v_h)) = 0$ for all $q_h \in \text{Ker} B_h^*$, we obtain

$$\| z_h - v_h \|_1^2 \leq C \| \pi_h + q_h^0 \| \| u - v_h \|_1$$

The infimum over all $q_h \in \text{Ker} B_h^*$ implies

$$\| z_h - v_h \|_1^2 \leq C \| \hat{\pi}_h \|_{Z^h} \| u - v_h \|_1,$$

By the inequality (4.141),

$$\| z_h - v_h \|_1 \leq \frac{C}{\beta_h} \| u - v_h \|_1$$

which gives

$$\| u - z_h \|_1 \leq \left(1 + \frac{C}{\beta_h} \right) \| u - v_h \|_1$$

$z_h \in \mathbb{X}^h$ according to the problem (4.140). The infimum over all $z_h \in \mathbb{X}^h$ gives

$$\inf_{z_h \in \mathbb{X}^h} \| u - z_h \|_1 \leq \left(1 + \frac{C}{\beta_h} \right) \| u - v_h \|_1 \quad \text{for all } v_h \in X^h \quad (4.142)$$

Substituting the (4.142) in (4.137) gives the estimate (4.128).

Now, let us derive the pressure estimate. From the discrete inf-sup condition (4.105) and substituting $q_h - p_h$ to q_h , we have

$$\| \hat{q}_h - \hat{p}_h \|_{Z^h} \leq \frac{1}{\beta_h} \sup_{v_h \in X^h} \frac{I((q_h - p_h)\nabla \cdot v_h)}{\| v_h \|_1}. \quad (4.143)$$

Using (4.99),

$$I((q_h - p_h)\nabla \cdot v_h) = (q_h - p, \nabla \cdot v_h) + (p - p_h, \nabla \cdot v_h) \quad (4.144)$$

Multiplying (4.4) by v_h and subtracting (4.110)

$$\begin{aligned} (p - p_h, \nabla \cdot v_h) &= \nu(\nabla(u - u_h), \nabla v_h) + ((u \cdot \nabla)u, v_h) - ((u_h \cdot \nabla)u_h, v_h) \\ &\quad - \frac{1}{2}((\nabla \cdot u_h), u_h \cdot v_h) + a|u|^\alpha u, v_h - a|u_h|^\alpha u_h, v_h \\ &\quad \text{for all } v_h \in X^h \end{aligned}$$

Using similar calculus as in (4.70)- (4.75), the triangle inequality and (4.102) to get

$$(p - p_h, \nabla \cdot v_h) \leq [\nu \| u - u_h \|_1 + 2\nu(1-r)\| u - u_h \|_1 + aC\| u - u_h \|_1] \| v_h \|_1$$

Injecting this result in (4.144) and using (4.141) yields to

$$\| \hat{q}_h - \hat{p}_h \|_{Z^h} \leq \frac{\nu(3-2r) + aC}{\beta_h} \| u - u_h \|_1 + \frac{C'}{\beta_h} \| p - q_h \|$$

Consequently

$$\begin{aligned} \| p - p_h \|_{Z^h} &\leq \| \hat{p} - \hat{q}_h \|_{Z^h} + \frac{\nu(3-2r) + aC}{\beta_h} \| u - u_h \|_1 + \frac{C'}{\beta_h} \| p - q_h \| \\ &\leq \frac{\nu(3-2r) + aC}{\beta_h} \| u - u_h \|_1 + \left(1 + \frac{C'}{\beta_h} \right) \| p - q_h \| \end{aligned}$$

which finish the proof. ■

Theorem 4.4.5. Let $(u, p) \in X \times Y$ be the solution of (4.4) and $(u_h^\varepsilon, p_h^\varepsilon)$ be defined by (4.100) then

$$\begin{aligned} \|u - u_h^\varepsilon\|_1 \leq & \left(\frac{3}{r} - 1 + \frac{a}{\nu r} C_1 \right) \left(1 + \frac{C}{\beta_h} \right) \inf_{v_h \in X^h} \|u - v_h\|_1 \\ & + \frac{C_2}{\nu r} \inf_{q_h \in Y^h} \|p - q_h\| + \frac{C_3}{\beta_h} \varepsilon \|p_h\| \end{aligned} \quad (4.145)$$

and

$$\begin{aligned} \|p - p_h^\varepsilon\|_{Z^h} \leq & \frac{\nu(3 - 2r) + aC_1}{\beta_h} \left(\frac{3}{r} - 1 + \frac{a}{\nu r} C_2 \right) \left(1 + \frac{C_3}{\beta_h} \right) \inf_{v_h \in X^h} \|u - v_h\|_1 \\ & + \left(1 + \frac{C_4}{\beta_h} \left(\frac{3}{r} - 1 + \frac{a}{\nu r} C_1 \right) \right) \inf_{q_h \in Y^h} \|p - q_h\| + \frac{C''}{\beta_h^2} \varepsilon \|p_h\| \end{aligned} \quad (4.146)$$

Proof. For the first inequality, we use the triangle inequality

$$\|u - u_h^\varepsilon\|_1 \leq \|u - u_h\|_1 + \|u_h - u_h^\varepsilon\|_1$$

Using the inequalities (4.128) and (4.114). The infimum over $v_h \in X^h$, $q_h \in Y^h$ implies the estimate (4.145).

With a similar manner

$$\begin{aligned} \|p - p_h^\varepsilon\|_{Z^h} & \leq \|p - \hat{p}_h\|_{Z^h} + \|\hat{p}_h - p_h^\varepsilon\|_{Z^h} \\ & = \|p - \hat{p}_h\|_{Z^h} + \|\hat{p}_h - p_h^\varepsilon\| \end{aligned}$$

■

Remark 4.4.1. For ε a small positive constant, the inequality (4.115) show that $\|p_h\|$ is bounded.

4.5 Numerical approximation and optimization algorithm

Here we will limit ourselves to the approximation of optimization problems involving fishways (Figure 4.1).

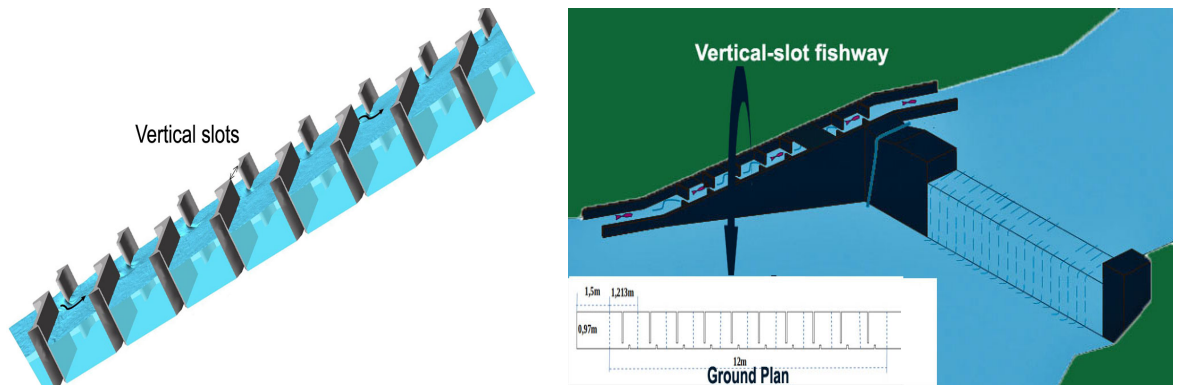


Figure 4.1: Schematic description of fishway structure

The design of any vertical slot relies on the use of guiding elements to conduct a regular hydraulic flow into the next slot. The placement of the guiding elements was done in two distinct locations, $a(y_1, y_2)$ and $b(y_3, y_4)$, that determine the shape of the fishway Ω (Figure 4.2).

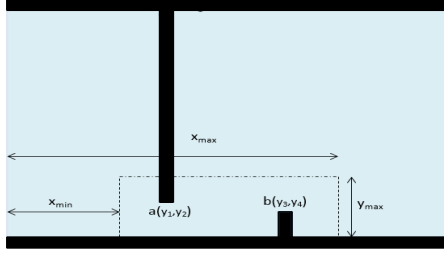


Figure 4.2: Fish pass geometry I shaped baffle for the central pool

In addition, the design variables a and b are subject to certain constraints in regard to their impact on the flow rate. These restrictions are expressed as the following

$$\begin{aligned} \frac{1}{4} 1.213 \leq y_1, y_3 \leq \frac{3}{4} 1.213 \\ 0 \leq y_2, y_4 \leq \frac{1}{4} 0.97 \end{aligned} \quad (4.147)$$

Fishways must be designed to allow all individuals in a population to have the opportunity to get through. To this end, the following requirements are added.

$$y_3 - y_1 \geq d_1 = 0.1 \quad (4.148)$$

$$y_2 - y_4 \geq d_2 = 0.05$$

4.5.1 Optimization procedure

We describe the approach called projected spectral gradient to tackle the shape optimization problem based on the minimization of the discrete cost function given by

$$\bar{\Phi}(y) = \frac{\Delta t}{2} \sum_{n=1}^N \sum_{e \in T_i} \left[\int_e \|\mathbf{u}^{n,i} - \vec{v}\|^2 + \alpha \int_e |\text{curl}(\mathbf{u}^{n,i})|^2 \right]. \quad (4.149)$$

We denote $a_1 = a_3 = \frac{1}{4} 1.213$, $b_1 = b_3 = \frac{3}{4} 1.213$, $a_2 = a_4 = 0$, $b_2 = b_4 = \frac{1}{4} 0.97$.

Let the admissible set Ω_0 be defined as

$$\Omega_0 = \{y = (y_1, y_2, y_3, y_4) \in \mathbb{R}^4 : \begin{aligned} & a_i \leq y_i \leq b_i, \quad i = 1, \dots, 4, \\ & y_3 - y_1 \geq d_1, \quad y_2 - y_4 \geq d_2 \end{aligned} \} \quad (4.150)$$

The optimization problem writes

$$\min_{y \in \Omega_0} \bar{\Phi}(y). \quad (4.151)$$

The optimal position $y \in \Omega_0$ is determined by an algorithm combining the calculation of the gradient of the cost function and the projected functions. Let $\eta = 1$, $\bar{y} \in \Omega$ and $\varepsilon > 0$ be a positive tolerance.

1. Compute $d = P_{\Omega_0}(\bar{y} - \eta \nabla J(\bar{y})) - \bar{y}$, with ∇J is the gradient of the cost function J and η is a positive constant given by
 - Consider \bar{y} the current point and \tilde{y} the previous point. Compute $x = \bar{y} - \tilde{y}$ and $y = \nabla J(\bar{y}) - \nabla J(\tilde{y})$. If $x^T y > 0$, take $\eta = \frac{x^T x}{x^T y}$; elsewhere, take η as a fixed positive value.
2. Stop when $d = 0$ (in practice, $\|d\| < \varepsilon$) and \bar{y} is a stationary point of J on Ω_0 .
3. Set $\tilde{y} = \bar{y} + \xi d$, with ξ is defined as the step size. And go to (1) with $\bar{y} = \tilde{y}$.

The value $y = P_{\Omega_0}(z)$ is the projection of $z \in \mathbb{R}^4$ onto Ω_0 . It is computed by minimizing a quadratic function of the distance of z to Ω as follow

$$\min_{y \in \Omega} \frac{1}{2} \|y - z\|^2 = \min_{y \in \Omega} \frac{1}{2} z^T z - z^T y + \frac{1}{2} y^T y \quad (4.152)$$

This is similar to

$$\min_{(y_1, y_2, y_3, y_4)} \sum_{i=1}^4 \left\{ \frac{1}{2} z_i^2 - z_i y_i + \frac{1}{2} y_i^2 \right\}$$

$$\text{subject to } a_i \leq y_i \leq b_i, i = 1, \dots, 4$$

$$y_3 - y_1 \geq d_1, \quad y_2 - y_4 \geq d_2$$

The two quadratic problems, the former for the abscissa and the latter for the ordinate, will be solved by the Karush-Kuhn-Tucker (KKT) technique. The KKT is a generalization of the augmented Lagrangian approach including inequality constraints and used to find optimal points. The algorithm works as shown below

Choose $a = a_1 = a_3$, and $b = b_1 = b_3$. We need three constraints with the optimization problem

$$\min_{(x_1, x_2)} c - (l_1 x_1 + l_2 x_2) + \frac{1}{2} (x_1^2 + x_2^2)$$

$$\text{subject to } x_2 \leq b,$$

$$x_1 \geq a,$$

$$x_2 - x_1 \geq d_1,$$

where ,a, b, d_1 , c, and l_i , $i=1,2$, are real numbers.

Consider the following matrix

$$A = \begin{pmatrix} 0 & -1 \\ 1 & 0 \\ -1 & 1 \end{pmatrix}, \quad b = \begin{pmatrix} -b \\ a \\ d_1 \end{pmatrix},$$

Then the linear constraints write

$$Ax - v = b, \quad v \geq 0,$$

where $v = (v_1, v_2, v_3)^T$ is the slack variables. The optimization problem is solvable with unique solution due to the convexity of the cost function in \mathbb{R}^2 . The obtained solution satisfies the KKT conditions

$$\begin{aligned} v &= Ax - b \\ -l + x &= A^T \lambda, \\ v \geq 0, \quad \lambda &\geq 0, \\ v^T \lambda &= 0, \end{aligned}$$

where $l = (l_1, l_2, l_3)$, and $\lambda = (\lambda_1, \lambda_2, \lambda_3)$ is the vector of the Lagrange multipliers associated to the three constraints above. The unique optimal solution writes

$$x = l + A^T \lambda$$

which gives

$$\begin{cases} x_1 = l_1 + \lambda_2 - \lambda_3 \\ x_2 = l_2 - \lambda_1 + \lambda_3 \end{cases}$$

For computing the Lagrange multipliers λ_i , we solve the above linear complementarity problem

$$\begin{aligned} v &= (-b + Al) + AA^T \lambda \\ v \geq 0, \quad \lambda &\geq 0 \\ v^T \lambda &= 0 \end{aligned}$$

Remark 4.5.1. *The gradient of the cost function is computed using the formula established in section 3.*

4.5.2 Numerical examples

In this part, we present numerical results concerning the optimization of the shape of fishways. We have combined all the techniques developed in the previous sections: the set of equations (4.33) is solved by the finite element method (4.100) combined with projected gradient for the resolution of the shape optimization problem (4.149)-(4.151). The numerical implementation is based on the use of the FreeFem++ [8], using the sparse linear solver for the linear systems.

The computational grids are unstructured. \mathbb{P}_2 - \mathbb{P}_1 finite elements have been used for the spatial discretization.

We analyze the approach for the calculation of the average flow in a vertical slot fishway (VSF) capable of dissipating the energy of the inlet jet and creating flow conditions in the pool that allow fish to ascend under comfortable conditions.

We conduct three different studies of VSF designs with I- and L-shaped baffles that are most adopted for upstream fish passage in river obstructions. The structure of a fishway is consisting of a succession of ten pools Figure 4.3. Each pool has a length of $1.213m$ with a width of $0.97m$ for "I" shaped baffle-rectangular slots and a length of $3m$ with a width of $2m$ for "L" shaped baffle-oblique slots. We also have two transition pools, one at the beginning and the other at the end of the channel with a length of $1.5m$ and a same width as the other pools.

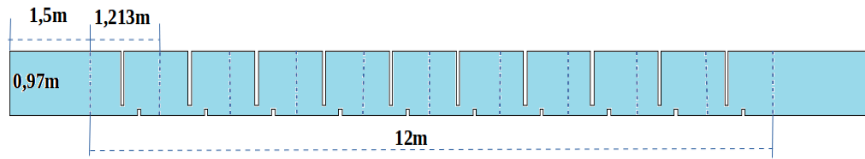


Figure 4.3: Conventional pool pass Ω : each pool is designed by dashed lines

The three numerical simulations are conducted under the same physical and numerical conditions: initial and boundary conditions are constants. The following crucial velocities must be respected if pool passes are to function correctly: the inflow velocity is $(0.1, 0, 0)$, the target velocity is $\mathbf{u}_d = (0.8, 0, 0)$ ideal for fish leaping and swimming abilities. The vorticity parameter is $\sigma = 0.3$. The viscosity is $\nu = 0.01$. The external function corresponding to the gravity effect is $\mathbf{f} = (0, 0, 9.81)$. The non-slip boundary condition was applied to all walls (bottom, lateral walls and baffles).

Vertical Slot Fishway (2-D "L" shaped baffle-oblique slots)

The central pool geometry is shown in Figure 4.4. The standard values are issued from current VSF designs [1; 3]: slot width 0.3 m, basin length 3 m, and width 2 m.

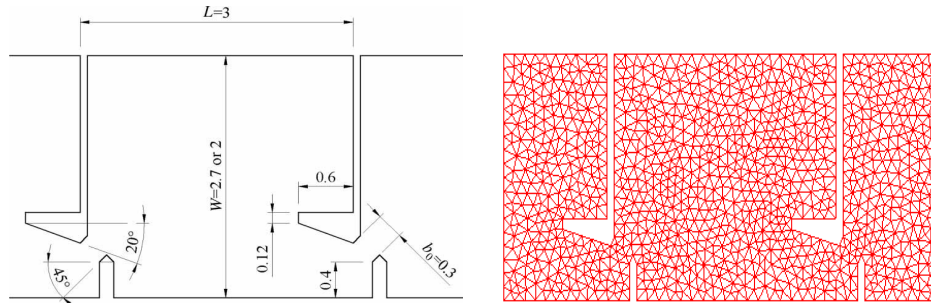


Figure 4.4: Fish pass geometry and mesh in the central pool

In Figure 4.5 calculated flow contour plots of the approximated velocity components both for the random and the optimal shape.

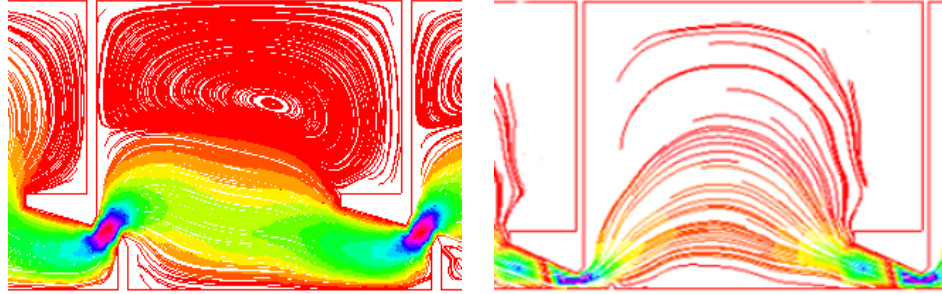


Figure 4.5: Initial (left) and optimal (right) velocities for central pool

The correct positioning of a slot pass and the location of its entrance at a dam for the optimal shape see Figure 4.5 (right) leads to a decrease in turbulence and allows to maintain the possibility of migration at dams for both strongly swimming fish, and for bottom oriented and small fish.

Slot Fishway (3-D "I" shaped baffle-rectangular slots)

A 3-D experiments are performed. The geometry of slots in each pool is rectangular as shown in Figure 4.6.

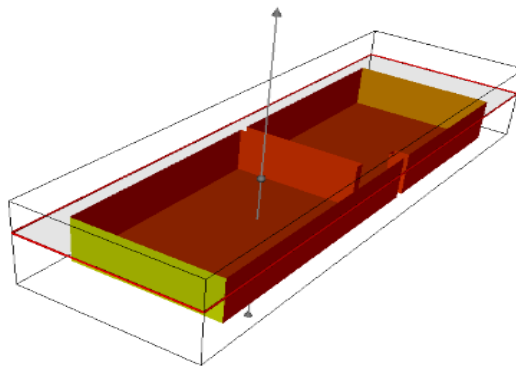


Figure 4.6: Configuration of central pool

The next results present the velocity for ten pools and compare the water flow in the random and optimum shapes.

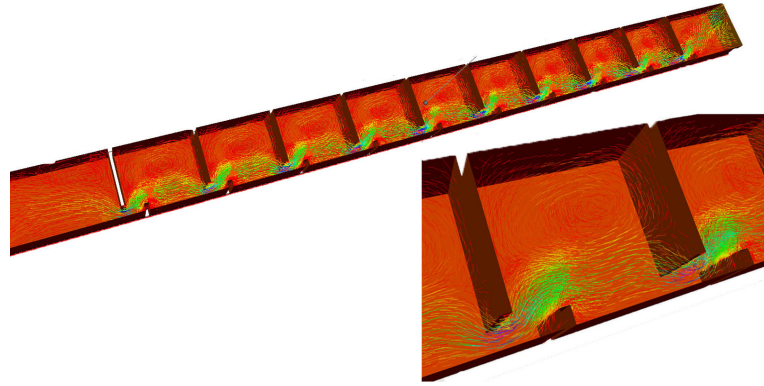


Figure 4.7: Velocity fields for non optimal ten pool configuration

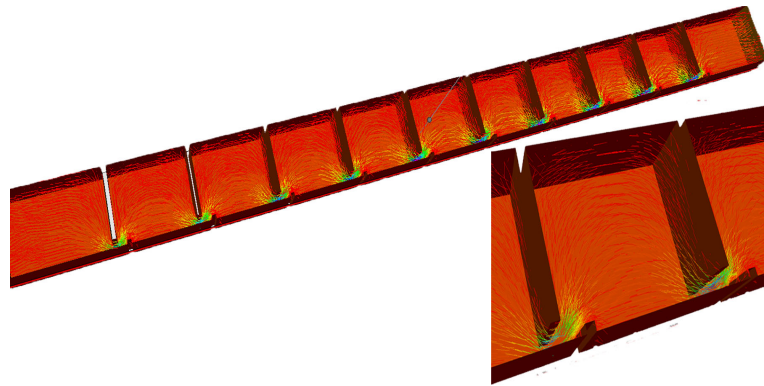


Figure 4.8: Velocity fields for optimal ten pool configuration

The calculation shows that reduction in flow velocities near the bottom of the slots and the turbulence conditions in the pass, obtained for the optimal shape (Figure 4.8), allow low performance fish such as loach, gudgeon or bullhead to ascend. The reduction of the corresponding cost function is given in Figure 4.9. As soon as the guide slots are optimally positioned, the objective function reaches a minimum value.

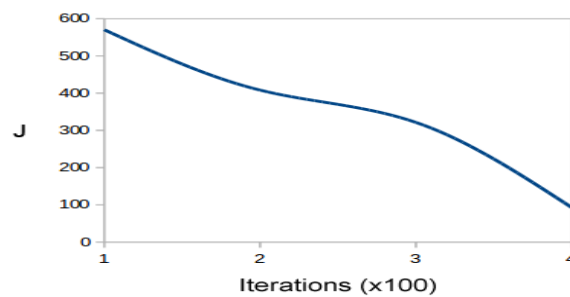


Figure 4.9: Convergence history

Slot Fishway (3-D "L" shaped baffle-oblique slots)

The 3-D version of the first experiment is presented in the following test. The standard values are selected [1; 3]: slot width 0.3 m, basin length 3 m, and width 2 m. A triangular discretization of the fluid domain Ω is used. The density of mesh is higher near slots compared to the other zones. Numerical simulation are done with 19000 triangles.

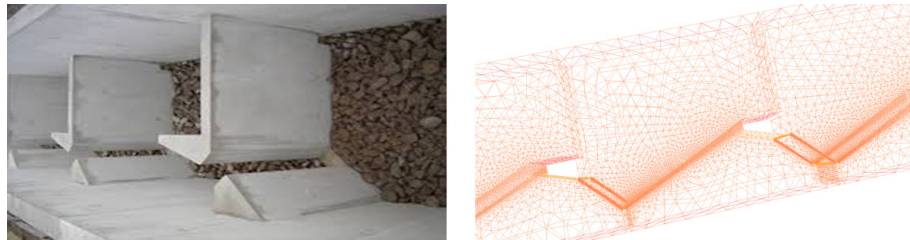


Figure 4.10: 3-D Example of Fiswhay with oblique slots and mesh in the central pool

The current results show the velocity for ten pools and compare the flow of water in both the initial (Figure 4.11) and optimal (Figure 4.12) shapes. We observe clearly the recirculation regions flowing in opposite directions for the initial structure compared to results in the optimal one. These hydrodynamic conditions reduce transit time to enable fish to continue their migratory movements and access habitats for growth, refuge, and reproduction.

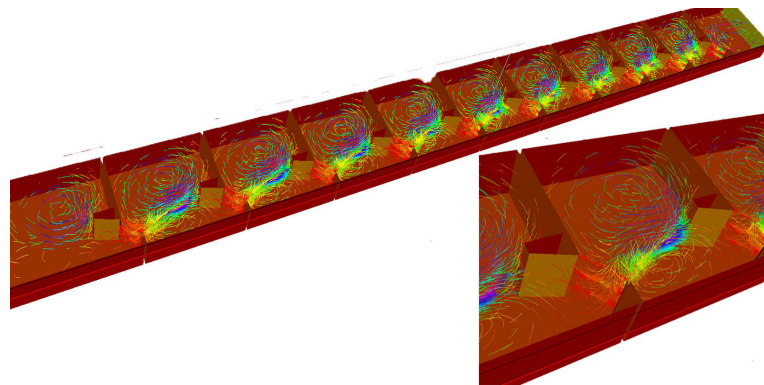


Figure 4.11: Non optimal velocity for ten pool

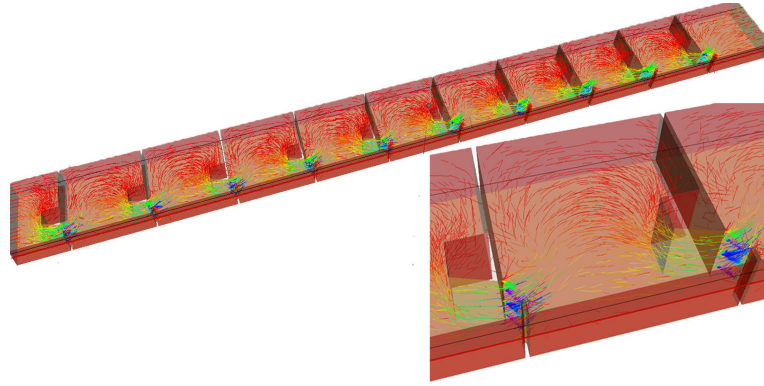


Figure 4.12: Optimal velocity for ten pool

Figure 4.13 shows the decay of the cost functional J as a function of the elements of the fishway structure.

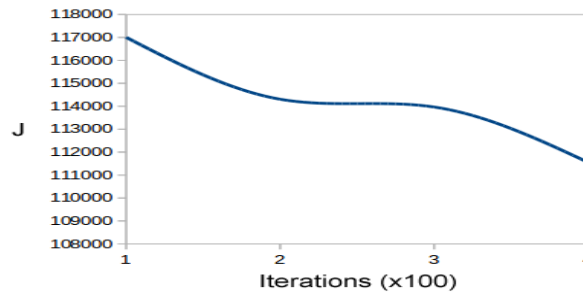


Figure 4.13: Convergence history

4.6 Conclusion

The design optimization is extended to the penalty porous media model and has been successfully used in hydraulic shape optimization. Based on the Navier Stokes Forchheimer model, the penalized system has been analyzed and a finite element method are considered. Error estimates of the velocity and the pressure are derived in term of H^1 and L^2 norm respectively. 2-D and 3-D examples have been presented, and the corresponding results have demonstrated the usefulness and robustness of the approach.

4.7 Annex: Control problem of mixed boundary conditions

For the case where Dirichlet and Neumann boundary conditions are chosen, we provide a description of the shape derivative. We express the shape gradients of the cost functions by means

of the corresponding linear adjoint state systems. Let the relaxed flow model

$$\begin{cases} -\nu\Delta u^\varepsilon + (u^\varepsilon \cdot \nabla)u^\varepsilon + \frac{1}{2}(\nabla \cdot u^\varepsilon)u^\varepsilon + a|u^\varepsilon|^\alpha u^\varepsilon + \nabla p^\varepsilon = f \text{ in } \Omega \\ \nabla \cdot u^\varepsilon + \varepsilon p^\varepsilon = 0 \text{ in } \Omega \\ u^\varepsilon = 0 \text{ on } \Gamma_1 \\ \nu \frac{\partial u^\varepsilon}{\partial n} - p^\varepsilon \mathbf{n} = 0 \text{ on } \Gamma_2 \end{cases} \quad (4.153)$$

where $\partial\Omega = \Gamma_1 \cup \Gamma_2$. We maintain the identical definition of the objective function (4.78) and the functional F in (4.79). Then the optimization problem can be expressed as

$$\begin{aligned} \min_{\Omega \in \Omega_{ad}} J(\Omega) &= \frac{1}{2} \int_{\Omega} |u^\varepsilon - u_d|^2 dx + \frac{\sigma}{2} \int_{\Omega} |\text{curl}(u^\varepsilon)|^2 dx \\ &\text{such that } (u^\varepsilon, p^\varepsilon) \text{ satisfies the equation (4.153)} \end{aligned} \quad (4.154)$$

4.7.1 Adjoint system

We begin by deriving an adjoint system associated with the penalized system (4.153).

Theorem 4.7.1. Let $(u^\varepsilon, p^\varepsilon) \in \hat{V}_g(\Omega) \times Y$. The adjoint system associated to the equation (4.153) takes the form

$$\begin{cases} -\nu\Delta v + (\nabla u^\varepsilon)^T \cdot v - (u^\varepsilon \cdot \nabla)v - \frac{1}{2}\nabla(u^\varepsilon \cdot v) + \frac{1}{2}(\nabla \cdot u^\varepsilon)v + a|u^\varepsilon|^{\alpha-2}(|u^\varepsilon|^2 v + \alpha(u^\varepsilon \cdot v)u^\varepsilon) \\ \quad + \nabla q = (u^\varepsilon - u_d) - \sigma \underline{\text{curl}}(\text{curl}(u^\varepsilon)) \text{ in } \Omega \\ \nabla \cdot v + \varepsilon q = 0 \text{ in } \Omega \\ v = 0 \text{ on } \Gamma_1 \\ \nu \frac{\partial v}{\partial n} + 2(u^\varepsilon \cdot n)v - nq = \sigma \text{curl}(u^\varepsilon) \cdot \tau \text{ on } \Gamma_2 \end{cases} \quad (4.155)$$

Proof. Let $L(\Omega, u^\varepsilon, p^\varepsilon, v, q)$ be a Lagrangian functional defined by

$$L(\Omega, u^\varepsilon, p^\varepsilon, v, q) = J(\Omega) - F(\Omega, u^\varepsilon, p^\varepsilon, v, q) \quad (4.156)$$

Firstly we derive L with respect to the state variable p in any direction $\tilde{p} \in M$ to get

$$\frac{\partial L}{\partial p^\varepsilon}(\Omega, u^\varepsilon, p^\varepsilon, v, q) \cdot \tilde{p} = \int_{\Omega} \tilde{p} \nabla \cdot v \, dx + \int_{\Omega} \varepsilon \tilde{p} q \, dx$$

The variation \tilde{p} is arbitrary, we deduce

$$\nabla.v + \varepsilon q = 0 \quad \text{on } \Omega \quad (4.157)$$

After deriving L with respect of the state variable u^ε in the arbitrary direction $\tilde{u} \in V_0(\Omega)$ one writes

$$\begin{aligned} 0 &= \frac{\partial L}{\partial u^\varepsilon}(\Omega, u^\varepsilon, p^\varepsilon, v, q) \cdot \tilde{u} \\ &= \int_{\Omega} (u^\varepsilon - u_d) \cdot \tilde{u} dx + \sigma \int_{\Omega} \text{curl}(u^\varepsilon) \cdot \text{curl}(\tilde{u}) dx \\ &\quad - \int_{\Omega} \left[\nu \nabla \tilde{u} : \nabla v + (\tilde{u} \cdot \nabla) u^\varepsilon \cdot v + (u^\varepsilon \cdot \nabla) \tilde{u} \cdot v + \frac{1}{2} (\nabla \cdot \tilde{u}) u^\varepsilon \cdot v + (\nabla \cdot u^\varepsilon) \tilde{u} \cdot v \right] dx \\ &\quad + \int_{\Omega} q \nabla \cdot \tilde{u} dx - \int_{\Omega} [a |u^\varepsilon|^\alpha \tilde{u} + a \alpha |u^\varepsilon|^{\alpha-2} (u^\varepsilon \cdot \tilde{u}) u^\varepsilon] \cdot v dx \\ &= \int_{\Omega} [(u^\varepsilon - u_d) - \sigma \underline{\text{curl}}(\text{curl}(u^\varepsilon)) + \nu \Delta u^\varepsilon - (\nabla u^\varepsilon)^T \cdot v + (u^\varepsilon \cdot \nabla) v \\ &\quad + \frac{1}{2} \nabla(u^\varepsilon \cdot v) - \frac{1}{2} (\nabla \cdot u^\varepsilon) v - (a |u^\varepsilon|^\alpha v + a \alpha |u^\varepsilon|^{\alpha-2} (u^\varepsilon \cdot v) u^\varepsilon - \nabla q) \cdot \tilde{u} dx \\ &\quad + \int_{\Gamma_2} \left(\sigma \text{curl}(u^\varepsilon) \tau - \left(\nu \frac{\partial v}{\partial n} + 2(u^\varepsilon \cdot n) v - n q \right) \right) \cdot \tilde{u} ds \end{aligned}$$

By taking an arbitrary direction \tilde{u} which vanishes in neighborhood of the boundary Γ_2 , we have

$$\begin{aligned} -\nu \Delta v + (\nabla u^\varepsilon)^T \cdot v - (u^\varepsilon \cdot \nabla) v - \frac{1}{2} \nabla(u^\varepsilon \cdot v) + \frac{1}{2} (\nabla \cdot u^\varepsilon) v + a |u^\varepsilon|^{\alpha-2} (|u^\varepsilon|^2 v + \alpha (u^\varepsilon \cdot v) u^\varepsilon) \\ + \nabla q = (u^\varepsilon - u_d) - \sigma \underline{\text{curl}}(\text{curl}(u^\varepsilon)) \end{aligned}$$

An arbitrary \tilde{u} in Γ_2 gives

$$\nu \frac{\partial v}{\partial n} + 2(u^\varepsilon \cdot n) v - n q = \sigma \text{curl}(u^\varepsilon) \cdot \tau \quad \text{on } \Gamma_2$$

Finally we get the adjoint system

$$\left\{ \begin{array}{ll} -\nu \Delta v + (\nabla u^\varepsilon)^T \cdot v - (u^\varepsilon \cdot \nabla) v - \frac{1}{2} \nabla(u^\varepsilon \cdot v) + \frac{1}{2} (\nabla \cdot u^\varepsilon) v + a |u^\varepsilon|^{\alpha-2} (|u^\varepsilon|^2 v + \alpha (u^\varepsilon \cdot v) u^\varepsilon) \\ \quad + \nabla q = (u^\varepsilon - u_d) - \sigma \underline{\text{curl}}(\text{curl}(u^\varepsilon)) & \text{in } \Omega \\ \nabla.v + \varepsilon q = 0 & \text{in } \Omega \\ v = 0 & \text{on } \Gamma_1 \\ \nu \frac{\partial v}{\partial n} + 2(u^\varepsilon \cdot n) v - n q = \sigma \text{curl}(u^\varepsilon) \cdot \tau & \text{on } \Gamma_2 \end{array} \right. \quad (4.158)$$

■

4.7.2 Shape gradient

We express the shape gradient using the state and adjoint systems using the derivative of the saddle point problem $j(t)$ with respect to t , where

$$j(t) = \min_{(u_t^\varepsilon, p_t^\varepsilon) \in V_0(\Omega_t) \times Y(\Omega_t)} \max_{(v_t, q_t) \in V_0(\Omega_t) \times Y(\Omega_t)} L(\Omega_t, u_t^\varepsilon, p_t^\varepsilon, v_t, q_t)$$

and (u_t, p_t) and (v_t, q_t) are solutions of (4.153) and (4.155) in the perturbed domain Ω_t , respectively.

We consider the Hilbert spaces which depend on the parameter t defined by

$$\begin{aligned} V_0(\Omega_t) &= \{u^\varepsilon \circ T_t^{-1} : u^\varepsilon \in V_0(\Omega)\} \\ Y(\Omega_t) &= \{p^\varepsilon \circ T_t^{-1} : p^\varepsilon \in Y(\Omega)\} \end{aligned}$$

Since T_t and T_t^{-1} are homeomorphisms, the parametrization do not influence $j(t)$, and we have

$$j(t) = \min_{(u^\varepsilon, p^\varepsilon) \in V_0(\Omega) \times Y(\Omega)} \max_{(v, q) \in V_0(\Omega) \times Y(\Omega)} L(\Omega_t, u^\varepsilon \circ T_t^{-1}, p^\varepsilon \circ T_t^{-1}, v \circ T_t^{-1}, q \circ T_t^{-1})$$

We introduce the following functions which depend on the parameter t

$$\begin{aligned} l_1(t) &= \frac{1}{2} \int_{\Omega_t} |u^\varepsilon \circ T_t^{-1} - u_d|^2 dx + \frac{\sigma}{2} \int_{\Omega_t} |\text{curl}(u^\varepsilon \circ T_t^{-1})|^2 dx, \\ l_2(t) &= \int_{\Omega_t} [\nu \nabla(u^\varepsilon \circ T_t^{-1}) : \nabla(v \circ T_t^{-1}) + ((u^\varepsilon \circ T_t^{-1}) \cdot \nabla)(u^\varepsilon \circ T_t^{-1}) \cdot (v \circ T_t^{-1}) \\ &\quad + a |u^\varepsilon \circ T_t^{-1}|^\alpha (u^\varepsilon \circ T_t^{-1}) \cdot (v \circ T_t^{-1}) - (p^\varepsilon \circ T_t^{-1}) \nabla \cdot (v \circ T_t^{-1})] dx \\ &\quad - \int_{\Omega_t} (f \circ T_t^{-1}) \cdot (v \circ T_t^{-1}) dx - \int_{\Omega_t} (q \circ T_t^{-1}) \nabla \cdot (u^\varepsilon \circ T_t^{-1}) dx \\ &\quad - \varepsilon \int_{\Omega_t} (q \circ T_t^{-1}) (p^\varepsilon \circ T_t^{-1}) dx \end{aligned}$$

The Lagrangian functional writes

$$L(\Omega_t, u^\varepsilon \circ T_t^{-1}, p^\varepsilon \circ T_t^{-1}, v \circ T_t^{-1}, q \circ T_t^{-1}) = l_1(t) - l_2(t)$$

If $\Phi : [0, \tau] \times \mathbb{R}^d \rightarrow \mathbb{R}$ is sufficiently smooth, we have the following Hadamard formula

$$\frac{d}{dt} \int_{\Omega_t} \Phi(t, x) dx |_{t=0} = \int_{\Omega} \frac{\partial \Phi}{\partial t}(0, x) dx + \int_{\partial \Omega} \Phi(0, x) V(0, X) \cdot n ds \quad (4.159)$$

Let $\mathbf{V}(0, X) \in V_{ad}$, and observe that $\mathbf{V}(0, X) = \mathbf{V}$. Therefore we can derive the shape gradient using the formula (4.159):

$$\frac{d}{dt} L(\Omega_t, u^\varepsilon \circ T_t^{-1}, p^\varepsilon \circ T_t^{-1}, v \circ T_t^{-1}, q \circ T_t^{-1}) |_{t=0} = l'_1(0) - l'_2(0) \quad (4.160)$$

where

$$\begin{aligned}
 l'_1(0) &= \int_{\Omega} (u^\varepsilon - u_d) \cdot (-\nabla u^\varepsilon \cdot \mathbf{V}) dx + \sigma \int_{\Omega} \operatorname{curl}(u^\varepsilon) \operatorname{curl}(-\nabla u^\varepsilon \cdot \mathbf{V}) dx \\
 &\quad + \frac{1}{2} \int_{\Gamma_1} (|u^\varepsilon - u_d|^2 \mathbf{V} \cdot \mathbf{n}) ds + \frac{\sigma}{2} \int_{\Gamma_1} (|\operatorname{curl}(u^\varepsilon)|^2 \mathbf{V} \cdot \mathbf{n}) ds
 \end{aligned} \tag{4.161}$$

$$\begin{aligned}
 l'_2(0) &= \int_{\Omega} [\nu \nabla(-\nabla u^\varepsilon \cdot \mathbf{V}) : \nabla v + \nu \nabla u^\varepsilon : \nabla(-\nabla v \cdot \mathbf{V}) \\
 &\quad + ((-\nabla u^\varepsilon \cdot \mathbf{V}) \cdot \nabla u^\varepsilon) \cdot v + (u^\varepsilon \cdot \nabla(-\nabla u^\varepsilon \cdot \mathbf{V})) \cdot v + (u^\varepsilon \cdot \nabla u^\varepsilon) \cdot (-\nabla v \cdot \mathbf{V}) \\
 &\quad + \frac{1}{2} \nabla \cdot (-\nabla u^\varepsilon \cdot \mathbf{V}) u^\varepsilon \cdot v + \frac{1}{2} \nabla \cdot u^\varepsilon (-\nabla u^\varepsilon \cdot \mathbf{V}) \cdot v + \frac{1}{2} \nabla \cdot u^\varepsilon u^\varepsilon \cdot (-\nabla v \cdot \mathbf{V}) \\
 &\quad + a \alpha |u^\varepsilon|^{\alpha-2} (-\nabla u^\varepsilon \cdot \mathbf{V} \cdot u^\varepsilon) (u^\varepsilon \cdot v) + a |u^\varepsilon|^\alpha (-\nabla u^\varepsilon \cdot \mathbf{V}) \cdot v \\
 &\quad + a |u^\varepsilon|^\alpha u^\varepsilon \cdot (-\nabla v \cdot \mathbf{V}) - (\nabla p^\varepsilon \cdot \mathbf{V}) \nabla \cdot v - p^\varepsilon \nabla \cdot (-\nabla v \cdot \mathbf{V}) \\
 &\quad - f \cdot (-\nabla v \cdot \mathbf{V}) \cdot - (f \cdot \mathbf{V}) \cdot v - q \nabla \cdot (-\nabla u^\varepsilon \cdot \mathbf{V}) - (\nabla \cdot u^\varepsilon) (-\nabla q \cdot \mathbf{V})] dx
 \end{aligned}$$

Thanks to Green's formula and the condition $u^\varepsilon = 0$ on Γ_1 , we get

$$\begin{aligned}
 l'_2(0) &= - \int_{\Omega} [(-\nu \Delta u^\varepsilon + (u^\varepsilon \cdot \nabla) u^\varepsilon + \frac{1}{2} \nabla \cdot u^\varepsilon u^\varepsilon + a |u^\varepsilon|^\alpha u^\varepsilon + \nabla p^\varepsilon - f) \cdot (\nabla v \cdot \mathbf{V})] dx \\
 &\quad + \int_{\Omega} (\nabla \cdot u^\varepsilon) (\nabla q \cdot \mathbf{V}) dx + \int_{\Omega} (\nabla \cdot v) (\nabla p \cdot \mathbf{V}) dx + \int_{\Omega} [-\nu \Delta v + (\nabla u^\varepsilon)^T \cdot v - (u^\varepsilon \cdot \nabla) v \\
 &\quad - \frac{1}{2} \nabla (u^\varepsilon \cdot v) + \frac{1}{2} (\nabla \cdot u^\varepsilon) v + a |u^\varepsilon|^{\alpha-2} (|u^\varepsilon|^2 v + \alpha (u^\varepsilon \cdot v) u^\varepsilon) - \nabla q] \cdot (\nabla u^\varepsilon \cdot \mathbf{V}) dx \\
 &\quad - \int_{\Gamma_1} [\nu \frac{\partial v}{\partial \mathbf{n}} + 2(u^\varepsilon \cdot \mathbf{n}) v - nq] \cdot (\nabla u^\varepsilon \cdot \mathbf{V}) ds - \int_{\Gamma_1} [\frac{\partial u^\varepsilon}{\partial \mathbf{n}} - np^\varepsilon] \cdot (\nabla v \cdot \mathbf{V}) ds \\
 &\quad + \int_{\Gamma_1} [\nu \nabla u^\varepsilon : \nabla v + (u^\varepsilon \cdot \nabla u^\varepsilon) \cdot v + a |u^\varepsilon|^\alpha u^\varepsilon \cdot v - p^\varepsilon \nabla \cdot v - q \nabla \cdot u^\varepsilon] \mathbf{V} \cdot \mathbf{n} ds
 \end{aligned} \tag{4.162}$$

Replacing (4.161) and (4.162) in (4.160) and using the fact that $(u^\varepsilon, p^\varepsilon)$ is solution of (4.153) and (v, q) is solution of (4.155) respectively yields to

$$\begin{aligned}
 dJ(\Omega; \mathbf{V}) &= \frac{d}{dt} L|_{t=0} \\
 &= \frac{1}{2} \int_{\Gamma_1} ((|u^\varepsilon - u_d|^2 + \sigma |\operatorname{curl}(u^\varepsilon)|^2) \mathbf{V} \cdot \mathbf{n}) ds + \int_{\Gamma_1} [\nu \frac{\partial v}{\partial \mathbf{n}} - nq] \cdot (\nabla u^\varepsilon \cdot \mathbf{V}) ds \\
 &\quad + \int_{\Gamma_1} [\nu \frac{\partial u^\varepsilon}{\partial \mathbf{n}} - np^\varepsilon] \cdot (\nabla v \cdot \mathbf{V}) ds - \int_{\Gamma_1} [(\nu \nabla u^\varepsilon : \nabla v) \mathbf{V} \cdot \mathbf{n} ds \\
 &\quad - \sigma \int_{\Gamma_1} (\frac{\partial u^\varepsilon}{\partial \mathbf{n}} \cdot (\operatorname{curl}(u^\varepsilon) \wedge \mathbf{n})) \mathbf{V} \cdot \mathbf{n} ds
 \end{aligned} \tag{4.163}$$

Notice the fact that $u^\varepsilon = 0$, $v=0$ in Γ_1 we have

$$\mathbf{n} \cdot (\nabla u^\varepsilon \cdot \mathbf{V}) = \nabla u^\varepsilon \cdot (\mathbf{n} \otimes \mathbf{n}) \cdot \mathbf{V} \cdot \mathbf{n} = \nabla u^\varepsilon \cdot \mathbf{n} \cdot \mathbf{n} (\mathbf{V} \cdot \mathbf{n}) = (\nabla \cdot u^\varepsilon)(\mathbf{V} \cdot \mathbf{n}) = 0, \quad \forall x \in \Gamma_1 \quad (4.164)$$

$$\frac{\partial v}{\partial \mathbf{n}} \cdot (\nabla u^\varepsilon \cdot \mathbf{V}) = \nabla u^\varepsilon \cdot (\mathbf{n} \otimes \mathbf{n}) \cdot \mathbf{V} \cdot \frac{\partial v}{\partial \mathbf{n}} = \frac{\partial u^\varepsilon}{\partial \mathbf{n}} \cdot \frac{\partial v}{\partial \mathbf{n}} (\mathbf{V} \cdot \mathbf{n}) = (\nabla u^\varepsilon : \nabla v) \mathbf{V} \cdot \mathbf{n} \quad (4.165)$$

In a similar way, one obtains

$$\mathbf{n} \cdot (\nabla v \cdot \mathbf{V}) = 0, \quad \frac{\partial u^\varepsilon}{\partial \mathbf{n}} \cdot (\nabla v \cdot \mathbf{V}) = \frac{\partial u^\varepsilon}{\partial \mathbf{n}} \cdot \frac{\partial v}{\partial \mathbf{n}} (\mathbf{V} \cdot \mathbf{n}) = (\nabla u^\varepsilon : \nabla v) \mathbf{V} \cdot \mathbf{n} \quad (4.166)$$

By replacing (4.164)-(4.166) in (4.163) the shape derivative takes the form

$$dJ(\Omega; \mathbf{V}) = \int_{\Gamma_1} \left[\frac{1}{2} |u^\varepsilon - u_d|^2 + \frac{\sigma}{2} |\text{curl}(u^\varepsilon)|^2 + \frac{\partial u^\varepsilon}{\partial \mathbf{n}} \cdot \left(2\nu \frac{\partial v}{\partial \mathbf{n}} - \sigma \text{curl}(u^\varepsilon) \wedge \mathbf{n} \right) \right] \mathbf{V} \cdot \mathbf{n} \, ds \quad (4.167)$$

Therefore, the shape gradient reads as

$$\nabla J = \left[\frac{1}{2} |u^\varepsilon - u_d|^2 + \frac{\sigma}{2} |\text{curl}(u^\varepsilon)|^2 + \frac{\partial u^\varepsilon}{\partial \mathbf{n}} \cdot \left(2\nu \frac{\partial v}{\partial \mathbf{n}} - \sigma \text{curl}(u^\varepsilon) \wedge \mathbf{n} \right) \right] \mathbf{n} \quad (4.168)$$

Bibliography

- [1] C.H. Clay, : Design of fishways and other Fish Facilities. Lewis Publishers, CRC Press, Boca Raton, (1995) p 248.
- [2] C. Katopodis, N. Rajaratnam, S. Wu, D. Towell: Denil Fishways of varying. ASCE J. Hydraul. Eng. 123 (1997) 624-631.
- [3] N. Rajaratnam, G. Van de Vinne, C. Katopodis, Hydraulics of vertical slot fishways. ASCE J. Hydraul. Eng. 130, (1986), 909-917.
- [4] L.J. Alvarez-Vazquez, A. Martinez, M.E. Vazquez Mendez and M.A Vilar, An optimal shape problem related to the realistic design of river fishways, Ecological engineering 32 (2008) 293-300.
- [5] Z. Chen, S. Lyons, G. Qin, Derivation of the Forchheimer law via homogenization. Transp. Porous Media. 44 (2001) 325-335.
- [6] J. Chorda, M. M. Maubourguet, H. Roux, M. Larinier, L. Tarrade, L. David, Two-dimensional free surface flow numerical model for vertical slot fishways. Journal of Hydraulic Research, 48:2. pp. 141-151. ISSN 1814-2079, (2010).
- [7] G.F Carey, R. Krishnan, Penalty finite element method for the Navier Stokes equations. Computer methods in applied mechanics and engineering 42, 183-224, (1984)

- [8] F. Hecht, O. Pironneau, A. Le Hyaric, K. Ohtsuka, FreeFem++ Manual, available at <http://www.freefem.org>.
- [9] S. Irmay, On the theoretical derivation of Darcy and Forchheimer formulas, *Trans. Amer. Geophys. Union.* 84 (1958) 702–707.
- [10] W. Li, W. Wang, Q. Jiu, Existence and uniqueness of the weak solutions for the steady incompressible Navier Stokes equations with damping, *African diaspora journal of mathematics*, volume 12, number 2, pp 57-72, (2011)
- [11] D. A. Nield, Resolution of a paradox involving viscous dissipation and nonlinear drag in a porous medium, *Transport in Porous Media*, 41, (2000) 349–357.
- [12] J. Su, Z. Chen, Z. Wang, G. Xi, An adaptive finite element method for shape optimization in stationary incompressible flow with damping, *International journal of numerical analysis and modelling* , series B, volume 5, number 1-2, pp 79-96, (2014)
- [13] M. Louaked, N. Seloula, S. Sun, S. Trabelsi, A pseudocompressibility method for the incompressible Brinkman-Forchheimer equations, *Differential Integral Equations*, 28:361-382, (2015)
- [14] M. Louaked, N. Seloula, S. Trabelsi, Approximation of the unsteady Brinkman-Forchheimer equations by the pressure stabilization method, *Numerical Methods for Partial Differential Equations*, 33: 1949-1965, (2017)
- [15] R. Temam, Une méthode d’approximation de la solution des équations de Navier Stokes, *Bull. Soc. Math. France*, 98(4):115-152, 1968.
- [16] R. Temam, Sur l’approximation de la solution des équations de Navier Stokes par la méthode des pas fractionnaires (ii), *Archive for Rational Mechanics and Analysis*, 33(5): 377-385, 1969.
- [17] J. Shen, On error estimates of the penalty method for unsteady Navier Stokes equations. *SIAM Journal on Numerical Analysis*, 32(2):386:403, 1995.
- [18] A. J. Chorin, Numerical solution for the Navier Stokes equations. *Mathematics of computation*, 22(104):745-762, 1968.
- [19] A. J. Chorin, On the convergence of discrete approximations to the Navier Stokes equations. *Mathematics of computation*, 23(106):341-353, 1969.
- [20] G.P. Galdi, An introduction to the Mathematical Theory of the Navier Stokes Equations. Vol. Linearized Steady Problems. Springer-Verlag. New York. Berlin. etc. 1994.
- [21] H. Sohr, The Navier-Stokes Equations: an elementary functional analytic approach. Birkhauser, 2001.

- [22] M. Kadiri, Shape optimization and applications to hydraulic structures : mathematical analysis and numerical approximation, Thèse doctorat, Université De Caen Normandie, 2019.

Chapter 5

The application of adjoint method for shape optimization in porous media model

Contents

5.1	Introduction	191
5.2	The Navier-Stokes Forchheimer equations	193
5.3	Main results	194
5.3.1	Existence of the weak solution	195
5.3.2	Uniqueness of weak solutions	198
5.4	A shape optimization problem and adjoint states	199
5.5	Finite Element approximation	203
5.5.1	Space discretization : the Finite Element method	205
5.5.2	Algorithmic description of the implemented method	206
5.5.3	Numerical results : academic case	208
5.5.4	Numerical results : practical case	212
5.6	Conclusions	215

5.1 Introduction

Nowadays, the conservation of the environment has become a major issue in order to keep the balance in our civilization. Some species move locally, such as pike that spawn in flooded meadows and marshes. Others make larger displacements, such as the highly migratory ones, which will move from the marine environment to the freshwater environment according to their reproductive cycle. For example, salmon or trout perform the reproductive phase in freshwater. To facilitate the migration of these species from saltwater to freshwater, the humans built the

fishway. The fishway is hydraulic structure constructed near dams. In the literature, some types of fishways are studied such as the vertical slot [1] and Denil [2] presented in Figure 5.1.

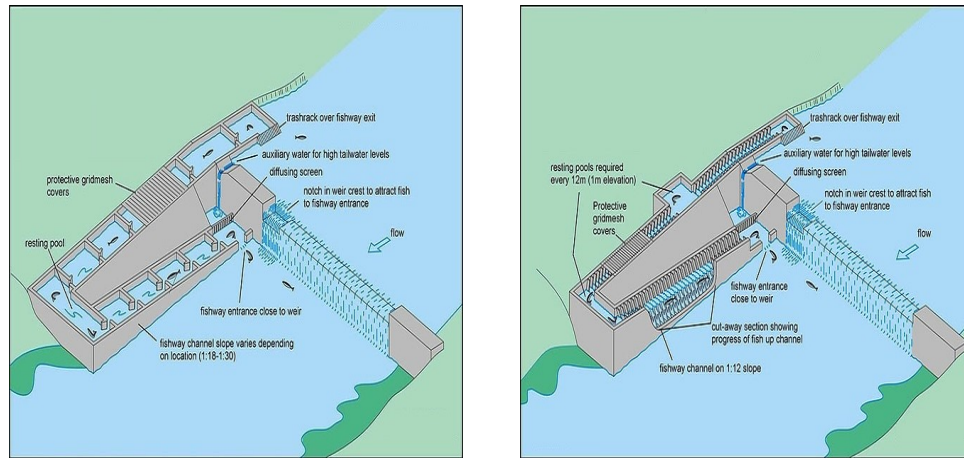


Figure 5.1: Exemple of vertical slot and Denil fishway

In recent years, much consideration has been given from the theoretical and experimental view point on hydraulic characteristics, the fluid flow regime and how to control the effect of the turbulence in all types of fishway. Several authors have studied these phenomena, [3] presented an application of mathematical modeling and optimal control theory related to enhance of the stockes of fish migrating between saltwater and freshwater, [4] they did an experimental study to characterize the turbulent flow for various structural configurations of vertical slot fishway and to determine how their characteristics could be modified to facilitate the passage of small species.

One of the important tasks in designing a fishway is to reduce the turbulence in the pools that allows rest and facilitate a movement of fish from pool to another without expending energy. The shape optimization problem consists to find an optimal shape in an admissible set. There are several optimization strategies in the literature used in the context of the fluid mechanics [5], [6]. In the case of structural mechanics the density-based methods and the SIMP method (Solid Isotropic Material with Penalisation)[7] are widely used. Some examples are discussed by [8], [9] and [10]. Another class of shape and topology optimization strategies relies on the Level Set Method introduced by [11; 12; 13; 14], and [24; 25].

The remainder of the chapter is organized as follows. in the next section, we introduce the physical model. In section 3, we analyze the existence and uniqueness of the solution for the Navier-Stokes Forchheimer system. In section 4, a 2D model is used to examine an optimal control problem, and we derive the adjoint state. In section 5 and 6, we describe the Finite Elements method by using the Euler scheme, the detail and the description of the implemented of the augmented Lagrangian algorithm. Finally, in order to show the efficiency of our method, some numerical results are presented.

5.2 The Navier-Stokes Forchheimer equations

Assume the $\Omega \subset \mathbb{R}^d$ ($d = 2$ or 3) is a regular bounded domain, corresponding to the fluid surface in the hydraulic structure, the flow is governed by the viscous stationary incompressible Navier-Stokes Forchheimer equations with kinematic viscosity $\nu > 0$. The structure is composed of four disjoint regions : $\partial\Omega = \Gamma_{in} \cup \Gamma_{out} \cup \Gamma$

- Γ_{in} the inflow boundary,
- Γ_{out} the outflow boundary,
- Γ no slip boundary condition

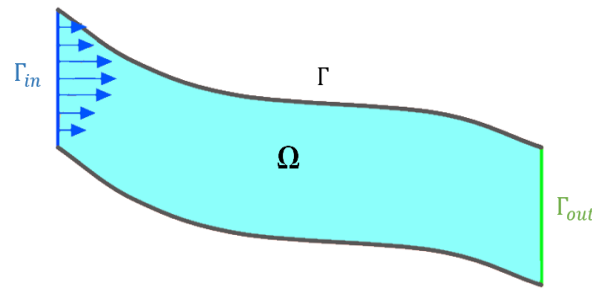


Figure 5.2: Schematic representation of the fluid domain

$$\begin{cases} -\nu\Delta u + (u.\nabla)u + \nabla p + au + b |u|^\alpha u = f & \text{in } \Omega \\ \text{div}(u) = 0 & \text{in } \Omega \end{cases} \quad (5.1)$$

The boundary conditions are either on the flow velocity or stress. Both Dirichlet-type and Newmann-type boundary condition are considered in the following form

$$\begin{cases} u = u_{in} & \text{on } \Gamma_{in} \\ u = 0 & \text{on } \Gamma \\ \sigma(u, p).n = 0 & \text{on } \Gamma_{out} \end{cases} \quad (5.2)$$

where $u(x, t) \in \mathbb{R}^d$ is the velocity field at point $x \in \Omega$ and time $t \in [0, T]$, $p(x, t) \in \mathbb{R}$ is the pressure, ∇ and Δ denote the gradient and Laplacian operators in \mathbb{R} respectively, f is a given function. The coefficient satisfy $a > 0$, $b > 0$ and $1 < \alpha < \infty$, ν denotes the reciprocal of the Reynolds number Re , $\nu(\cdot) = \frac{1}{Re} : \mathbb{R} \rightarrow \mathbb{R}$. n is the unit normal vector on the smooth boundary $\partial\Omega$. The classical mechanical stress $\sigma(u, p)$ of the fluid is defined by

$$\sigma(u, p) = 2\nu\mathbf{e}(u) - p\mathbf{I}, \quad \text{where } \mathbf{e}(u) = \frac{1}{2}(\nabla u + {}^T\nabla u)$$

where $\mathbf{e}(u)$ is the strain tensor.

We consider the weak solution of the Navier-Stokes Forchheimer system giving by eq. (5.3),

and we define the Hilbert spaces for the unknown functions u and p . Thus, the problem is to find a solution satisfies that the couple $(u, p) \in \hat{V}_{in}(\Omega) \times \hat{M}(\Omega)$. The weak formulation of the Navier-Stokes Forchheimer equations (5.1) is to :

$$\left\{ \begin{array}{l} \text{Find } (u, p) \in \hat{V}_{in}(\Omega) \times \hat{M}(\Omega) \text{ such that} \\ \int_{\Omega} [\nu \nabla u : \nabla v + (u \cdot \nabla)u \cdot v + au \cdot v + b |u|^\alpha u \cdot v - p \operatorname{div} v] dx = \int_{\Omega} f v, \quad \forall v \in \hat{V}(\Omega) \\ \int_{\Omega} \operatorname{div} u q = 0, \quad \forall q \in \hat{M}(\Omega) \end{array} \right. \quad (5.3)$$

Let Ω be a bounded domain $\mathbb{R}^d, (d = 2, 3)$. if $\|u\|_r = \left(\int_{\Omega} |u|^r dx \right)^{\frac{1}{r}} < \infty, 1 \leq r < \infty$, we say $u \in L^r(\Omega)$ under the norm define above. Let $C_{0,div}^\infty(\Omega)$ denotes the set of all C^∞ real vector-valued functions $u = (u^1, u^2, \dots, u^d)$ with compact support in Ω such that $\operatorname{div} u = 0$. We denote by $H^r(\Omega)$ the Sobolev space and $H^{-r}(\Omega)$ dual space with the norm $\|u\|_{H^r}$. The Hilbert spaces are define in the following form :

$$\begin{aligned} \hat{V}_0(\Omega) &= \{u \in (H^1(\Omega))^d | u = 0 \text{ on } \Gamma\} \\ \hat{V}(\Omega) &= \{v \in (H^1(\Omega))^d | v = 0 \text{ on } \Gamma_{in}\} \\ \hat{V}_{in}(\Omega) &= \{u \in (H^1(\Omega))^d | u = 0 \text{ on } \Gamma, u = u_{in} \text{ on } \Gamma_{in}\} \\ \hat{M}(\Omega) &= \left\{ p \in L^2(\Omega); \int_{\Omega} p dx = 0 \right\} \\ M(\Omega) &= \{p \in H^1(\Omega)\} \\ V_0(\Omega) &= \{u \in (H^2(\Omega))^d | u = 0 \text{ on } \Gamma\} \\ V_{in}(\Omega) &= \{u \in (H^2(\Omega))^d | u = 0 \text{ on } \Gamma, u = u_{in} \text{ on } \Gamma_{in}\} \end{aligned}$$

5.3 Main results

Before stating the main results of the existence of the weak solution and the uniqueness solution, we recall some definitions of functional analysis. The following Lemma will be needed later for the proof.

Theorem 5.3.1. Rellich-Kondrachov (for more details see reference [16]). Consider Ω is bounded and of class C^1 and $1 \leq p \leq \infty$. Then we have the following injections

$$\begin{aligned} H^{1,p}(\Omega) &\hookrightarrow L^q(\Omega) \quad \forall q \in [1, p^*), \quad \text{where } \frac{1}{p^*} = \frac{1}{p} - \frac{1}{N}, \quad \text{if } p < N, \\ H^{1,p}(\Omega) &\hookrightarrow L^q(\Omega) \quad \forall q \in [p, +\infty), \quad \text{if } p = N, \\ H^{1,p}(\Omega) &\hookrightarrow C(\bar{\Omega}), \quad \text{if } p > N \end{aligned}$$

and all these injections are continuous.

Lemma 5.3.2. (for more details see reference [22]). We consider Ω a bounded locally Lips-

chitzian domain in $\mathbb{R}^d, (d \geq 2)$. if for any $\mathcal{F} \in H^{-1}(\Omega)$ and $v \in (H_0^1(\Omega))^d$

$$(\mathcal{F}, v) = 0$$

then there existe a unique $P \in L^2(\Omega)$ satisfying

$$(\mathcal{F}, v) = \int_{\Omega} P \operatorname{div}(v) dx \quad \text{and} \quad \int_{\Omega} P dx = 0$$

Lemma 5.3.3. (for more detail see reference [22]). Let Ω be an arbitrary domain in $\mathbb{R}^d, (d = 2, 3)$. Then a vector $V \in H_{loc}^1(\Omega)$ satisfies the system (5.3) for all $\varphi \in C_{0,div}^{\infty}(\Omega)$ if and only if there $P \in L_{loc}^2$ satisfying the identity

$$\nu (\nabla V : \nabla \psi) + (aV, \psi) + (b |V|^{\alpha} V, \psi) - (P, \nabla \cdot \psi) = (f, \psi) \quad (5.4)$$

for all $\psi \in C_0^{\infty}(\Omega)$, if, moreover, Ω is bounded and Lipschitzian and $f \in H^{-1}(\Omega)$, $V \in (H_0^1(\Omega))^d$ then

$$P \in L^2(\Omega) \quad \text{with} \quad \int_{\Omega} P dx = 0 \quad (5.5)$$

and (5.4) holds for all $\psi \in (H_0^1(\Omega))^d$

Lemma 5.3.4. (for more detail see reference [22]). We consider \mathcal{F} a continuous function $\mathcal{F} : \mathbb{R}^m \rightarrow \mathbb{R}^m$, for $(m \geq 1)$ and such that for some $k > 0$

$$\mathcal{F}(\xi) \cdot \xi > 0$$

for all $\xi \in \mathbb{R}^m$ with $|\xi| = k$. Then there exists $\xi_0 \in \mathbb{R}^m$ with $|\xi_0| \leq k$ such that $\mathcal{F}(\xi_0) = 0$

5.3.1 Existence of the weak solution

In this part, we consider the existence of the weak solutions of the problem (5.3) with Dirichlet's and Neumann boundary condition, the domain $\Omega \in \mathbb{R}^d, (d = 2, 3)$.

Theorem 5.3.5. We consider Ω a bounded domain in $\mathbb{R}^d, (d = 2, 3)$, $f \in H^{-1}(\Omega)$ is an given function (external force g). If $u = 0$ on $\partial\Omega$ and $0 \leq \alpha < 10$, there exists at least a weak solutions of (5.3) satisfying

$$\frac{\nu}{2} \|\nabla u_m\|^2 + a \|u_m\|_{L^2}^2 + b \|u_m\|_{L^{\alpha+2}}^{\alpha+2} \leq c \|f\|_{H^{-1}}^2 \quad (5.6)$$

and

$$\|p\| \leq C \left[(\nu + c_1 + c_2 a) \|u\|_{H^1} + c_3 b \|u\|_{L^{2\alpha+2}}^{\alpha+1} - c_4 \|f\|_{H^{-1}} \right] \quad (5.7)$$

where C, c_1, c_2, c_3 and c_4 are a positive constants and $\nu > 0$

Proof. (of theorem)

We consider the sequence an orthogonal basis $\psi \in \hat{M}(\Omega)$ and for each $m \in \mathbb{N}$, we define the

approximate solutions $u_m \in M(\Omega)$ as follows

$$u_m = \sum_{k=1}^m \xi_{km} \psi_k \quad (5.8)$$

and

$$\nu (\nabla u_m : \nabla \psi_k) + (u_m \cdot \nabla u_m, \psi_k) + (a u_m, \psi_k) + (b |u_m|^\alpha u_m, \psi_k) = (f, \psi_k) \quad 1 \leq k \leq m \quad (5.9)$$

Substituting in equations (5.8) and (5.9), we obtain a system of nonlinear differential equations for the coefficients ξ_{km} , by using the Lemma 8.2.1 in [15], we have

$$\sum_{k=1}^m (u_m \cdot \nabla u_m, \xi_{km} \psi_k) = (u_m \cdot \nabla u_m, u_m) = 0 \quad (5.10)$$

We multiply (5.9) by ξ_{km} on both sides and summing with respect to k , we have

$$\nu (\nabla u_m : \nabla u_m) + (u_m \cdot \nabla u_m, u_m) + (a u_m, u_m) + (b |u_m|^\alpha u_m, u_m) = (f, u_m) \quad 1 \leq k \leq m \quad (5.11)$$

using the property giving in (5.10), we get

$$\nu \|\nabla u_m\|^2 + a \|u_m\|_{L^2}^2 + b \|u_m\|_{L^{\alpha+2}}^{\alpha+2} = (f, u_m) \quad (5.12)$$

Using Schwarz and Poincaré's inequality for the right hand side of (5.12), we have

$$\frac{\nu}{2} \|\nabla u_m\|^2 + a \|u_m\|_{L^2}^2 + b \|u_m\|_{L^{\alpha+2}}^{\alpha+2} \leq c \|f\|_{H^{-1}}^2 \quad (5.13)$$

In the first step we have approximate the solutions and in this second step, we will find the existence of the approximate solutions. So, we introduce the following function

$$\mathcal{F}(u_m, u_m) = \nu (\nabla u_m : \nabla u_m) + (a u_m, u_m) + (b |u_m|^\alpha u_m, u_m) - (f, u_m)$$

Correspondingly, one has

$$\begin{aligned} \mathcal{F}(u_m, u_m) &\geq \nu \|\nabla u_m\|_{L^2}^2 + a \|u_m\|_{L^2}^2 + b \|u_m\|_{L^{\alpha+2}}^{\alpha+2} - \|f\|_{H^{-1}} \|\nabla u_m\|_{L^2} \\ &= (\nu \|\nabla u_m\|_{L^2} - \|f\|_{H^{-1}}) \|\nabla u_m\|_{L^2} + a \|u_m\|_{L^2}^2 + b \|u_m\|_{L^{\alpha+2}}^{\alpha+2} \end{aligned}$$

when $\|\nabla u_m\|_{L^2} = k$, $k > \frac{1}{\nu} \|f\|_{H^{-1}}$, by the Lemma (5.3.4), there exist the approximative solutions to (5.9) for $m \in \mathbb{N}$. Since the sequence (u_m) are uniformly bounded by (5.3.1), there exist a subsequence of (u_m) such that

$$u_m \longrightarrow u \quad \text{in} \quad (H_0^1(\Omega))^d \cap L^{\alpha+2} \quad (5.14)$$

It follows from Sobolev embedding $H^1 \hookrightarrow L^6$ from the theorem (5.3.1) ($p = N = 2$) we have

that

$$u_m \longrightarrow u \quad \text{in } L^{6-\varepsilon} \quad (5.15)$$

where $\varepsilon > 0$ is so constant. We summarize the convergence of the fifth terms in (5.9) when $m \longrightarrow \infty$

$$\lim_{m \rightarrow \infty} |(\nabla u_m, \nabla \psi_k) - (\nabla u, \nabla \psi_k)| = 0 \quad (5.16)$$

$$\lim_{m \rightarrow \infty} |(u_m \cdot \nabla u_m, \psi_k) - (u \cdot \nabla u, \psi_k)| = 0 \quad (5.17)$$

$$\lim_{m \rightarrow \infty} |(au_m, \psi_k) - (au, \psi_k)| = 0 \quad (5.18)$$

$$\lim_{m \rightarrow \infty} |(b | u_m |^\alpha u_m, \psi_k) - (b | u |^\alpha u, \psi_k)| = 0 \quad (5.19)$$

By (5.16), (5.17), (5.18) and (5.19), it follows that the field $u \in H_0^1(\Omega)$ satisfies the equation

$$\nu (\nabla u : \nabla \psi_k) + (u \cdot \nabla u, \psi_k) + (au, \psi_k) + (b | u |^\alpha u, \psi_k) = (f, \psi_k) \quad 1 \leq k \leq m \quad (5.20)$$

for all $k = 1, 2, \dots$, for any $\varphi \in (H_0^1(\Omega))^d$ can be approximated by linear combinations of ψ_k . Since

$$\frac{\nu}{2} \|\nabla u_m\|^2 + a \|u_m\|_{L^2}^2 + b \|u_m\|_{L^{\alpha+2}}^{\alpha+2} \leq c \|f\|_{H^{-1}}^2$$

For the existence for the pressure field, we consider Ω locally lipschitzian, from Lemma (5.3.3), there exist $p \in L^2(\Omega)$ satisfying (5.4) and (5.5). So, we consider the problem

$$\begin{cases} \nabla \cdot \eta = p \\ \eta \in (H_0^1(\Omega))^d \\ \|\eta\|_{H_0^1} \leq C \|p\|_{L^2} \end{cases} \quad (5.21)$$

Knowing that $p \in L^2(\Omega)$ and satisfies (5.5), the problem (5.21) admits a solution. We consider $\psi = \eta$ the system (5.4) is written in the following form

$$\nu (\nabla u : \nabla \eta) + (au, \eta) + (b | u |^\alpha u, \eta) - (p, \nabla \cdot \eta) = (f, \eta) \quad (5.22)$$

From the system (5.21) we have $\nabla \cdot \eta = p$, so the system (5.22) become

$$\nu (\nabla u : \nabla \eta) + (au, \eta) + (b | u |^\alpha u, \eta) - (p, p) = (f, \eta)$$

$$\|p\|^2 = \nu (\nabla u : \nabla \eta) + (au, \eta) + (b | u |^\alpha u, \eta) - (f, \eta)$$

Using Cauchy-Schwarz inequality we have

$$\begin{aligned}
\|p\|^2 &\leq \nu \|u\|_{H^1} \|\eta\|_{H^1} + c_1 \|u\|_{H^1} \|\eta\|_{H^1} + c_2 a \|u\|_{H^1} \|\eta\|_{H^1} \\
&\quad + c_3 b \|u\|_{L^{\alpha+1}}^{\alpha+1} \|\eta\|_{H^1} + c_4 \|f\|_{H^{-1}} \|\eta\|_{H^1} \\
\|p\|^2 &\leq C \left[(\nu + c_1 + c_2 a) \|u\|_{H^1} + c_3 b \|u\|_{L^{2\alpha+2}}^{\alpha+1} - c_4 \|f\|_{H^{-1}} \right] \|p\| \\
\|p\| &\leq C \left[(\nu + c_1 + c_2 a) \|u\|_{H^1} + c_3 b \|u\|_{L^{2\alpha+2}}^{\alpha+1} - c_4 \|f\|_{H^{-1}} \right]
\end{aligned} \tag{5.23}$$

■

5.3.2 Uniqueness of weak solutions

In order to prove the uniqueness of the weak solution of the Navier-Stokes Forchheimer problems (5.4). We begin to show our main result and then we give the proof of this theorem.

Theorem 5.3.6. *We consider Ω a bounded domain \mathbb{R}^d , ($d = 2, 3$) and locally Lipschitz, $u = 0$ on $\partial\Omega$, $f \in H^{-1}(\Omega)$. The solutions of (5.3) exist for any Reynolds number; however, if ν big enough and $\frac{2}{3} \leq \alpha \leq 4$, then the weak solution of the Navier-Stokes Forchheimer (5.3) is unique.*

Proof. We consider the two weak solutions u_1 and u_2 satisfying the equations

$$\nu (\nabla u_1 : \nabla \psi) + (u_1 \cdot \nabla u_1, \psi) + (a u_1, \psi) + (b |u_1|^\alpha u_1, \psi) = (f, \psi)$$

$$\nu (\nabla u_2 : \nabla \psi) + (u_2 \cdot \nabla u_2, \psi) + (a u_2, \psi) + (b |u_2|^\alpha u_2, \psi) = (f, \psi)$$

$$\nu (\nabla(u_1 - u_2) : \nabla \psi) + (u_1 \cdot \nabla u_1 - u_2 \cdot \nabla u_2, \psi) + (a u_1 - a u_2, \psi) + (b |u_1|^\alpha u_1 - b |u_2|^\alpha u_2, \psi) = 0$$

Let $\psi = u_1 - u_2$, we obtain

$$\begin{aligned}
&\nu (\nabla(u_1 - u_2) : \nabla(u_1 - u_2)) + (u_1 \cdot \nabla u_1 - u_2 \cdot \nabla u_2, u_1 - u_2) \\
&\quad + (a u_1 - a u_2, u_1 - u_2) + (b |u_1|^\alpha u_1 - b |u_2|^\alpha u_2, u_1 - u_2) = 0
\end{aligned}$$

moreover, we have

$$\begin{aligned}
\nu \|\nabla(u_1 - u_2)\|^2 &= \underbrace{-((u_1 - u_2) \cdot \nabla u_1, u_1 - u_2)}_{T_1} \\
&\quad - \underbrace{(b |u_1|^\alpha (u_1 - u_2), u_1 - u_2)}_{T_2} \\
&\quad - \underbrace{b ((|u_1|^\alpha - |u_2|^\alpha) u_2, u_1 - u_2)}_{T_3} \\
&\quad - \underbrace{(a (u_1 - u_2), u_1 - u_2)}_{T_4}
\end{aligned} \tag{5.24}$$

For the first term on the right hand side in (5.24),

$$\begin{aligned} |T_1| &\leq \|\nabla u_1\|_{L^2} \cdot \|u_1 - u_2\|_{L^4}^2 \\ &\leq c_5 \|f\|_{H^{-1}} \cdot \|u_1 - u_2\|_{L^6}^2 \\ &\leq c_5 \|f\|_{H^{-1}} \|\nabla(u_1 - u_2)\|_{L^2}^2 \end{aligned} \quad (5.25)$$

For the second term, using $1 \leq \frac{3\alpha}{2} \leq \alpha + 2$, we obtain

$$\begin{aligned} |T_2| &\leq \|b |u_1|^\alpha\|_{\frac{3}{2}} \| |u_1 - u_2|^2 \|_{L^3}^2 \\ &\leq b \| |u_1|^\alpha \|_{\frac{3}{2}} \|u_1 - u_2\|_{L^6}^2 \\ &\leq c_6 b \|f\|_{H^{-1}} \|\nabla(u_1 - u_2)\|_{L^2}^2 \end{aligned} \quad (5.26)$$

For the above estimate, using $1 \leq \frac{3\alpha}{2} \leq \alpha + 2$ for the third term, we obtain

$$|T_3| \leq c_7 b \alpha \|f\|_{H^{-1}} \|\nabla(u_1 - u_2)\|_{L^2}^2 \quad (5.27)$$

And for the last term, we obtain

$$\begin{aligned} |T_4| &= |a |u_1 - u_2|^2| \\ &\leq c_8 a \|\nabla(u_1 - u_2)\|_{L^2}^2 \end{aligned} \quad (5.28)$$

Substituting the differents terms, we obtain

$$\nu \|\nabla(u_1 - u_2)\|_{L^2}^2 - \left[c_5 + c_6 b + c_7 b \alpha + \frac{c_8 a}{\|f\|_{H^{-1}}} \right] \|f\|_{H^{-1}} \|\nabla(u_1 - u_2)\|_{L^2}^2 \leq 0 \quad (5.29)$$

■

5.4 A shape optimization problem and adjoint states

From numerical methods, our aim is to find the optimal shape Ω to minimize the total dissipative energy in the flow domain governed by the stationary incompressible Navier-Stokes Forchheimer equations. We define the set of admissible domains

$$Q_{ad} = \left\{ \Omega \subset \mathbb{R}^d : [\Gamma_{in} \cup \Gamma_{out} \cup \Gamma_{fix}] \subset \partial\Omega \text{ is fixed, } \int_{\Omega} dx = constant \right\}$$

The shape optimization problem can be written

$$\min_{\Omega \in Q_{ad}} J(\Omega) \quad \text{subject to} \quad G(\Omega) = 0 \quad (5.30)$$

where the objective function $J(\Omega)$ can take the form of the total dissipative energy $E(\Omega)$ related to the viscous forces of the fluid domain and a least-square discrepancy $D(\Omega)$ given by the

following equations respectively

$$E(\Omega) = \int_{\Omega} \sigma(u, p) : \mathbf{e}(u) dx = 2\nu \int_{\Omega} \|\mathbf{e}(u)\|^2 dx \quad (5.31)$$

$$D(\Omega) = \frac{1}{2} \int_{\Omega} |u - u_{ref}|^2 dx \quad (5.32)$$

In our case, we take into consideration the sum of the both previous function plus the dissipative energy and the least-square discrepancy. We have the following form:

$$\begin{aligned} J(\Omega) &= D(\Omega) + E(\Omega) \\ &= \frac{1}{2} \int_{\Omega} |u - u_{ref}|^2 dx + 2\nu \int_{\Omega} \|\mathbf{e}(u)\|^2 dx \end{aligned} \quad (5.33)$$

The shape optimization is a set of methods allowing to find the optimal shape of a given structure by minimizing the cost function $J(\Omega)$ while respecting a constraint of the form $G(\Omega)$. In the case of an optimization approach, first we discretize the optimized domain in a set of design variables, and in finite elements the PDE system. we use the approach of the derivatives of $J(\Omega)$ and $G(\Omega)$ with respect to the domain. In the case of this work, we rely on Hadamard's boundary variation method [19]. See also [20] for an overview of the rival notion of topological derivatives and the topological derivatives in the context of fluid mechanics [21].

According to the Hadamard method, the sensitivity of a function of the domain is assessed with respect to small perturbations of its boundary where the variations of the shape take the form

$$\Omega_{\theta} = (\text{Id} + \theta)(\Omega) \quad (5.34)$$

where $\theta : \mathbb{R}^d \rightarrow \mathbb{R}^d$ is a small vector field, Id is the identity mapping from \mathbb{R}^d into itself.

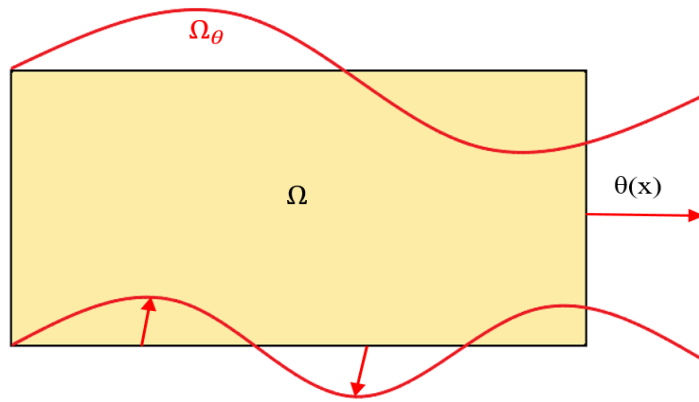


Figure 5.3: Example of a variation Ω_{θ} of shape Ω

Since the admissible shapes $\Omega \in Q_{ad}$ are smooth and only Γ is subject to optimization, it is natural that θ belong the set Θ_{ad} of admissible perturbations defined by

$$\Theta_{ad} = \left\{ \theta : \mathbb{R}^d \longrightarrow \mathbb{R}^d \text{ smooth, } \theta = 0 \text{ on } \Gamma_{in} \cup \Gamma_{out} \right\}$$

so that variations (5.34) of admissible shapes stay admissible.

Theorem 5.4.1. (for more detail see reference [23]). Consider Ω be a smooth shape. Then

1. The volume $Vol(\Omega)$ is shape differentiable and its derivative reads:

$$\forall \theta \in \Theta_{ad}, Vol'(\Omega)(\theta) = \int_{\Gamma} \theta \cdot n ds$$

2. The perimeter $Per'(\Omega)$ is shape differentiable and its derivative reads:

$$\forall \theta \in \Theta_{ad}, Per'(\Omega)(\theta) = \int_{\Gamma} \kappa \theta \cdot n ds$$

where $\kappa : \partial\Omega \longrightarrow \mathbb{R}$ is the mean curvature of $\partial\Omega$

Theorem 5.4.2. Let $\Omega \in Q_{ad}$; then the cost function $J(\Omega)$ given by (5.33) is shape differentiable and its derivative reads :

$$\forall \theta \in \Theta_{ad}, \nabla J(\Omega)(\theta) = 4\nu \int_{\Omega} e(u) : e(u) + \int_{\Omega} |u - u_{ref}| \quad (5.35)$$

and the adjoint system associated to the equations (5.1) (5.2) take the form

$$\left\{ \begin{array}{ll} -\nu \Delta v + (\nabla u)^T \cdot v - (u \cdot \nabla)v + av + b |u|^\alpha v + \alpha b |u|^{\alpha-2} (u \cdot v)u + \nabla q & \text{in } \Omega \\ = -(2\nu \Delta u + |u - u_{ref}|) & \text{in } \Omega \\ \operatorname{div}(v) = 0 & \text{in } \Omega \\ v = 0 & \text{on } \Gamma_{in} \\ v = 0 & \text{on } \Gamma \\ \sigma(v, \pi)n + (u \cdot n)v = 4\nu e(u) \cdot n & \text{on } \Gamma_{out} \end{array} \right. \quad (5.36)$$

Proof. We construct a Lagrangian fonctionnal by introducing the adjoint state variables (v, q) :

$$\mathcal{L}(\Omega, u, p, v, q) = J(\Omega) - F(\Omega, u, p, v, q) \quad (5.37)$$

where

$$F(\Omega, u, p, v, q) = \int_{\Omega} [\nu \nabla u : \nabla v + (u \cdot \nabla)u \cdot v + au \cdot v + b |u|^\alpha u \cdot v - p \operatorname{div}v] dx - \int_{\Omega} \operatorname{div}u q dx \quad (5.38)$$

Since

$$\max_{(v,\pi) \in V_0(\Omega) \times M(\Omega)} \mathcal{L}(\Omega, u, p, v, q) = \begin{cases} J(\Omega) & \text{if } F(\Omega, u, p, v, q) = 0 \\ +\infty & \text{if } F(\Omega, u, p, v, q) \neq 0 \end{cases} \quad (5.39)$$

then the solution of the optimization problem (5.30) is the minimum of the shape of the following problem

$$\min_{\Omega \in Q_{ad}} \min_{(u,p) \in V_g(\Omega) \times M(\Omega)} \max_{(v,q) \in V_0(\Omega) \times M(\Omega)} \mathcal{L}(\Omega, u, p, v, q) \quad (5.40)$$

Setting the first variation of \mathcal{L} with respect to the state arbitrary direction $\tilde{p} \in M(\Omega)$ to zero is equivalent to the condition

$$\frac{\partial \mathcal{L}}{\partial p}(\Omega, u, p, v, q) \cdot \tilde{p} = \int_{\Omega} \tilde{p} \operatorname{div} v dx \quad (5.41)$$

Since the variation \tilde{p} , we obtain

$$\operatorname{div} v = 0 \quad (5.42)$$

Next, we derive \mathcal{L} with respect to the state variable u in the arbitrary direction $\tilde{u} \in V_0(\Omega)$ and using the Green's formula

$$\begin{aligned} 0 &= \frac{\partial \mathcal{L}}{\partial u}(\Omega, u, p, v, q) \cdot \tilde{u} \\ &= 4\nu \int_{\Omega} \mathbf{e}(u) : \mathbf{e}(\tilde{u}) + \int_{\Omega} |u - u_{ref}| \\ &\quad - \int_{\Omega} [\nu \nabla \tilde{u} : \nabla v + (\tilde{u} \cdot \nabla) u \cdot v + (u \cdot \nabla) \tilde{u} \cdot v] dx + \int_{\Omega} \operatorname{div} \tilde{u} q dx \\ &\quad - \int_{\Omega} a \tilde{u} v dx - \int_{\Omega} [b |u|^{\alpha} \tilde{u} + \alpha b |u|^{\alpha-2} (u \cdot \tilde{u}) u] \cdot v dx \\ &= \int_{\Omega} [-4\nu \operatorname{div} \mathbf{e}(u) + \nu \Delta v - (\nabla u)^T \cdot v + (u \cdot \nabla) v] dx \\ &\quad - \int_{\Omega} a \tilde{u} v dx - \int_{\Omega} [b |u|^{\alpha} v + \alpha b |u|^{\alpha-2} (u \cdot v) u + \nabla q] \tilde{u} dx \\ &\quad + \int_{\partial \Gamma} \left[4\nu \mathbf{e}(u) \cdot n - \nu \frac{\partial v}{\partial n} + (u \cdot n) v - n q \right] \tilde{u} ds \\ &= \int_{\Omega} [-4\nu \operatorname{div} \mathbf{e}(u) + \nu \Delta v - (\nabla u)^T \cdot v + (u \cdot \nabla) v] dx \\ &\quad - \int_{\Omega} a \tilde{u} v dx - \int_{\Omega} [b |u|^{\alpha} v + \alpha b |u|^{\alpha-2} (u \cdot v) u + \nabla q] \tilde{u} dx \\ &\quad + \int_{\partial \Gamma} [4\nu \mathbf{e}(u) \cdot n - (\sigma(v, q) n + (u \cdot n) v)] \tilde{u} ds \end{aligned}$$

First, we consider an arbitrary direction \tilde{u} in the boundary $\partial \Gamma$, we obtain

$$-\nu \Delta v + (\nabla u)^T \cdot v - (u \cdot \nabla) v + a v + b |u|^{\alpha} v + \alpha b |u|^{\alpha-2} (u \cdot v) u + \nabla q = -(4\nu \operatorname{div} \mathbf{e}(u) + |u - u_{ref}|) \quad (5.43)$$

We have the deformation tensor $\mathbf{e}(u) = \frac{1}{2}(\nabla u^T + \nabla u)$, we have $\nabla \cdot u = 0$ and ν is constant, then

$$\nabla \cdot 4\mathbf{e}(u) = 2\nu \nabla \cdot \nabla u + 2\nu \nabla \cdot \nabla^T u = 2\nu \nabla \cdot \nabla u + 2\nu \nabla \nabla \cdot u = \nu \nabla^2 u = 2\nu \Delta u$$

The equation (5.43) can be rewritten in the following form

$$-\nu \Delta v + (\nabla u)^T \cdot v - (u \cdot \nabla)v + av + b |u|^\alpha v + \alpha b |u|^{\alpha-2} (u \cdot v)u + \nabla q = - (2\nu \Delta u + |u - u_{ref}|) \quad (5.44)$$

On the other side, taking an arbitrary \tilde{u} in $\partial\Gamma$ gives

$$\sigma(v, q)n + (u \cdot n)v = 4\nu \mathbf{e}(u) \cdot n \quad (5.45)$$

Finally, the adjoint systems are obtained

$$\left\{ \begin{array}{ll} -\nu \Delta v + (\nabla u)^T \cdot v - (u \cdot \nabla)v + av + b |u|^\alpha v + \alpha b |u|^{\alpha-2} (u \cdot v)u + \nabla q \\ = - (2\nu \Delta u + |u - u_{ref}|) & \text{in } \Omega \\ \operatorname{div}(v) = 0 & \text{in } \Omega \\ v = 0 & \text{on } \Gamma_{in} \\ v = 0 & \text{on } \Gamma \\ \sigma(v, q)n + (u \cdot n)v = 4\nu \mathbf{e}(u) \cdot n & \text{on } \Gamma_{out} \end{array} \right. \quad (5.46)$$

■

5.5 Finite Element approximation

The numerical resolution of the stationary Navier-Stokes Forchheimer system at low Reynolds number is performed using the Finite Element method. The optimal design is a set of methods to find the best shape. These methods are used in many fields such as aerodynamics, hydrodynamics and mechanical engineering where we talk about structural optimization. In our case, we use the augmented Lagrangian algorithm to obtain the optimal shape of a hydraulic structure such as the fishway.

We consider $\Omega \subset \mathbb{R}^2$ the shape of the fishway a rectangular shape divide into ten pools with baffles of the same size, and two transition pools located in the upstream and downstream of the channel showing in Figure (5.4). Each pool has a width of $0.97m$ and a length of $1.213m$. The baffles separating the pools have a thickness of $0.061m$.

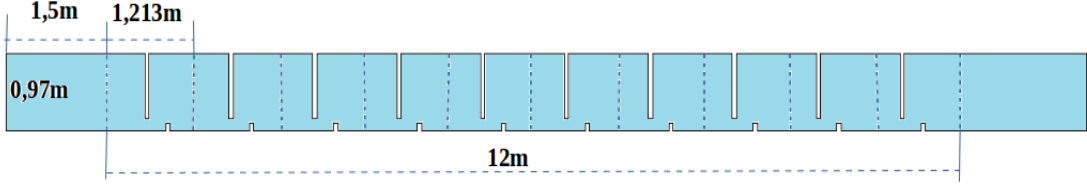


Figure 5.4: 2D schematic representation of the Denil fishway

The equilibrium behavior of the fluid inside the domain Ω is described with the velocity field and the pressure, which solve the stationary incompressible Navier-Stokes Forchheimer equations

$$\begin{cases} -\nu\Delta u + (u.\nabla)u + \nabla p + au + b |u|^\alpha u = 0 & \text{in } \Omega \\ \operatorname{div}(u) = 0 & \text{in } \Omega \\ u = u_{in} & \text{on } \Gamma_{in} \\ u = 0 & \text{on } \Gamma \\ \sigma(u, p).n = 0 & \text{on } \Gamma_{out} \end{cases} \quad (5.47)$$

In practice, the resolution of the Navier-Stokes Forchheimer system is modified. We introduce the penalty method that gives us the modified version of the system describing in (5.47) of the following form

$$\begin{cases} -\nu\Delta u^\varepsilon + (u^\varepsilon.\nabla)u^\varepsilon + \nabla p^\varepsilon + au^\varepsilon + b |u^\varepsilon|^\alpha u^\varepsilon = 0 & \text{in } \Omega \\ \operatorname{div}(u^\varepsilon) + \varepsilon p^\varepsilon = 0 & \text{in } \Omega \\ u^\varepsilon = u_{in}^\varepsilon & \text{on } \Gamma_{in} \\ u^\varepsilon = 0 & \text{on } \Gamma \\ \sigma(u^\varepsilon, p^\varepsilon).n = 0 & \text{on } \Gamma_{out} \end{cases} \quad (5.48)$$

where ε is very small parameter ($\varepsilon = 10^{-6}$). The reason is to get a well-posed system, the matrix associated to its resolution by the Finite Element method is positive definite, which allows to use efficient numerical linear algebra solvers.

In order to compute in a simpler manner the derivatives of the objective function (5.33), we introduce the adjoint system of the following form :

$$\begin{cases} -\nu\Delta v + (\nabla u)^T.v - (u.\nabla)v + av + b |u|^\alpha v + \alpha b |u|^{\alpha-2} (u.v)u + \nabla q \\ = -(2\nu\Delta u + |u - u_{ref}|) & \text{in } \Omega \\ \operatorname{div}(v) = 0 & \text{in } \Omega \\ v = 0 & \text{on } \Gamma_{in} \\ v = 0 & \text{on } \Gamma \\ \sigma(v, \pi).n + (u.n)v = 4\nu\mathbf{e}(u).n & \text{on } \Gamma_{out} \end{cases} \quad (5.49)$$

5.5.1 Space discretization : the Finite Element method

For the space discretization we consider a Lagrange-Galerkin finite element triangulation mesh \mathcal{T}_h of the domain Ω . For the numerical resolution of the systems define in (5.47) and (5.49), the choice of the Finite Element spaces used for the discretization of the unknown velocity and the pressure are the \mathbb{P}_2 Lagrange elements for the velocity and \mathbb{P}_1 for the pressure. We define the following Finite Element spaces

$$U_h = \{w_1 \in [C(\Omega)]^n : w_1|_T \in [\mathbb{P}_2(T)]^n, \forall T \in \mathcal{T}_h, w_1 \cdot n = 0 \text{ on } \partial\Omega\}$$

$$X_h = \{w_2 \in [C(\Omega)]^n : w_2|_T \in [\mathbb{P}_2(T)]^n, \forall T \in \mathcal{T}_h, w_2 \cdot n = 0 \text{ on } \partial\Omega\}$$

$$M_h = \{\tilde{q} \in C(\Omega) : \tilde{q}|_T \in \mathbb{P}_1(T), \forall T \in \mathcal{T}_h\}$$

$$Q_h = \{q \in L^2(\Omega) : w_2|_T \in \mathbb{P}_1(T), \forall T \in \mathcal{T}_h\}$$

Let (u^{n+1}, p^{n+1}) the solution of the following variational formulation

$$\left\{ \begin{array}{l} \text{Find } (u_h^\varepsilon, p_h^\varepsilon) \in U_h \times M_h \text{ such that} \\ \int_{\Omega} \nu \nabla u_h^\varepsilon : \nabla w_1 dx + \int_{\Omega} (u^n \cdot \nabla) u_h^\varepsilon w_1 dx - \int_{\Omega} p_h^\varepsilon \nabla \cdot w_1 dx - \int_{\Omega} \tilde{q} \nabla \cdot u_h^\varepsilon w_1 dx \\ - \int_{\Omega} \varepsilon p_h^\varepsilon \tilde{q} w_1 dx + \int_{\Omega} a u_h^\varepsilon w_1 dx + \int_{\Omega} b |u_h^\varepsilon| |u_h^\varepsilon| w_1 dx = 0 \quad \forall w_1 \in U_h \text{ and } \forall \tilde{q} \in M_h \end{array} \right. \quad (5.50)$$

and (v_h, q_h) the solution of the following variational formulation of the system adjoint

$$\left\{ \begin{array}{l} \text{Find } (v_h, q_h) \in X_h \times M_h \text{ such that} \\ \int_{\Omega} \nu \nabla v_h : \nabla w_2 dx - \int_{\Omega} (u_h \cdot \nabla) v_h w_2 dx + \int_{\Omega} (\nabla u_h)^T \cdot v_h w_2 dx + \int_{\Omega} v_h w_2 dx \\ + \int_{\Omega} b |u_h|^\alpha v_h w_2 dx + \int_{\Omega} \alpha b |u_h|^{\alpha-2} (u_h \cdot v_h) u_h w_2 dx - \int_{\Omega} q_h \nabla \cdot w_2 dx \\ + \int_{\Omega} 2\nu \nabla u_h : \nabla w_2 dx + \int_{\Omega} |u_h - u_{ref}| w_2 dx + \int_{\Gamma_{out}} \sigma(v_h, q_h) \cdot n w_2 ds \\ + \int_{\Gamma_{out}} (u_h \cdot n) v_h w_2 ds - 4\nu \mathbf{e}(u_h) \cdot n w_2 = 0 \quad \forall w_2 \in X_h \text{ and } \forall q \in Q_h \end{array} \right. \quad (5.51)$$

Theorem 5.5.1. *Let $(u^\varepsilon, p^\varepsilon)$ the solution of the problem (5.48) and (u, p) the solution $(H_0^1(\Omega))^d \times L^2(\Omega)$ of the problem (5.1). Then we have*

$$p^\varepsilon \in L^2(\Omega) \text{ is uniformly bounded in } \varepsilon \quad (5.52)$$

and as $\varepsilon \rightarrow 0$

$$u^\varepsilon \rightarrow u \text{ in } (H_0^1(\Omega))^d \quad (5.53)$$

and

$$p^\varepsilon \rightarrow \tilde{p} \text{ in } L^2(\Omega) \quad (5.54)$$

where \tilde{p} is the orthogonal projection in $L^2(\Omega)$ of p into $(\text{Ker}B^*)^\perp$. For the demonstration of this theorem we refer [17]

In order to evaluate the cost function J , we first need to solve the Navier-Stokes Forchheimer system (5.48) with initial and boundary conditions. The functionnal $J(\Omega)$ is approximated by

$$J(\Omega) = \frac{1}{2} \sum_{E \in \mathcal{T}_h} \left[\int_E |u_h - u_d|^2 + 4\nu \int_E \|\mathbf{e}(u_h)\|^2 \right] \quad (5.55)$$

In the lower third of the channel near the slots, the velocity must be as possible to a typical horizontal velocity u_{ref} to facilitate the movement of fish from one pool to another and in the remaining of the fishway the velocity must be close to zero to allow fish to rest. The choice of the target velocity depends on the maximum swimming speed according to the species of migratory fish. The velocity of the fluid must be close to the following target velocity

$$u_d(x, y) = \begin{cases} (u_{ref}, 0), & \text{if } y \leq \frac{1}{3}H \\ (0, 0), & \text{otherwise} \end{cases}$$

where H is the the width of the fishway and u_d is the desired velocity.

5.5.2 Algorithmic description of the implemented method

There are numerical methods to solve some optimization problems with or without constraints. Generally, a problem of optimization of structures is defined by a model of partial differential equations which allows us to evaluate the mechanical behavior of a structure, a criterion to be minimized and an admissible set of optimization variable under constraints that we impose these variables. In the literature, there are three categories in the case of shape optimization problems: parametric, geometric and topologic shape optimization. Several types of conventional optimization algorithms are used to numerically solve a shape optimization problem, such as gradient descent methods, conjugate gradient, projection method and constraint penalty, Level Set method and others. In our case, to solve the problem define in (5.30) we rely on the augmented Lagrangian method we refer to [18].

The augmented Lagrangian algorithm for equality-constrained problems

The augmented Lagrangian algorithm transforms the constrained optimization problem into the series of unconstrained problems.

$$\inf_{\Omega \in Q_{ad}} \mathcal{L}(\Omega, \lambda^n, b^n)$$

where the Lagrangian of the penalized problem take the following form

$$\mathcal{L}(\Omega, \lambda, b) = J(\Omega) - \lambda G(\Omega) + \frac{b}{2} G(\Omega)^2$$

where $G(\Omega)$ as a constraint functional, we limit to an equality constraint on the volume of the domain $V(\Omega) = \int_{\Omega} dx$ for some given volume target V_T , we have

$$G(\Omega) = V(\Omega) - V_T$$

To update the value of the Lagrange multiplier λ and the penalty coefficient in the augmented Lagrangian. The parameter b is a penalty factor defined positive for the violation of the constraint $G(\Omega) = 0$.

$$\lambda^{n+1} = \lambda^n - b^n G(\Omega^n)$$

$$b^{n+1} = \begin{cases} \delta b^n & \text{if } b < b_d \\ b & \text{otherwise} \end{cases}$$

The different steps of the shape optimization algorithm are summarized as follows

1. INITIALIZATION

- The initial domain Ω^0 with a triangular mesh \mathcal{T}_h^0
- Choose the initial value of the coefficients of the augmented Lagrangian algorithm (λ^0, b^0)

2. MAIN LOOP For $n = 0, \dots, k$

- Compute the Navier-Stokes Forchheimer system (u^n, p^n) on the mesh \mathcal{T}_h^n of Ω^n
- Compute the adjoint system (v^n, π^n)
- Compute the shape gradient of $\Omega \mapsto \mathcal{L}(\Omega, \lambda^n, b^n)$
- Infer a descent direction Θ^n for $\Omega \mapsto \mathcal{L}(\Omega, \lambda^n, b^n)$ on the mesh \mathcal{T}_h^n
- Find a descent step τ^n such that

$$\mathcal{L}((Id + \tau^n \theta^n)(\Omega^n), \lambda^n, b^n) < \mathcal{L}(\Omega, \lambda^n, b^n)$$

- Move the vertices of \mathcal{T}_h^n according to τ^n and θ^n

$$x_i^{n+1} = x_i^n + \tau^n \theta^n(x_i^n)$$

- If the resulting mesh is invalid, go back to step and take a small value of τ^n
- Else the new mesh \mathcal{T}_h^{n+1}

- Update the augmented Lagrangian parameters (λ^{n+1}, b^{n+1})

3. ENDING CRITERION Stop if $e^k < \varepsilon_{stop}$

4. RETURN Ω^n

5.5.3 Numerical results : academic case

We present some numerical results for three academic tests. We consider an exemple for the two-dimensional domain $\Omega = [0, 1.5] \times [0, 1]$ which can interpreted as a rectangular domain, with a circular, square and double square hole. The parameters values are taken as follow: the inlet velocity $u_{in} = 1m.s^{-1}$, for the Lagrangian parameters $\lambda_{in} = 10$ and $b_{in} = 0.02$, for the descent step $\tau = 0.001$. The number of iteration 100. All computations are done at a low Reynolds number $Re = 200$ and $\alpha = 1$. The results obtained for the first geometry with circular hole are showing in Figure (5.5)

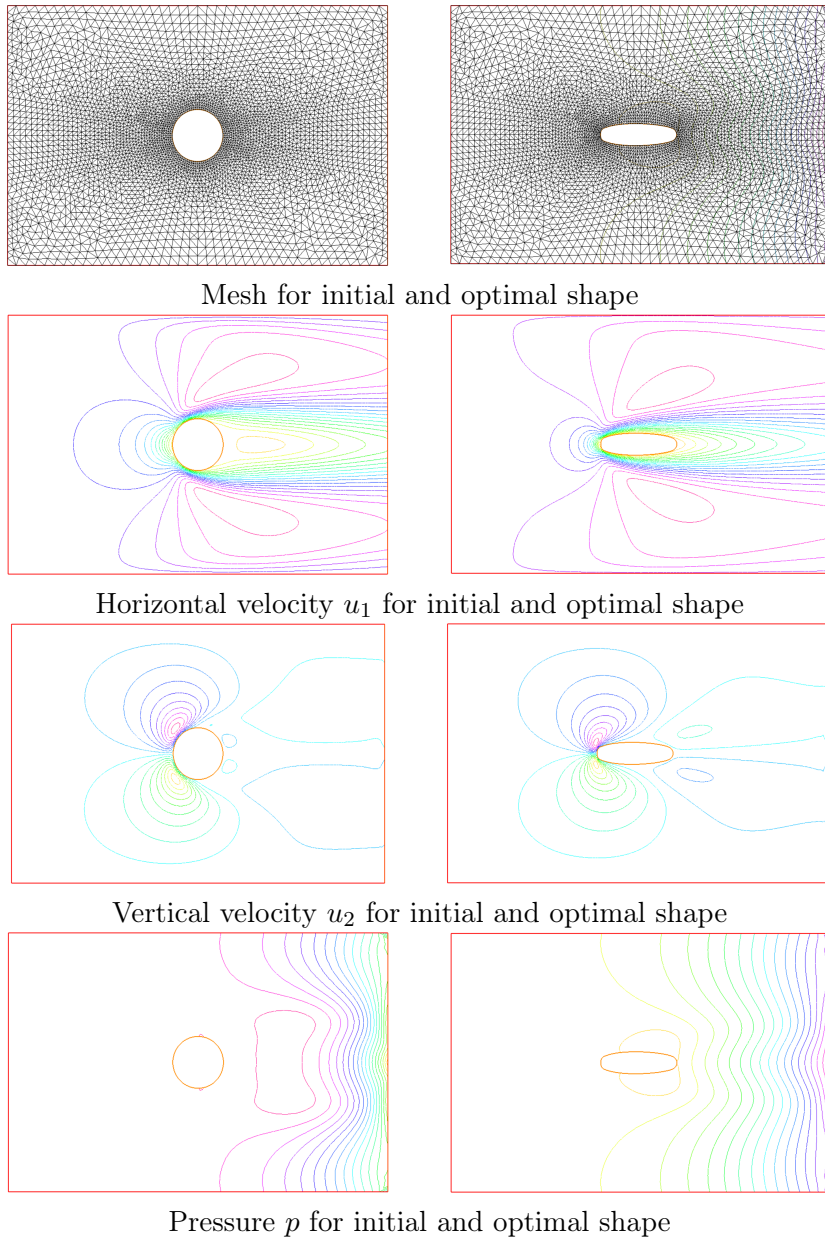


Figure 5.5: Comparison of the initial shape and optimal shape $Re = 200$

For the second test with the same parameters, we have the following results showing in Figure (5.6)

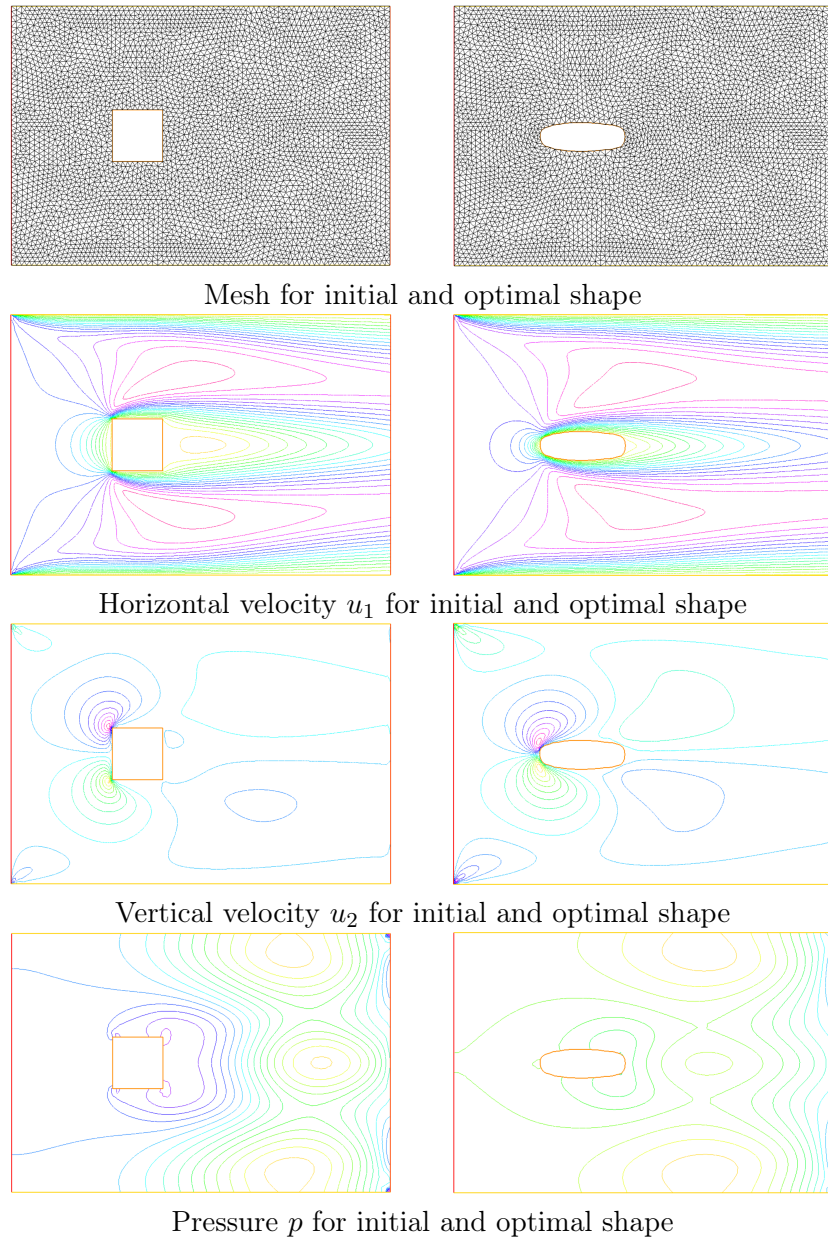
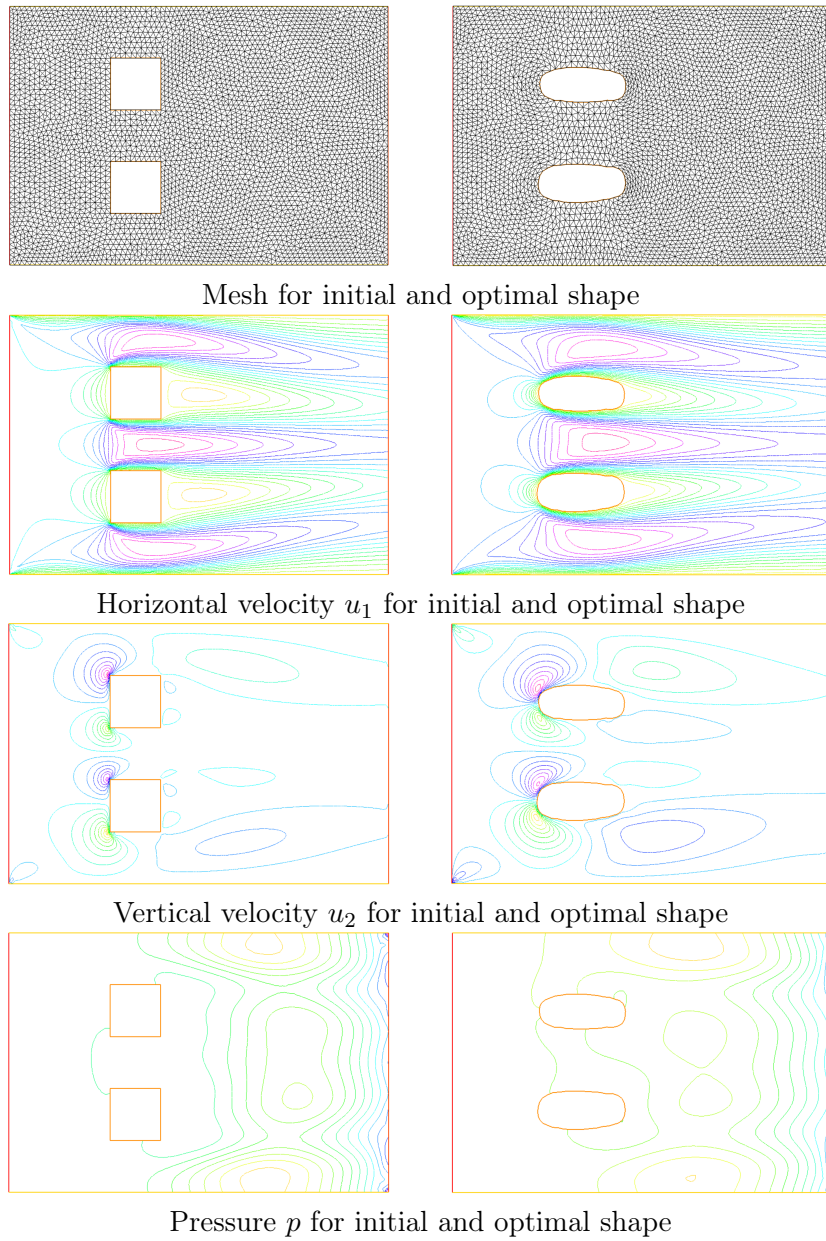
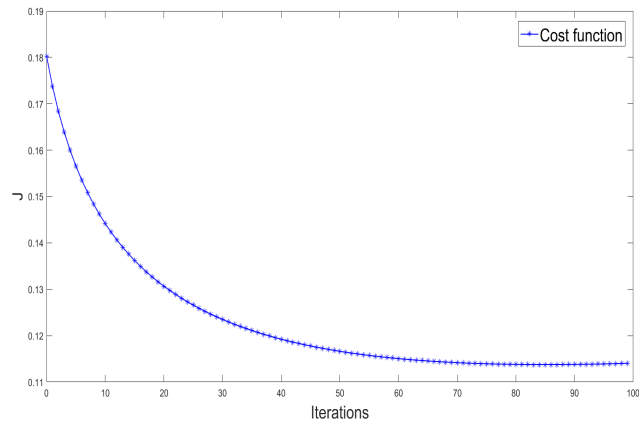


Figure 5.6: Comparison of the initial shape and optimal shape $Re = 200$

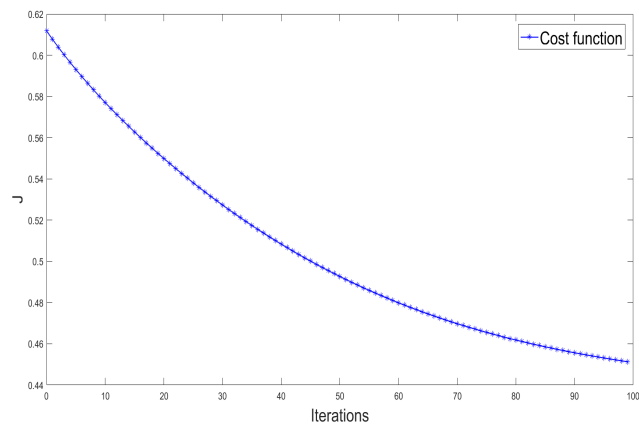
And for the third test case, we have obtained the result showing in Figure (5.7)

Figure 5.7: Comparison of the initial shape and optimal shape $Re = 200$

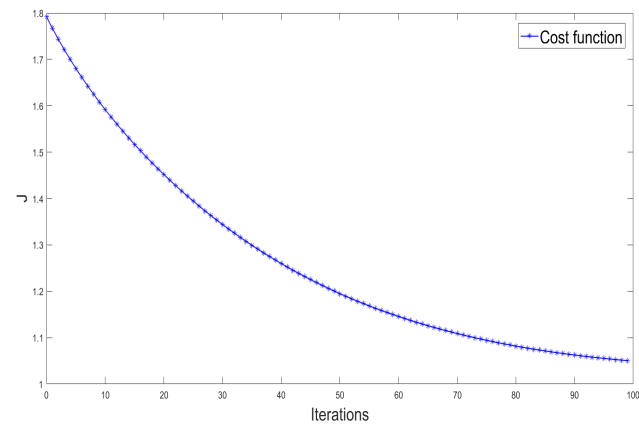
The convergence of the cost function in each case



Case 1 : circle hole



Case 2 : square hole



Case 3 : double square hole

Figure 5.8: Convergence history of the cost function for the three cases $Re = 200$

5.5.4 Numerical results : practical case

In this subsection, we presented some numerical results we have obtained. We consider the hydraulic structure given in Figure (5.4). The goal is to find the optimal shape in an admissible set in order to minimize in all the channel the flow turbulence to avoid fish disorientation. Before showing and analyzing the results obtained, all computations have been initialized with a constant initial and boundary conditions and at low Reynolds Number $Re = 20$. The different parameters of the numerical tests we have used, the inlet velocity $u = 1m.s^{-1}$, and the desired velocity u_d for the objective function we are taking the horizontal reference speed $u_{ref} = 0.8m.s^{-1}$, the number of iterations is $N = 4000$. For the initial value of the multiplier and the penalty parameter are respectively $\lambda = 5$ and $b = 1$, the descent step $\tau = 10^{-2}$, and for the computational domain a triangular mesh of 13063 triangles.

The following results present the velocity for ten pools and compare the water flow in the initial and the optimal shape. The results obtained is showing in Figure (5.10) show the fields velocity corresponding to the initial shape of the fishway. Using the augmented Lagrangian method and after 4000 iterations we get the optimal shape presented in Figure (5.11). From this results we observe that the effect of the turbulence is reduced. The detail results in central pool is showing in Figure (5.12)

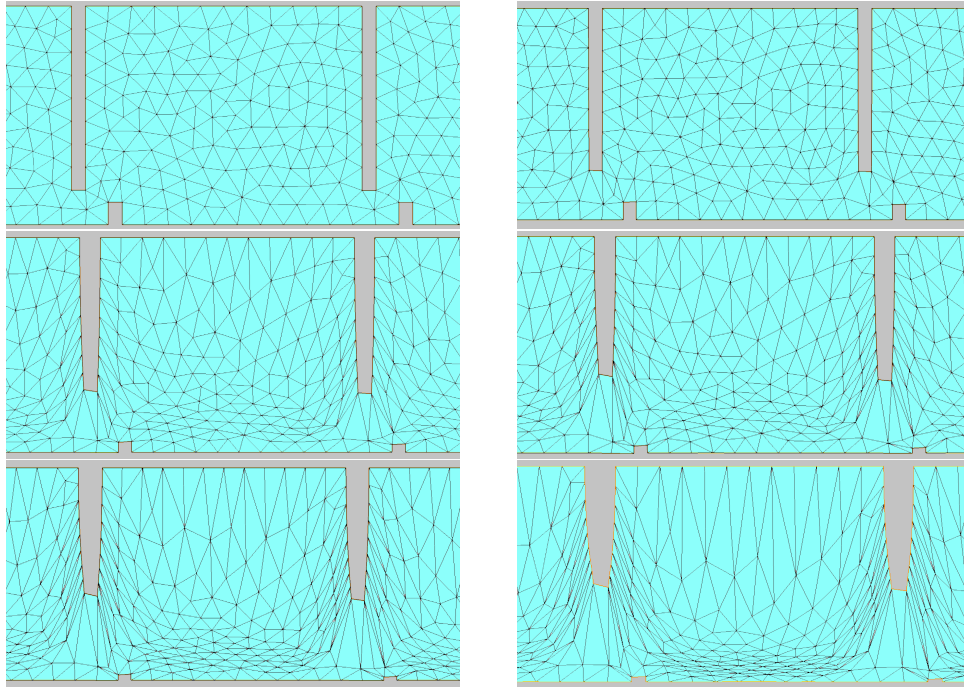


Figure 5.9: From left to right, top to bottom the initial and the optimal shapes Ω^n from $n = 0$, to $n = 4000$ iterations.

We also present the velocity fields in the different zones of the pass where we see the presence of turbulence in each pool in the case of the non-optimal shape which causes the difficulty and a very important energy for the movement of the fish from the pool to another Figure (5.12) (left).

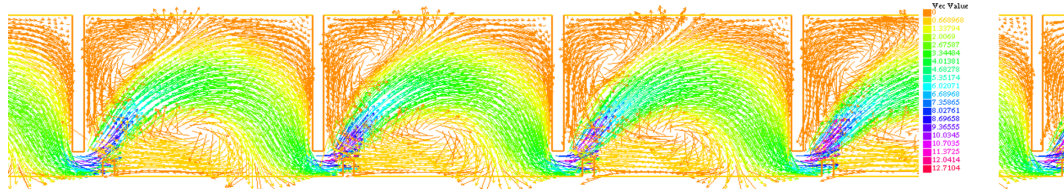


Figure 5.10: The non-optimal structure of the fields velocity

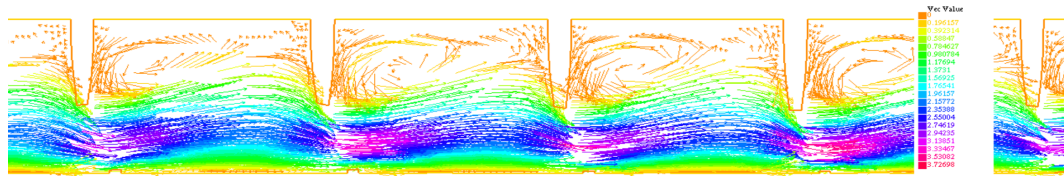


Figure 5.11: The optimal structure of the fields velocity

For the optimal shape (5.12) (right), the nature of the velocity close to zero in the upper part of the pool between the two successive slots, which facilitates the passage of fish and allows them to rest.

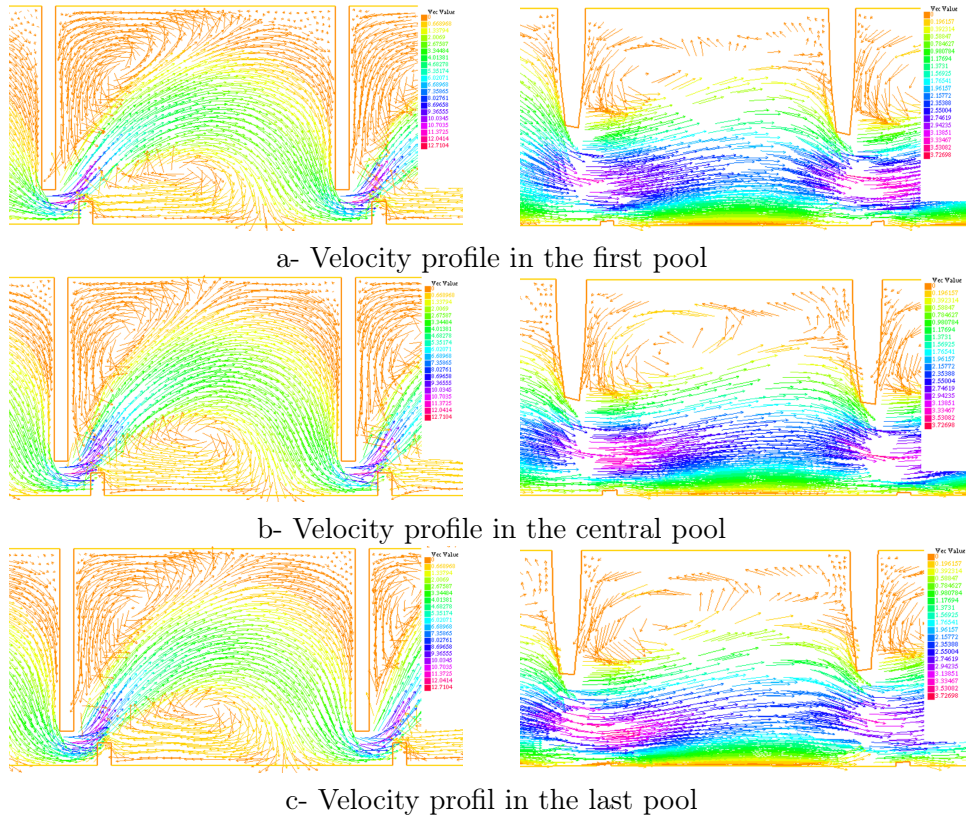


Figure 5.12: Initial (left) and optimal (right) velocities for the fishway

The evolution of the objective function J according to the number of iterations of the optimization process, is presented on Figure (5.13). The value of the objective functional decreases very strongly according to the iterations, passing from a value equal to 979.734 at the beginning of the iterative process to a value equal to 83.8794 after convergence.

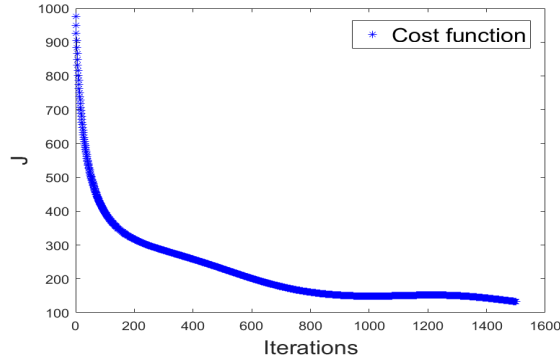


Figure 5.13: Convergence history of the cost function $J(\Omega)$

Then, we vary the Forchheimer coefficient α and the parameter b , to show the influence of the parameters on the topology and the optimal shape of the structure. We take some examples $\alpha = \frac{3}{2}$, $\alpha = 0$, $b = 0$ and $b = 5$, the numerical results obtained are presented in Figure (5.14).

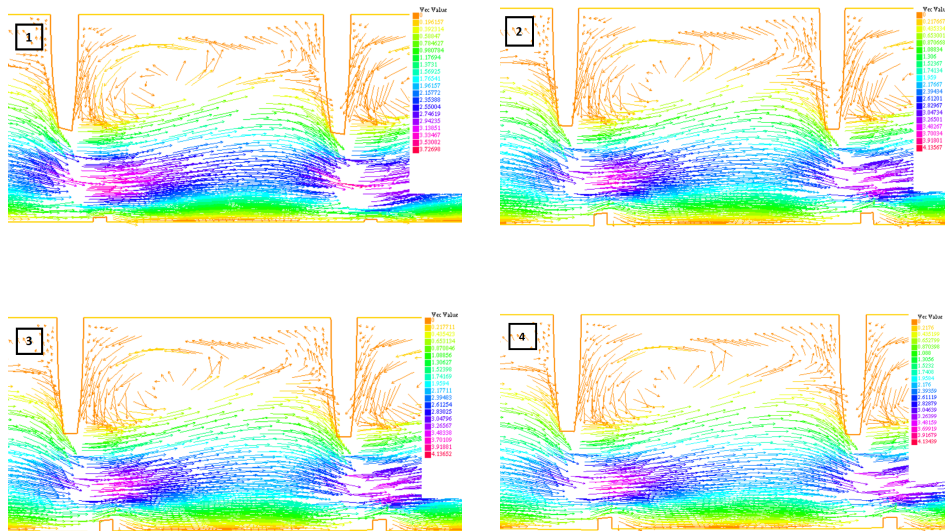


Figure 5.14: Velocity profiles of the optimal shape in the case :

- 1- $\left[\alpha = \frac{3}{2} \right]$, 2- $[\alpha = 0]$, 3- $[b = 0]$, 4- $[b = 5]$

The convergence history of the objective function according to some of the change in parameters such as the Darcy and Forchheimer parameters showing in Figure (5.15).

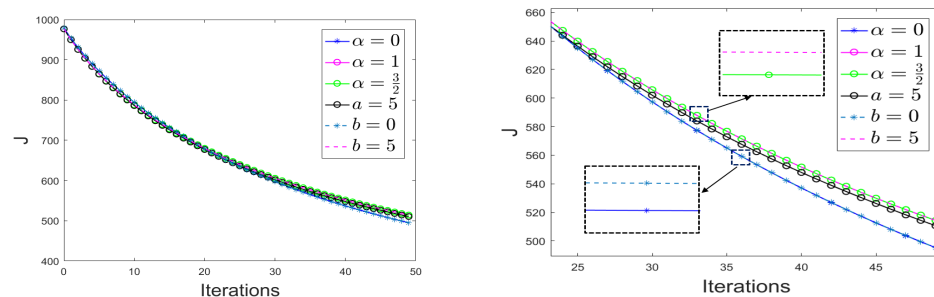


Figure 5.15: Convergence history of the cost function $J(\Omega)$ for the different parameters

5.6 Conclusions

In this chapter, we presented a numerical method for the shape optimization problem governed by steady Navier-Stokes Forchheimer equations at low Reynolds number. We proposed a Lagrangian algorithm based on the first order by shape derivatives. The numerical examples indicated the reliability and the robustness of the proposed algorithm for the practical applications.

Bibliography

- [1] N. Rajaratnam, C. Katopodis, Hydraulics of Denil fishways, J Hydraulic Eng. 110 : 1219 – 1233(1984).
- [2] N. Rajaratnam, V. de Vinne, C. Katopodis, Hydraulics of vertical slot fishways, J Hydraul. Eng. 112 : 909 – 917(1986).
- [3] L.J. Alvarez-Vazquez, J.J. Judice, A. Martinez, C. Rodriguez, M.E. Vasquez-Mendez, M.A. Vilar, On the optimal design of river fishways, Optim Eng (2013)14 : 193 – 211.
- [4] L. David, R. W. Wang, F. M. Chambon, A. Texier, M. Larinier, F. Baran, Control of turbulent flow in vertical slot fishways for the migration of small fish species. (2011) In: 7th International Symposium on Ecohydraulics, 12 January 2009 - 16 January 2009 (Concepcion, Chile).
- [5] M. D. Gunzburger, Perspectives in flow control and optimization, vol. 5, Siam, 2003.
- [6] B. Mohammadi and O. Pironneau, Applied shape optimization for fluids, Oxford University Press, 2010.
- [7] M. P. Bendsoe and O. Sigmund, Topology optimization: theory, methods, and applications, Springer Science & Business Media, 2013.
- [8] N. Aage, T. H. Poulsen, A. Gersborg-Hansen, and O. Sigmund, Topology optimization of large scale stokes flow problems, Struct. Multidisc. Optim., 35(2008), pp.175 – 180.

-
- [9] T. Borrvall and J. Petersson, Topology optimization of fluids in stokes flow, *Int. J. Numer. Meth. Fluids*, 41(2003), *pp.*77 – 107.
- [10] G. Pingen, A. Evgrafov, and K. Maute, Topology optimization of flow domains using the lattice boltzmann method, *Structural and Multidisciplinary Optimization*, 34(2007), *pp.*507 – 524.
- [11] J. A. Sethian and A. Wiegmann, Structural Boundary Design via Level Set and Immersed Interface Methods, *Journal of Computational Physics* 163, 489 – 528(2000).
- [12] A. Takezawa, S. Nishiwaki, M. Kitamura, Shape and topology optimization based on the phase field method and sensitivity analysis, *Journal of Computational Physics* 229(2010)2697 – 2718.
- [13] M. Y. Wang, X. Wang, D. Guo, A level set method for structural topology optimization, *Comput. Methods Appl. Mech. Engrg.* 192(2003)227 – 246.
- [14] P. Wei, M. Y. Wang, X. Xing, A study on X-FEM in continuum structural optimization using a level set model, *Computer-Aided Design* 42(2010)708 – 719.
- [15] G. P. Galdi, An introduction to the Mathematical Theory Of the Navier-Stokes Equations. Vol. Linearized Steady Problems. Springer-Verlag. New York. Berlin. etc. 1994.
- [16] H. Brezis, *Functional Analysis, Sobolev Spaces and Partial Differential Equations*, Springer New York Dordrecht Heidelberg London, 2010.
- [17] M. Louaked, M. Kadiri, N. Sellila, H. Mechkour, Analysis and Finite Element Approximation of Optimal Control Problem Based on Porous Media Model.
- [18] J. Nocedal and S. Wright, *Numerical Optimization*, Springer, 2006.
- [19] A. Henrot, M. Pierre, *Variation et optimisation de formes*, vol 48 (2005). Springer, Berlin.
- [20] A.A. Novotny, J. Sokołowski, *Topological derivatives in shape optimization*, Springer Science & Business Media.
- [21] S. Amstutz, The topological asymptotic for the Navier-Stokes equations. *ESAIM: Control Optim Calc Var* 11(3) : 401 – 425(2005).
- [22] W. Li, X. Wang, Q. Jiu, Existence and uniqueness of the weak solutions for the steady incompressible Nvaier-Stokes equations with damping, *African Diasporama Journal of Mathematics*, Volume 12, Number 2, pp. 57 – 72(2011).
- [23] C. Dapogny, P. Frey, F. Omnès, Y. Privat, Geometrical shape optipization in fluid mechanics using FreeFem++, *Structural and Multidisciplinary* (2018)50 : 2761 – 2788.
- [24] F. Jouve, H. Mechkour, Level set based method for design of compliant mechanisms , *Eur. J. of Comp. Mech.*, 17/5-6-7 (2008), pp.957-971.

- [25] F. De Gournay, G. Allaire, F. Jouve, Shape and topology optimization of the robust compliance via the level set method , ESAIM COCV, 4/1 (2008), pp.43-70. (Internal report 593, CMAP, Ecole Polytechnique).

List of Figures

1	Champs de température de l'air pour les emplacements des espaces verts optimaux et non optimaux (Campus universitaire Caen Normandie).	5
2	Champs de vitesse et de température dans la cavité.	8
3	Champs de vitesse et de température dans une île isolée.	8
4	Contrôle optimal de la concentration du polluant dans le golf Normand-Breton. .	13
5	Exemple d'une passe à poissons à fentes obliques et son maillage.	14
6	Vitesse non optimale pour dix bassins.	17
7	Vitesse optimale pour dix bassins.	17
8	De gauche à droite, de haut en bas de la forme initiale à la forme optimale Ω^n de $n = 0$, à $n = 4000$ iterations.	22
9	Champs de vitesses non optimal (gauche) et optimal (droite) dans le bassin central d'une passe à poisson.	22
1.1	2D Schematic representation.	51
1.2	Air temperature profile for non optimal green locations.	59
1.3	Air temperature profile for optimal green locations.	59
1.4	Temperature profiles corresponding to the non optimal and optimal and green locations.	60
1.5	Decreasing cost function.	60
1.6	Different positions.	60
1.7	Velocity and temperature profiles according to the height in city.	61
1.8	Fields Temperature profiles for the difference value of $\varepsilon = 10^{-3}$, $\varepsilon = 10^{-4}$ and $\varepsilon = 10^{-5}$	61
1.9	Profile temperature and velocity according to the variation of ε	62
1.10	Fields Temperature profiles for 3D build: nonoptimal in the left and the optimal in the right	62
1.11	Initial mesh of Caen university.	63
1.12	Air temperature and velocity profiles for non optimal in the left and optimal green locations in the right.	63
1.13	3D air temperature profile for optimal green locations of Caen university.	64
2.1	Square cavity with free wall.	94

2.2	Velocity fields in driven cavity $b = 1$, $b = 5$ and $b = 10$	95
2.3	Temperature fields in driven cavity $\kappa = 0.01$, $\kappa = 0.001$ and $\kappa = 0.0001$	95
2.4	Physics model of cavity flows.	95
2.5	Velocity and temperature fields in driven cavity $\lambda = 1$, $\kappa = 1$	96
2.6	The boundary conditions, initial mesh and adaptative mesh.	99
2.7	Velocity fields in the city $b = 1$, $b = 5$ and $b = 10$ from the left to the wright for $\lambda = 0.01$	99
2.8	Temperature fields in the city $b = 1$, $b = 5$ and $b = 10$ from the left to the right for $\lambda = 0.01$, $\kappa = 0.01$	99
2.9	Velocity fields in the city $\varepsilon = 10^{-3}$, $\varepsilon = 10^{-4}$ and $\varepsilon = 10^{-6}$ from the left to the right for $\lambda = 1$	99
2.10	Temperature fields in the city $\varepsilon = 10^{-3}$, $\varepsilon = 10^{-4}$ and $\varepsilon = 10^{-6}$ from the left to the right for $\lambda = 0.01$, $\kappa = 0.01$	100
2.11	Computational domain and 3D mesh of the free-frost refrigerator.	100
2.12	Temperature profile in the frost-free refrigerator without shelves in the left and with shelves in the right.	101
2.13	Horizontal temperature profile in the freezer compartment without shelves in the left and with shelves in the right.	102
2.14	Velocity profiles in the refrigerator without shelves in the left and with shelves in the right.	102
3.1	Examples of wastewater in the left and a Normand-Breton golf oil spill 1967 in the right.	106
3.2	2D geometric model of Normand-Breton gulf.	130
3.3	The nonoptimal solution of the pollutant.	132
3.4	Optimal control of the pollutant with $\alpha = 1$ and $\mu = 1m^2.s^{-1}$	133
3.5	Optimal control of the pollutant with $\alpha = 1$ and $\mu = 0.1m^2.s^{-1}$	133
3.6	Optimal control of the pollutant with $\alpha = 1$ and $\mu = 0.01m^2.s^{-1}$	133
3.7	Optimal control of the pollutant with $\alpha = 0$ and $\mu = 1m^2.s^{-1}$	134
3.8	Optimal control of the pollutant with $\alpha = 0.1$ and $\mu = 1m^2.s^{-1}$	134
3.9	Optimal control of the pollutant with $\alpha = 0.01$ and $\mu = 1m^2.s^{-1}$	134
3.10	Gradient of the cost function evolution depending iteration number.	135
3.11	The discrete state $\Phi_{h\tau}$ at time $t = 0.1$ with 12106	136
3.12	Nonoptimal (left) and optimal control (right) of the pollutant in the Normand- Breton Gulf.	137
3.13	Zoom for the differents sources of the pollutant.	137
4.1	Schematic description of fishway structure	174
4.2	Fish pass geometry I shaped baffle for the central pool	175
4.3	Conventional pool pass Ω : each pool is designed by dashed lines	178
4.4	Fish pass geometry and mesh in the central pool	178

4.5	Initial (left) and optimal (right) velocities for central pool	179
4.6	Configuration of central pool	179
4.7	Velocity fields for non optimal ten pool configuration	180
4.8	Velocity fields for optimal ten pool configuration	180
4.9	Convergence history	180
4.10	3-D Example of Fiswhay with oblique slots and mesh in the central pool	181
4.11	Non optimal velocity for ten pool	181
4.12	Optimal velocity for ten pool	182
4.13	Convergence history	182
5.1	Exemple of vertical slot and Denil fishway	192
5.2	Schematic representation of the fluid domain	193
5.3	Example of a variation Ω_θ of shape Ω	200
5.4	2D schematic representation of the Denil fishway	204
5.5	Comparison of the initial shape and optimal shape $Re = 200$	208
5.6	Comparison of the initial shape and optimal shape $Re = 200$	209
5.7	Comparison of the initial shape and optimal shape $Re = 200$	210
5.8	Convergence history of the cost function for the three cases $Re = 200$	211
5.9	From left to right, top to bottom the initial and the optimal shapes Ω^n from $n = 0$, to $n = 4000$ iterations.	212
5.10	The non-optimal structure of the fields velocity	213
5.11	The optimal structure of the fields velocity	213
5.12	Initial (left) and optimal (right) velocities for the fishway	213
5.13	Convergence history of the cost function $J(\Omega)$	214
5.14	Velocity profils of the optimal shape in the case : 1- $\left[\alpha = \frac{3}{2}\right]$, 2- $[\alpha = 0]$, 3- $[b = 0]$, 4- $[b = 5]$	214
5.15	Convergence history of the cost function $J(\Omega)$ for the different parameters	215

List of Tables

2.2	Uniform meshes for $\lambda = 0.1, \kappa = 1, a = 1, b = 1$	97
2.3	Uniform meshes for $\lambda = 0.001, \kappa = 1, a = 1, b = 1$	97
2.1	Uniform meshes for $\lambda = 1, \kappa = 1, a = 1, b = 1$	97
2.4	Uniform meshes for $\lambda = 1, \kappa = 0.1, a = 1, b = 1$	97
2.5	Uniform meshes for $\lambda = 1, \kappa = 1, a = 5, b = 1$	98
2.6	Uniform meshes for $\lambda = 1, \kappa = 1, a = 1, b = 5$	98
2.7	Boundary conditions	101